Evaluation of Arsenic Contamination in Texas

Report Prepared for
Texas Commission on Environmental Quality
Austin, Texas

August 2005

Prepared by
Bureau of Economic Geology
Scott W. Tinker, Director
John A. and Katherine G. Jackson School of Geosciences
The University of Texas at Austin
Austin, Texas 78713-8924

FINAL REPORT – August 2005

Evaluation of Arsenic Contamination in Texas

Prepared for
Texas Commission on Environmental Quality
Austin Texas

under
Umbrella Contract No. 582-4-56385
Work Order No. UT-08-5-70828

Bridget R. Scanlon, Principal Investigator
Jean-Philippe Nicot
Robert C. Reedy
J. Andrew Tachovsky
Seay H. Nance
Rebecca C. Smyth
Kelley Keese
Randi E. Ashburn
Lance Christian

Bureau of Economic Geology
Scott W. Tinker, Director
John A. and Katherine G. Jackson School of Geosciences
The University of Texas at Austin
Austin, Texas 78713-8924

TABLE OF CONTENTS

LIST OF FIGURES

LIST OF TABLES

ACRONYMS

DO	Dissolved Oxygen
Fm., Fms.	Formation(s)
GLF	Geophysical Log Facility
MCL	Maximum Contaminant Limit
NLCD	National Land Cover Data
NURE	National Uranium Resource Evaluation
NWIS	National Water Information System
PWS	Public Water Supply
TDS	Total Dissolved Solids
TCEQ	Texas Commision on Environmental Quality
TOC	Total Organic Carbon
TWDB	Texas Water Development Board

ACKNOWLEDGMENTS

Many people contributed in various ways to this project. We very much appreciate help from many property owners and other facilitators during the soil sampling campaign: Ken Carver, Permian Basin Underground Water Conservation District, Jason Coleman, South Plains Underground Water Conservation District, Deanya Williams, Mesa Underground Water Conservation District, Casey Barrett, Dawson County Agricultural Extension Agent, Kent Lewis, Lamb Agricultural Extension Agent, George Gonzales, Benavides, Duval County NRCS office, Adrien Perez, Field Representative for District III of the State Soil and Water Conservation Board, Felo Guerra, former director of the Red Sands Groundwater Conservation District, and John Freeman, Robstown, Nueces County NRCS office.

Steve Walden Steve Walden Consulting, facilated communication with TCEQ. Gary Franklin, TWDB, contributed the results of the Duval County recent sampling campaign. George Fitzgerald, TCEQ, and Mark Rhodes and Jon Brandt, both at RRC, provided information on the south Texas uranium district. Arten Avakian, TCEQ, assisted in gathering data on the petrology of the High Plains aquifer. The report was partially edited by Susie Doenges.

EXECUTIVE SUMMARY

Lowering the Federal standard for arsenic in drinking water from 50 ug/L to 10 ug/L, results in much more widespread arsenic contamination in groundwater in Texas. The objectives of this study were to (1) determine the distribution of arsenic in Texas groundwater; (2) assess the potential of past application of arsenical pesticides as a source of arsenic in groundwater in the southern High Plains and southwestern Gulf Coast; (3) evaluate the role of phosphate fertilizers in mobilizing arsenic; and (4) assess geologic sources of arsenic in Texas. The study focused on geographic areas of domestic drinking water wells affected by high arsenic levels.

The Bureau of Economic Geology (BEG) conducted a number of tasks to accomplish the above objectives. (1) Groundwater arsenic concentrations in surrounding states were reviewed and research related to elevated arsenic studies in the US was evaluated. (2) Potential anthropogenic sources of arsenic, such as arsenical pesticides in the southern High Plains and the southwestern Gulf Coast, were examined using GIS overlay analyses and soil sampling. (3) Potential geologic sources of elevated arsenic concentrations in groundwater were evaluated in the southern High Plains and southwestern Gulf Coast using relationships between arsenic concentrations and different geologic units. Relationships between arsenic concentrations and other ions, particularly oxyanions, were evaluated using existing databases (TWDB, NURE, and TCEQ) to assess sources of arsenic. The impact of different redox conditions on the distribution of arsenic was examined. Limited additional groundwater sampling was conducted in Duval County in the Gulf Coast.

Arsenic contamination is widespread in surrounding states, particularly New Mexico where 16% of wells exceed the MCL (10 ug/L). Arsenic contamination is focused in the Middle Rio Grande Basin and is attributed to desorption of arsenic from iron oxyhydroxides. Only 5% of wells in Oklahoma had arsenic levels exceeding the MCL. Contamination is found primarily in central Okalhoma in Permian formations where arsenic is found in iron oxide coatings and is desorbed under high pH. Arsenic contamination in Arkansas represented 8% of the wells and is found in alluvial aquifers in eastern Arkansas. Arsenic is associated with iron oxide coatings and is released by reductive dissolution of iron oxides. Arsenic contamination in Louisiana is limited.

Groundwater arsenic contamination is widespread in Texas. Approximately 6% of wells exceed the MCL of 10 ug/L. Contamination is focused in the southern High Plains (32% of wells exceed than the MCL) and the southwestern Gulf Coast (29% of wells exceed than the MCL).

Southern High Plains

The southern High Plains (SHP) was subdivided into two areas: a northern area (SHP-N) characterized by low total dissolved solids (TDS < 500 mg/L) and a southern area (SHP-S) characterized by high TDS (> 500 mg/L). Arsenic contamination is much greater in the SHP-S region (51% of wells > 10 ug/L) than in the SHP-N region (7% of wells > 10 ug/L). Regional analyses of groundwater arsenic concentrations do not support a surfical source of arsenic contamination. Arsenic concentrations are not correlated with land use, i.e. percent cultivated land within a 500 m buffer of each well. Correlations between arsenic concentrations and normalized county areas planted with cotton are low (r^2=0.09, SHP-S). Arsenic concentrations do not vary systematically with distance from cotton gins. Arsenic concentrations were not correlated with nitrate concentrations. Although arsenic concentrations decrease with increasing clay content throughout the southern High Plains, there is no systematic variation with clay content within the SHP-N and SHP-S regions. The lack of correlation between arsenic concentrations and water table depth does not support a surface source for arsenic. Arsenic concentrations do not correlate with aquifer saturated thickness.

Unsaturated zone studies were conducted to assess the potential for arsenical pesticides to provide a source of arsenic to groundwater. Results of drilling and sampling 18 boreholes in the

southern High Plains indicate that the distribution of arsenic is not related to the distribution of cotton production and application of arsenical pesticides. High arsenic concentrations in a rangeland profile (peak 77 ug/kg) indicate that background levels of water soluble arsenic are high in soils. Arsenic levels in cultivated areas are variable. Some profiles have highest arsenic levels near the surface which are correlated with nitrate and phosphate that may suggest a fertilizer or arsenical pesticide source. These data indicate that arsenic related to arsenical pesticides is probably restricted to the near surface zone. Other profiles have peak concentrations in the middle of the profile or at depth. Chloride profiles provide information on historical water flux conditions. High chloride concentrations at depth in many profiles in cultivated areas indicate low rates of water movement. It is unlikely that arsenical pesticides associated with cotton production would have reached the water table. The unsaturated zone data indicate a widespread source of water soluble arsenic in soils in the southern High Plains that may contribute to groundwater arsenic contamination.

Groundwater arsenic contamination occurs in generally oxidizing conditions in the High Plains and arsenic is expected to be in the form of arsenate. Groundwater arsenic concentrations were compared with concentrations of other ions to evaluate potential arsenic sources. Correlations between arsenic and other constituents (vanadium, r^2 0.65; fluoride r^2 0.30; molybdenum r^2 0.18; boron r^2 0.17; selenium r^2 0.14) suggest a geologic rather than an anthropogenic source. Arsenic concentrations are related to geologic units and are highest in the Ogallala aquifer and much lower in the Dockum aquifer. Arsenic concentrations in the Edwards Trinity (High Plains) aquifer are highest in the area where it is underlain by the Ogallala and much lower elsewhere. Potential sources of arsenic include volcanic ash beds in the Ogallala, black shales in the Cretaceous (Kiamichi Shale), and saline lakes. Analysis of existing geophysical logs indicates that high gamma zones, representative of volcanic ash beds, are restricted primarily to the southwestern area of the southern High Plains and are not collocated with most of the high groundwater arsenic concentrations. Arsenic concentrations are not related to distance from saline lakes, indicating this is not the only source of arsenic in the region. Additional studies will be required to assess geologic sources, including geophysical logging and stratified water sampling.

Southwestern Gulf Coast

Groundwater arsenic concentrations are much higher in the southwestern area of the Gulf Coast (29 percent of wells exceed the MCL) than elsewhere in the Gulf Coast (3.5 percent of wells exceed the MCL).

It is more difficult to evaluate surface sources of arsenic in the Gulf Coast than in the High Plains because aquifers in the Gulf Coast are confined except in the narrow outcrop areas. GIS analysis indicates that groundwater arsenic concentrations are not related to cotton production. Some counties with high levels of arsenic contamination do not have any cotton production (Live Oak and Duval Counties). Results of drilling and sampling 10 boreholes in the unsaturated zone indicate that arsenic concentrations are highest in a rangeland site where gin waste was ploughed into the field (1854 ug/kg at 1.3 m depth). Restriction of elevated arsenic related to gin waste to the upper ~ 2 m soil zone suggests that this is an unlikely source of groundwater arsenic. High chloride concentrations below the arsenic peak indicate that there is little water movement below this zone. High arsenic concentrations in the shallow subsurface and correlation with nitrate suggests fertilizer or arsenical pesticide sources for another profile. High arsenic concentrations were found throughout an irrigated profile. The remaining profiles had low arsenic levels (< 10 ug/kg) that showed no systematic variation with land use or with depth.

Redox conditions range from mildly oxidizing to reducing in the Gulf Coast. Although arsenic concentrations are not related to dissolved oxygen, high arsenic concentrations do not occur at low redox potentials ~ -100 mV). However, conditions are not reducing enough to immobilize arsenic in sulfides. High arsenic concentrations occur along the Rio Grande valley, in

the few counties west and southwest of Corpus Christi, and along the Catahoula Formation outcrop extending into the north eastern Gulf Coast. Correlations between arsenic and other constituents (vanadium, r^2 0.43; molybdenum r^2 0.36; boron r^2 0.12) suggest a geologic rather than an anthropogenic source. Arsenic concentrations are highest in the Jasper aquifer (48 percent > 10 ug/L) which immediately overlies the Catahoula Formation and are much less in younger stratigraphic aquifers (Evangeline aquifer; 21 percent > 10 ug/L and Chicot aquifer; 27 percent > 10 ug/L). Therefore, volcanic ashes associated with or reworked from the Catahoula Fm. are the most likely source of high arsenic concentrations in the southwestern Gulf Coast aquifer. Correlations between arsenic and other oxyanions typically associated with volcanism (molybdenum, vanadium) as well as the general decrease in arsenic contamination away from this formation strongly support this hypothesis.

This study represents an initial assessment of arsenic contamination in the southern High Plains and southwestern Gulf Coast and has resulted in a number of questions that may be addressed in future studies. The widespread distribution of water soluble arsenic in soils in both regions should be evaluated to determine if arsenic in rangeland and in deeper portions of cultivated profiles is related to volcanic ashes. Gamma logs should be conducted in boreholes to determine if there are high gamma levels that would indicate ashes. Water from leaching the soils should be analyzed for oxyanions and fluoride to assess relationships between soluble arsenic and these ions. Arsenic speciation should be conducted on selected samples to determine whether there are any organic arsenicals in the water. Playa water and saline lake water should be sampled to determine arsenic levels in these potential sources. Groundwater sampling should be conducted in different geologic units to assess potential correlations with arsenic contamination. Geophysical logging and multilevel sampling of groundwater should be conducted to determine if arsenic concentrations are stratified and if arsenic contamination can be linked to specific geologic units.

INTRODUCTION

The reduction in the arsenic Maximum Contaminant Level from 50 to 10 ug/L has resulted in widespread groundwater contamination with arsenic in the state. The objectives of this study were to determine the distribution of arsenic in Texas groundwater; assess the potential of past application of arsenical pesticides as a source of arsenic in groundwater in the Southern High Plains and Southern Gulf Coast; evaluate the role of phosphate fertilizers in mobilizing arsenic in areas of arsenical pesticide application and high groundwater arsenic concentrations; evaluate geologic sources of arsenic in Texas, and, target geographic areas of domestic drinking water wells potentially affected by high arsenic levels. To accomplish the above objectives, the following tasks were conducted:

Task A: Review of elevated arsenic concentrations (> 10 ug/L) in surrounding states and evaluation of research related to elevated arsenic (concentrations > 10 ppb) in groundwater nationwide.

Task B: Develop a quality assurance project plan for water quality and soil sampling and analyses

Task C: Evaluate potential anthropogenic sources of arsenic, such as arsenical pesticides in the Southern High Plains and the Southern Gulf Coast using GIS overlay analyses and soil sampling. The ability of phosphate fertilizers to mobilize arsenic from arsenical pesticide applications will also be evaluated where information on phosphate fertilizer application can be obtained.

Task D: Assess potential geologic sources of elevated arsenic concentrations in groundwater in Texas using relationships between arsenic concentrations and different geologic units. Relationships between arsenic concentrations and other ions, particularly oxyanions and uranium, were evaluated using existing databases to determine geologic rather than anthropogenic sources of arsenic. The impact of different redox conditions on the distribution of arsenic was also examined. Limited additional groundwater sampling was conducted in the southwestern Gulf Coast.

GENERAL BACKGROUND

On January 22, 2001 EPA adopted a new standard for arsenic in drinking water at 10 ug/L, replacing the old standard of 50 ug/L (Occupational Safety and Health Administration (OSHA) formally determined in 1978 that arsenic is a human carcinogen). The rule became effective on February 22, 2002. The date by which systems must comply with the new 10 ug/L standard is January 23, 2006. The health risks of inorganic arsenic in humans based on chronic exposure usually in drinking water include cancers and other effects. Studies have found the skin to be the area most susceptible to chronic arsenic exposure with skin lesions being common and the first indications of arsenic poisoning (Yoshida et al., 2004). Skin cancer effects from arsenic exposure include: hyperpigmentation, darkening of skin color usually occurring in patches, and keratosis, small raised warty lesions usually on the palms and soles (from a study in India by Mazumder et al., 1998), skin malignancies in Taiwan (Tseng et al., 1968 and Wu et al., 1989), and other skin lesions (in Chile by Borgono et al., 1977, Japan by Tsuda et al., 1995, Bangladesh by Tondel et al., 1999, and China by Guo et al., 2001). However, a study in the U.S. showed no relation between skin lesions and arsenic exposure for low (<0.40 mg/l) concentrations (Valentine et al., 1992). Lung cancer is also related to arsenic exposure as shown from studies in Taiwan (Chiou et al., 1995 and Wu et al., 1989), Japan (Tsuda et al., 1995), Argentina (Hopenhayn-Rich et al., 1998), and Chile (Smith et al., 1998). Bladder cancer is also related to arsenic exposure as shown by studies in Taiwan (Chiang et al., 1993, Guo et al., 1994, and Wu et al., 1989), Argentina (Hopenhayn-Rich et al., 1996), Finland (Kurttio et al., 1999) and Chile (Smith et al., 1998). However, studies with lower (0.5 - 160 ug/l; average of 5.0 ug/l) arsenic concentrations show no significant relationship with bladder cancer (US, Bates et al., 1995; Belgium (Buchet and Lison, 1998). In contrast, a study in Finland showed that bladder cancer can be caused by exposure to relatively low (1.0 ug/l) arsenic concentrations (Kurttio et al., 1999). Liver cancers in Japan (Tsuda et al., 1995) and Taiwan (Wu et al., 1989), kidney cancers in Argentina (Hopenhayn-Rich et al., 1998) and Taiwan (Wu et al., 1989) and urinary tract and uterine cancers in Japan (Tsuda et al., 1995), and prostate (in Taiwan Wu et al., 1989) have all shown relations to chronic arsenic exposure. Other effects of arsenic poisoning include: vascular disease including blackfoot (Chen et al., 1995; Lewis et al., 1999 in the U.S.; Chiou et al., 1997; Wu et al., 1989 in Taiwan), diabetes mellitus (Lai et al., 1994; Rahman et al., 1998 in Bangladesh) and hypertension, respiratory disease, and gastroenteritis (Rahman et al., 1999a, 1999b). Neurological effects have also been cited for effects of chronic arsenic exposure (Abernathy et al., 2003, Yoshida et al., 2004).

Arsenic is an element that occurs naturally in air, water, soil, and rocks. Arsenic minerals include realgar (AsS), orpiment (As_2S_3), arsenopyrite (FeAsS), and arsenian pyrite. The geochemistry of arsenic is dominated by the strong interaction of most arsenic compounds with soil particles, particularly iron oxides (and to a lesser degree aluminum and manganese oxides). The fully deprotonated arsenate AsO_4^{-3} is the expected form of arsenic in most soils under aerobic conditions only at high pH (Figure 1). At more neutral and acid pH's, the $HAsO_4^{-2}$ and $H_2AsO_4^-$ forms, respectively, are dominant. The general understanding of arsenic mobility in soil and aquifers is that it increases with increasing pH and phosphate concentration and with decreasing clay and iron oxide content. As pH increases, the negative charge of the arsenate ion increases making it less likely to sorb on negatively charged soil particles. Phosphates have a chemical structure similar to arsenates and sorb to soils more than arsenate in some conditions. Other structurally similar oxyanions, sulfate and selenate, are weak sorbers. Under less oxidizing conditions, arsenite H_3AsO_3 is most stable. The lack of charge renders this ion less likely to sorb to soil particles and more mobile. Its pH stability spread ranges from very acid to alkaline. Under even more reducing conditions, arsenide is the stable ionic form of arsenic. Arsenic metal –As(0)- rarely occurs. Methylated arsenic compounds are generally present at low aqueous concentrations (<1 ug/L), if at all, except maybe when there is an abundance of

organic matter (Welch et al., 2000). Methylated arsenic compounds are stable in both oxic and anoxic environments (Stollenwerk, 2003). As(V) and As(III) minerals are fairly soluble and do not control arsenic solubility in oxiding and mildly reducing conditions except maybe if barium is present (Henry et al., 1982a, p.21). In reducing conditions, As precipitates as arsenopyrite (FeAsS) but more commonly in solid solution with pyrite (arsenian pyrite).

Arsenic in groundwater can originate from anthropogenic or natural sources. Anthropogenic sources of arsenic include: industrial effluents (copper smelters), herbicides, insecticides, defoliants, animal feed amendment (promote growth), wood preservatives, and industrial wastes (glass production, paints, drugs, dyes, lead batteries, and metal alloys and semiconductors (Lederer and Fensterheim, 1983; Loebenstein, 1994). Agricultural usages were dominant until ~1980 when wood preservatives became the main avenue for arsenic consumption. Inorganic arsenic has been used in a wide variety of agricultural practices. Lead arsenate ($PbHAsO_4$) was used as the main insecticide in fruit orchards prior to the use of DDT (DichloroDiphenylTrichloroethane) in the late 1940s (Shepard, 1951) and resulted in soil contamination (100 mg/kg As in soil) in Washington (Davenport and Peryea, 1991; Welch, 2000). Background arsenic in soil is < 10 mg/kg (Wauchope, 1983; Shacklette and Borengen, 1984). Adsorption generally restricts downward movement of arsenical pesticides; however, phosphate fertilizer has been found to mobilize arsenical pesticides to greater depths (Peryea, 1991; Peryea and Kammereck, 1997). Although elevated groundwater arsenic concentrations are associated with the use of arsenical pesticides in many areas (Hudak, 2000), studies indicate that groundwater contamination in some of these areas is related to natural geologic sources rather than anthropogenic sources (Carter et al., 1998). High arsenic concentrations in groundwater in the southern High Plains in Texas have been attributed to cotton gin waste (Aurelius, 1988). Arsenic is also used as a feed amendment for poultry and swine; however, little information is available on the fate of arsenic from this process (Welch, 2000). Elevated arsenic concentrations are also found in many contaminated sites. Arsenic is the contaminant of concern in ~ 30 percent of 1191 Superfund Sites (Welch, 2000). Disposal sites can result in locally very high concentrations of arsenic in groundwater (e.g. <2.5 g/L in Texas; Welch, 2000). Plants producing arsenical pesticides often have locally high arsenic concentrations. Studies associated with arsenic contamination from smelter emissions indicate that contamination is restricted to the soil zone (e.g. Tacoma Smelter Plume, Washington). In addition to providing a source of arsenic, anthropogenic activities may also release arsenic from natural sources. For example, organic carbon leaching from a landfill site in Maine resulted in release of arsenic from iron oxyhydroxides through reductive dissolution (Stollenwerk and Colman, 2003).

Natural sources of arsenic include (Welch et al., 2000): geothermal waters (T ≥50°C), iron oxides, sulfide minerals, and evapotranspirative concentration. The sources of arsenic in groundwater in the US have been summarized by Welch (2000). The dominant cause of widespread high groundwater arsenic concentrations (> 10 ug/L) in the US is release from iron oxides, particularly in Arizona (Robertson, 1989), South Dakota (Carter et al., 1998) and Minnesota (Kanivetsky, 2000). Sulfide sources predominate in New England, Michigan, Illinois, and Wisconsin (Ayotte et al., 2003; Schreiber et al., 2000, 2003). Geothermal sources are important in California and Wyoming (Ball et al., 1998; Wilkie and Hering, 1998). Evapotranspiration is listed as an important process in generating groundwater with high arsenic concentrations in arid regions of California and Nevada (Swartz et al., 1996; Welch and Lico, 1998). The natural arsenic content in soils varies with the composition of the parent material and could be as high as 20 to 30 mg/kg but averages 5 – 6 mg/kg (Yan-Chu, 1994). Arsenic concentrations vary among rock types (1.8 ppm, igneous, 1.0 ppm, sandstone; 9 ppm, shale; and 1.8 ppm, carbonate) (Hem, 1985; table 10). Most is sorbed to soil particles because of the strong attraction between positively charged arsenate and generally negatively charged soil particles.

Major sources of arsenic and processes releasing arsenic to groundwater were summarized by Smedley and Kinniburgh (2002) (Table 1). The processes include mixing of upwelling geothermal water with shallow groundwater, reductive desorption and dissolution of iron oxides in reducing environments and desorption from iron oxides in oxidizing environments, and pyrite oxidation. The most widespread process resulting in elevated groundwater arsenic concentrations is dissolution or desorption of arsenic from iron oxyhydroxides under reducing conditions. Extremely widespread high arsenic concentrations in Bangladesh are attributed to this process. Reducing conditions in this area are attributed to rapid burial of young sediments. Dissolution or desorption of iron oxyhydroxides is also the dominant process resulting in mobilizing arsenic in groundwater in the US (Welch et al., 2000). Desorption of arsenic under oxidizing conditions generally occurs under high pH. Dissolution of sulfide minerals is also an important process for releasing arsenic and occurs in New England, Michigan, Illinois, and the central valley in California (Welch, 2000). Various lines of evidence are used to distinguish different processes releasing arsenic to groundwater, including source location in geologic units, relationships among different ions, and pH and Eh conditions.

Task A: Review

Subtask A1: Review Elevated Arsenic Concentrations (>10 ppb) in Groundwater in Surrounding States

Many of the states surrounding Texas, including New Mexico, Oklahoma, Arkansas, and Louisiana, have a significant number of freshwater aquifer wells that produce water with arsenic concentrations that exceed the new EPA national standard of 10 ug/L. The following summarizes the status of arsenic contamination in surrounding states (Figure 4 and Figure 5), including the most likely sources of arsenic and processes affecting arsenic concentrations.

A1-1 New Mexico

Data Source: United States Geological Survey (USGS) National Water Information System (NWIS) database; National Uranium Resource Evaluation (NURE) database; New Mexico Bureau of Geology and Mineral Resources

Range of arsenic concentrations: <0.1 to 1,100 ug/L (1,100 groundwater wells analyzed)

784 wells (70.6%) had arsenic concentrations <5 ug/L

326 wells (29.4%) had arsenic concentrations ≥5 ug/L

180 wells (16.2%) had arsenic concentrations >10 ug/L

Aquifers:

Middle Rio Grande Basin:

Recent (post-Santa Fe Group) flood-plain, channel, and basin-fill deposition of Pleistocene – Holocene age.

Santa Fe Group: unconsolidated – moderately consolidated basin-fill sediments (Oligocene–middle Pleistocene age) (≤40 m thick)

Sources of arsenic:

Middle Rio Grande Basin
Silicic volcanic rocks in the Jemez Mountains that have had contact with geothermal water (north of Albuquerque)
Deep (thousands of feet) mineralized groundwater mixing with shallow groundwater. Upwelling occurs along faults. This source is supported by correlations between arsenic and chloride, SO_4, Na, Ba, and ^{14}C age.

Socorro Basin: Thermal springs

Geochemical Controls on Arsenic Mobilization (Middle Rio Grande Basin):

Reductive dissolution of iron oxides is an unlikely source of arsenic because the aquifer is predominantly oxidizing as shown by the presence of dissolved oxygen and nitrate. In Albuquerque As is present as As(V) in 90% of public water supply wells sampled.

Dissolution of sulfide minerals is not a likely source of arsenic because sulfides are not common in the Santa Fe Group aquifer (Stanton et al., 2001).

Desorption of As from Iron Oxyhydroxides under high pH may cause high As concentrations west of Albuquerque. Arsenic concentrations <20 ug/L have pH values <8.5, whereas As concentrations ≥20 ug/L have pH values ≥8.5.

References: Bexfield (2002), Bexfield et al. (2003), Brandvold (1999), Brandvold (2001), and Brandvold (2002).

A1-2 Oklahoma

Data Source: United States Geological Survey (USGS) National Water Information System (NWIS) database; National Uranium Resource Evaluation (NURE) database; Association of Central Oklahoma Governments (ACOG)

Range of arsenic concentrations: <0.5 to 4,000 ug/L (5,299 groundwater wells analyzed)

4,715 wells (89.0%) had arsenic concentrations < 5 ug/L

584 wells (11.0%) had arsenic concentrations ≥ 5 ug/L

268 wells (5.1%) had arsenic concentrations > 10 ug/L

Aquifers:

Central Oklahoma Aquifer:
Alluvium and terrace deposits (Quaternary age) along streams (0 – 30 m thick).

Garber Sandstone and Wellington Formation of Permian age fine-grained sandstone interbedded with siltstone and mudstone (355 – 490 m thick).

Chase, Council Grove, and Admire Groups Permian-age fine-grained sandstone, shale, and thin limestone (170 – 290 m thick).

The Permian units dip to the west and become confined by the Hennessey Group in the west.

Sources of arsenic:

Central Oklahoma Aquifer
Red iron oxide grain coatings (high As, Cr, Se, and U)
Yellow-brown goethite-cemented sandstone (high As)

Geochemical Controls on Arsenic Mobilization (Central Oklahoma Aquifer):

Oxidizing redox conditions required to mobilize As and other elements (> 1 mg/L DO). Arsenic, Cr, and Se desorb from iron oxide coatings of mineral grains at higher pH; dissolved concentrations increase with increased pH.

References: Christenson and Havens (1998), Christenson et al. (1998), Mosier (1998), and Schlottmann et al. (1998).

A1-3 Arkansas

Data Source: United States Geological Survey (USGS) National Water Information System (NWIS) database; Arkansas Department of Environmental Quality

Range of arsenic concentrations: <0.5 to 80 ug/L (515 groundwater wells analyzed)

440 wells (85.4%) had arsenic concentrations < 5 ug/L

75 wells (14.6%) had arsenic concentrations ≥ 5 ug/L

42 wells (8.2%) had arsenic concentrations > 10 ug/L

Aquifers:

Alluvial Aquifer of Eastern Arkansas (Bayou Bartholomew Watershed)

Upland terrace deposits and flat-lying delta deposits.

Arsenic concentrations exceeded MCL in 21 of 118 wells sampled. All high arsenic concentrations were in the delta portion of the watershed.

Sources of arsenic:

Iron oxides coatings in the delta deposits

Geochemical Controls on Arsenic Mobilization:

Reductive dissolution of iron oxides is the most likely release mechanism for arsenic. Low arsenic concentrations in water with TDS ≤175 mg/L; elevated As, Fe, Mn, total phosphorus, and low NO_3 in water with TDS ≥175 and ≤ 350 mg/L.

High TOC indicates that carbon as organic carbon is available and is reduced along the flow path (TDS ≥175 mg/L). Development of reducing conditions results in release of As from iron or manganese oxyhydroxides (FeOOH, MnOOH), along with Fe and Mn. At higher TDS (≥ 350 mg/L), As concentrations decrease and the decrease is attributed to mixing with low-As water or precipitation with As containing Fe sulfides.

References: Kresse and Fazio (2003)

A1-4 Louisiana

Data Source: United States Geological Survey (USGS) National Water Information System (NWIS) database

Range of arsenic concentrations: <0.5 to 200 ug/L (428 groundwater wells analyzed)

410 wells (95.8%) had arsenic concentrations < 5 ug/L
18 wells (4.2%) had arsenic concentrations ≥ 5 ug/L
11 wells (2.6%) had arsenic concentrations > 10 ug/L

Information on sources and distribution of elevated arsenic in groundwater in Louisiana is limited. A local source from cattle dips is cited in Cow Island.

Subtask A2: Evaluate Research Related to Elevated Arsenic in Groundwater Conducted by EPA, the U.S. Geological Survey, and Other Agencies that is Relevant to Texas

Groundwater arsenic contamination is widely distributed throughout the United States, particularly in the western United States. The new EPA Maximum Contaminant Level of 10 ug/L has resulted in many public water supply systems not being in compliance with the regulations. A survey of ~ 30,000 arsenic analyses in groundwater indicated that about 10% exceeded 10 ug/L (Welch et al., 2000). Known sources of arsenic in the United States include iron oxide coatings, sulfide minerals, geothermal waters, and evaporite deposits. Processes releasing arsenic include dissolution or desorption of iron oxides under reducing conditions or desorption under high pH under oxidizing conditions. Pyrite oxidation can also release arsenic into groundwater. Understanding the sources and release mechanisms for arsenic in groundwater will provide valuable information to water managers to modify existing water supplies or develop alternative water supplies that comply with the new EPA arsenic regulations.

A2-1 Distribution of Elevated Arsenic in the United States

Elevated arsenic concentrations in groundwater are widely distributed within the United States, particularly in the western United States, the Great Lakes region, and New England (Ryker, 2001; 2003). Various approaches have been used to show the arsenic distribution in groundwater, including point data and percentiles, to evaluate the degree to which various populations would be impacted by the new EPA regulations. The 75th percentile of arsenic concentration per county (calculated for counties having at least five wells) is shown in Figure 2 and indicates widespread arsenic contamination throughout the western United States, Great Lakes region, and New England.

A2-2 Research Related to Groundwater Arsenic Contamination

Intensive research is being conducted related to arsenic contamination in groundwater in the US and globally. Most research is related to source attribution, mobilization processes, treatment options and other topics. Within the US, widespread research is conducted by

government agencies such as the USGS and EPA and many other groups. The USGS has formed an arsenic studies group (http://wwwbrr.cr.usgs.gov/Arsenic/). Reviews of the status of arsenic contamination have been conducted by USGS researchers (Welch et al., 2000; Welch and Stollenwerk, 2000). The USGS has conducted arsenic studies in many states throughout the US, including California (Fuji and Swain, 1995), Nevada (Welch and Lico, 1998); Dakota (Berkas and Komar, 1996), Oklahoma (Schlottmann et al., 1998), New Mexico (Bexfield et al., 2003), and New Jersey (Ayotte et al., 2003). The general approaches used by USGS researchers in evaluating arsenic contamination ranges form reconnaissance mapping, relating arsenic to geologic or anthropogenic sources, and evaluation of mobilization mechanisms. Borehole geophysical applications related to arsenic studies are described in Paillet and Williams (2001). Detailed core sampling, X-ray diffraction analyses, sequential leaching, and arsenic speciation studies were conducted on core from the Middle Rio Grande Basin to understand the source and mobilization mechanisms related to arsenic contamination at this site (Stanton et al., 2001; Stanton and Cole, 2002). Assessing vertical stratification of arsenic concentrations in groundwater is being evaluated using depth dependent sampling techniques in production wells (Izbicki et al., 1999). Groundwater velocity distributions have been determined using dye tracing techniques to determine flow contributions from different depths. Depth dependent sampling and dye tracing are used to isolate zones with high arsenic in California and Oklahoma (Izbicki and Christenson, pers. comm. 2004). Once elevated groundwater arsenic concentrations have been determined, they may be related to particular geologic sources through geophysics and evaluation of cores and cuttings. This approach to determining vertical stratification of arsenic concentrations is of particular interest to groundwater managers because it may allow them to isolate sources and reduce groundwater arsenic contamination without the need for costly treatment options.

Research at EPA covers a wide range of topics including drinking water standards, exposure research, risk assement, remediation, and treatment technologies. A total of $20 million was pledged for research and development of more cost effective technologies and technical assistance and training to operators of small systems to reduce compliance costs (http://www.epa.gov/ORD/NRMRL/arsenic/). Research topics included cost evaluation of arsenic control technologies, studies to modify treatment methods to reduce residuals, and verification testing of package drinking water treatment technologies for small systems.

Task A: Conclusions

The above analysis of elevated arsenic concentrations in states surrounding Texas provides an indication of the level of arsenic contamination, the dominant sources of arsenic, and the primary mechanisms releasing arsenic to groundwater. This information is useful for assessing sources and distribution of arsenic in groundwater in Texas.

The status of current understanding of sources and mobilization mechanisms of elevated arsenic in groundwater provides valuable background information for assessing elevated arsenic concentrations in Texas aquifers. The results of the analyses indicate that the dominant sources of arsenic in the US include iron oxide coatings, sulfide minerals, geothermal waters, and evaporite deposits. The dominant mechanisms releasing arsenic to groundwater in the U.S. include dissolution or desorption of iron oxides under reducing or oxidizing conditions. Pyrite oxidation can also release arsenic into groundwater. Understanding the sources and release mechanisms for arsenic in groundwater is essential for predicting the distribution of elevated arsenic in groundwater in Texas.

Task B: Quality Assurance Project Plan (QAPP) for Water Quality and Soil Sampling and Analyses

A Quality Assurance Project Plan (QAPP) was approved on May 16, 2005 to govern the collection of samples in the field, and analysis of samples in the lab by the Lower Colorado River Authority (LCRA). In accordance with the QAPP, The Bureau of Economic Geology (BEG) conducted soil core collection in the field, core processing, and water extraction for total dissolved arsenic and anion analysis. Collection of soil cores began in the Southern High Plains on May 22, 2005 and continued through June 4, 2005. During this time, 18 soil cores were collected. Collection of soil cores began in the Southwestern Gulf Coast on June 15, 2005 and continued through June 22, 2005. During this time, 10 soil cores were collected. Soil cores were processed, and water extracts were prepared at the UT BEG Core Research Facility in Austin, TX from June 22, 2005 through July 19, 2005.

Soil samples and water extracts were sent to the LCRA for analysis. LCRA analyzed the water extract for total dissolved arsenic using EPA Method 200.8 (ICP-MS). Soil samples were digested by the LCRA and analyzed for total (acid leachable) arsenic using EPA Method 6020 rev. 0. Analytical reports were provided as MS Excel spreadsheets, and formal reports were provided as pdf files. All standard operating procedures (SOPs) used by LCRA were included in the QAPP.

The QAPP was then amended on June 15, 2005 to include The University of Texas at Austin, Environmental and Water Resources Engineering Program (UT-EWRE) in the Civil Engineering Department. The first samples analyzed by UT-EWRE were sent on June 27, 2005. UT EWRE analyzed water extracts prepared by UT BEG for anions by ion chromatograph (IC) according to EPA Method 300.0. Water extracts were analyzed for dissolved arsenic by graphite furnace atomic absorption spectroscopy (GFAA) according to EPA Method 300.0. A refined analysis was also conducted on selected water extracts for dissolved arsenic using hydride generating graphite furnace atomic absorption spectroscopy (HG-GFAA), to achieve lower detection limits. HG-GFAA was based on EPA Method 300.0 and the work of Korte and Fernando (1991). All SOPs used by UT were included in the QAPP as amended on June 15, 2005.

Task C: Evaluation of Potential Anthropogenic Sources of Arsenic in the Southern High Plains and Southwestern Gulf Coast Regions

There are several potential anthropogenic sources of arsenic in the High Plains and Gulf Coast. These two areas were chosen for study because they show high arsenic aqueous concentrations relative to the rest of Texas (Figure 6). Both regions have almost a century-old tradition of cotton growing. The cotton industry used arsenical products as pesticides (first half of 20th century), harvest-aid desiccants (from late 50's to late 80's in High Plains), and currently organo-arsenicals (particularly in the Gulf Coast region). Related activities, such as waste piles near cotton gins or on fields, gin waste spread on fields, or gin waste used for winterizing wells, can also lead to contamination, as well as atmospheric deposition when gin wastes were burned. There is also anecdotal evidence that isolated arsenic contamination cases may include old cattle dipping pits, especially within the Chicot aquifer in Kenedy County (Vickers, pers. comm., 2005).

Other anthropogenic sources of arsenic are also possible. Phosphate fertilizers, in addition to possibly mobilizing arsenic, can also contain arsenic because of their similar chemistry (Campos, 2002). Arsenic concentration in synthetic and natural phosphate fertilizers can be as high as 13 mg/kg. Campos (2002) argued that arsenic traces in overused fertilizers were sufficient to increase aqueous arsenic concentrations to more than 100 ug/L in Brazil. Direct anthropogenic contamination by oil field brines is unlikely except locally. Contamination by uranium mining in south Texas will be addressed under Task D. This section devoted to Task C will exclusively deal with arsenic related to cotton industry.

Subtask C1: Compilation of Arsenic Data from Existing Sources (TWDB, TCEQ, NURE, USGS) for Domestic and Public Water Supply Systems.

C1-1 Description of Data Sources

Arsenic concentrations in groundwater were compiled from the following databases:

1) Texas Water Development Board (TWDB) database available at http://www.twdb.state.tx.us/DATA/waterwell/well_info.asp
2) Texas Commission on Environmental Quality (TCEQ) Public Water System (PWS) database not publicly available (http://www.tceq.state.tx.us/)
3) National Uranium Resource Evaluation (NURE) database available for the State of Texas at http://pubs.usgs.gov/of/1997/ofr-97-0492/state/nure_tx.htm
4) U.S. Geological Survey (USGS) National Water Information System (NWIS) database available at: http://waterdata.usgs.gov/nwis/
5) Miscellaneous small databases

The Texas Water Development Board conducts ambient groundwater monitoring. All the major and selected minor aquifers are sampled on a 5-yr rotating basis. Water quality data are available for 55,000 ground-water sites (wells, springs), resulting in a total of 104,000 analyses, each analysis being done for major anions and cations. The earliest water chemistry data available is from the late 19th century. Groundwater quality information includes state well number, date of sampling event, time, collection remarks, reliability of sampling method remarks, collecting agency, indication of whether the sample is balanced or unbalanced, lab-calculated pH, phenol and total alkalinity, hardness, specific conductance, sodium adsorption ratio (SAR), total dissolved solids, and major anions and cations (Ca, Mg, K, Na, Sr, SO_4^{-2}, HCO_3^{-1}, CO_3^{-2}, Cl^{-1}, F^{-1}, NO_3^{-1}, SiO_2). In some instances, analyses are performed for infrequent constituents (metals), organics, nutrients, and radioactive constituents. Approximately 500,000 infrequent constituent analyses (each corresponding to one single constituent) have been

entered in the database. Additional well information is provided in the database, including well depth, main aquifer, and groundwater level. The TWDB database includes some but not all the water quality data in the USGS database. The database is provided as a Microsoft Access file and can be downloaded from the TWDB website.

The TCEQ PWS database includes water quality data for all public water systems in the state. Water sources of public water systems include surface water, groundwater, and/or mixed sources. Water chemistry data in the PWS database represent the water entry points, which may represent a blend of groundwater from different wells, or groundwater and surface water, or surface water. For this study, we are only interested in raw groundwater chemistry data; therefore, we selected water quality samples that can be associated with a single well and included raw and entry point data. The database obtained from TCEQ is a subset of the larger PWS database that includes only inorganic chemical constituents of concern, including arsenic. The list of constituents in this modified database: specific conductance, TDS, alkalinity, total hardness, pH, Al, An, Be, N, NH_3, As, Ba, Ca, Cd, Cl, Cr, Cu, Fl, Fe, Pb, Mg, Mn, Hg, Ni, NO_3, NO_2, K, Se, Ag, Na, SO_4, Th, Zn, gross alpha, U, Rd, radium 226 and radium 228, gross beta, tritium, gross alpha, and Sr90. Additional well information in the database includes well depth, screened interval, aquifer designation, and geology. Well depth is available for most of the wells, but screen depth and geologic descriptions are not available for all the wells in the database. TCEQ PWS has limited spatial coverage because it excludes rural areas. The database is provided as a Microsoft Access file.

The National Uranium Resource Evaluation (NURE) database hydrogeochemical and stream sediment reconnaissance includes data from stream sediments, soils, groundwater, and surface water over the entire United States. The reconnaissance survey began in 1975 and ended in 1980 under the responsibility of four DOE national laboratories: Lawrence Livermore National Laboratory (LLNL), Los Alamos National Laboratory (LANL), Oak Ridge Gaseous Diffusion Plant (ORGDP), and Savannah River Laboratory (SRL) (Smith, 2001; USGS, 2004). The purpose of the program was to explore for undiscovered uranium. This database provides chemical data for Ag, Al, As, Au, B, Ba, Be, Bi, Br, Ca, Cd, Ce, Cl-, Co, Cr, Cs, Cu, Cy, Eu, F, Fe, Ga, He, Hf, Hg, K, La, Li, Lu, Mg, Mn, Mo, Na, Nb, Ni, P, Pb, Pt, Rb, Sb, Sc, Se, Si, Sm, Sn, Sr, Ta, Tb, Th, Ti, U, V, W, Y, Yb, Zn, Zr, PO_4 (phosphate), NO_3 (nitrate), SO_4 (sulfate), methane, ethane, propane, and butane in samples of stream sediment, spring sediment, lake or pond sediment, soil, rock, well water, stream water, and spring water. In addition, the database provides location and descriptive information for each sample. The NURE database covers only the eastern half of the southern High Plains, and there were gaps in the southwestern Gulf Coast as well. The database is provided as text files that were consolidated and imported into Microsoft Access and Excel.

The USGS database includes water quality data for selected areas of Texas, mostly in the Houston area. It contains data on major ions and trace metals, as well as additional well information. The database is provided as downloadable text files. A report recently published on perchlorate in the High Plains by Texas Tech University (Jackson et al., 2004) contains approximately an additional 40 arsenic analyses from private wells.

Geophysical logs were also obtained from the Geophysical Log Facility (GLF) at the Bureau of Economic Geology (BEG). The GLF is a repository for geophysical data received from private donations, BEG research projects, and the Railroad Commission of Texas (RRC), which by law receives a copy of geophysical logs from every new, deepened, or plugged well drilled in Texas. These data are available for public viewing and copying, and include wireline electric logs, well records, and scout tickets from hundreds of thousands of wells located in Texas.

C1-2 Database Analysis

In the High Plains study area, the main aquifers are the Ogallala aquifer and the underlying Edwards Trinity (High Plains) aquifer. These aquifers are sometimes difficult to differentiate and are often grouped as the High Plains aquifer where they are thought to be hydraulically connected. In addition, because individual wells can be screened in both aquifers, water quality samples may carry mixed signatures. We examined and analyzed data from the NURE and TWDB databases, as well as the TCEQ PWS, USGS, and Texas Tech databases. Typically, only the most recent analysis was used. Some wells were sampled multiple times within the past 15 years; one well has time series of five samples, and 23 wells have time series of four samples. The limited data available on temporal trends suggest that there is no systematic variation in arsenic concentrations over time (Figure 7a).

The lack of aquifer data for the NURE database is more of an issue for the southwestern Gulf Coast samples than the High Plains samples because the Gulf Coast comprises multiple aquifers. Aquifer subunits of the Gulf Coast aquifers are, from oldest to youngest, the Jasper, Evangeline, and Chicot aquifers. It is sometimes difficult to reconcile well depth and aquifer. The TWDB has a list of seven- to eight-character aquifer codes for most of the water-bearing units in Texas (Nordstrom and Quincy, 1999). These codes were defined using either rock- or hydro-stratigraphic unit names. Of the wells sampled for arsenic by TWDB, each of the three aquifer subunits of the Gulf Coast aquifer (Jasper, Evangeline, and Chicot) contains as many as eight different aquifer codes. Geologic and hydrologic units that compose the Gulf Coast aquifer vary in name and character and are not consistently identified from one area to another. For example, two wells near La Gloria, Texas, in Starr County that were drilled one year apart, have the same total depth, and are separated horizontally by only 50 m. One of the wells has an aquifer designation 122OKVL (Oakville), which is in the Jasper aquifer, whereas the other well is labeled 121EVGL, which is in the Evangeline aquifer. Even with this degree of variability in aquifer code assignment to wells, there are clear trends between arsenic concentration in wells in the Gulf Coast and aquifer unit.

Data were analyzed without consideration for the specific aquifer within the Gulf Coast or by subdividing the database into three units corresponding to the three main Gulf Coast aquifers. In the latter case, wells designated as Gulf Coast Aquifer were excluded. All wells in Jackson County, for which there are TWDB infrequently analyzed constituents, have been given the undifferentiated Gulf Coast Aquifer designation are not included in plots discriminating among units. Wells identified as being completed in the Fleming Fm. were also excluded because this unit is lumped with the Oakville rock stratigraphic unit and included in either the Jasper or Evangeline aquifers in south Texas. In northeast Texas the Fleming Fm. is included in the Jasper aquifer, the Burkeville confining unit, or the Evangeline aquifer. Eight of the nine samples analyzed for arsenic in wells with the 122FLMG (Fleming) aquifer code were below detection limits, so excluding this unit does not affect the statistics to be presented later. The conventional hydrostratigraphic unit defined for the Catahoula Fm. is the Catahoula confining system (Baker, 1979). However, in the southwestern Gulf Coast there are numerous domestic and public water supply wells completed in a unit with the TWDB aquifer code designation 122CTHL. These wells were included in the Jasper aquifer subunit of the Gulf Coast aquifers. Also excluded from the well statistics by layers are wells completed in both the Chicot and Evangeline aquifers.

Analysis of Gulf Coast data focused on the most recent samples. Wells were sampled multiple times during the past 15 years. Only wells with most of the samples >10μg were retained. One well was sampled 13 times, 26 wells were sampled 5 times, and 100 wells were sampled at least 4 times. There is no systematic trend in the time series data (Figure 7b).

Detection limits are variable. The TWDB database, for arsenic data, listed detection limits include 0.5, 1, 1.5, 2, 4, 5, 10, or even 20 ug/L in a few instances. The NURE database has

more consistent detection limit at 1 or 0.5 ug/L. An analysis of variance revealed that both TWDB and NURE databases (data above detection limits) in the southwestern Gulf Coast belong to the same population at a 5% significance level. The lack of coverage of the NURE database in the southern High Plains precludes such an analysis.

C1-3 Spatial Distribution of Arsenic

Groundwater arsenic concentrations in Texas are highest in the southern High Plains and southwestern Gulf Coast (Figure 6). The map of arsenic concentrations is mainly based on data from the TWDB database because this database includes water quality from many of the TCEQ PWS wells and from the USGS NWIS database. The NURE database consists of samples from an earlier time period (1976 to 1980) and was only used in this report for analytes where little or no information was available from other databases.

The most striking feature of arsenic distribution in the southern High Plains is the contrast in groundwater concentrations between the northern and southern sections of this aquifer. Arsenic concentrations are much higher in an area south and east of a line that extends from Lubbock, Texas, to Clovis, New Mexico. The limit between the northern and southern sections of the southern High Plains was operationally defined as the 500 mg/L TDS line. Approximately 50 percent of the 609 samples in the southern section sampled during the past five years exceed the EPA recommended maximum contaminant level (MCL) of 10 ug/L (~2 percent > 50 ug/L), whereas the percentage of samples exceeding the MCL in the northern section is 7% (Figure 9, Table 2). Only 20 percent of samples exceed the MCL throughout the High Plains in the Texas Panhandle. The area of high arsenic concentrations generally coincides with high total dissolved solids.

Similarly to the High Plains aquifer, the Gulf Coast aquifers offer a contrast in arsenic concentration between the southwestern and northeastern sections. Throughout much of the report, these two sections are compared. The contrast is more diffuse than that in the High Plains and broadly corresponds to the geologic feature called the San Marcos Arch (see geology section). The southwestern section of the Gulf Coast aquifer is operationally defined as limited by and including De Witt, Victoria, and Calhoun counties. Approximately 13 percent of the 1,120 samples in the Gulf Coast aquifer sampled during the past five years have arsenic concentrations > 10 ug/L (2.1 percent > 50 ug/L) (Figure 9, Table 3). Arsenic concentrations were greater in the southwestern Gulf Coast (29 percent > 10 ug/L; 6 percent > 50 ug/L) than in the northeastern Gulf Coast (3.5 percent > 10 ug/ and none > 50 ug/L).

Subtask C2. Evaluation of Arsenical Pesticides for Cotton Production as a Potential Source of Groundwater Arsenic

In the High Plains, groundwater arsenic contamination has been attributed to arsenical product application on cotton (Hudak, 2000; Welch et al., 2000; Nativ, 1988, p.43; Nativ and Guttierez, 1988, p.14; Lee, 2005), particularly in areas of shallow groundwater. Hudak (2000) suggested that arsenic contamination is of anthropogenic origin in selected counties in the High Plains. He based his conclusion on the following:

- higher arsenic levels in areas of shallower water table depths,
- presence of other agricultural chemicals in groundwater (such as nitrate),
- downward cross-formational flow eliminating deep sources of arsenic,
- and low dissolved arsenic concentrations in potentially arsenic-rich horizons in deeper formations (e.g., Dockum Fm.).

Nativ (1988) and Nativ and Guttierez (1988) attributed the source to arsenical products on the basis of a general spatial relationship between high groundwater arsenic concentrations, shallow water table depths, and use of arsenical pesticides. Lee (2005) observed, using kriging techniques, that areas having the most arsenic lack higher concentrations in other oxyanions and concluded that in the High Plains the origin of the arsenic contamination must be anthropogenic. Welch et al. (2000) also noted the general spatial overlap between high groundwater arsenic concentrations in the United States and use of arsenical pesticides. In the Gulf Coast aquifer, arsenic contamination has generally been attributed to abundant volcanic ash fall or reworked volcanic material and possibly the presence of a uranium mining province.

C2-1 Arsenic as an Industrial Product

Nearly all of the world's supply of arsenic has been and is recovered as a byproduct of copper, lead, and zinc production. Most of the arsenic currently consumed in the United States is imported. Since the mid-1920's arsenic consumption has mostly oscillated between 15,000 and 30,000 metric tons per year (Figure 10). The U.S. production, concentrated in the western states, essentially ended in 1985 because of the high cost required to reduce atmospheric emissions to meet environmental regulations (Loebenstein, 1994). OSHA formally determined in 1978 that arsenic is a human carcinogen. Smelters released arsenic both locally in tailings and other waste dumps and also in the atmosphere. Those releases are not believed to have impacted Texas, although the Asarco smelter operating in El Paso produced arsenic for sale from 1938 to 1949 (Loebenstein, 1994).

Over the last 100 years, arsenic compounds have had several major industrial uses (Table 4) as a component of animal feed (to promote growth), herbicides, pesticides, lead batteries, metal alloys, semiconductors, wood preservatives, and glass manufacturing (Loebenstein, 1994; Lederer and Fensterheim, 1983). Agricultural usages were dominant until ~1980, when wood preservatives became the main avenue for arsenic consumption (Figure 10). Table 5 shows a rough timeline of arsenic usage. Arsenic trioxide [As_2O_3], or white arsenic, is the most common base product for arsenic derivatives. It has a valence of 3, whereas most of its commercial derivatives have a valence of 5. Inorganic arsenical products, such as lead or calcium arsenate or sodium arsenite, were used as herbicides and insecticides in the first half of the 20th century and until they were banned by EPA in 1988 for such usage. Calcium arsenate was specifically used to fight a cotton pest, the boll weevil. Sodium arsenite was used in sheep and cattle dips. Another inorganic arsenical product, arsenic acid, was massively used as a desiccant in Texas from ~1965 to 1992, when it was banned by EPA. Beginning in 1977 and still in use today (<1,000 tons elemental As consumed in the U.S.), organo-arsenical compounds such as monosodium methyl arsonate (MSMA), disodium methyl arsonate (DSMA), and

cacodylic acid have been used as herbicides. MSMA represents the bulk of organo-arsenical compounds used in the cotton industry.

C.2-2 Arsenic Use in the Cotton Industry

The historical centers of cotton production in Texas are the Blackland Prairie of central and east Texas, where cotton production exploded after the Civil War. A major shift in cotton production occurred at the beginning of the 20th century when irrigation techniques made cotton growth possible in north and west Texas and in south Texas. In the past three decades between 20 and 30 percent of the total land surface in the southern High Plains has been dedicated to cotton, of which ~50 percent is irrigated.

A cotton production cycle (Table 6) starts with preparation measures including spraying of herbicides at the end of the winter to control weed growth. It is followed by further pre-plant steps such as application of herbicides and pesticides, irrigation, if appropriate, and treatment with a fertilizer. In April/May, planting occurs, followed by a new application of herbicides to control weed species growing alongside cotton and by fertilizer treatment to support growth. Later in the season, insecticides are also applied. Both irrigation and precipitation events fall mainly in the May-to-September time range (Figure 11 and Figure 12). Harvest-aid products (boll-openers, defoliants, and desiccants) are applied in late summer/fall to facilitate harvesting. The operational details of the harvest depend on the cotton variety and climate. Cotton from taller varieties is machine-picked after being treated with a defoliant (e.g., thidiazuron, dimethipin), whereas shorter varieties, usually grown in dry plains of Texas and Oklahoma, are machine-stripped and treated with desiccants (previously, arsenic acid; currently, organic desiccants, e.g., paraquat). Machine stripping collects more plant material that is dropped to the ground after processing, whereas machine picking is more discriminatory and leaves plants erect (EPA, 2005). Harvesting is done from mid/late summer in the southwestern Gulf Coast to late fall in the northern Panhandle (EPA, 2005). Table 6 presents a basic picture of cotton agricultural practices. Many variations, depending on climate (temperature, precipitation), irrigation status, local practices, and cotton variety, exist. Application rates gathered from multiple references are summarized in Table 7.

Early Arsenic Use: Ca Arsenate - Insecticide

The cotton industry has been using arsenical compounds for more than a century. Before DDT and other more efficient organic insecticides were introduced in the late 1940's, the most widespread insecticides were metal arsenates. Calcium arsenate [$Ca_3(AsO_4)_2$] was used in the early fight against boll weevil, while lead arsenate [$PbHAsO_4$] was used in orchards across the United States. Inorganic arsenic compounds were banned from insecticide and herbicide use by EPA in 1988. Aurelius (1988) reported anecdotal evidence of calcium arsenate insecticide use near Knott, Howard County, Texas, from the 1930's to the 1960's. The application rate was described as 10-15 lb/acre (equivalent to 420-630 mg/m^2 elemental As).

The Main Arsenic Compound: Arsenic Acid - Desiccant

Arsenic acid [H_3AsO_4] became a popular defoliant in the 1960's after becoming commercially available in 1956 (Miller and Bailey, 1979) and until it was banned by EPA in 1992. Arsenic acid was produced and marketed at the Pennwalt Corporation facility (now Elf Atochem) in Bryan, Texas, and also marketed at Volunteer Purchasing Group (VPG) in Boham, Texas. Arsenic acid is commercially available as a powder but more commonly as a liquid. Commercial formulations contain 6.22 lb of elemental arsenic per gallon (Warrick et al, 1992). However, field application rates are measured in pints/acre. Typical dosage for cotton desiccation is 2-3 pints/acre (equivalent to 175-260 mg/m^2 elemental As) that could be delivered in variable water dilution (Warrick et al., 1992). Miller and Bailey (1979) recommended an

approximate dosage of 3 pints of arsenic acid per acre, whereas Aurelius (1988) reported an application rate of 2.94-4.42 lb/acre of arsenic acid in an area around Knott, Howard County.

Arsenic acid was generally sprayed from a ground-based vehicle or from an airplane. In the process, the desiccant was deposited on the lint of the open bolls, as well as on the plant foliage and stems and on the ground. Past agricultural practices required most of the plant material to remain on the field or be reused as compost because burning of waste had been banned earlier. Arsenic acid spraying occurs toward the end of the heavy rain period (Figure 12) and certainly after irrigation.

Current Arsenic Uses: Organo-arsenicals - Herbicides

Arsenic-based herbicides, such as MSMA and DSMA, are still being applied, although at a smaller application rate than arsenic acid, often in conjunction with other herbicides to control weed growth in cotton fields. Jordan et al. (1997) and Bridges et al. (2002) cited dosages of 1.7 kg/ha (78 mg/m^2 elemental As) and 0.6-0.8 kg/ha (27-37 mg/m^2 elemental As), typically applied before planting or after emergence, early in the growing season. Baumann (1998) indicated that commercial formulations of MSMA consist of 4 or 6 lb of elemental arsenic per gallon, whereas DSMA is often marketed in a 3.6 lb/gal formulation. Baumann (1988) suggested an application rate of 1.33 qt/acre of MSMA at 6 lb/gal (equivalent to 100 mg/m^2 of elemental arsenic) and 4 qt/acre of DMSA at 3.6 lb/gal (equivalent to 165 mg/m^2 of elemental arsenic).

Texas cotton growers currently make little use of organo-arsenical herbicides (only a few percent of the total acreage is treated with organo-arsenical herbicides), but it can be locally important, such as in central/east and south Texas, where pressure from weeds is highest (Abernathy in Lederer and Fensterheim, 1983, p. 57). Organo-arsenical herbicides are used mainly in the southeastern United States. Gianessi and Marcelli (2000) reported that in 1992 and 1997, approximately 3% and 5% of the total cotton acreage was treated with 0.76 lb/a (39 mg/m^2 elemental As) and 1.14 lb/acre (59 mg/m^2 elemental As) of MSMA, respectively. DSMA was used on 1% of the acreage at a dosage of 2 lb/acre (91 mg/m2 elemental As) in 1992. No DSMA use was reported in 1997. The year 1997 is the most recent year for which comprehensive data are available. Data are reported on a state-wide basis. However, Thelin and Gianessi (2000) detailed a simple method to distribute state pesticide data to the county level by using U.S. Department of Agriculture crop statistics available at that level. This approach merely assumes that crop management practices are similar across a given state and that pesticide consumption is distributed proportionally to cotton production. A study by Coupe et al. (1998) in northwest Mississippi suggested that those cotton pesticides are not present in surface waters, despite the fact that MSMA is the most widely used pesticide.

C2-3 Arsenic Concentrations in Soil in Agricultural Settings

After repeated applications, soil arsenic loading reaches a balance between additions and removal processes (leaching, volatilization, biomobilization). An order-of-magnitude mass balance helps in understanding the total arsenic loading of a cotton tract and suggests that most of the arsenic is trapped in the soil (very little is needed to contaminate water resources; 50 ug/L As in a saturated thickness of 30 m with 25% porosity translates into ~0.4 mg/m^2 elemental arsenic). Assuming no crop rotation and 25 years of arsenic acid treatment at 200 mg/m^2, 1 square meter of the parcel would have received ~200 mg x 25 = 5,000 mg/m^2 of elemental arsenic. If the arsenic is generally evenly distributed to a depth of 3 m, as suggested by soil sampling in Aurelius (1988, Table 4), and assuming a dry soil density of 2, typical soil arsenic concentrations would be ~1 mg/kg. This value is consistent with previous observations (e.g., Aurelius, 1988, Table 4). Background arsenic concentrations in soil are in the 0.1 to 40 mg/kg range but typically about 5 mg/kg.

Arsenic loading of crops is variable (Table 7) and is a function of both the crop and the climate. A typical application rate in the High Plains would be 200 mg/m^2 elemental arsenic. Lead arsenate for orchards was applied at a much higher rate than arsenic acid on cotton fields. Welch et al. (2000) mentioned that annual loading in orchards could be as high as 490kg/ha of lead arsenate (11 g/m^2 As) and could lead to soil concentration as high as 100 mg/kg. Davenport and Peryea (1991) cited a loading rate of 80 kg/ha (8 g/m^2 As). Peryea and Creger (1994) stated that arsenic soil concentration in apple orchards in Washington State could be as high as ~360 mg/kg. However, contamination was limited to the topsoil (< 40 cm). Peryea and Davenport (1994) also referenced two other studies in the northeast with the same conclusion. Arsenic contamination was limited to the top soil. On the other hand, evidence of leaching was also presented. They stated that arsenic mobility is related to soil texture. Arsenic is more mobile in coarse sand because of a relative lack of substances that would retard arsenic such as iron oxides, clay particles, organic matter, or calcite.

C2-4 Relationship between Cotton Distribution and Groundwater Arsenic Contamination Based on GIS Analysis

C2-4.1 Southern High Plains

Groundwater well information was separated into two groups based on the spatial distribution of groundwater quality in the Southern High Plains. The concentration of total dissolved solids (TDS) displays a distinct transition from the northern region (SHP-N) where TDS is generally < 500 mg/L to the southern region (SHP-S) where TDS is generally > 500 mg/L. Median arsenic concentration for wells in the SHP-N region is 4.5 ug/L whereas it is 11.2 ug/L in the SHP-S region. GIS analysis was performed separately on the two regions.

General Land Use

Groundwater arsenic concentrations were evaluated relative to general land use categories in the vicinity of each well in the southern High Plains according to the National Land Cover Data (NLCD; satellite imagery from ~1992; Vogelmann *et al*. 2001). Cultivated land use categories (crops, pasture, fallow) account for 61% of the area while rangeland categories (shrubland, grassland) account for 38% (Figure 15). Urban areas were excluded because they constitute only 1% of the area. For each well, percentages of cultivated and rangeland categories within a 500 m radius were calculated for each region. The distributions of arsenic concentrations were determined for 25th percentile intervals of cultivated (Figure 16) and rangeland category percentages. An arsenic source associated with agricultural chemicals should indicate a trend toward higher arsenic concentrations with increasing percentage of cultivated land use and a trend toward lower concentrations with increasing percentage of rangeland land use. The results indicate no significant trends for any percentile for either category or region.

Cotton-Producing Areas

Groundwater arsenic concentrations were evaluated relative to the distribution of cotton which should be related to arsenical pesticides. The fraction of county area planted with cotton in the Southern High Plains varies from negligible south of Amarillo to one-fourth to almost half of the county in the 9-county area centered on Lubbock county and in Gaines and Dawson counties (Figure 13). Values shown are based on median annual planted cotton acreage for the period 1970 to 1995 (from the National Agricultural Statistics Service, NASS, database), corresponding to the main period of arsenical product usage. There seems to be a spatial match between high arsenic concentrations and cotton production although other Panhandle counties with relatively high cotton production outside of the High Plains aquifer (Hall, Childress, and Cottle counties) do not have arsenic in groundwater (Figure 6). This is also true for the cotton-producing counties northwest of Abilene. Arsenic concentrations were plotted versus median

cotton production in each county (Figure 14). Spatial average arsenic values were estimated for each county using GIS and groundwater well data. Normalized areas planted with cotton were calculated using National Agricultural Statistics Service (NASS) median planted cotton acreages for the 1970 to 1995 period divided by aquifer outcrop area within each county. Three counties (Bailey, Lamb, and Lubbock) were omitted because they straddle the demarcation line between the SHP-N and SHP-S regions. Comparison of arsenic concentrations with higher resolution cotton production data would be more appropriate; however, this information is not available. The results indicate no significant correlation between cotton production and groundwater arsenic concentrations at the county scale

Cotton Gins

Cotton gins are distributed across the southern High Plains but are not as numerous in the high-arsenic region (Figure 17). Arsenic concentrations in wells within 1,000 m of cotton gin locations were compared with concentrations in wells at distances greater than 1,000 m for both regions (Figure 18). Within each region, F-tests were used to determine if the variances are significantly different between each population, and two sample student's t-tests were used to determine if population means are significantly different (α=0.05) (Table 8). Log values were used because concentration distributions are skewed toward high values. Results for the SHP-S region indicate that no significant difference between arsenic concentration variance (p=0.002) or $\log_{10}$ mean values (p=0.987) for wells closer than and farther than 1,000 m from cotton gins. Results for the SHP-N region are inconclusive because of the small number of wells located within 1,000 m of gins.

Soil Texture

If groundwater arsenic contamination is attributed to surficial sources, one might expect arsenic contamination in areas of coarser soil because infiltration and recharge should be higher. Soil texture distribution (Figure 19) was obtained primarily from Soil Survey Geographic (SSURGO) Database county soil survey data. SSURGO soil texture data are not available for Martin, Howard, or Dickens counties where data are available from State Soil Geographic (STATSGO) database (USDA, 1994). Soils are in general coarser in the SHP-S region. Soil clay content increases where the Blackwater Draw Fm. is present, primarily in the SHP-N region. Groundwater arsenic concentrations in each well were plotted against percent clay content within 500 m of each well. Results indicate that within each region there is no correlation between groundwater arsenic concentrations and soil clay content. There is only a slight correlation across regions, with lower clay contents and higher arsenic concentrations in the SHP-S region.

Depth to Water Table

Higher groundwater arsenic concentrations would be expected in areas of shallow water tables if land surface applications of arsenic are the dominant source of arsenic. Predevelopment depth to water in the SHP-S region is generally less than 30 m (100 ft) (Figure 21). There is no correlation between arsenic concentrations and depth to water within regions (Figure 22).

Saturated Thickness

Higher groundwater arsenic concentrations would be expected in areas of smaller saturated thickness if land surface applications of arsenic are the dominant source of arsenic because dilution would be less important. Predevelopment saturated thickness is in general much smaller in the SHP-S region than in the SHP-N region (Figure 23). Except in Gaines County, saturated thickness is less than ~30 m (100 ft) in most of the SHP-S region. There is no correlation between predevelopment saturated thickness and arsenic concentration in either the SHP-S or SHP-N regions (Figure 24).

Nitrate Concentrations

Arsenical pesticide applications may be related to fertilizer applications; therefore, correlations between groundwater arsenic and nitrate concentrations may reflect an arsenical pesticide source. Groundwater arsenic concentrations are not correlated with nitrate concentrations (Figure 26).

C2-4.2 Southwestern Gulf Coast

Cotton production is generally much lower in the southwestern Gulf Coast. The lack of a relationship between cotton production and arsenic concentrations is obvious because some counties with no cotton production have high arsenic concentrations (Live Oak and Duval Counties) whereas some coastal cotton-producing counties have little arsenic contamination (Willacy and Kleberg Counties). Therefore, it is unlikely that cotton production can explain the distribution of arsenic contamination in the Gulf Coast. Similarly, no high phosphate concentrations accompany arsenic hot spots (may possibly be affected by the high detection limit for phosphate of 1 ppm) (Figure 54g). Groundwater arsenic concentrations are not correlated with nitrate concentrations (Figure 56k). An anthropogenic agricultural origin for arsenic contamination in the southwestern Gulf Coast is unlikely, except maybe locally.

Subtasks C3/5: Relationship between Cotton Distribution and Groundwater Arsenic Contamination Based on Unsaturated Zone Sampling

This section describes the results of field studies to assess relationships between cotton distribution and elevated arsenic concentrations in groundwater (subtask C3), the impact of phosphate fertilizer on arsenic transport (subtask C4), and the effect of different soil types on arsenic transport (subtask C5). Arsenic from pesticide applications may follow one of two pathways to groundwater in the High Plains—either direct downward movement through soils in cotton areas or through surface-water movement to playas and downward beneath playas. Extensive research in the southern High Plains indicates that playas are the main source of recharge to the Ogallala aquifer (Wood and Sanford, 1985; Scanlon and Goldsmith, 1987).

Boreholes were drilled and soil samples were collected and analyzed for various parameters, including arsenic concentrations (Table 9), to evaluate relationships between land use (cotton distribution) and arsenic concentrations in the unsaturated zone. Field studies were conducted in the southern High Plains and southwestern Gulf Coast. These two areas are described separately. In both areas, information on land cover was obtained from the National Land Cover Data (NLCD; satellite imagery, 1992; Vogelmann *et al*. 2001). Irrigated areas were identified using the NLCD imagery classification results of Qi *et al*. (2002).

C3/5-1 Site Descriptions

C3/5-1.1 Southern High Plains

Locations of drilling sites were chosen relative to land use and distributed across the southern High Plains (Figure 30a). Information on land cover was obtained from the National Land Cover Data (NLCD; satellite imagery, 1992; Vogelmann *et al*. 2001). Irrigated areas were identified using the NLCD imagery classification results of Qi *et al*. (2002). Approximately 38% of land in the SHP is rangeland and 61% is cultivated and 23% of cultivated land is irrigated. Cotton production accounts for approximately 38% of all cultivated areas and for 23% of the entire Texas SHP area. From 1968 through 2004, cotton production in the Texas SHP accounted for an average of 17% of US production, ranging from 9% to 23%.

A total of 18 boreholes were drilled in the Southern High Plains: 2 in rangeland, 2 in irrigated, 1 in a playa, and 13 in dryland settings (Figure 30a). Boreholes are in Andrews, Terry, Lamb, Bailey, Gaines, Howard, Dawson, and Martin counties. Boreholes drilled in rangeland settings in Andrews County were used to provide baseline information on arsenic concentrations in soils relative to cultivated areas. A total of 15 borehholes were drilled in areas cultivated with cotton in Bailey, Dawson, Gaines, Howard, Lamb, Martin, and Terry Counties. Two of these boreholes were in irrigated sites in Terry County. One borehole was drilled in a playa surrounded by irrigated cotton fields in Terry County to test the conceptual model that downward arsenic movement occurs in response to focused recharge in playas from runoff from irrigated cotton fields.

Boreholes were also drilled in areas of different soil texture based on STATSGO and/or SSURGO data to evaluate the impact of soil texture on arsenic concentrations (Figure 19). The soil data from these databases only represents the upper 1.5 to 1.8 m of the profile but were used as a preliminary indicators of soil type. Soil clay content at the rangeland and cultivated sites averaged 25% and ranged from 18 to 33%, and was 48% at the playa site.

C3/5-1.2 Southwestern Gulf Coast

Locations of drilling sites were chosen relative to landuse and distributed across the southwestern Gulf Coast. A total of 10 boreholes were drilled: 5 in rangeland, 1 in irrigated, and 3 in dryland locations. Boreholes are located in Kenedy, Duval, Hidalgo, Starr, and Nueces

counties. The smaller borehole total depth in the Gulf Coast can be attributed to generally higher clay content and drier soil conditions relative to the southern High Plains. Boreholes were also drilled in areas of different soil texture based on STATSGO and/or SSURGO data to evaluate the impact of soil texture on arsenic concentrations. Boreholes in coastal counties are located in predominantly clay rich sediments whereas those in inland counties are in sandier soils.

C3/5-2 Methods

C3/5-2.1 Methods (Southern High Plains)

A total of 18 boreholes were drilled with a 6620DT rig (Geoprobe, Salina, KS) without any drilling fluid in the southern High Plains (Figure 30a, Table 9). Continuous cores were obtained using a core tube (1.22 m long, 29 mm inside diameter) from the ground surface to depths ranging from 3.1 to 12.7 m (average 7.6 m). Boreholes were drilled until auger refusal. Core sample tubes were cut in various length sections and capped and sealed to prevent evaporative loss. Sample tubes were stored on ice in the field and in a refrigerator in the laboratory. Core samples were used for laboratory measurement of water content, matric potential, anions, and arsenic concentrations.

In addition to borehole drilling, noninvasive measurements of near-surface apparent electrical conductivity (EC_a) were performed at 17 borehole locations using a downhole EM39 instrument (Geonics, Mississaugua, ON). The EM39 has a nominal measurement radius of 0.75 m and provides high resolution measurements of EC_a. The instrument signal response is a function of several soil parameters, including texture (clay content), water content, and salinity.

Soil samples were analyzed for pressure head (to determine direction of flow). The term pressure head is generally equivalent to the term matric potential, which refers to the potential energy associated with the soil matrix. Matric potentials ≥ -8 m were measured in the laboratory with tensiometers (Model T5, UMH, Munich) whereas matric potentials ≤ -8 m were measured in the laboratory with a dewpoint potentiameter (Model WP4-T, Decagon Devices Inc., Pullman, WA).

Chemical parameters included arsenic concentrations and anions (chloride, sulfate, nitrate + nitrite, bromide, and phosphate) in water leached from 288 unsaturated zone soil samples. The distribution of arsenic in the unsaturated zone provides information on potential transport of arsenic from surface arsenical pesticide applications to underlying aquifers and may also be related to natural arsenic in the soil zone that could provide a source for groundwater contamination. Chloride concentrations were used to estimate the rate of water movement through the unsaturated zone using the chloride mass balance approach (App. 1). Nitrate + nitrite concentrations in the unsaturated zone were used to evaluate transport of nitrogen fertilizers. Soils were air dried. Approximately 40 mL of double deionized water (≥18.2 Mohm) was added to about 25 g of soil. The mixture was placed in a reciprocal shaker for 4 hr, centrifuged at 7000 rpm for 20 minutes, and the supernatant was filtered to 0.2 um. Approximately 10 mL was acidified with nitric acid (reagent grade) to pH < 2 for arsenic analysis using graphite furnace atomic absorption spectroscopy and 20 mL was used for anion analysis using ion chromatography at the University of Texas Environmental and Water Resources Engineering Analytical Services Center. Soil samples were oven dried at 105^{o}C for 48 hr to determine gravimetric water content.

Arsenic concentrations are represented as ug/kg by multiplying the arsenic concentrations in the supernatant by the ratio of the volume of DI water to the weight of dried soil (extraction ratio). Arsenic concentrations can also be represented as ug/L of pore water by dividing the concentrations in the supernatant by the gravimetric water content (Figure 32). The latter representation may not be reliable because the leaching process may have removed more

arsenic than would generally be present in soil pore water. Arsenic concentrations are discussed primarily in terms of ug/kg of soil. The concentrations from the leaching process indicate that there is soluble arsenic or water extractable arsenic in the soil and may overestimate actual arsenic concentrations in soil pore water.

C3/5-2.2 Methods (Southwestern Gulf Coast)

A total of 10 boreholes was drilled in the southwestern Gulf Coast in areas of different land use (rangeland, cotton, other crops) under dryland (rainfed) and irrigated conditions (Figure 30b, Table 9). Borehole depths ranged from 0.9 to 7.3 m (average 4.3 m). In addition, downhole electromagnetic induction was used to evaluate stratification. Soil sample analyses for a total of 107 samples were similar to those described for the southern High Plains.

C3/5-3 Results

C3/5-3.1 Results (Southern High Plains)

Arsenic concentrations in soils are quite variable, with median arsenic concentrations in individual profiles ranging from 2.6 to 23 ug/kg (Figure 31, Table 9). There is no systematic variation in arsenic concentrations with land use (Figure 31, Table 9). Arsenic concentrations in rangeland were expected to be low and to represent background levels for arsenic in cultivated areas; however, arsenic concentrations in rangeland were high (≤ 77 ug/kg at 6.4 m depth; Figure 31). The second borehole drilled in rangeland had low arsenic levels; however, it was only 3 m deep. Arsenic concentrations in areas of cotton production were quite variable with peak values in different boreholes ranging from 17 – 62 ug/kg. These concentrations are generally slightly lower than those in the rangeland setting (Figure 31). Arsenic concentrations in irrigated cotton settings were similar to those in dryland cotton settings. There is more variation in arsenic profiles within irrigated sites than between irrigated and dryland sites (Figure 31). There is no systematic variation in arsenic concentrations with depth in the cultivated profiles. Some profiles have peak concentrations at the surface (Figure 31 T4, D1, H2, M1, M2, M3, M4) whereas others have peak concentrations toward the center of the profile (T3, T1, L1, B1, B2, G2, H1). The playa profile has the highest peak arsenic concentration (204 ug/kg) at a depth of 2.8 m and arsenic concentrations decreased with depth to values of 0.6 – 7.1 ug/kg.

Total arsenic concentrations in soils were compared with water soluble or water extractable arsenic in selected soil samples that represented a range of soluble arsenic concentrations. Total arsenic concentrations ranged form 0.7 to 4.0 mg/kg (Table 9) which are similar to global average values of soil arsenic estimated by Shacklette and Boerngen (1984) and Hem (1985). The lack of a strong relationship between total and water soluble arsenic is consistent with what is generally reported in the literature and indicates that arsenic solubility is not the controlling process in arsenic mobility.

Arsenic concentrations were evaluated relative to concentrations of other anions to assess sources and transport mechanisms of arsenic. Arsenic is highly correlated with phosphate (r^2=0.73) in the T4 irrigated site. The restriction of arsenic to the upper ~ 1 m and correlation with arsenic suggests an arsenical pesticide source for arsenic at this site. High correlations between arsenate and nitrate in D1, M3, and M4 dryland cotton sites and highest arsenic concentrations near the surface suggest arsenical pesticide sources for arsenic in the near surface zone.

Many dryland cotton profiles have low chloride concentrations in the shallow subsurface and increasing chloride concentrations at depth (T1, L1, B1, B2, G1, G2). Low chloride concentrations are attributed to leaching of chloride related to higher downward water fluxes beneath cultivated areas. The increase in chloride at depth is attributed to the transition from rangeland to dryland agriculture. High chloride at depth is associated with high sulfates in some

profiles, particurarly L1 and H2. Increases in sulfate are shallower than chloride increases in some profiles. Low correlations between arsenic and chloride in these profiles indicates that arsenic levels are independent of water fluxes in the system. Some profiles in dryland settings have low chloride concentrations throughout the profile (H1, D1, M1, M3) which may result from the profiles not being deep enough to show the transition from rangeland to cultivated agriculture.

Relationship between Arsenic Concentrations and Soil Type

Soil texture based on SSURGO and STATSGO was variable for boreholes drilled in the Southern High Plains. However, while clay content ranged from 18 to 48%, most (14 of 18 boreholes) were between 20 and 29%. There is no systematic variation in arsenic concentrations with clay content based on SSURGO/STATSGO data. Soil texture data are not available for individual boreholes; however, soil water content is often highly correlated with soil texture; therefore, water content was used as a proxy for soil texture. Correlations between arsenic concentrations and water content for individual profiles were generally low (r^2<0.2), with the exception of D1 (r^2=0.5). The low correlations suggest that arsenic concentrations may not be related to soil texture, assuming that soil water content is a reliable proxy for soil texture.

C3/5-3.2 Results (southwestern Gulf Coast)

Arsenic concentrations in soils are quite variable, with median concentrations for individual profiles ranging from 3.3 to 102 ug/kg (Figure 33 and Figure 34). Some of the profiles are too shallow to evaluate arsenic distribution in the profile (DU1, DU2, DU3, HI1). The highest arsenic concentration (1,854 ug/kg) was found in a pasture area where cotton gin waste had been ploughed into the soil (HI1). The high arsenic peak occurs at a depth of 1.3 m. High arsenic concentrations are restricted to the upper~ 2 m where chloride concentrations are low as shown by the negative correlation between arsenic and chloride (r=-0.78). This profile indicates that contamination related to gin waste application is restricted to the shallow soil profile. High chloride concentrations below the arsenic peak indicate that there is little water movement at depth; therefore, chloride is not leached. High arsenic concentrations in the ST3 profile are also restricted to the shallow subsurface and are highly correlated with nitrate which may indicate a fertilizer source for arsenic. Although the H12 profile is shallow (1 m), high arsenic concentrations near the surface correlate with high nitrate and phosphate and may suggest a fertilizer source. The profile with the second highest arsenic level is DU1. Arsenic concentrations are high throughout the profile. Median arsenic levels in all the remaining profiles are < 10 ug/kg and show no systematic variation with land use.

C3/5-4 Modeling Analyses

C3/5-4.1 Modeling of Arsenic Behavior in the Unsaturated Zone

The Modeling Tool

Modeling studies were performed with the USGS PHREEQC geochemical code (Parkhurst and Appelo, 1999). The code has pseudo-1D transport capabilities. Advection (and diffusion) can be modeled when the water moves from cell to cell in a piston flow fashion. Each cell contains 1 kg of water by default. Each cell can have its own reactive surface minerals and initial water composition. In an advection step (“shift” in PHREEQC terminology), water moves from a cell to the one downstream and equilibrates with the minerals and surfaces present in that cell. Comments on the thermodynamic database used in the modeling are given in Appendix I.

Conceptual Model and Assumptions

This section details a modeling exercise describing the competing behavior of phosphate and arsenic in a generic unsaturated zone considered typical of the southern High Plains. The

model illustrates the behavior of arsenic and phosphate as they are transported downward by advection. It consists in loading the soil with arsenical products and with (or without) phosphates by following the historical pattern in monthly time steps for the duration of arsenical products use (~35 years). Rainfall and possibly irrigation water will leach sorbed arsenic and phosphate from the upper topsoil levels where they have deposited or have been incorporated to the uncontaminated subsoil. There, they can also sorb.

We made the following assumptions:

1) all anthropogenic arsenic is available to be leached
2) oxidizing conditions exist and As(V) only is present
3) all oxide-sorbing minerals (amorphous iron oxide, ferrihydrite, green rust, goethite, hematite, amorphous aluminum oxide, gibbsite, boehmite, diaspore) are lumped into one category and modeled as amorphous iron oxide ($Fe(OH)_3$). Iron oxide weight fraction is estimated at 0.5 percent, and its specific surface area is assumed to be 300 m^2/g (see Appendix I).
4) unsaturated zone average porosity is 40 percent; water saturation is 50 percent
5) local chemical equilibrium is reached (no kinetics)
6) diffusion is neglected; only advection is considered
7) organo-arsenicals have a minor role and can be neglected
8) water movement is only downward

The model contains 150 cells, each ~0.1 m long in the vertical direction. Initially all cells are at chemical equilibrium with the resident water and, as appropriate, typical phosphate loading (see below). Arsenic is then added to the first cell in an amount consistent with its historical use pattern, and the arsenic front slowly moves downward with the infiltrating water. After a period of ~35 years, no arsenic is added to the top cell, only phosphate, as appropriate. It is recognized that some, if not all, of that water will evapotranspirate back into the atmosphere. However, assuming only downward water movement is conservative relative to the location of the arsenic pulse.

Soil Information

High Plains soils are mostly derived from the Blackwater Draw eolian deposits (Holliday, 1989). Wood and Sanford (1995) suggested that a porosity of 40 percent and a bulk density of 1.60 g/cm^3 are reasonable values following hundreds of measurements in multiple studies by different authors. Measurements made for this study support the bulk density value of ~1.6 g/cm^3. The same measurements also produced an average water content by weight of ~11 percent, that is, a volumetric water content of approximately 20 percent. Bryant (1977) measured an average total porosity of ~43 percent on a few sites across the High Plains. He indicated that ~36 percent is microporosity and ~7 percent is macroporosity.

Playa soils consist mainly of smectite clays. Soils in the shallow subsurface of a playa in Andrews County consisted of clay (>50%) (Lipan soil down to a depth of 2 m) transitioning to fine sand of the Blackwater Draw Fm (Allen et al., 1972). The clay minerals are mainly illite (>50% in coarse clay fraction), interstratified illite-montmorillonite and montmorillonite (>50% in fine clay fraction), roughly in equal proportions. Kaolinite is generally present in small quantities (<10%). The upland areas (Arvana soils) are shallower (~1m) with a lower clay content (down to ~20%) but otherwise little different in terms of composition (maybe slightly higher illite fraction). The cation exchange capacity (CEC) of playa and upland soils was estimated at ~15-35 and 10-15 meq/100g of soil, respectively (Allen et al., 1972, their Tables 11 and 12). The organic carbon content decreases from 1% to 0.05% across the soil profile of the playa floor, whereas it did not reach 0.5% in the upland areas. The upland areas had a deep calichified horizon which was absent in the playa soils. Films of manganese and iron oxides are often present in the C horizon. Another study of eight upland areas (Bryant, 1977, his Table 2) determined that clay

fraction varies between 15 and 35% with little silt-size material. CEC was in the range 5-20 meq/100g of soil, and pH was generally between 6.5 and 7.8, typically increasing with depth. Higher pH values were associated with free calcium carbonate. Organic carbon was generally below 0.5%. All sampled soils showed calcic enrichment in the B and/or C horizons.

Given the geochemistry of arsenic (see Appendix I), it is important to understand the nature, amount, location and surface properties of iron oxides and hydroxides in the unsaturated zone. The modeler must provide sorption site density and specific surface area exposed to water. The first parameter is extracted from the literature, whereas the second must be provided by study of grain mineralogy.

Water Composition

The input pore water composition is taken from a variety of sources. This study collected only anion data (chloride, sulfate, nitrate/nitrite, phosphates, and bromide). Bryant (1977) presented results for soluble cations (calcium, magnesium, potassium, and sodium), whereas Jackson et al. (2004) in a recent perchlorate study in the High Plains published both anion and cation data. Not all those analyses are fully consistent. Nevertheless, a representative analysis can be built. The average TDS should be in the 400-500 mg/L. Calcium and magnesium should be approximately equal at ~2 milliequivalent per liter (meq/L) each. Sodium would be present at a concentration of ~1 meq/L, whereas potassium would be much lower at 0.1-0.2 meq/L. Anions are dominated by bicarbonate. Bicarbonate is not analyzed but can be backcalculated through electrical balance. Chloride and sulfate should both be below 0.5 meq/L. This is also consistent with recharge water composition presented in Fryar et al. (2001). The biggest discrepancy among all the analyses is the amount of sulfate relative to chloride. Jackson et al. (2004) also reported high fluoride concentrations. To simplify the model and avoid dealing with issues such as rainwater dissolving soil elements, the infiltration is assumed to have the pore water composition from the start.

Chemical Loadings

Compilation of chemical loading for arsenic (Table 7) suggests a range of 175-260 mg As/m^2 for cotton-producing areas. A worst-case scenario of application of 260 mg/m^2/year (3.45 mmol/yr/m^2) is assumed starting in 1956 until 1992 (37 years). This amounts to an arsenic soil concentration over 0.305 m of 260x38/(1x1x0.305x1000)/0.6/2.65 ~ 20.4 mg/kg with a porosity of 40 percent (50 years of Ca arsenate at 500 mg/kg would be an additional 117 mg/kg over 0.305 m) consistent with current observations. Phosphate application is done in different formulations but assumed to be all orthophosphates. We assume also a rate of 20 lb P_2O_5/ac, that is, 0.454 kg/lb / (4047 m^2/ac)=2243 mg/m^2 x (62 of P / 142 of P_2O_5) = 980 mg P/m^2 = 32 mmol P/m^2. With a footprint of 0.059 m^2 (see below), the monthly loading becomes 0.0169 mmol As/liter/month and 0.157 mmol P/liter/month.

Infiltration Rates

As mentioned above, PHREEQC default option computes geochemical changes relative to the 1 kg (that is, we assume, occupies 1 liter) of water in a cell. The cell can be shaped according to the user's understanding of the system. The key question to be addressed in this section is how much soil surface area is in contact with 1 liter of water. If we use a vertical dimension of 0.305 m for a cell, given that the volume/volume water content of the soil is 20 percent, a square cell would have a dimension *a* so that a^2 = 0.3048/0.2/1000=0.00152 m^2, that is, *a* = 4 cm. Rainfall in Lubbock is ~18" (14" in Midland). We assume that half of it infiltrates (most of it will go back up as ET). This translates into 8" x 2.54 cm/inch = 0.203m, /0.2 taking into account water content, that is, 1.016 m^3/m^2, that is, 0.085m^3/m^2/month. It follows that, on average, the wetting front will move by 0.085 m each month. We eventually choose this as the cell vertical dimension. Given that the volume/volume water content of the soil is 20 percent, a

square cell would have a dimension *a* so that a^2 (in m) = 0.001/0.085/0.2=0.059 m^2, that is, *a*=24 cm.

C3/5-4.2 Modeling Results

Even using conservative numbers for arsenic and phosphate loadings, as well as infiltration rates, iron oxides strongly retard both arsenic and phosphates. Despite total arsenic concentration in the 30-50 mg/kg, aqueous concentrations remain low (more than 99% of the arsenic is sorbed to iron oxides). Figure 35a (presence of phosphates) shows a rapid increase of aqueous arsenic in water to a maximum of ~1,200 ug/L. In contrast, Figure 36a (no phosphates) displays a much slower increase in arsenic aqueous concentration and a much lower maximum concentration at ~300 ug/L. In both cases, arsenic concentrations in water slowly decrease starting at the end of the application period (37 years). The tail is longer in the no-phosphate case because there is a larger reservoir of arsenic. A couple of meters away from that first cell, the impact of phosphate competition is more dramatic. Figure 36b and c (no phosphate) show that arsenic aqueous concentrations are extremely low, on the order of 1 ug/L, whereas Figure 35b and c (with phosphates) displays a lower concentration than in the first cell but still much higher than in the no-phosphate case.

Vertical profiles (Figure 37) include the same information as breakthrough curves. The cases with and without phosphates are plotted side by side. Arsenic aqueous concentration increases in the loading period (first 37 years), then the pulse moves downward very slowly in the phosphate case. In the no-phosphate case, the arsenic bulge does not move from the first cell (upper meter). In both cases, arsenic aqueous concentrations are below 10 ug/L at a depth of 15 m. Note that this modeling is generic in nature and that specific conclusions for a given site cannot be reached unless site-specific data are used.

Task C: Conclusions on Anthropogenic Origin of Arsenic Contamination

Southern High Plains

The southern High Plains was subdivided based on differences in TDS into a northern area (SHP-N: TDS < 500 mg/L) and a southern area (SHP-S: TDS > 500 mg/L). Arsenic contamination is much higher in the SHP-S region (51% of wells > 10 ug/L) than in the SHP-N region (7% of wells > 10 ug/L).

Regional analysis of groundwater does not support a surficial source of arsenic. The lack of correlation between groundwater arsenic concentrations and land use, distance from cotton gins, soil texture, water table depth, and aquifer saturated thickness suggests that anthropogenic surface sources are not dominant. Low correlation between groundwater arsenic and nitrate (r2 = 0.05) in the SHP-S region suggests that fertilizer is not a dominant source.

Results of drilling and sampling 18 boreholes in the southern High Plains indicate that the distribution of arsenic contamination is not related to cotton production or application of arsenical pesticides. High arsenic concentrations in rangeland profiles where arsenical pesticides have never been applied, indicate that there are other sources of soluble arsenic in the soils. Elevated arsenic concentrations in near surface soils related to nitrate and phosphate concentrations may reflect a fertilizer or arsenical pesticide source. Other profiles have peak arsenic concentrations at depth that cannot be explained by arsenical pesticides. The unsaturated studies indicate a widespread natural source of water soluble arsenic in the southern High Plains that may contribute to groundwater arsenic contamination.

Southwestern Gulf Coast

Groundwater arsenic concentrations are much higher in the southwestern area of the Gulf Coast (29 percent of wells exceed the MCL) than elsewhere in the Gulf Coast (3.5 percent of wells exceed the MCL).

It is more difficult to evaluate surface sources of arsenic in the Gulf Coast than in the High Plains because aquifers in the Gulf Coast are confined except in narrow outcrop areas. No indicator points toward an anthropogenic origin of the arsenic contamination in the southwestern Gulf Coast. GIS analysis indicates that groundwater arsenic concentrations are not related to cotton production. Some counties with the highest arsenic contamination do not have any cotton production (Live Oak and Duval Counties). Results of drilling and sampling 10 boreholes in the unsaturated zone indicate that arsenic concentrations are highest in a rangeland site where gin waste was ploughed into the field (≤1854 ug/kg at 1.2 m depth). Restriction of elevated arsenic related to gin waste to the upper ~ 2 m soil zone suggests that this is an unlikely source of groundwater arsenic. High chloride concentrations below the arsenic peak indicate that there is little water movement below this zone. High arsenic concentrations in the shallow subsurface and correlation with nitrate suggests fertilizer or arsenical pesticide sources for another profile. High arsenic concentrations were found throughout an irrigated profile. The remaining profiles had low arsenic levels (< 10 ug/kg) that showed no systematic variation with land use or with depth.

Task D: Evaluate Geologic Sources of Arsenic Occurrence in Groundwater

This section describes deliverables for subtasks described in Task D. Elevated arsenic concentrations in groundwater may be related to natural geologic sources. Geologic sources are evaluated separately for the southern High Plains and southwestern Gulf Coast because the geology of each region is markedly different.

Subtask D1. Compare Arsenic Concentrations in Groundwater with the Distribution of Different Hydrogeologic Units.

D1-1 Arsenic in Nature

Typical whole-rock arsenic content is approximately 2 mg/kg with higher concentrations in shales based on global average values reported by Hem (1985) (Table 11). Shales generally accumulate more trace metals than other sedimentary rocks because of their slow accumulation and the properties of clay minerals. For example, elevated levels of trace metals in Cretaceous marine shales are attributed to extensive volcanic activity during Cretaceous time (Presser, 1994). Volcanic rocks are also generally enriched relative to their intrusive counterparts. Soil concentrations often reflect concentrations in the parent material. Table 12, gives average abundance of selected elements in soils (Shacklette and Boerngen, 1984). The geometric average arsenic concentration in soils is ~ 7 mg/kg (range 0.1 – 100 mg/kg) based on data from Shacklette and Boerngen (1984) (Table 12). Global average arsenic concentrations in soils of 5 – 6 mg/kg were also reported by Yan-Chu (1994). An average arsenic concentration in soil of 5 – 10 mg/kg was cited by Smedley and Kinniburgh (2002). Most arsenic is adsorbed onto soil particles because of the strong attraction between positively charged arsenic ions, particularly arsenates and generally negatively charged clays and iron oxides. Rock degradation products, such as iron and other metal oxides and clays, are more abundant in soils and scavenge arsenic compounds. This explains the average slightly higher arsenic concentrations in soils than in rock. Soils contaminated by agricultural products have arsenic concentrations as high as ~100 mg/kg (Peryea and Kammereck, 1997) or 366-732 mg/kg (Smedley and Kinniburgh, 2002). Table 14 presents typical concentrations in groundwater. They range from 1 to 50 ug/L, two to three orders of magnitude less than in an average soild phase. Welch et al. (2000) presented a summary figure reproduced in Table 15.

Henry and Kapadia (1980) studied concentrations of As, U, Se, and Mo in soils in the southwestern Gulf Coast area both in background samples and in the vicinity of mines. Table 13 presents baseline concentration for trace elements in the southwestern Gulf Coast and elsewhere in the United States. Most soils in south Texas have Mo, As, and Se concentrations similar to those of natural soils elsewhere. However, sampling of mined and mineralized areas shows much higher concentrations. The average arsenic concentration for the Catahoula Fm. is lower than the world average, despite the fact that the Catahoula Fm. is mainly composed of volcanic degradation products.

D1-2 Geology of the Analysis Areas

D1-2.1 Geology of the High Plains

The major aquifer in the Texas Panhandle is the High Plains aquifer. The Texas Panhandle includes part of the central High Plains aquifer and the southern High Plains aquifer. The main geologic unit that makes up the High Plains aquifer is the Ogallala Fm., which is late Tertiary (Miocene-Pliocene, about 4-12 Ma) in age (Nativ, 1988). The Ogallala Fm. consists of coarse fluvial sandstone and conglomerate, that were deposited in paleovalleys in a mid-Tertiary erosional surface with eolian sands in intervening upland areas (Gustavson and Holliday, 1985). The Ogallala Fm. is generally thicker in the northern region (100-200 m Dallam – Hartley

counties) and thins to ~ 30 m in the south (Ector-Midland counties). The thickest deposits are found in paleovalleys (≤ 250 m, e.g. Carson County) that trend to the southeast. Paleovalley fills are separated by interfluvial upland areas where the Ogallala is much thinner and sediments are finer grained. The Ogallala Fm. has been partially eroded locally in the southern High Plains where groundwater discharges at the surface as saline lakes (Figure 38). The top of the Ogallala Fm. is marked by a resistant calcite layer termed the “caprock” caliche.

The Ogallala Fm. is overlain by Quarternary-age (Pleistocene-Holocene) eolian, fluvial, and lacustrine sediments called the Blackwater Draw Fm. (Holliday, 1989). The texture of the formation ranges from sands and gravels along riverbeds and mostly clay in playa floors.

The Ogallala Fm. is underlain by lower Cretaceous (Comanchean) strata in the southern High Plains (Figure 39). The top of the Cretaceous sediments is marked by an erosional surface that represents the end of the Laramide orogeny. Nonuniform erosion resulted in topographic relief on the Cretaceous beneath the Ogallala Fm. Cretaceous strata are absent beneath the thick Ogallala paleovalley fill deposits because they were removed by erosion. The Cretaceous sediments were deposited in a subsiding shelf environment and consist of (1) the Trinity Group (basal sandy, permeable Antlers Fm.), (2) Fredericksburg Group (limy to shaly formations including the Walnut, Comanche Peak, and Edwards Fm., as well as the Kiamichi Fm.), and (3) the Washita Group (low-permeability, shaly sediments of Duck Creek Fm.) (Nativ, 1988). The sequence results in two main aquifer units: the Antlers Sandstone (also termed the Triinty or Paluxy sandstone, ~ 15 m thick) and the Edwards Limestone (~ 30 m thick). The term Edwards Trinity (High Plains) Aquifer is generally used to describe these units (Ashworth, 1991). The limestone decreases in thickness to the northwest and transitions into the Kiamichi Fm. and Duck Creek Fm. (predominantly shale).

The Ogallala Fm. is underlain by the Triassic Dockum Group in much of the southern High Plains. The Dockum Group is exposed along the margins of the High Plains (~150 m thick). The uppermost sediments consist of red mudstones (termed red beds) that generally form an aquitard. Underlying units (Trujillo Sandstone [Upper Dockum] and Santa Rosa Sandstone [lower Dockum]) are aquifers. Water quality in the Dockum is generally poor (Dutton and Simpkins, 1986, Figure 10b). The sediments of the Dockum were deposited in a continental fluvio-lacustrine environment that included streams, deltas, lakes, and mud flats (McGowen et al., 1977) and included alternating arid and humid climatic conditions. The Triassic rocks are thickest in the Midland Basin (≤ 600 m).

The Ogallala Fm. is directly underlain by Permian rocks in the northeastern Texas Panhandle. The Permian is also present across all of the area. The top of the upper Permian consists of sediments deposited in tidal flats and sabkha environments of a shallow hypersaline sea in arid conditions. The filling of paleovalleys during Ogallala times approximately reproduces long-lasting structural features. In the late Paleozoic, three main basins trending W-E/NW-SE existed in the Texas Panhandle from north to south: the Anadarko, Palo Duro, and Midland basins. They are defined by the presence of structural highs: the Amarillo Uplift between the Anadarko and Palo Duro basins and the Matador Arch between the Palo Duro and Midland basins. Since Permian time, the region has been tectonically stable. The area has been tilted and warped, but deep-seated faults are rare (Bachman and Johnson, 1973). Subsidence due to salt dissolution (halite, NaCl, and anhydrite, $CaSO_4$) has been and still is common in the geological history of the area. The maximum cumulative evaporite thickness of the Salado and Castile Fms. of Permian age is ~ 600 m and is centered across the Texas-New Mexico state line along the current Pecos River valley in the Delaware basin. The cumulative thickness decreases toward the northeast across the Central Basin Platform to negligible values northeast of the Lubbock area (Bachman and Johnson, 1973, their Figure 3). Sinkholes of Triassic age are known (Bachman and Johnson, 1973, p. 10).

D1-2.2 Geology of the Southwestern Gulf Coast

During the Cretaceous, sediments deposited from shallow inland seas formed broad continental shelves that covered most of Texas. In the Tertiary (starting 65 million years ago), the Rocky Mountains to the west started rising, and large river systems flowed toward the Gulf of Mexico, carrying abundant sediment, similar to today's Mississippi River. Most of Texas, particularly west Texas, was also uplifted, generating a local sediment source, including erosional detritus from the multiple Tertiary volcanic centers in West Texas and Mexico. Six major progradational events occurred where sedimentation built out into the Gulf Coast Basin. These progradational sequences include the most recent Vicksburg-Catahoula-Frio, Oakville-Fleming, and Plio-Pleistocene sand-rich wedges. A general stratigraphic column is presented in **Figure 40**. Hydrostratigraphic units do not necessarily correspond to stratigraphic units. The former are defined in terms of flow (i.e., in terms of "shales" vs. "sands"), whereas the latter are defined in terms of age. Three main aquifers define the Gulf Coast aquifer: the Jasper, Evangeline, and Chicot aquifers that broadly include the Oakville Sandstone, the Goliad Sand, and Quaternary units, respectively. The Fleming Fm. is a confining unit between the Jasper and Evangeline aquifers and is named the Burkeville confining unit. A more accurate model would take into account the fact that the top of the Catahoula Fm. is sometimes included in the Jasper as the top of the Fleming Fm. is included in the Evangeline aquifer.

The component geologic units of the Gulf Coast aquifers are, from oldest to youngest, (1) Catahoula Fm., (2) Oakville Sandstone/Fleming Fm., (3) Goliad Fm., (4) Pleistocene formations: Willis Fm., Lissie Fm., and Beaumont Fm., and (5) Quaternary terrace deposits and alluvium (Doering, 1935; Baker, 1979) (Figure 41 and Figure 42). Rocks of the Jackson Group and Frio Fm. underlie the Gulf Coast aquifer formations and are pertinent to this study because they contain volcanic deposits, which are associated with uranium deposits and presumably arsenic concentrations in groundwater. The geologic units range in age from Eocene (Jackson Group) to Recent (Figure 40). Stratigraphic relationships and definitions are inconsistent and sometimes ambiguous for this group of Tertiary rocks, which are discussed below from oldest to youngest.

Jackson Group – Eargle (1959) defined four component formations of the Jackson Group and noted that the uppermost Whitsett Fm. consists of bentonitic clay and tuff at the top and sandstone at the base. Lignite is also present in some horizons of the Jackson Group. It generally behaves as a confining unit between the Yegua and Jasper aquifers. Uranium deposits have been found in the uppermost portions of the Whitsett Fm., where it is unconformably overlain by Catahoula Tuff Fm. Uranium deposits occur in Jackson Group rocks in Karnes County as oxidized deposits near the outcrop and as deeper (25 – 30 m), unoxidized, roll-front-type deposits (Eargle et. al., 1975). Fluvial sand to gray-green clay sedimentary deposits "yield variable amounts of highly mineralized water" from upper Jackson Group rocks (Adidas, 1991). Fewer than half a dozen wells on the western edge of the Gulf Coast aquifers in Webb County penetrate upper Jackson Group rocks, and arsenic concentrations in these wells were below detection limits. Frio Clay – This formation, of the Jackson Group, should not be confused with the Frio Fm**. (Figure 40), downdip** expression of the Catahoula Fm. (Baker, 1979).

Catahoula (Gueydan) Formation = Catahoula Confining System – The Catahoula Fm. has different lithology and provenance in the southwestern Gulf Coast than it does in the northeastern Gulf Coast. Several authors suggest the Catahoula Fm. in the southwest should be referred to as the Gueydan Fm. (McBride et. al., 1968; and Parker, et. al., 1988), which is the name originally given to it by Bailey (1924). Baker (1979) noted that this unit is referred to as Catahoula Tuff in the southwest and Catahoula Sandstone to the northeast of the Colorado River, where it contains more sand and less volcanic material than in the southwest. In the southwestern counties of Duval and McMullen, the Gueydan Fm. reaches a thickness of ~ 300

m and contains the coarsest volcanic material of any Gulf Coast Tertiary unit (McBride, et. al., 1968). In this region the Catahoula Fm. lies unconformably on either the Frio Fm. or Whitsett Fm. of the Jackson Group. In the southwest the Catahoula/Gueydan formations are unconformably overlain by either the Oakville Fm. or the Goliad Fm., whereas in the northeast they are overlain by the Fleming Fm. (Aronow et. al., 1987 and Shelby et. al., 1992).

McBride et al. (1968) describe cross-bedding in Gueydan strata that suggests deposition of the coarser grained volcaniclastics by streams flowing down a NW-SE-oriented paleoslope in Duval and Karnes counties. Farther north in Fayette County paleocurrent data suggest more of an east to west flow direction. Sediments in the lower Catahoula Fm. are predominantly gray tuff, whereas pink tuffaceous clay is more common in the upper strata, suggesting a change to more humid climatic conditions during deposition. Volcanic conglomerates and sandstone are most common in mid levels of the unit. Bentonite and opalized clay layers and alteration products of volcanic glass (zeolites, Ca-montmorillonite, opal, and chalcedony) are present throughout the formation and indicate syndepositional alteration of tuffaceous beds. Widespread areas of calichification indicate long periods of exposure to soil-forming conditions at the surface (McBride et al., 1968).

Galloway (1977) described the Catahoula Fm. as being deposited by two separate fluvial systems, Gueydan in the southwest and Chita-Corrigan in the northeast parts of the Gulf Coast. The Gueydan bedload fluvial system was deposited in the Rio Grande embayment and is dominated by plagioclase and volcanic rock fragments from a distal western source. The Chita-Corrigan mixed-load fluvial system was deposited in the Houston Embayment and is dominated by quartz-rich material from mixed sedimentary terranes. Both depositional systems contain volcanic ash; however, Galloway (1977) cites differences in alteration clay minerals as evidence that Gueydan deposition occurred in an arid environment, whereas the depositional environment of Chita-Corrigan was more humid.

Oakville Sandstone/Fleming Formation – These two units are commonly grouped because they are both composed of varying amounts of interbedded sand and clay. In the central part of the Gulf Coast (Brazos River to central Duval County) they are easily recognized as stratigraphically adjacent units because the Oakville is sand-rich and the Fleming is more clay-rich. To the northeast of the Brazos River, the two units are indistinguishable. Baker (1979, 1986) assigned the Miocene Oakville/Fleming geologic units to the Jasper aquifer, which has been best characterized along the northeastern Texas Gulf Coast, north of the Brazos River. Galloway et al. (1982) described the Oakville in the southwest Gulf Coast as a sand-rich fluvial system overlying the Catahoula Fm. They associated the Oakville Sandstone with the Jasper aquifer and stated that the Evangeline aquifer includes most of the Fleming Fm.

Goliad Formation – The Goliad Fm. is only present at surface as far as Lavaca County, just south of the Colorado River as seen on the Seguin GAT sheet (Proctor et. al., 1974) and is absent farther to the northeast (not present on the Beaumont GAT sheet (Shelby et. al., 1992). The Goliad Fm. was deposited during the Pliocene or as recently as 5 Ma. Hoel (1982) mapped the Pliocene Goliad Fm. in detail for her Master's thesis research at UT Austin. She found the Goliad Fm. to be genetically and compositionally similar to the underlying Oakville and Catahoula formations as they exist in the southwest Gulf Coast. Hoel (1982) also stated that preliminary exploration shows potential for the Goliad Fm. to have economically mineable uranium deposits similar to those found in the underlying Oakville Sandstone. Hoel (1982) noted a distinct change in character of the Goliad Fm. along a line perpendicular to the coast, just north of the Nueces River roughly coincident with the San Patricio-Refugio county line. Southwest of this line the Goliad Fm. was deposited by rivers carrying bed load or very coarse sediments containing a large proportion of orthoclase and plagioclase feldspar crystals and volcanic rock fragments from a "distant western source." Northeast of this line the rivers carried

finer grained sediments composed primarily of calc-lithic particles presumably derived from Edwards Plateau rocks of central Texas.

The Evangeline aquifer is composed of water-bearing zones primarily within the Goliad Sand and secondarily in underlying portions of the Fleming Fm. (Ryder and Ardis, 1991) The Goliad Sand is only identified as an aquifer unit in the TWDB well database within and to the south and west of Lavaca and Jackson counties. However, the Evangeline aquifer is present throughout the Gulf Coast aquifer in the northeast into Louisiana. Clearly there is a difference in the geologic units that compose the Evangeline aquifer in the southwest and northeast sections of the Gulf Coast aquifer. According to Baker (1979), the Evangeline aquifer was originally only defined as far west as Austin, Brazoria, Fort Bend, and Washington counties in Texas. He stated that extending the Evangeline farther west is speculative; however, in 1976 the USGS decided to extend the Evangeline to the Rio Grande.

Pleistocene and Recent Alluvial Deposits – Since Pleistocene time, packages of fluvial sediments representing successively younger progradational cycles have been deposited along the Texas Gulf Coast (Blum, 1992). The fluvial sediments range in texture from gravel to clay and are commonly poorly indurated. Decreasing dip of the strata toward the coast through time reflects changes in relative uplift of inland areas (southern Rocky Mountains, Great Plains, and the Edwards Plateau) and subsidence in the Gulf of Mexico (Doering, 1935; Blum, 1992). The older portions of this depositional sequence are coarser grained and dip 3 to 7 m per mile (Willis Sand), whereas the younger units are finer grained and dip only approximately 2×10^{-4} (1 ft/mi) (Beaumont Fm.) (Doering, 1935). Major Pleistocene to Recent formations along the Texas Gulf Coast, listed from oldest to youngest, include Willis Fm., Lissie Fm., Beaumont Fm., and Quaternary terrace deposits and alluvium (Doering, 1935; Baker, 1979). These units plus Quaternary alluvial deposits are all assigned to the Chicot aquifer.

Northeast of the Colorado River, Miocene- to Pliocene-age Fleming Fm. clay is unconformably overlain by the Willis Sand, which is in turn unconformably overlain by the sand and clay of the Lissie Fm. South of the Colorado River, the Pliocene-age Goliad Fm. is overlain by the Lissie Fm., which consists of sand, silt, clay, and minor amounts of gravel. The Lissie Fm. is overlain by clay, silt, and fine-grained sand of the Pleistocene-age Beaumont Fm. throughout the Texas Gulf Coast. Although the Beaumont Fm. as a whole is much finer grained than directly underlying formations, it contains localized sand channel deposits. The base of the Pleistocene (thought to be Willis Fm. in the northeast Gulf Coast and Lissie Fm. in southwest Gulf Coast) is very difficult to identify on geophysical logs (Baker, 1979). Because of this the bottom of the Chicot aquifer, which has in the past been defined as the base of the Pleistocene, is ambiguously defined and is often lumped together with the Evangeline aquifer.

The structural map of the Gulf Coast area (Figure 43) shows the abundance of growth faults that strike parallel to the Gulf of Mexico. Each major progradation package has a series of growth faults associated with it. An interesting feature of the map is that the Wilcox fault zone impacts the Catahoula Fm. and Oakville Sandstone close to their outcrop area in the southwestern Gulf Coast but there is no major fault associated with the outcrop of the same formations farther north and in East Texas.

D1-3 Arsenic Distribution

D1-3.1 Arsenic Distribution in the High Plains Aquifers

High arsenic concentrations seem mostly to overlap Cretaceous subcrops. However, there are also localized pockets of higher concentrations farther north, in particular, on the escarpment, south of the Palo Duro Canyon (Figure 44a). In order to better visualize arsenic distribution in the High Plains, a probability map that highlights areas having high arsenic concentrations was constructed (Figure 44b). It is based on the strong correlation between

fluoride and arsenic, and it possibly enhances the distribution visualization because fluoride data are more abundant. High arsenic concentrations (>50 ug/L) are mostly restricted to the eastern side of the southern High Plains in Lynn, Terry, Dawson, and Martin Counties. Intermediate arsenic concentrations are present in most or all of Lubbock, Yoakum, Terry, Lynn, Gaines, Dawson, Martin, and Howard Counties, as well as on the Ogallala footprint of Ector, Midland, and Glasscock Counties and in the eastern half of Andrews County. Some counties farther north (Bailey and Hockley Counties) and located along the escarpment (Randall, Briscoe, and Floyd Counties) also show intermediate arsenic values. Low arsenic values are present across most of the northern section of the southern High Plains and in the Texas section of the central High Plains. In the center of the arsenic-contaminated area, in Dawson and eastern Gaines Counties, few samples show arsenic <10 ug/L. The western section of the southern High Plains shows an apparent general decrease in arsenic concentrations (western side of Yoakum, Gaines, and Andrews Counties). There is a lack of arsenic analyses in the Ogallala across the New Mexico state line to confirm whether the trend continues. The Cenozoic-Pecos Alluvium aquifer (TWDB major aquifer) which is similar in origin and age to the Ogallala aquifer also contains higher arsenic concentrations.

Arsenic concentration in aquifers underlying the Ogallala aquifer and next to it are displayed in Figure 45. The TWDB database includes, in the footprint of the High Plains aquifer, water samples whose source well could also be screened mostly in the Cretaceous and/or in a few instances in the Triassic Dockum. There is a total of 177 such samples (out of a total of 6,433). There are several data points with As>10 ug/L in Andrews, Terry, and Dawson counties. This is consistent with the Nativ and Guttierez (1988) study of the Cretaceous aquifers that found only one out of eight samples with As>10 ug/L (in Terry County).

Analyses for arsenic in the Dockum Fm. are mainly from the outcrop area (outside of the Ogallala footprint) and that portion of the aquifer having a TDS <5,000 mg/L (sometimes within the Ogallala footprint). Only 10% of the ~200 Dockum data points are above the 10 ug/L threshold (with a maximum of 26 ug/L). Arsenic concentrations >10 ug/L in the Dockum aquifer are more uniformly distributed than in the Ogallala aquifer, but no sample is > 50 ug/L. The currently available samples do not suggest that arsenic would be more abundant downdip in the center of the basin.

High arsenic values in the Edwards-Trinity aquifer are clearly spatially associated with the underlying Ogallala Fm.. There are no high arsenic concentrations outside of the Ogallala footprint. The Cenozoic Pecos Alluvium aquifer presents an interesting pattern, the Monument Draw Trough, on the east, contains several samples >10 ug/L, whereas the Pecos Trough, on the West, contains only background values.

D1-3.2 Arsenic Distribution in the Gulf Coast Aquifers

Similarly to the High Plains aquifer, the Gulf Coast aquifers offer a contrast in arsenic concentrations between the southwestern and northeastern sections. Approximately 13 percent of the 1,120 samples in the Gulf Coast aquifer sampled during the past five years have arsenic concentrations > 10 ug/L (2.1 percent > 50 ug/L) (Figure 9, Table 3). Arsenic concentrations were greater in the southwestern Gulf Coast (29 percent > 10 ug/L; 6 percent > 50 ug/L) than in the northeastern Gulf Coast (3.5 percent > 10 ug/ and none > 50 ug/L).

From a spatial standpoint, high arsenic concentrations are present along the Rio Grande valley, in the few counties west and southwest of Corpus Christi, as well as along the Catahoula outcrop extending into the northeastern Gulf Coast region (Figure 46). The highest arsenic concentrations (>50 ug/L) are located mostly along the Catahoula Fm. outcrop, as well as in Jim Hogg, Webb, and Duval Counties on one side and Karnes County on the other side. Elevated arsenic concentrations occur in both the outcrop and confined sections of the Gulf Coast aquifers. The highest arsenic concentrations are in the Jasper aquifer, stratigraphically located

next to and above the Catahoula Fm (48 percent of wells > 10 ug/L; 20 percent of wells > 50 ug/L). The Chicot aquifer, which is the youngest and stratigraphically most distant from the Catahoula Fm. displays much lower levels of arsenic contamination (27 percent of wells > 10 ug/L). The intermediate Evangeline aquifer has 21 percent of wells > 10 ug/L. A few isolated high arsenic sample points across the whole Gulf Coast may or may not be of local anthropogenic origin. Intermediate concentrations (10 – 50 ug/L) are more widespread and exist across all counties south of the San Antonio River. They are also present sporadically in the northeastern Gulf Coast (Brazoria and Galveston Counties). However, numerous concentrations <10 ug/L are also present within the areas of high concentrations. This is characteristic of arsenic hot spots across the world (Smedley and Kinniburgh, 2002).

Subtask D2. Evaluate Geologic Sources of Arsenic by Comparing Groundwater Arsenic Concentrations with Concentrations of Other Ions Using Existing Databases.

D2-1 General Geochemistry

D2-1.2 Geochemistry of High Plains Aquifer

The High Plains aquifer is generally unconfined, saturating the lower section of the Ogallala Fm. Rain water is concentrated by evapotranspiration in interplaya areas and flushed periodically to the playas during higher intensity events (Fryar et al., 2001; Wood and Sanford, 1995a). Playas are the main recharge features in the Texas High Plains (Scanlon and Goldsmith, 1987; Scanlon et al., 1994; Mullican et al., 1997). The imprints of calcite dissolution and ion exchange are added on the downward path to the water table or within the aquifer. The water has a resulting calcium bicarbonate or calcium/magnesium bicarbonate character with a pH in the 7-8 range and is oxidizing. Nativ (1988, Figure 25) showed that south and west of Lubbock, the water has higher TDS and has evolved into a mixed anion-mixed cation type (Ca-Mg-Na-HCO_3-Cl).

Groundwater is at equilibrium with calcite, as defined by a saturation index between -0.3 and 0.3, in about 60% of the samples with an additional 40% slightly supersaturated with a saturation index mostly between 0.3 and 1 (Figure 47). It has also exchanged some Ca and Mg ions for Na ions. Groundwater has also received minor contributions from the weathering of aluminosilicates. Fryar et al. (2001) studied chemical evolution of the groundwater along a few flow paths east of Amarillo in the southern part of the Central High Plains aquifer. Supported by inverse geochemical modeling, they suggested that most of the controlling chemical reactions occur while the water is moving through the unsaturated zone and that mixing is the major process occurring in the saturated zone.

The evolution of groundwater chemistry is sometimes more complex when interactions with underlying formation waters occur. Permian evaporite dissolution results in high TDS in groundwater just south of the Canadian River, as suggested by high chloride and sulfate, as well as isotopic studies (Mehta et al., 2000). McMahon (2001) also explained variations from low-TDS calcium bicarbonate water composition at a few locations by upward flow of Permian brines farther north on the Oklahoma-Kansas state line. Several explanations have been proposed for the regional increase in salinity in the southern High Plains, west and south of Lubbock. The spatial association of higher groundwater salinity and saline lakes (Figure 38) where groundwater discharges and evaporates led Wood and Sanford (1995b) to the conclusion that an oft-repeated cycle of wind deflation, particle deposition and dissolution, and discharge and evaporation caused the increase in TDS. Nativ (1988, p. 38) and Nativ and Guttierez (1988) suggested that the increase in sodium and chloride in both the Ogallala aquifer and the underlying Cretaceous aquifers implies a connection between them, particularly on the paleodivides. Isotopic studies also supported that hypothesis (Nativ and Guttierez, 1988). Nativ (1988), Nativ and Guttierez (1988), and Hopkins (1993) presented data suggesting that groundwater south and west of Lubbock results from the mixing of typical recharging water (as seen north of this NW-SE line) and of Cretaceous water. Studies north of Lubbock by McMahon et al. (2004b), in an area where the TDS is <500 mg/L (e.g., Figure 24 of Nativ, 1988) but close to Cretaceous subcrops, suggest that deeper water in the Ogallala aquifer resulted from mixing of Ogallala with about 20 percent Cretaceous waters. The conclusion was supported by an upward vertical hydraulic gradient in nested wells (p.14-15), consistent with the map presented in Nativ (1988), sulfur isotopes (p.19), and inverse modeling of geochemical reactions along flow paths (p. 28). Formation brines from leaking oil and gas wells, abundant in this area, have

also been suggested as a source for the higher TDS (Nativ, 1988). Several authors (Figure 8 of McMahon et al., 2004b; Nativ 1988) have noted that TDS close to the water table can be higher than in deeper sections of the aquifer as a result of downward transport of anthropogenic contaminants (mainly fertilizers).

A striking feature of the spatial distribution of TDS is its sharp increase west and south of Lubbock along the southern edge of the Clovis-Plainview paleovalley (e.g., Figure 12 sketches in Seni, 1980) and also noted by Hopkins (1993). The TDS distribution is affected by the NW-SE direction omnipresent in the High Plains. Seni (1980, p. 23) described a 15- to 30-m buried Cretaceous escarpment. This paleovalley approximately follows the Paleozoic Palo Duro Basin. High Plains aquifer pH distribution is uneven. The southern area southwest of Lubbock where most of the highest arsenic concentrations are located generally has a lower pH than the rest of the Ogallala aquifer (**Figure 48**a and b and Figure 49m).

Detailed petrology and mineralogy analyses of the Ogallala and Blackwater Draw Fms. are presented in Avakian (1988). These analyses are based on cores of 14 wells drilled in five counties in a transect from Lamb to Dickens counties. McMahon et al. (2004b, p. 9-14) evaluated petrology and mineralogy from cores of two wells drilled in Hale and Castro Counties. Both formations have very similar mineralogy. Quartz is by far the most common framework mineral. McMahon et al. (2004b) stated that feldspar, especially K-feldspar (85 percent of all feldspar grains), is minor detrital grains (~5-10%), whereas Avakian (1988) noted that both K-felspar and plagioclase make up from 5 to sometimes 50 percent of the framework grains. Clay minerals (illite ~ mixed layer illite-smectite > kaolinite) are ubiquitous, although in minor proportion in siltstones, sandstones, and conglomerates. The authigenic fibrous clay mineral attapulgite is widely distributed, albeit always in minor proportions (Avakian, 1988, p. 20). Calcite is locally an important authigenic cementing mineral. Rock fragments are also locally abundant. Through study of numerous thin sections, Avakian (1988) noticed that authigenic iron oxides and hydroxides are common and disseminated throughout the rock (grains <0.01 mm, Avakian, 1988, p. 36). The iron oxides coat the abundant quartz grains. McMahon et al. (2004b) also reported that in southeast Hale County, quartz is sometimes coated by clay and/or Fe-Mn oxides. In addition, detrital iron oxides (magnetite and hematite) make up most of the accessory minerals (up to a few percent of the framework minerals) (Avakian, 1988, p. 17). Magnetite is more abundant in the upper sections of the Ogallala Fm., whereas hematite is concentrated in the lower portions. Biotite is also described but is easily weathered. Both magnetite and biotite contain reducing Fe(II).

D2-1.2 Geochemistry of Gulf Coast Aquifers

Oakville Sandstone / Jasper Aquifer: The Oakville sandstone / Jasper aquifer is typical of Gulf Coast aquifers. A thin oxidizing recharge zone is located updip in the formation outcrop, whereas waters slowly become more reducing downdip. In the southwestern Gulf Coast area, the Oakville sandstone is between 100 and 200 m thick in the outcrop (Smith et al, 1982), consists of sandy deposits from several major fluvial systems, and grades downdip into finer deposits. Axes of higher transmissivity such as George West in Live Oak County include most of the uranium mines. TDS in the Oakville are generally in the brackish range (>1,000 mg/L) because of the impact of fault discharge (Smith et al., 1982, p.10) except in the outcrop area and initially along high-transmissivity zones. High concentrations of sulfate and chloride are associated with those faults (Figure 43, Wilcox Fault Zone, and Figure 2 of Henry et al., 1982a). Sulfate could also originate from dissolution of evaporites locally present in playa-floodplain facies (Henry et al., 1982a). In the northeastern Gulf Coast, the same aquifer does not show such high TDS and remains mostly below 1,000 mg/L (Henry et al., 1982a). Hydrochemical facies evolution ranges from calcium bicarbonate in the recharge zone to sodium bicarbonate chloride farther downdip with a strong sulfate component (Smith et al., 1982, p.13-14) in the

southwestern Gulf Coast, whereas in the northeastern Gulf Coast, the hydrogeochemical composition is in the sodium bicarbonate range.

In the southwestern Gulf Coast, geochemical evolution reflects the impact of both Ca/Na cation exchange on clay and fault discharge, possibly from different depths. Following a pattern similar to that of TDS, Eh conditions vary from strongly oxidizing in the recharge area (470 mV) to reducing farther downdip (-170 mV), with variations due to conductivity changes and proximity to faults. The decrease is not progressive but moves through plateaus at ~400, ~50 and ~-100 mV (Henry et al., 1980; Galloway, 1982, p. 21 and his Figure 18). Values of pH increase more or less regularly from ~7 to 8.

Smith et al. (1982, their Figures 19 and 21 to 23) presented spatial distribution of uranium, molybdenum, selenium, and arsenic with inferred isopleths. All ions increase from the northeast to the southwestern Gulf Coast. Galloway (1982, his Figure 18) presented a typical downflow evolution with uranium and selenium decreasing downdip while Mo stays high.

The Oakville sands consist of quartz-poor litharenites or feldspathic litharenites (classification of Folk, 1974) (Galloway et al., 1982, p. 23). Galloway (1982, p. 2-3) and Galloway et al. (1982, p. 24) suggested that sediments were deposited in an arid environment in a typical redbed system with hematitic alteration. Whole-rock analysis suggests that iron oxides are common in the subsurface (2% in Table 1 of Galloway, 1982). Diagenetic calcite cement is also abundant. Fine-grained sediments within the formation mainly consist of montmorillonite and illite. Galloway et al. (1982, p.23) suggested that montmorillonite is derived from older strata rather than an alteration product of ash material.

Catahoula Formation. The Catahoula Fm. comprises two large fluvial systems: the Gueydan system southwest of the San Marcos Arch and the Chita-Corrigan system to the northeast. The Gueydan system was deposited under semiarid conditions, and sediments show a strong volcanic influence, including numerous occurrences of airborne volcanic ash (Galloway, 1977). Thickness ranges from 60 to 300 m (Galloway, 1977, p.3). Fant Tuff, Soledad Conglomerate, and Chusa Tuff are members of the Catahoula Fm. The petrologic composition of the Gueydan system consists of a mixture of feldspar plagioclase, quartz, and volcanic fragments in subequal proportions (feldspathic litharenite or lithic arkose according to Folk's classification, 1974) in sandy intervals. They also contain up to 4% magnetite/ilmenite (Galloway, 1977, p.23). The dominant clay mineral in the clayey petrofacies is montmorillonite, most likely derived from alteration of volcanic ash rather than reworking of older units.

Subsequent diagenesis decreased the permeability of the sand as a result of clay coating and calcite cement. Clayey facies have low permeability, although before alteration they may have had much higher permeability, allowing leaching of uranium and other trace metals very soon after the depositional event. Current trace metal concentrations in the Catahoula Fm. rocks do not show any particular enrichment, suggesting that leaching occurred early after deposition.

Within the Catahoula Fm., the Chita-Corrigan system of central and northeastern Gulf Coast has lower TDS than its southwestern counterpart, the Gueydan system. The Chita-Corrigan system also has a more typical hydrochemical evolution, albeit complex, starting with calcium bicarbonate waters, then increasing in sodium by ion exchange and chloride. The Catahoula Fm. in the southwest has relatively high TDS, attributed to the impact of deep water, except in sandy lobes following major depositional sandy channels (Galloway and Kaiser, 1980, p.25). Current water composition of the Catahoula Fm. is dominated by sodium bicarbonate chloride and sodium chloride (Galloway and Kaiser, 1980, p.19). High chloride content in the shallow subsurface suggests the long-term influence of deep brines mixing with recharging waters. The formation pH varies from neutral to alkaline with values locally >10 in ash beds (Galloway and Kaiser, 1980, p. 27).

D2-2 Crossplot Analyses

Groundwater arsenic concentrations were plotted against a variety of variables to better understand sources and mobilization mechanisms of arsenic. Crossplots include arsenic vs. oxyanions (B, Mo, Se, V) and other trace elements (F, U, perchlorate), arsenic vs. environmental parameters (pH, alkalinity, TDS/conductivity), arsenic versus major ions (sulfate, chloride, bicarbonate) and minor ions (silica, nitrate, iron). Other environmental parameters such as dissolved oxygen/Eh, well depth, water table depth, and aquifer saturated thickness were also plotted or are discussed in other sections.

D2-2.1 Arsenic and Covariates (southern High Plains)

Arsenic distribution in the southern High Plains was already discussed in a previous section. There is a clear spatial association between arsenic and other oxyanions (B, Mo, Se, V), as well as with fluoride. Table 16 presents a summary of the correlations displayed in Figure 50. The highest correlation is with vanadium (r2=0.65) followed by fluoride (r2=0.30) then by molybdenum (r2=0.18), boron (r2=0.17) and selenium (r2=0.14). Arsenic concentration also increases with that of major anions (chloride, sulfate, bicarbonate) but only when the whole High Plains data set is considered. Correlations are low when applied to only the SHP-S region (presented r2 values are only computed for SHP-S).

All of the more than 800 analyses for beryllium presented in the TWDB database for the area south and southwest of Lubbock are less than the detection limit of 1 ug/L. However, this does not preclude a relationship with arsenic because beryllium concentrations are typically lower than 1 ug/L.

A recent perchlorate study (Jackson et al., 2004) found that perchlorate correlates with Cl, Br, F, SO_4, K, and Mg but not with NO_3, Na, or Ca. Potential sources for perchlorate include anthropogenic fertilizers and natural sources (possibly in association with evaporites). Other sources such as industrial sources from explosives (unlikely given the spread of the contamination in a largely agricultural area) or in-situ generation by redox reactions (lightning strikes on buried metallic objects, cathodic protections for oil wells) were eliminated. High-perchlorate waters are concentrated in the upper half of the aquifer. However, the only other local aquifer with perchlorate > 4 ug/L is the underlying Dockum aquifer.

D2-2.2 Arsenic and Covariates (southwestern Gulf Coast)

High arsenic concentrations are present along the Rio Grande valley, in the few counties west and southwest of Corpus Christi, as well as along the Catahoula outcrop extending into the northeastern Gulf Coast (**Figure 54**a). In the southwestern Gulf Coast, the Jasper aquifer contains the most samples larger than 10 ug/L (47.5 percent > 10 ug/L; 20 percent > 50 ug/L), whereas the Evangeline and Chicot aquifers contain 21 percent > 10 ug/L and 27 percent > 10 ug/L (**Figure 53**). Molybdenum (**Figure 54**b) and vanadium (**Figure 54**d) follow the same pattern. However, Se (**Figure 54**c) is mainly present along the Rio Grande valley and much less in those counties west and southwest of Corpus Christi. Uranium is also high along the Catahoula outcrop, west and southwest of Corpus Christi, and along the Rio Grande (**Figure 54**g). There is a clear spatial association on the regional level between As, Mo, Se, V, and U. This regional association is less clear on cross-plots for reasons to be detailed later (Table 17 and **Figure 55** and Figure 56).

Similarly to the High Plains area, arsenic concentration has been plotted against a variety of variables to understand its behavior. Plots were made for two databases: TWDB and NURE. The NURE database has incomplete spatial coverage and produces noisy crossplots, but most samples were analyzed for major, minor, and trace elements. It also provides total well depth but gives no information about the sampled aquifer. Coverage by the TWDB database is more uniform and does includes aquifer information, but samples were more rarely analyzed for trace

elements. Cross-plots were built by using data from the same samples (same well, same date). Data from the same well with, for example,arsenicconcentration in year 1 and Mo concentration in year 2 were not retained. In addition, two cross-plots per element (for Mo, Se, V, and B) are displayed for the TWDB database. One set of cross-plots represents those data points where both As and the companion ion were above detection limits. The other set includes all data points, regardless of detection limits. The latter was used to assess concentrations of one ion when arsenic concentrations were below the detection limit. **Figure 54** shows a clear contrast between arsenic concentrations in the southwestern and northeastern Gulf Coast. When appropriate and as noted, some of the figures include the whole Texas Gulf Coast, whereas in other instances, only the southwestern Gulf Coast samples were used. In addition, most plots do not discriminate between the different units of the Gulf Coast aquifers (Jasper, Evangeline, and Chicot aquifers). The highest correlation is with vanadium (0.43) followed by molybdenum (0.36). Other covariates do not have correlations as strong as in the High Plains aquifer.

Molybdenum (**Figure 55**a and **Figure 56**a and b) and vanadium (**Figure 55**c and **Figure 56**e and f) still correlate relatively strongly with arsenic, whereas selenium (**Figure 55**b and **Figure 56**c and d) seems independent of arsenic. Nevertheless As, Mo, Se, and V, as well as U, are spatially associated at the regional scale, pointing to a regional origin of the arsenic contamination (volcanic ash?). Ions of those five elements do not always behave similarly in the subsurface, explaining the discrepancies in the details. Fluoride has, for the most part, concentrations below the MCL of 4 ppm (**Figure 54**f) and seems to be correlated with arsenic (**Figure 56**i). In addition, silica (**Figure 55**f and **Figure 56**i), bicarbonate (**Figure 55**h and **Figure 56**j), and sulfate (**Figure 55**i and **Figure 56**j) do not seem to controlarsenic distribution. A weak correlation with TDS (**Figure 54**h and **Figure 56**l) suggests that longer residence time or mixing with more saline waters may explain part of the high arsenic concentrations. Redox conditions do not seem to impact arsenic distribution, as noted by several authors, as long as they are not too reducing and the sulfur activity is low (**Figure 69**). High arsenic concentrations seem to be present in an optimal depth range, particularly in the Jasper aquifer (**Figure 57**).

D2-3 General Mechanisms of Arsenic Release

A review of the global distribution of arsenic contamination provided by Smedley and Kinniburgh (2002) indicates that there are several potential release mechanisms (Welch et al., 2000; Smedley and Kinniburgh, 2002):

1) dissolution of arsenic-bearing minerals,
2) mixing with geothermally influenced water, and
3) desorption from iron oxides.

Oxidation and dissolution of arsenic-bearing minerals such as arsenic-rich pyrite or arsenopyrite can lead to high arsenic concentrations. It also leads to low pH and favors the production of iron oxides that can mitigate the impact of arsenic release. Lowering of the water table can bring those sulfides to oxidizing conditions. Magnetite (Fe_3O_4) and ilmenite ($FeTiO_3$) can also contain arsenic and vanadium (Smedley et al., 2002, p. 280; Smedley and Kinninburgh, 2002, their Table 3) and other trace elements. Geothermal waters can bring arsenic to the shallow subsurface. This case can be generalized by adding mixing from deeper formations lacking geothermal character.

Desorption from iron oxides is commonly invoked to explain high arsenic concentrations in water. It could occur because the oxides themselves are being dissolved (reductive dissolution, most likely biomediated), as suggested in Bangladesh (Smedley and Kinniburgh, 2002). Kresse and Fazio (2003) suggested that As contamination in an alluvial aquifer in Arkansas is related to reductive dissolution of iron oxides rather than anthropogenic soil arsenic compounds. This hypothesis is supported by spatial correlations between As, Fe, nitrate, and ammonium ions and by the presence of abundant organic matter (Kresse and Fazio, 2003, p.18). Alternatively,

desorption can be due to a change in environmental conditions such as an increase in pH, competition from introduced oxyanions (e.g., phosphates), or mutual competition by other sorbates. Crystallized iron oxides, such as hematite, do not sorb as much arsenic as less ordered and hydrated species (ferrihydrite, goethite). Yet iron oxides typically precipitate under the latter form in conditions expected in a shallow aquifer and then age into the former (see Appendix I). There are indications that the process involves destruction of the mineral structure and reprecipitation of hematite, whose crystallographic structure can accommodate more arsenic. More generally, as described in Appendix I, arsenic sorption on iron oxides could be impacted by phosphates, carbonates (Appelo et al., 2002), organic matter (Redman et al., 2002), and maybe silica (Dixit and Hering, 2003).

Dissolution of silicates and carbonates generally leads to an increase in pH. Alteration of silicates raises pH because it consumes protons (Smedley and Kinniburgh, 2002; Sracek et al., 2004). This is particularly true in the presence of plagioclase because plagioclase feldspars are less stable than potassium feldspars. When the degradation product is kaolinite, the reaction is written as:

$2NaAlSi_3O_8 + H_2O + 2H^+ = Al_2Si_2O5(OH)_4 + 2Na^+ + 4SiO_2$

$CaAl_2Si_2O_8 + H_2O + 2H^+ = Al_2Si_2O5(OH)_4 + Ca^{+2}$

Silica is also generated, along with clay minerals, in the alteration of plagioclases. Silica can compete with arsenic for sorption sites. Calcite dissolution by carbonic acid consumes H^+ and also raises pH

$CaCO_3 + H^+ + HCO_3^- = Ca^{+2} + 2HCO_3^-$

Increase in CO_2 pressure in the presence of calcite will raise pH. An increase in CO_2 pressure can result from biological activity. Mixing with higher-pH waters can also raise pH with no need for extrinsic arsenic. Ion exchange, which typically consumes Ca, also impacts pH.

Hydrodynamic factors are also important to consider for all of the three general mechanisms. The rate of arsenic release relative to the flushing rate of the aquifer impacts arsenic concentration (Table 1 and Smedley and Kinninburgh, 2002, p. 556). Arsenic released at a high rate into an aquifer can be quickly flushed from the system with the overall arsenic aqueous concentration remaining low. Alternatively, stagnant or very slow moving water may have high arsenic concentrations even if the release rate is low.

D2-4 Potential Natural Sources of Arsenic

D2-4.1 Potential Natural Sources of Arsenic in the High Plains

Elevated arsenic concentrations in the High Plains have been attributed to various natural sources, including Permian brines (McMahon, 2001), upward or lateral flow from Cretaceous subcrops (Nativ, 1988), volcanic ash of variable origin, and saline lakes. Understanding arsenic behavior in the High Plains aquifer requires knowledge of the source and mobilization mechanism, and ensuring an accurate mass balance of arsenic. Any hypothesis should include an explanation for the sharp contrast between northern and southern areas of the Texas High Plains. Considering the High Plains aquifer as an open system, the origin of arsenic in the formation may be intrinsic to the aquifer system (volcanic ash layers, detrital minerals, evaporative concentration) or extrinsic through water originating from underlying formations (Cretaceous, Dockum, Permian) and/or from the Rocky Mountain area.

Arsenic accumulation may still be active (arsenic is added to the system) or relict (no mass of arsenic is added to the formation). In the latter case, arsenic will be flushed progressively out of the formation. The overall young age of the Ogallala water (less than 10,000 years, Figure 12 of McMahon et al., 2004b) suggests that flushing may still be active today. Additional data by Dutton (1995) confirm the relatively young age of the Ogallala water. He reports a percent

modern carbon (pmc) of 40.3±13.8 in the southern High Plains in six wells in Randall, Swisher, and Floyd counties in the north section of the southern High Plains. This translates into an average age of ~7,300 years. Isotopic analyses also suggest that Ogallala water was recharged under the current warm and dry climate that followed the last glaciation about ~10.000 years ago. By contrast a similar analysis of the confined Dockum aquifer yielded an age of 25,000 to 50,000 years.

A crude computation sheds light on the arsenic mass balance. If the Ogallala sediments are 5 millions years (Ma) old on average, a total of at least 5×10^6 yr / 1×10^4 yr = 500 pore volumes has flowed through them. For an average arsenic groundwater concentration of 20 ug/L, this represents a mass of 0.02 × 500 = 10 mg/L of water. Assuming a porosity of n = 0.2, this translates into depleting the rock of $10\times n/(1-n)/2.65$ ~ 1 mg/kg. This simple calculation can be linearly scaled by the sediment age (10 Ma translates into 2 mg/kg), arsenic aqueous concentration (50 ug/L translates into 2.5 mg/kg), or the average water residence time (5,000 years translates into 2 mg/kg). This most likely represents only a fraction of the whole rock amount of arsenic, although the world-wide average arsenic concentration for sandstone is ~ 1 mg/kg (Table 11).

Most of the arsenic is likely to be associated with a solid phase, either part of the mineral structure (in pyrite, arsenopyrite, and other minerals), or sorbed to a mineral or organic surface. Iron and manganese oxides are common in the formation and can sorb and scavenge most of the arsenic. A change in environmental conditions may not change the total mass of arsenic in the formation but will change the balance between sorbed and dissolved fractions, as well as possibly the redox state of the arsenic. A change from reducing to oxidizing conditions will mobilize arsenic contained in sulfides. Conversely a change from oxidizing to reducing conditions can desorb arsenic from the iron oxides that are being dissolved (reductive dissolution). A raise in pH with no change in redox conditions will also mobilize sorbed arsenic. Addition of new competing ions could have the same results without a change in either pH or Eh.

Volcanic Ash Layers of Ogallala Age

Rhyolitic ash layers have been described within the Ogallala and Blackwater Draw Fms. (Table 18). Those ash layers are collectively described as Pearlette ash. Pliocene and Pleistocene ash falls in the United States originated from three main centers: the Yellowstone area in Idaho and Wyoming, the Long Valley–Glass Mountain area in California, and the Jerez Mountain area in New Mexico (Izett, 1981). Some events, such as the Lava Creek B or Huckleberry Ridge event, blanketed most of the western United States, including the Texas Panhandle (event name is related to the location where the ashfall was studied and generally not to the source). Ash layers of similar age have been recognized in the Blackwater Draw Fm. (Frye and Leonard, 1957, p.22). Gustavson et al. (1991) mentioned Lava Creek B, dated at 0.62 Ma, and Huckleberry Ridge (2.2 Ma) volcanic ash layers present on terraces of the Pecos and Canadian River valleys, north and east of the southern High Plain aquifer, respectively. Gustavson (1996, p. 46) also noted the Guaje ash (1.4 Ma) present in Crosby County. Izett (1981) also cited the Mount Blanco event (2.3 Ma). Ash-bed thickness is on the order of 0.3 m (e.g., Figure 5 in Gustavson et al., 1991). Cepeda (2001) suggested that there are at least 10 volcanic beds in the Ogallala and Blackwater Draw Fms. originating from the Yellowstone area in the past 12 million years and varying in thickness from 0.3 to 1.5 m. He described a 1-meter-thick ash bed in the northern Panhandle in Potter County. Hanan et al. (1998) found expression of those ashfalls in Gulf of Mexico turbiditic sediments.

Volcanic ash, some with high U content and As by inference, is not uncommon in Pliocene and Pleistocene sediments. Because the source of the ash was hundreds to thousands of miles away in most cases and blanketed most of the Texas Panhandle, it still leaves open the

question of the presence of As only in the southern section of the southern High Plains. Assuming that the whole Texas High Plains aquifer had been subjected to the same conditions, one would expect higher concentrations in the north than in the south because volcanic sources are mostly in the northwest United States. A preliminary study performed for this work and presented in Appendix III suggests that ash bed relicts (Figure 58) may be more abundant in the southern region of the southern High Plains. However, a simple mass balance calculation suggests that the mass of arsenic available may not be sufficient to explain the current elevated arsenic concentrations.

Desorption from Iron Oxide Coatings

Most of the Ogallala sediments originated from the ancestral Rocky Mountains before the Pecos River valley cut this supply source (~4 Ma ago). Intense calichification and eolian mobilization and deposition were the two mains processes affecting the High Plains after this event. Ogallala sediments are rich in secondary iron oxides, and it is conceivable that arsenic was incorporated during mineral growth or sorbed at a later time to the oxide surfaces. The arsenic would have originated in the Rocky Mountains area or in now-eroded local Cretaceous rocks, would have been transported either in losing surface streams or in groundwater, and would have been immobilized in the Ogallala sediments. Only the area south of the southern High Plains aquifer would have been contaminated by arsenic because only the most recent alluvial fan moved sediments from farther west arsenic-rich areas such as Colorado uranium deposits (also rich in arsenic) and other volcanic rocks.

Saline Lakes

A total of ~ 40 saline lakes having total concentration as high as 430 g/L have been described in the southern High Plains (Wood and Jones, 1990) (**Figure 38**). They vary in size from less than 1 km^2 to tens of square kilometers. They are different from the ~25,000 playas that dot the Texas Panhandle. Playas are generally smaller and have a circular shape (< 1 km of diameter, Osterkamp and Wood, 1987) and are venues for recharge to the aquifer (Scanlon and Goldsmith, 1987; Scanlon et al., 1994; Mullican et al., 1997). They are also more abundant toward the north of the panhandle. Saline lakes discharge groundwater, are oftentimes elongated in shape, and are restricted to the southwest of Lubbock. Wood and Jones (1990) dismissed the hypothesis of migrating brines as the source of the high salinity on the basis of chemical ratios, particularly Br/Cl. They presented convincing evidence that groundwater discharge and runoff water feed the lakes. Most of the lake bottoms are lower than the Ogallala-Cretaceous contact, and the discharging groundwater is mainly from the Cretaceous aquifer. Some of the lake water is also recycled as it infiltrates through the lake bottom and is mixed with groundwater discharging into the lake, possibly generating saline springs (Wood and Jones, 1990).

The spatial association of higher groundwater salinity and saline lakes where groundwater discharges and evaporates led Wood and Sanford (1995b) to the conclusion that an oft-repeated cycle of wind deflation, particle deposition and dissolution, and discharge and evaporation caused the high TDS in the south section of the southern High Plains aquifer. There is no question that the TDS is locally impacted by the saline lakes (e.g., study of Double Lake by Wood and Sanford 1995b). However, the problem of the origin of the large spatial distribution of higher TDS remains. A crossplot of chloride vs. arsenic in the south of the southern High Plains show no correlation between the conservative solute and arsenic, as would be expected (Figure 50j)

Arsenic would be passively concentrated in the brine and transported along with other particle constituents. Wood (2002) suggested a similar mechanism to explain the relatively high uranium concentrations in the sand dunes associated with the lakes. Gypsum, halite, and sodium sulfate are present in the lake bottom, as are clays (Parry and Reeves, 1968). Arsenic

would most likely be transported with the clay fraction. In that case, arsenic behavior should be similar to anthropogenic arsenic. A similar hypothesis of atmospheric deposition with saline lakes as source was postulated for perchlorate contamination occurring roughly in the same regional area of the southern High Plains. Perchlorate is known to form or integrate evaporites. However, no perchlorate was detected within the saline lakes (Jackson et al., 2004, p. 140).

This hypothesis, however, cannot explain elevated arsenic concentrations in areas without saline lakes such as Yoakum and most of Gaines and Terry Counties unless currently buried saline lakes have been recurrent during the Ogallala depositional history.

Cretaceous Subcrops:

Cretaceous subcrops in the Panhandle consist of mainly marine shales in their upper section overlying a lower section dominated by limestones (Nativ and Gutteriez, 1988). Walnut, Comanche Peak, and Edwards limestones, as well as the Trinity/Paluxy/Antlers sandstones farther down in the section, are aquifers (Figure 39). Figure 39 displays two somewhat similar interpretations of cores and well logs mapping the extent of the Cretaceous. The largest Cretaceous subcrop in the interpretation by Nativ (1988) has been used by the TWDB as the outline of the High Plains Edwards-Trinity minor aquifer. Interpretation by Brandt (1953) is consistent with that of Nativ (1988) in that most of the Cretaceous, except maybe some Antlers (Paluxy) remnants, is missing in the southernmost main depositional axis of the Ogallala Fm. The Ogallala aquifer overlies the shaly upper section of the Cretaceous profile when present, that is, mostly on the northern limit of the Cretaceous subcrop. Both shale formations (Kiamichi shale and Duck Creek shale of the Frederickburg and Washita groups) are described as yellow-brown to dark-gray color with thin intercalations of limestone and sandstone. The maximum cumulative observed thickness of the shale section is 45 m (148 ft). The Kiamichi Shale Fm. crops out in some localities in Lynn, Terry, Hockley, Lamb, and Bailey counties (Brandt, 1953).

Kiamichi shale could be a source of arsenic because Cretaceous times are known for higher than average volcanic activity and because clay minerals scavenge and accumulate trace metals, especially if they are organic matter rich such as black shales (Guilbert and Park, 1980, p. 702-703). Selenium contamination in the Central Valley in California is thought to originate in the Moreno Shale cropping out in the nearby Coastal Range (Presser, 1994). The Kiamichi Fm. is described as a black shale between the Hill Country in Central Texas and the Red River in the east Texas Basin (Neeley, 1994). However, Sidwell (1936) described the Kiamichi shale in the Panhandle as composed of quartz primarily. Some pyrite is also present. He did not describe any feldspar (actually specified as absent) or clay minerals. However, Brandt (1953, Table 3) gave a normative composition with 17% Al_2O_3 showing the presence of clays (more likely than feldspar at that grain size). This is corroborated by Kessinger (1967), who indicated influx of a quartz mud in Kiamichi sediments but also the presence of dark-gray shale with a paucity of fossils, reflecting a reducing environment and analogous to the black shale accumulation to the East. Bishop (1967) published a detailed stratigraphy of the Kiamichi Fm. but with little information about its facies in the Texas Panhandle. Eargle (1956) reported 10 ppm uranium in the Kiamichi Clay Fm. at King Mountain in Upton Country, south of the High Plains. A large segment of the Kiamichi Fm. is slightly radioactive in that area. No arsenic analysis was made.

There are two possible scenarios to account for a Cretaceous origin of the arsenic: current cross-formational flow and/or paleo-accumulation following erosion of the Cretaceous material. Nativ and Gutteriez (1988) and McMahon (2001) described potential areas of upward flow in association with Cretaceous subcrops by mapping and comparing heads in both the Ogallala and the Cretaceous aquifers. Upward flow would be present in the larger northern subcrop. Blandford and Blazer (2004), using a model recently constructed for the regional Groundwater Availability Model (GAM) groundwater studies (Blandford et al., 2003), suggested that cross-

formational flow is downward, at least in the smaller southern subcrop (**Figure 39**). In addition, along paleovalleys Cretaceous subcrops are at higher elevation than the bottom of the Ogallala sediments, making cross-formational flow possible without head difference in the vertical direction. The second scenario does not involve current hydrogeology but would rely on iron oxide coatings that would have been enriched during the erosion of some arsenic-rich layers. This scenario is similar to the one described above with the Rocky Mountains as a source, except that the source is more local. The lack of good spatial fit between the elevated arsenic concentrations and the Cretaceous subcrops suggests that, although some of the contamination may be genetically linked to them, other elements are at play. The lack of arsenic in the Edwards-Trinity Plateau aquifer (Figure 45b) demonstrates than there is no intrinsic arsenic source in the Cretaceous water-bearing formations (Antlers and Edwards Fms).

Dockum Formation:

Analyses for arsenic in the Dockum Fm. are mainly from the outcrop area (outside of the Ogallala footprint) and that portion of the aquifer having a TDS <5,000 mg/L (sometimes within the Ogallala footprint). Only 10% of the ~200 Dockum data points are above the 10 ug/L threshold (with a maximum of 26 ug/L). Distribution of arsenic concentrations >10 ug/L in the Dockum aquifer seems more even than in the Ogallala aquifer. However, water-bearing beds in the Dockum are mostly in the lower section of the formation, although some local sandy layers exist within the red beds forming most of the upper section. Red beds are mostly made of clays and silts and have very low permeability. It would not be easy to leak water to the High Plains aquifer. In addition, heads in the Dockum are lower than that of the High Plains aquifer (Bradley and Kalaswad, 2003). The currently available data do not suggest that arsenic would be more abundant downdip in the center of the basin underneath the region with elevated arsenic concentrations or that this area.

Permian and Older Formation Brines

There are few available analyses of arsenic concentration in Permian rocks and brines. A request to oil and gas vendors of geochemical data was unsuccessful because very few formation waters are analyzed for arsenic. Parkhurst et al. (1995) studied the Central Oklahoma aquifer developed on rocks of Permian age and described high concentrations of arsenic, molybdenum, selenium, and vanadium. Trace analyses performed on 220 samples yielded 90th percentile and maximum values for As (8 and 110 ug/L), Mo (7.5 and 80 ug/L), Se (20 and 190 ug/L), and V (91 and 560 ug/L) (their Table 1). Those values can be considered low, given the generally high TDS of the formations. In addition, high uranium concentrations are also known to occur in the aquifer. In their study of perchlorate distribution in the High Plains, Jackson et al. (2004) suggested that perchlorate could diffuse from the Permian evaporites to overlying aquifers through fractures. Permian heads do not reach the elevation of the High Plains aquifer. Permian Fms are not considered viable arsenic sources for the Ogallala contamination.

D2-4.2 Potential Natural Sources of Arsenic in the Gulf Coast

In the southwestern Gulf Coast, arsenic contamination has been attributed to the presence of the uranium mining province and of abundant ashfall or reworked volcanic materials. Other felsic rocks also contain high uranium concentrations. Volcanic ash, however, fully degrades in a short time, maximizing release of trace elements. Numerous abandoned and reclaimed open pits and solution mining operations (some active as of August 2005) are in the same general area as the high arsenic concentrations (Figure 59). Worldwide, arsenic is often associated with uranium. A genetic link is often made (e.g., Nugent et al., 1994), although no specific mechanism is invoked. It could then be due to direct natural contamination through economical but also substandard uranium accumulations or possibly anthropogenic contamination through mining operations and tailings.

Volcanic Ash / Uranium Deposits

Numerous small uranium deposits were exploited from the 1950's to the early 1990's in the southwestern Gulf Coast. Those deposits are thought to be genetically linked to the arsenic anomalies. Appendix II contains a more detailed description of the uranium province. The deposits are all geographically associated with the Oligocene Catahoula Fm., as well as the upper section of the underlying Eocene Jackson group and the overlying Miocene Oakville sandstone (Henry et al., 1982b, p. 6). A few deposits have also been exploited in the Pliocene Goliad sands. The main mining and exploration area encompassed a large section of the southwestern Gulf Coast from the Mexican border to San Marcos Arch, although uranium showings have been described as far as the northeastern Gulf Coast (Ledger, 1981). The strong relationship of most uranium deposits with high transmissivity sands suggests a genetic connection. The deposits are strata-bound and belong to the epigenetic type (Figure 22 of Galloway, 1982) where multiple influx stages of reducing fluids into the aquifer or products thereof reacted with the uranium-bearing oxidizing waters. The mineralization consists mainly of a matrix of iron sulfides (1-2%) cementing the sandstone silicic clasts with interstitial grains of uranium minerals. The deposits initially exploited resulted from the surface oxidation of the original deposits. RRC (Nugent et al., 1994) did a study of the impoundment waters lying in the excavations before reclamation and of the soil/spoils. Soil/spoil arsenic grade is ≤ 300 ppm (single outlier), but the average value is ~20 ppm (their Table 16). All arsenic aqueous concentrations were less than 30 ug/L, despite TDS being above 1,000 mg/L. The water pH was between 7.6 and 8.2. All selenium aqueous concentrations were below the detection limit of 6 ug/L. Uranium and molybdenum concentrations were often in the hundreds of micrograms per liter (their Appendix A.6). The source of the impoundment water is both runoff and groundwater. The RRC observation is consistent with conclusions by Brandenberger et al. (2004), who found that mine tailings have little impact on the regional surface water quality. Henry et al. (1982a) also stated that the chemical composition of the water matches that of the regional aquifer except in the middle of the ore body. Adidas (1991) studied the impact of local uranium mines on the water quality of the small town of Bruni in Webb County and found no relationship.

Deposits were exploited mainly in open pits, very rarely in underground mines. In a later phase, the exploitation shifted to solution mining, particularly for deeper, reduced deposits. Alkaline-leach mining where sodium or ammonium bicarbonate is injected with oxidants (O_2, H_2O_2, $NaClO_3$) to solubilize uranium as uranyl-carbonate complexes (Henry et al., 1982b, p. 13) was employed at many locations. At such high pH, most of the sorbed oxyanions are released into the fluid stream despite the oxidation of pyrite into iron oxides. Aquifer contamination could be a problem if hydraulic control is not mastered. Another process at low pH, the acid leach method, seldom used in the southwestern Gulf Coast, would solubilize uranium but not as much the oxyanions. Kingsville Dome uranium mine is active as of 2005. Deposits have formed with and without organic matter. In the latter case, H_2S from underlying hydrocarbon accumulations or Cretaceous brines flowing up along faults is thought to be the reducing material (Goldhaber et al., 1978) directly or indirectly through pyrite formation before encountering uranium-rich waters. However, brines did not transport uranium to the district (and very likely not As) but only provided reducing material.

Henry et al. (1982a, p.46) stated that higher concentrations of trace elements were to be expected in the Oakville sandstone. It has been postulated that solutions genetically connected to the mineralizations were more concentrated than current groundwater. The most likely reason is the lack of current source. The likely sources, ash layers in the Catahoula, Fleming, and possibly Oakville Fms., had been depleted, although some authors (e.g., Ledger, 1984) argue that leaching is still ongoing. Actual concentrations in oxidizing waters may reflect equilibrium between adsorbed and dissolved phases rather than dissolution from the source. Henry et al.

(1982a, p. 46) did not try to model the chemistry of adsorption of uranium and other trace elements including arsenic.

Galloway et al. (1982) hypothesized that the current position of the redox front is apparently updip of what is was during mineralization owing to additional H_2S. They identified three distinct redox zones within the Oakville aquifer: An upper oxidizing zone with Eh>200mV extends to ~ 250 m depth. A farther downdip intermediate zone has Eh between 300 and -40 mV and low but detectable H_2S, and a lower zone has Eh<-40 mV. The third zone is located in deeper sections of the aquifer but also closer to the surface along fault traces. In deposits where the redox gradient is sharp, uranium, molybdenum, selenium, arsenic, and vanadium minerals are found next to each other. However, where the redox gradient is low, more separation is expected with molybdenum and arsenic precipitating farther dowdip and vanadium even farther.; It follows that arsenic, molybdenum and vanadium aqueous concentrations can stay high if conditions are not too reducing.

Granite and volcanic ash derived from high-silica igneous systems are the sources of uranium in sedimentary mineral deposits (Finch, 1967). Some early workers thought there were nearby volcanic sources of uranium in south Texas (e.g. Bailey, 1924, 1926). More recent workers (McBride et al., 1968; and Parker, et al., 1988) have discounted this idea and shown there to be three possible distant sources of volcanic material: (1) the Trans-Pecos Volcanic Field located in the Big Bend region of Texas and adjacent Chihuahua, Mexico. (2) the Sierra Madre Occidental of central Mexico, and (3) Cretaceous intrusive rocks near Uvalde, Texas.

Volcanic activity in the Trans-Pecos Volcanic Field began approximately 35 to 40 million years ago (Ma), or during middle to late Eocene, coincident with deposition of the upper Jackson Group units. A period of active caldera-forming volcanism occurred between 38 and 32 Ma (late Eocene to early Oligocene), resulting in generation of large amounts of volcanic air-fall and ash-flow deposits know as ignimbrites (Henry et. al, 1986). This volcanic activity may have been ongoing during deposition of the Catahoula Fm. Between 34 and 23 Ma, explosive volcanic activity from large caldera complexes in central Mexico produced huge volumes of rhyolitic ignimbrite (McDowell and Claubaugh; 1979). Volcanic material in the Goliad Fm. is probably reworked volcanic debris from the Catahoula Fm. because it is much younger than the period during which rhyolitic volcanism was active in Trans-Pecos Texas and central Mexico.

Parker et al. (1988) confirmed through petrologic analysis that volcanic clasts found in coarse-grained Gueydan deposits in northwestern Duval County were transported from the Trans-Pecos Volcanic Field. They showed these clasts to be distinct from Cretaceous-age intrusive igneous rocks near Uvalde, Texas. The dominant clasts identified were mafic trachyte and basalt, but high-silica devitrified rhyolite and welded ash-flow tuff clasts were also noted (Parker et al., 1988). Welded ash-flow tuff is composed of volcanic glass shards that became sintered soon after deposition and is therefore capable of being transported without disintegrating. Southwest to northeast high-altitude wind patterns have most likely persisted in southern North America since the beginning of the Tertiary Period (McBride, 1968) and could easily have transported ash from central Mexico and Trans-Pecos Texas into the Gulf Coast Plain of Texas.

It is informative to understand why the Catahoula Fm. did not yield economic uranium deposits in east Texas where it is also present (100-200 meters thick as opposed to 300 m thick south of the San Marcos Arch, Ledger, 1981, p.5). This lack of uranium deposits is associated with lower arsenic concentrations in groundwater. Farther away from the emission centers in west Texas, ashfall deposits are common in the Catahoula Fm. of the northeastern Gulf Coast. However, this region is missing the stream-transported volcanoclastics abundant in the southwestern Gulf Coast. The key observation relates to the degree of degradation of the glassy material whose alteration mobilizes and solubilizes uranium. Glass shards are pervasively altered in the southwestern Gulf Coast and much less in the northeastern Gulf Coast (Ledger,

1981; Ledger et al., 1984). Galloway and Kaiser (1980) expressed the somewhat contradictory opinion that uranium in the northeastern Gulf Coast was leached and diluted because of the more humid climate and was then unable to precipitate except maybe downdip. The more humid conditions in Catahoula times were inferred by Galloway (1977) because of the relatively abundant kaolinite in the northeastern Gulf Coast, but Ledger et al. (1984) stated that it could be detrital and not authigenic. However, Ledger et al. (1984) also described numerous montmorillonite beds resulting from the degradation of ashfall layers in the northeastern Gulf Coast. Uranium solutions could also have been diluted as a result of the large volume of sandstones of nonvolcanic origin. Another factor to take into account is the possible lack of a reducing agent in the northeastern Gulf Coast. Several other workers (McBride et. al., 1982; Hoel, 1982) have also suggested that great differences in climate between the southwestern and northeastern Gulf Coast could have influenced the nature of depositional environments. For example, the Goliad Fm. is thought to have been deposited as a primary red-bed sequence (syn-depositionally-oxidized) as a result of the arid conditions. Even though there are air-fall tuff deposits (ash) all along the Texas Gulf Coast, there is a greater thickness of sediments containing volcanic material in the southwestern Gulf Coast. Not only would this have provided a greater thickness of sediments from which to leach uranium, arsenic, and other elements contained in volcanic aerosols, these larger and more interconnected sediment packages would also have allowed more extensive groundwater circulation patterns to have developed.

Arsenic contamination may originate from leaching of volcanic ash and volcaniclastic layers. Arsenic contamination can also be the product of erosion and solubilization of a myriad of small uranium/arsenic accumulations. Similarly to what was presented in the High Plains section, it could also be mobilized from the iron oxides.

Other Natural Potential Sources

Additional potential sources include upwelling of highly mineralized water from salt domes. However, the spatial mismatch between salt dome distribution and areas of high arsenic concentration (Figure 54a and Figure 60), as well as the lack of correlation between chloride and arsenic concentrations, precludes such an association.

D2-5 Modeling Arsenic Behavior in the Saturated Zone

Conceptual Model and Assumptions

This section describes a modeling exercise shedding light on arsenic behavior in the southern Ogallala aquifer. We used a statistical approach by considering the ~6,000 TWDB major ion analyses of the southern High Plains. A concentration of 15 ug/L arsenic is then assumed in the presence of trace elements competing for sorption sites. The model equilibrates this imposed aqueous arsenic and trace element concentrations with iron oxides. In a second step, the pH is raised or lowered by a half pH unit, and the resulting aqueous arsenic concentration is noted.

In contrast to experiments, where almost everything can be controlled, modeling of field data is challenging. Little is known about the sorbing minerals, except in the most general sense, and much less is known of their effectiveness, in particular relative to their reactive surface area. The general environment such as geological setting, hydrologic conditions, water chemistry, particle mineralogy, and subsurface microbiology should be considered. The key point is to capture the first-order processes by the modeling, even if, because of the complexity, not everything is included. We made the following assumptions:

1) oxidizing conditions and presence of As(V) only
2) closed system
3) all oxide sorbing minerals (amorphous iron oxide, ferrihydrite, green rust, goethite, hematite, amorphous aluminum oxide, gibbsite, boehmite, diaspore) are lumped into one

category and modeled as amorphous iron oxide ($Fe(OH)_3$). Iron oxide weight fraction is estimated at 0.5 percent, and its specific surface area is assumed 300 m^2/g.

4) aquifer average porosity is 15 percent.

We now successively examine these assumptions. Dissolved oxygen data suggest that conditions are mostly oxidizing and have been so for a long time. It is then reasonable to assume that arsenic is mostly under As(V). Because, the amount of arsenic and other anions sorbed is dependent on the mineral-specific area, it is important to understand the mineralogy of the iron oxides (nature, location, grain size, coatings, etc.). EPA, in its help manual for superfund sites (1996, Part 5, Table 44), proposes a low, medium, and high value for iron oxide content of 0.01, 0.31, and 1.1 weight percent (Fe_2O_3), respectively. The iron oxide and hydroxide (FeOx) content in the Ogallala aquifer seems to be higher than the average of U.S. aquifers. It is estimated at 0.5 percent from Avakian's work (1988). Since it is finely disseminated mostly as coating on framework grains, a specific surface area for FeOx of 300 m^2/g is used. Dzombak and Morel (1990) recommended a value of 600 m^2/g for amorphous iron oxide specific surface area. Welch and Lico (1988) also opted for 600 m^2/g. However, this value applies to fresh oxide aqueous suspensions used in laboratory experiments. In the subsurface, unless ferric iron is actively precipitating, specific surface areas are probably smaller because of aging. Crosby et al. (1983) determined that ~ 10% of initially amorphous iron oxide had been transformed into goethite in 2 weeks. Fuller at al. (1996) mentioned that sorption decreased by 20% on a ferrihydrite after six days, presumably owing to goethite transformation. In addition, despite the internal porosity of the natural iron oxide coating, it is likely that contact between aqueous solution and mineral surface is not as good as in a suspension. For modeling purposes, we assume that there is no gas exchange—in particular, that carbon dioxide partial pressure is fixed by carbonate concentration. Blandford et al. (2003) attributed a specific yield of 15 percent to the Ogallala aquifer in agreement with other sources cited in the report, whereas Nativ (1988) mentioned an average value of 16.1 percent (it ranges from 7.2 to 19.5 percent) measured from cores. The value of 15 percent is retained in this document for porosity.

In addition, because other chemical elements could compete for the same absorption sites, it is important to add their approximate concentrations. The following values were chosen from the average calculated from the TWDB database: boron (0.61 mg/L), molybdenum (0.012 mg/L), phosphate (0.05 mg/L), selenium (0.036 mg/L), and vanadium (0.081 mg/L). Uranium average concentration was extracted from the NURE database at 0.013 mg/L. Fluoride average is approximately 3 ppm, but it is provided with the major elements and thus varies in each run. Litke (2001, Table 7) reported median phosphate concentrations ranging from less than 0.01 to 0.09 mg/L in other areas of the High Plains aquifer, as well as a median of 0.009 mg/L for arsenic, 0.318 mg/L for boron, 0.021 mg/L for dissolved iron, and 0.011 mg/L for selenium in the southern High Plains aquifer, in agreement with the values used here. Carbonate ions and silica were not assumed to sorb on iron oxides.

The choice of thermodynamic data impacts the modeling results (see Appendix I, Section I-3). A modified version of the database llnl.dat is used in the simulations. All surface species listed in the wateq4f.dat database and not listed in the llnl.dat database were copied to the latter. In addition, data for vanadate and molybdate, copied from Chapter 10 of Dzombak and Morel (1990), were added. Because of numerical instabilities during the run, the fluoroarsenate species, AsO_3F^{-2} and $HAsO_3F^{-1,}$ were also deleted from the database. Modeling studies by Smedley et al. (2002, p. 269) suggested that they are minor, even with high arsenic and fluoride concentrations. Sorption reaction constants of some species, such as borate, have higher uncertainties than that of arsenic.

Modeling Results

With the assumptions of an arsenic aqueous concentration of 15 ug/L, an iron oxide content of 0.5 percent, and a surface area of 300 m^2/g, most of the arsenic is sorbed to the iron oxides

(>99 percent). With the knowledge of arsenic sorption decreasing with pH, it was expected that aqueous arsenic concentrations would increase with increasing pH and decrease with decreasing pH. This, however, did not fully occur during the modeling. About 50 percent of the samples showed an increase in arsenic aqueous concentration (total arsenic constant) with decreasing pH (Figure 61a), whereas about 60 percent of the samples showed a decrease in arsenic concentration with increasing pH (Figure 61b). This behavior could be due to the presence of other trace elements competing for sorption sites. Figure 62a demonstrates that although other trace elements do have a negative impact on arsenic sorption, it is minor. The origin of this behavior is the competition of magnesium. Runs that do not allow magnesium to sorb onto iron oxide surfaces show the expected behavior of increasing arsenic aqueous concentration with increasing pH (Figure 61c). Because the reaction constant of magnesium sorption on iron oxides is not accurately known (Dzombak and Morel, 1990, Table 10.5) and to ensure that those results are not an artifact due to the lack of accuracy, sensitivity runs on the value of the reaction constant were performed (a value of logK of -5.6 was used in addition to the baseline value of -4.6). Figure 62 suggests that this behavior is real although less pronounced with a lower magnesium sorption strength (logK=-5.6). The number of samples whose arsenic aqueous concentration decreases with increasing pH is smaller with logK=-5.6 (below the horizontal line at 15 ug/L) than with logK=-4.6 (to the left of the vertical line at 15 ug/L) (Figure 62b). Conversely, a decrease in pH leads to more samples with an increase in arsenic aqueous concentration, assuming a logK=-5.6, than the baseline logK=-4.6 (Figure 62c). This behavior does not occur in most experimental work on arsenic sorption because workers tend to simplify the object of their studies by using conservative salts (NaCl or $NaClO_4$).

Two observations corroborate the impact of magnesium on the High Plains aquifer. Highest arsenic concentrations do not correlate with the highest pH values but rather with more neutral pH values (Figure 50m). There is also a negative correlation between the ratio Ca/Mg and arsenic (Figure 52) supplemented by a satisfying spatial correlation between high arsenic concentrations and low Ca/Mg ratios (Figure 63). This working hypothesis needs more work to be developed and integrated within the history of the High Plains aquifer.

Subtask D3. Assess the Redox Conditions of Groundwater with and without High Arsenic Concentrations Using Existing Databases.

Redox conditions can be assessed by measuring dissolved oxygen concentration if conditions are at least somewhat oxidizing. Direct measurement of the redox potential can also be done with a redox meter. A third method to estimate redox conditions is to analyze redox couples appropriate to the anticipated Eh level (nitrate/nitrite; sulfate/sulfide).

D3-1 Redox Conditions in the Southern High Plains Aquifer

Redox conditions in the High Plains aquifer are in general oxidizing. Numerous anecdotal measurements support this statement. The TWDB database stores Eh measurements, whereas the NURE database provides information on dissolved oxygen. The median of 1,152 NURE measurements taken in the footprint of the southern High Plains and east of a north-south line going through Lubbock is 7.9 ug/L (Figure 64a). The average is 7.3 ug/L, the 10th percentile is 3.3 ug/L, and the minimum is ~0 ug/L. At the aquifer temperature, water can hold ~10 mg/L of dissolved oxygen at equilibrium with water vapor-saturated air (Langmuir, 1997, p. 16-17). Measurement of dissolved oxygen can be considered accurate down to a concentration of 0.1 ppm. TWDB Eh measurements (Figure 64c) show a bimodal distribution with a larger mode at ~125 mV and a much smaller one at ~-125 mV. Dissolved oxygen is theoretically related to Eh and pH through the following reaction:

$2H_2O = 4H^+ + O_2(aq) + 4e^-$ log10{K} = -86.08 (from wateq4f.dat database)

Eh (mV) = 59.2(21.52 -pH + 0.25log{[O_2(aq)]/1000/32} at 25^oC (O_2(aq) in mg/L)

which runs parallel to the water stability lines in (pH, Eh) diagrams. This equation is dominated by the pH term unless oxygen concentrations are low (not measurable). A pH of 7.5 then yields an Eh of 778 mV (DO = 10 mg/L) and 748 (DO = 0.1 mg/L). Those values are much higher than the measured values. In addition, frequency of negative Eh values in the TWDB database is higher than frequency of low dissolved oxygen values (<0.5 ppm). This can be explained by a difference in the spatial coverage of the sampling, by the well-known difficulties in measuring accurately low DO values and Eh values, or by the presence of true reducing conditions. Additional explanations are given in the section on recent sampling in Duval County. Arsenic concentrations show no obvious relationship with redox potential or dissolved oxygen ((Figure 64b and d).

Dissolved oxygen shows no obvious trend with depth (Figure 65) but is plotted against the only available well depth information: total well depth, a rough proxy for screened depth. Those dissolved oxygen numbers are similar to those provided in the multistate study of the High Plains aquifer (Table 7 of Litke, 2001). McMahon et al. (2004b, p.17, Appendix 1) multilevel well shows that conditions can be locally mildly reducing. The multilevel wells in Castro and Hale Counties described in McMahon et al. (2004b) match the area of lower dissolved oxygen as recorded by the NURE project (Figure 66). Areas of low dissolved oxygen in Figure 66 in Hale, Moore, and Huchinson Counties generally correspond to areas having large saturated thickness. Reducing conditions are more likely to exist at the bottom of the aquifer, and vertical mixing due to heavy pumping may homogenize the water column more than it was under pristine conditions.

D3-2 Redox Conditions in the Gulf Coast

Redox conditions of the southwestern Gulf Coast aquifers are weakly oxidizing (Figure 67) to reducing. Henry et al., 1980 and Galloway, 1982 stated that in the Oakville sandstone, Eh conditions range from strongly oxidizing in the recharge area (470 mV) to reducing farther downdip (-170 mV) with variations due to conductivity changes and fault proximity. The decrease is not progressive but moves through plateaus at ~400, ~50 and ~-100 mV (Henry et

al., 1980; Galloway, 1982, p.21 and his Figure 18). The Catahoula Fm. is overall reducing in the downdip area.

Arsenic concentrations do not correlate with dissolved oxygen (Figure 68), but there are no high concentrations at low redox potential (~-100 mV) (Figure 69).

The median of 1,725 dissolved oxygen NURE measurements irregularly distributed across the area of interest is 3.9 mg/L. The average is 4.4 mg/L, the 10th percentile is 1.5 mg/L, and the minimum is ~0 mg/L. The trend with increasing depth seems to be a slow decrease in dissolved oxygen (Figure 70). Henry et al. (1982a) with a few sampling lines approximately parallel to groundwater flow lines showed that the redox conditions from oxidizing at the outcrop of the Oakville sandstone become progressively reducing (Figure 72). The gradient is a function of the depositional systems. Large channel sand bodies maintain their oxidizing character farther downdip, as seen with the few data points that maintain a higher Eh than most data points.

Subtask D4. Conduct Additional Groundwater Sampling Where Feasible and Necessary to Evaluate Geologic Sources

D4-1 Data Analysis

BEG provided equipment to the TWDB regular sampling team to perform additional measurements in selected wells in Duval County (southwestern Gulf Coast). Some of the same wells had already been sampled through the years for major ions and arsenic and other trace elements. The new analyses are consistent with previous sampling events (Figure 73). In addition to routine chemical analyses, groundwater was also analyzed for redox pairs: sulfate/sulfide, nitrate/ammonia. An assessment of redox conditions of the 33 samples can be made by comparing dissolved oxygen data and that of the two redox pairs. All measurements were made in the field. Ammonia and dissolved oxygen were measured on all samples, whereas sulfide was measured only on those samples having a dissolved oxygen content of less than 1 mg/L. The maximum amount of oxygen dissolved in a water at 28^{o}C (average temperature in Duval County aquifer according to measurements in the TWDB database) is slightly less than 8 mg/L. Four samples report a D.O value between 7 and 8, and two samples have a D.O value higher than 10 mg/L (most likely because they were sampled from windmills). Those six samples are fully oxygenated, but four of them also contain a significant amount of ammonia (none was analyzed for sulfide). Six samples have D.O. values below 1 mg/L, and they all contain sulfide between 20 and 60 ug/L. Another test of the accuracy of the data can be performed by comparing iron concentrations measured in both the field and the laboratory (Figure 74a). In the presence of oxygen and at a neutral-alkaline pH, ferrous iron would be quickly oxidized, leaving only a few micrograms per liter of dissolved ferric iron (Figure 12.4 of Langmuir, 1997). This is the first instance of thermodynamic disequilibrium. There might be a slight trend in increasing iron with decreasing dissolved iron (Figure 74b). Sulfide and ammonia concentrations show no correlation (Figure 74c).

In order to calculate the theoretical Eh associated with those measurements, PHREEQC runs were done with the 33 chemical analyses as input and the Eh computed at equilibrium. As expected, all Eh values involving dissolved oxygen (including those D.O<1 mg/L) are between 600 and 700 mV, whereas the nitrate/ammonia redox couple yields Eh values from 270 to 390 mV and the sulfate/sulfide couple Eh values range from -120 to -40 mV. Measurements of low DO values are notoriously unreliable, and the presence of sulfide, typically quickly oxidized, is evidence of reducing conditions.

D4-2 Data Interpretation

Dissolved oxygen decreases with depth as expected (Figure 74d) and similarly to the rest of the Gulf Coast (Figure 70). On the contrary, ammonia and sulfide do not show a trend with depth. Henry et al. (1980) suggested that H_2S is still leaking from the Wilcox Fault zone, preventing the system from reaching equilibrium.

Henry et al. (1980) and Galloway (1982, p. 21 and his Figure 18) have shown that Eh decreases downdip through plateaus at ~400, ~50, and ~-100 mV (Section D1-1.2). The -100 mV plateau corresponds to the sulfide stability domain, and its presence in the Gulf Coast aquifers is again verifed in this sampling campaign. The Eh = ~50 mV is controlled by the ferrous-ferric reaction and is not well represented in this sampling event because of a lack of iron speciation in the analyses. The plateau at ~400 mV typically represents oxygenated and oxidizing conditions (Langmuir, 1997, p. 410). Only rarely does groundwater Eh reach values of Eh = 600-700 mV for thermodynamic equilibrium with dissolved oxygen because of extremely slow kinetics and because dissolved oxygen is not the only redox pair controlling Eh (Langmuir,

1997, p.409). From these observations, Henry et al. (1980, p. 17) concluded that measured Eh might be the best indicator of the true average redox conditions.

Coexistence of redox pairs in thermodynamic desequilibrium is common in groundwater. Lindberg and Runnels (1994) presented compelling evidence of this (Figure 76). Each vertical band on the figure corresponds to a computed Eh from a given redox pair. The cloud of field-measured Eh spans the whole Eh scale. Redox reactions unless microbially mediated are notoriously slow.

As a conclusion, recent measurements of redox conditions in Duval County are consistent with previous studies. Arsenic behavior (Figure 75) compares well with that of the Gulf Coat as a whole (Figure 68 and Figure 69). Eh values used in Figure 75b are based either on a single redox pair (O_2(aq)/H2O, ammonia/nitrate, or sulfide/sulfate) or on the average of at most two redox pairs (ammonia/nitrate and sulfide/sulfate or O_2(aq)/H2O and ammonia/nitrate). Arsenic is soluble until it reaches an Eh value of ~-100 mV, when it precipitates, especially in presence of sulfur.

Task D: Conclusions on Natural Origin of Arsenic Contamination

Southern High Plains

Arsenic contamination is much greater in the SHP-S region (51% of wells > 10 ug/L) than in the SHP-N region (7% of wells > 10 ug/L). Groundwater arsenic contamination occurs in generally oxidizing conditions in the High Plains and arsenic is expected to be in the form of arsenate. Correlations between arsenic and other constituents (vanadium, r2=0.65; fluoride r2=0.30; molybdenum r2=0.18; boron r2=0.17; selenium r2=0.14) suggests a geologic rather than an anthropogenic source. Arsenic concentrations are related to geologic units and are highest in the Ogallala aquifer and much lower in the Dockum aquifer. Arsenic concentrations in the Edwards Trinity (High Plains) aquifer are highest in the area where it is underlain by the Ogallala aquifer and much lower elsewhere. Potential sources of arsenic include volcanic ash beds in the Ogallala aquifer, black shales in the Cretaceous (Kiamichi Shale), saline lakes, and relict sorption on metal oxice coatings and clays. Analysis of existing geophysical logs indicates that high gamma zones, indicative of volcanic ash beds, are restricted primarily to the southwestern area of the SHP and are not collocated with most of the high groundwater arsenic concentrations. Similarly, the Kiamichi shale and the elevated arsenic concentrations do not fully overlap. Arsenic concentrations are not related to distance from saline lakes, indicating this is not a likely source of arsenic in the region. Additional studies will be required to assess geologic sources, including additional geophysical logging and stratified sampling.

Southwestern Gulf Coast

Groundwater arsenic concentrations are much higher in the southwestern area of the Gulf Coast (29 percent of wells exceed the MCL) than elsewhere in the Gulf Coast (3.5 percent of wells exceed the MCL). High arsenic concentrations occur along the Rio Grande valley, in the few counties westna dn southwest to of Corpus Christi, and along the Catahoula Formation outcrop extending into the north eastern Gulf Coast. Correlations between arsenic and other constituents (vanadium, r^2 0.43;; molybdenum r^2 0.36; boron r^2 0.12) suggest a geologic rather than an anthropogenic source. Arsenic concentrations are highest in the Jasper aquifer (48 percent > 10 ug/L) which immediately overlies the Catahoula Formation and are much less in younger stratigraphic aquifers (Evangeline aquifer; 21 percent > 10 ug/L and Chicot aquifer, 27 percent > 10 ug/L). Therfore, volcanic ashes associated with or reworked from the Catahoula Fm. are the most likely source of high arsenic concentrations in the southwestern Gulf Coast aquifer. Correlations between arsenic and other oxyanions typically associated with volcanism (molybdenum, vanadium) as well as the general decrease in arsenic contamination away from this formation strongly support this hypothesis.

References

Abernathy, C., J. Thomas, and R. L. Calderon. 2003. Health effects and risk assessment of arsenic. Journal of Nutrition 133:1536S-1538S.

Adidas, E. O. 1991. Ground-water quality and availability in and around Bruni, Webb County, Texas. Texas Water Development Board Report LP-209, 51 p.

Allen, B. L., B. L. Harris, K. R. Davis, and G. B. Miller. 1972. The mineralogy and chemistry of High Plains playa lake soils and sediments. Agronomy Department, Texas Tech University, report prepared for Office of Water Resources Research, U.S. Department of Interior under contract No B-004-TEX, 75 p.

Appelo, C. A. J., M. J. J. van der Weiden, C. Tournassat, and L. Charlet. 2002. Surface complexation of ferrous iron and carbonate on ferrihydrite and the mobilization of arsenic. Environmental Science and Technology 36:3096-3103.

Aronow, S., T. E. Brown, D. H. Eargle, and V. E. Barnes. 1987. Beeville - Bay City Sheet. in Geologic Atlas of Texas, scale 1:250,000. University of Texas at Austin, Bureau of Economic Geology.

Ashworth, J. B., and R. R. Flores. 1991. Delineation criteria for the major and minor aquifer maps of Texas. Texas Water Development Board Report LP-212, 27 p.

Aurelius, L. 1988. Investigation of arsenic contamination of groundwater occurring near Knott Texas. Texas Department of Agriculture, Austin, TX, 53 p.

Avakian, A. J. 1988. Mineralogy of the Ogallala Formation, southern High Plains: new lithologic, petrographic, and X-ray diffraction data from West Texas cores. The University of Texas at Austin, Bureau of Economic Geology, unpublished report.

Ayotte, J. D., D. Baris, G. P. Robinson, J. Lubin, K. P. Cantor, D. T. Silverman, D. Grauman, R. N. Hoover, and J. F. Fraumeni. 2001. Relation of bladder cancer mortality rates in New England to water use data. Epidemiology 12:S97.

Bachman, G. O., and R. B. Johnson. 1973. Stability of salt in the Permian salt basin of Kansas, Oklahoma, Texas, and New Mexico. U.S. U.S. Geological Survey Open File Report 73-0014, 66 p.

Bailey, T. L. 1926. The Gueydan, a new middle Tertiary formation from the southwestern coastal plain of Texas. University of Texas Bulletin no. 2645, 187 p. + 1 plate.

Baker, E. T. 1979. Stratigraphic and hydrogeologic framework of part of the Coastal Plain of Texas. Texas Department of Water Resources Report no. 236, 43 p.

Baker, E. T., Jr. 1986. Hydrology of the Jasper Aquifer in the southeast Texas Coastal Plain. Texas Water Development Board Report 295, 64 p.

Bates, M. N., A. H. Smith, and K. P. Cantor. 1995. Case-control study of bladder cancer and arsenic in drinking water. American Journal of Epidemiology 141:523-530.

Baumann, P. A. 1998. Suggestions for weed control. Texas Agricultural Extension Service, The Texas A&M University System, Report B5039, 22 p.

Bexfield, L. M. 2002. Spatial patterns and temporal variability in water quality from City of Albuquerque drinking water supply wells and piezometer nests, with implications for the groundwater flow system. U.S. Geol. Surv. Water Resour. Inv. Rept. 01-4344, 101 p.

Bexfield, L. M., and L. N. Plummer. 2003. Occurrence of arsenic in ground water of the Middle Rio Grande Basin, central New Mexico. Pages 295-331 in A. H. Welch and K. G. Stollenwerk, editors. Arsenic in Groundwater: Geochemistry and Occurrence. Kluwer Academic Publishers.

Bishop, B. A. 1967. Stratigraphic study of the Kiamichi Formation of the Lower Cretaceous of Texas. Pages 158-180 in L. Hendricks, editor. Comanchean (Lower Cretaceous) stratigraphy and paleontology of Texas, Vol 67-8. The Permian Basin Section, Society of Economic Paleontologists and Mineralogists.

Blandford, N. T., D. J. Blazer, K. C. Calhoun, A. R. Dutton, T. Naing, R. C. Reedy, and B. R. Scanlon. 2003. Groundwater availability of the southern Ogallala Aquifer in Texas and New Mexico: numerical simulations through 2050. Report prepared by Daniel B. Stephens and Associates for the Texas Water Development Board, February 2003.

Blandford, T. N., and D. J. Blazer. 2004. Hydrologic relationships and numerical simulations of the exchange of water between the southern Ogallala and Edwards-Trinity aquifers in southwest Texas, aquifers of the Edwards Plateau. Pages 115-131 in R. E. Mace, E. S. Angle, and W. F. I. Mullican, editors. Texas Water Development Board Report No 360.

Blum, M. D. 1992. Modern depositional environments and recent alluvial history of the lower Colorado River, gulf coastal plain of Texas. unpublished PhD. dissertation. Department of Geological Sciences, University of Texas at Austin.

Borgono, J. M., P. Vicent, H. Venturino, and A. Infante. 1977. Arsenic in the drinking water of the city of Antofagasta: Epidemiological and clinical study before and after the installation of a treatment plant. Environmental Health Perspectives 19:103-105.

Bowell, R. J. 1994. Sorption of arsenic by iron oxides and oxyhydroxides in soils. Applied Geochemistry 9:279-286.

Bradley, R. G., and S. Kalaswad. 2003. The groundwater resources of the Dockum aquifer in Texas. Texas Water Development Board report No. 359.

Brandenberger, J., P. Louchouarn, B. E. Herbert, and P. Tissot. 2004. Geochemical and hydrodynamic controls on arsenic and trace metal cycling in a seasonally stratified US sub-tropical reservoir. Applied Geochemistry 19:1601-1623.

Brandt, J. P. 1953. Cretaceous of Llano Estacado of Texas. The University of Texas at Austin, Bureau of Economic Geology Report of Investigations No 20, 59 p.

Brandvold, L. 1999. Arsenic in wells and springs in the Socorro, New Mexico area. Proc. Southwest and Rocky Mountain Div., Am. Assoc. Adv. Sci., 75th Annual Mtg., 36 p.

Brandvold, L. 2001. Arsenic in groundwater in the Socorro Basin, New Mexico. New Mexico Geology 23:2 p.

Brandvold, L. 2002. Water quality of drinking water supplies in Socorro, New Mexico. Am. Geophys. Union Fall Mtg. Prog. with Abs., No. H61C-0805.

Bridges, D. C., T. L. Grey, and B. J. Brecke. 2002. Pyrithiobac and bromoxynil combinations with MSMA for improved weed control in bromoxynil-resistant cotton. Journal of Cotton Science 6:72-75.

Bryant, R. B. 1977. A comparison of physical and chemical properties of selected irrigated, dryland, and native range Texas High Plains soils. Masters of Science Thesis. Texas Tech University.

Buchet, J. P., and D. Lison. 1998. Mortality by cancer in groups of the Belgian population with a moderately increased intake of arsenic. International Archives of Occupational and Environmental Health 71:125-130.

Campos, V. 2002. Arsenic in groundwater affected by phosphate fertilizers at Sao Paulo, Brazil. Environmental Geology 42:83-87.

Cepeda, J. C. 2001. A 10Ma silicic fallout tuff in the Texas panhandle; comparisons with the Pearlette Ash. Geological Society of America Abstracts with Programs 33:397 p.

Chen, C. J., Y. M. Hsueh, M. S. Lai, P. Shyu, S. Y. Chen, M. M. Wu, T. L. Kuo, and T. Y. Tai. 1995. Increased prevalence of hypertension and long-term arsenic exposure. Hypertension 25:53-60.

Chiang, H. S., H. R. Guo, C. L. Hong, S. M. Lin, and E. F. Lee. 1993. The incidence of bladder cancer in the blackfoot disease endemic area in Taiwan. British Journal of Urology 71:274-278.

Chiou, H. Y., Y. M. Hsueh, K. F. Liaw, S. F. Horng, M. H. Chiang, Y. S. Pu, J. S. N. Lin, C. H. Huang, and C. J. Chen. 1995. Incidence of internal cancers and ingested inorganic arsenic: a seven-year follow-up study in Taiwan. Cancer Research 55:1296-1300.

Chiou, H. Y., W. I. Huang, C. L. Su, S. F. Chang, Y. H. Hsu, and C. J. Chen. 1997. Dose-response relationship between prevalence of cerebrovascular disease and ingested inorganic arsenic. Stroke 28:1717-1723.

Chowdhury, A. H., and R. E. Mace. 2003. A groundwater availability model of the Gulf Coast aquifer in the Lower Rio Grande Valley, Texas: Numerical simulations through 2050. Texas Water Development Board Report, October 2003, 171 p.

Christenson, S., and J. S. Havens. 1998. Ground-water quality assessment of the central Oklahoma aquifer, Oklahoma: Summary of investigations. in Ground-water quality assessment of the central Oklahoma aquifer, Oklahoma: Results of investigations. U. S. Geological Survey Water Supply Paper 2357-A, 44 p.

Christenson, S., D. L. Parkhurst, and G. N. Breit. 1998. Summary of geochemical and geohydrologic investigations o fhte central Oklahoma aquifer. Pages 107-117 in S. Christenson and J. S. Havens, editors. Ground-water quality assessment of the Central Oklahoma aquifer, Oklahoma: Results of investigations. U. S. Geological Survey Water Supply Paper 2357-A.

Coupe, R. H., E. M. Thurman, and L. R. Zimmerman. 1998. Relation of usage to the occurrence of cotton and rice herbicides in three streams of the Mississippi delta. Environmental Science and Technology 32:3673-3680.

Crosby, S. A., D. R. Glasson, A. H. Cuttler, I. Gutler, D. R. Turner, M. Whitfield, and G. E. Millward. 1986. Surface areas and porosities of iron(III)- and iron(II)-derived oxyhydroxides. Envirnomental Science & Technology 17:709-713.

Davenport, J. R., and F. J. Peryea. 1991. Phosphate fertilizers influence leaching of lead and arsenic in a soil contaminated with lead arsenate. Water, Air and Soil Pollution 57-58:101-110.

De Soto, R. H. 1978. Uranium geology and exploration. Lecture notes and references published by the Colorado School of Mines, Golden, Co, March 1978, 396 p.

Dickinson, K. A. 1976. Geologic controls of uranium deposition, Karnes County, Texas. U. S. Geological Survey Open File Report 76-331, 16 p.

Dixit, S., and J. G. Hering. 2003. Comparison of arsenic(V) and arsenic(III) sorption onto iron oxide minerals: implications for arsenic mobility. Environmental Science and Technology 37:4182-4189.

Doering, J. 1935. Post-Fleming surface formations of coastal southeast Texas and south Louisiana. American Association of Petroleum Geologists Bulletin 19:651-688.

Dutton, A. R., and W. W. Simpkins. 1986. Hydrogeochemistry and water resources of the Triassic lower Dockum Group in the Texas Panhandle and eastern New Mexico. University of Texas, Bureau of Economic Geology Report of Investigations No 161, 51p.

Dutton, A. R. 1995. Groundwater isotopic evidence for paleorecharge in U.S. High Plains aquifers. Quaternary Research 43:221-231.

Dzombak, and Morel. 1990. Surface complexation modeling: Hydrous Ferric Oxide. Wiley-Interscience, New York.

Eargle, D. H. 1956. Some uranium occurrences in West Texas. The University of Texas at Austin, Bureau of Economic Geology Report of Investigations No. 27, 23 p.

Eargle, D. H. 1959. Stratigraphy of Jackson Group (Eocene), South-Central, Texas. American Association of Petroleum Geologists Bulletin 43:2623-2635.

Eargle, D. H., K. A. Dickinson, and B. O. Davis. 1975. South Texas uranium deposits. American Association of Petroleum Geologists Bulletin 59:766-779.

EPA. 1996. Soil screening guidance: Technical background document. Environmental Protection Agency, USA, document 540/R-95/128. http://www.epa.gov/superfund/resources/soil (2005/07/29).

EPA. 2005. AP 42, Food and Agricultural Industries, Vol. 1, Chpt. 9. 5th Ed., http://www.epa.gov/ttn/chief/ap42/ch09/ (2005/04/14).

Ewing, T. E. 1990. Tectonic map of Texas. The University of Texas at Austin Bureau of Economic Geology State Map No SM0001.

Finch, W. I. 1967. Geology of epigenetic uranium deposits in sandstone of the United States. U. S. Geological Survey Professional Paper 538, 212 p.

Finch, W. I. 1975. Uranium in West Texas. American Association of Petroleum Geologists Bulletin 59:909 p.

Finch, W. I. 1996. Uranium provinces of North America - their definition, distribution, and models. U.S. Geological Survey Bulletin 2141:18 p. +12 plates.

Finch, W. I. 1997. Uranium, its impact on the national and global energy mix - and its history, distribution, production, nuclear fuel-cycle, future, and relation to the environment. U.S. Geological Survey Circular 1141, 24p.

Fisher, W. L., W. E. Galloway, C. V. S. Proctor, and J. S. Nagle. 1970. Depositional systems in the Jackson group of Texas. Their relationship to oil, gas, and Uranium. Gulf Coast Association of Geological Societies Transactions 20:234-261.

Fishman, N. S., R. S. Reynolds, and M. R. Goldhaber. 1982. Geochemical and mineralogical data from the Lamprecht and Felder uranium deposits, Live Oak County, Texas. U.S. Geological Survey Open-File Report 82-749, 32 p.

Folk, R. L. 1974. Petrology of sedimentary rocks. Hemphill Publishing Co., Austin, Texas.

Fryar, A. E., W. F. Mullican, and S. A. Macko. 2001. Groundwater recharge and chemical evolution in the southern High Plains of Texas, USA. Hydrogeology Journal 9:522-542.

Frye, J. C., and A. B. Leonard. 1957. Studies of Cenozoic geology along eastern margin of Texas High Plains, Armstrong to Howard Counties. The University of Texas at Austin, Bureau of Economic Geology Report of Investigations No 32, 62 p.

Fuller, R. R., J. A. Davis, J. A. Coston, and E. Dixon. 1996. Characterization of metal absorption variability in a sand and gravel aquifer, Cape Cod, Massachusetts, USA. Journal of Contaminant Hydrology 22:165-187.

Galloway, W. E. 1977. Catahoula Formation of the Texas coastal plain: depositional systems, composition, structural development, ground-water flow history, and uranium deposition. University of Texas at Austin, Bureau of Economic Geology Report of Investigations No. 87, 59 p.

Galloway, W. E., R. J. Finley, and C. D. Henry. 1979. South Texas uranium province geologic perspective. University of Texas at Austin, Bureau of Economic Geology Guidebook No. 18, 79 p.

Galloway, W. E., and W. R. Kaiser. 1980. Catahoula Formation of the Texas coastal plain: origin, geochemical evolution, and characteristics of uranium deposits. The University of Texas at Austin, Bureau of Economic Geology Report of Investigations No. 100, 81 p.

Galloway, W. E. 1982. Epigenetic zonation and fluid flow history of uranium-bearing fluvial aquifer systems, south Texas uranium province. The University of Texas at Austin, Bureau of Economic Geology Report of Investigations No. 119, 31 p.

Galloway, W. E., C. D. Henry, and G. E. Smith. 1982. Depositional framework, hydrostratigraphy, and uranium mineralization of the Oakville sandstone (Miocene), Texas coastal plain. The University of Texas at Austin, Bureau of Economic Geology Report of Investigations No. 113, 51 p.

Gianessi, L. P., and M. B. Marcelli. 2000. Pesticide use in U.S. crop production: 1997. National Center for Food and Agriculture Policy, Washington, D.C., November 2000, http://www.ncfap.org/database/default.php (2005/04/12).

Goh, K. H., and T. T. Lim. 2005. Arsenic fractionation in a fine soil fraction and influence of various anions on its mobility in the subsurface environment. Applied Geochemistry 20:229-239.

Goldhaber, M. B., and R. L. Reynolds. 1977. Geochemical and mineralogical studies of a South Texas roll-front uranium deposits. U.S. Geological Survey Open-File Report 77-821, 34 p.

Goldhaber, M. B., R. L. Reynolds, and R. O. Rye. 1978. Origin of a South Texas Roll-type uranium deposit: II. Sulfide petrology and sulfur isotope studies. Economic Geology 73:1690-1705.

Guilbert, J. M., and C. F. J. Park. 1986. The Geology of Ore Deposits. W. H. Freeman and Company, New York.

Guo, H. R., H. S. Chiang, H. Hu, S. R. Lipsitz, and R. R. Monson. 1994. Arsenic in drinking water and urinary cancers: a preliminary report. Pages 119-128 in W. R. Chappell, C. O. Abernathy, and C. R. Cothern, editors. Arsenic: Exposure and Health. Science and Technology Letters, Northwood England.

Guo, X. J., and Y. Fujino. 2001. Arsenic contamination of groudwater a prevalence of arsenical dermatosis in the Hetao plain area, Inner Mongolia, China. Molecular and Cellular Biochemistry 222:137-140.

Gustavson, T. C., and V. T. Holliday. 1985. Depositional architecture of the Quaternary Blackwater Draw and Tertiary Ogallala Formations, Texas Panhandle and eastern New Mexico.

The University of Texas at Austin Bureau of Economic Geology Open File Report of West Texas Waste Isolation 1985-23, 60 p.

Gustavson, T. C., R. W. J. Baumgartner, S. C. Caran, V. T. Holliday, H. H. Mehnert, J. M. O'Neill, and C. C. J. Reeves. 1991. Quaternary geology of the southern Great Plains and an adjacent segment of the Rolling Plains. Pages 477-501 in R. B. Morrison, editor. Quaternary nonglacial geology; Conterminous U.S., The Geology of America, v. K-2. Geological Society of America, Boulder, Colorado.

Gustavson, T. C. 1996. Fluvial and eolian depositional systems, paleosols, and paleoclimates of the upper Cenozoic Ogallala and Blackwater Draw Formations, southern High Plains, Texas and New Mexico. The University of Texas at Austin, Bureau of Economic Geology Report of Investigations No. 239, 62 p.

Halbouty, M. T. 1979. Salt domes Gulf Region, United States & Mexico, Chapter 5, 2nd edition. Gulf Publishing Company.

Halter, W. E., and H.-R. Pfeifer. 2001. Arsenic(V) adsorption onto alpha-Al2O3 between 25 and 70 degrees C. Applied Geochemistry 16:793-802.

Hanan, M. A., M. W. Totten, B. B. Hanan, and T. Kratochovil. 1998. Improved regional ties to global geochronology using Pb-isotope signatures of volcanic glass shards from deep water Gulf of Mexico ash beds. Gulf Coast Association of Geological Societies Transactions 48:95-106.

Hem, J. D. 1985. Study and interpretation of the chemical characteristics of natural water. U.S. Geological Survey Water Supply Paper 2254, ed. 3, Alexandria, VA, 263 p.

Henry, C. D., and R. R. Kapadia. 1980. Trace elements in soils of the south Texas uranium district: concentrations, origin, and environmental significance. The University of Texas at Austin, Bureau of Economic Geology Report of Investigations No. 101, 52 p.

Henry, C. D., W. E. Galloway, G. E. Smith, C. L. Ho, J. P. Morton, and J. K. Gluck. 1982. Geochemistry of ground water in the Miocene Oakville sandstone - a major aquifer and uranium host of the Texas coastal plain. The University of Texas at Austin, Bureau of Economic Geology Report of Investigations No. 118, 63 p.

Henry, C. D., W. E. Galloway, and G. E. Smith. 1982. Considerations in the extraction of uranium from a fresh-water aquifer - Miocene Oakville sandstone, South Texas. The University of Texas at Austin, Bureau of Economic Geology Report of Investigations No. 126, 36 p.

Henry, C. D., F. W. McDowell, J. G. Price, and R. C. Smyth. 1986. Compilation of potassium-argon ages of Tertiary igneous rocks, Trans-Pecos Texas. The University of Texas at Austin, Bureau of Economic Geology Geological Circular 86-2, 34 p.

Hiemstra, T., and W. H. Van Riemsdijk. 1999. Surface structural ion adsorption modeling of competitive binding of oxyanions by metal (hydr)oxides. Journal of Colloid and Interface Science 210:182-183.

Hitchon, B., E. H. Perkins, and W. D. Gunter. 1999. Introduction to groundwater geochemistry. Geoscience Publishing Ltd., Canada.

Hobday, D. K., and W. E. Galloway. 1999. Groundwater processes and sedimentary uranium deposits. Hydrogeology Journal 7:127-138.

Hoel, H. D. 1982. Goliad Formation of the south Texas gulf coastal plain: regional genetic stratigraphy and uranium mineralization. unpublished Master's Thesis. Department of Geological Sciences, University of Texas at Austin.

Holliday, V. T. 1989. The Blackwater Draw Formation (Quaternary): a 1.4-plus-m.y. record of eolian sedimentation and soil formation on the Southern High Plains. Geological Society of America Bulletin 101:1598-1607.

Hopenhayn-Rich, C., M. L. Biggs, and A. Smith. 1998. Lung and kidney cancer mortality associated with arsenic in drinking water in Cordoba, Argentina. International Journal of Epidemiology 27:561-569.

Hopkins, J. 1993. Water-quality evaluation of the Ogallala aquifer, Texas. Texas Water Development Board Report No. 342, 41 p.

Hudak, P. F. 2000. Distribution and sources of arsenic in the Southern High Plains aquifer, Texas, USA. Journal of Environmental Science and Health Part A-Toxic/Hazardous Substances & Environmental Engineering 35(6):899-913.

Ilger, J. D., W. A. Ilger, R. A. Zingaro, and M. S. Mohan. 1987. Modes of occurrence of uranium in carbonaceous uranium deposits: characterization of uranium in a South Texas (U.S.A.) lignite. Chemical Geology 63:197-216.

Izett, G. A. 1981. Stratigraphic sucession, isotopic ages, partial chemical analyses, and sources of certain silicic volcanic ash beds (4.0 to 0.1 m.y.) of the western United States. U.S. Geological Survey Open-File Report 81-763:2 sheets.

Jackson, W. A., K. Rainwater, T. Anderson, T. M. Lehman, R. Tock, S. Rajagopalan, and M. Ridley. 2004. Distribution and potential sources of perchlorate in the High Plains region of Texas. Report by Texas Tech University Water Resources Center, Lubbock, TX submitted to the Texas Commission on Environmental Quality, August 2004, 170 p.

Jordan, D. N., M. McClelland, A. Kendig, and R. Frans. 1997. Monosodium methanearsonate influence on broadleaf weed control with selected postemergence-directed cotton herbicides. Journal of Cotton Science 1:72-75.

Kessinger, W. P. J. 1967. Cretaceous (Kiamichi and Duck Creek) foraminifera from Lynn, Terry, Hockley, and Lamb Counties, Texas. Pages 301-308 in L. Hendricks, editor. Comanchean (Lower Cretaceous) stratigraphy and paleontology of Texas. The Permian Basin Section, Society of Economic Paleontologists and Mineralogists, 67-8.

Korte, N. E., and Q. Fernando. 1991. A review of arsenic(III) in groundwater. Critical Reviews in Environmental Control 21:1-39.

Kresse, T., and J. Fazio. 2003. Occurrence of arsenic in ground waters of Arkansas and implications for source and release mechanisms. Arkansas Deptartment of Environmental Quality, Water Quality Report WQ03-03-01, 35 p.

Kurttio, P., E. Pukkala, H. Kahelin, A. Auvinen, and J. Pekkanen. 1999. Arsenic concentrations in well water and risk of bladder and kidney cancer in Finland. Environmental Health Perspectives 107:705-710.

Lai, M. S., Y. M. Hsueh, C. J. Chen, M. P. Shyu, S. Y. Chen, T. L. Kuo, M. M. Wu, and T. Y. Tai. 1994. Ingested inorganic arsenic and prevalence of diabetes mellitus. American Journal of Epidemiology 139:484-492.

Langmuir, D. 1997. Aqueous Environmental Chemistry. Prentice Hall, New Jersey.

Lederer, W. H., and R. J. Fensterheim, editors. 1983. Arsenic: Industrial, Biomedical, Environmental Perspectives, Proceedings of the Arsenic Symposium, Gaithersburg, Maryland, Van Nostrand Reinhold Environmental Engineering Series, 443 p.

Ledger, E. B. 1981. Evaluation of the Catahoula Formation as a source rock for uranium mineralization, with emphasis on East Texas. Ph.D thesis. Texas A&M University.

Ledger, E. B., T. T. Tieh, and M. W. Rowe. 1984. An evaluation of the Catahoula Formation as a uranium source rock in east Texas. Gulf Coast Association of Geological Societies Transactions 34:99-108.

Lee, L. M. 2005. Regional survey of Arsenic and associated trace metals in Texas groundwater: a multivariate and geostatistical approach. Submitted to Ground Water.

Lewis, D. R., J. W. Southwick, R. Ouellet-Helstrom, J. Rench, and R. L. Calderon. 1999. Drinking water arsenic in the United States: a cohort mortality study. Environmental Health Perspectives 107:359-365.

Lin, T.-F., and J.-K. Wu. 2001. Adsorption of arsenite and arsenate within activated alumina grains: equilibrium and kinetics. Water Research 35:2049-2057.

Lindberg, R. D., and D. D. Runnells. 1994. Ground water redox reactions: an analysis of equilibrium state applied to Eh measurements and geochemical modeling. Science 255:925-927.

Litke, D. W. 2001. Historical water-quality data for the High-Plains regional ground-water study area in Colorado, Kansas, Nebraska, New Mexico, Oklahoma, South Dakota, Texas and Wyoming, 1930-1998. U.S. Geological Survey Water Resources Investigation Report 00-4254, 66 p.

Loebenstein, R. J. 1994. The materials flow of arsenic in the United States. U.S. Bureau of Mines Information Circular 9382, 12 p.

Lombi, E., W. W. Wenzel, and R. S. Sletten. 1999. Arsenic adsorption by soils and iron-oxide coated sand: kinetics and reversibility. Journal of Plant Nutrition and Soil Science 162:451-456.

Lopez, J. A. 1995. Salt Tectonism of the United States Gulf Coast Basin, map, 2nd ed., New Orleans Geological Society.

LSU (Lousiana State University). 2005. Louisiana suggested chemical weed control guide. Louisiana Cooperative Extension Service, Louisiana Agricultural Experiment Station, and the United States Department of Agriculture, Publication 1565, January 2005, http://www.agctr.lsu.edu/guides/weedguide/01weeds.htm (2005/04/16):148 p.

Lumsdon, D. G., and L. J. Evans. 1994. Surface complexation model parameters for Goethite (alpha-FeOOH). Journal of Colloid and Interface Science 164:119-125.

Manning, B. A., and S. Goldberg. 1996. Modeling competitive adsorption of arsenate with phosphate and molybdate on oxide minerals. Soil Science Society of America Journal 60:121-131.

Manning, B. A., S. E. Fendorf, B. Bostick, and D. L. Suarez. 2002. Arsenic(III) oxidation and arsenic(V) adsorption reactions on synthetic birnessite. Environmental Science & Technology 36:976-981.

Mazumder, D., N. Guha, J. Das Gupta, A. Santra, A. Pal, A. Ghose, S. Sarkar, N. Chattopadhaya, and D. Chakraborti. 1997. Non-cancer effects of chronic arsenicosis with special reference to liver damage. Pages 112-123 in C. O. Abernathy, R. L. Calderon, and W. R. Chappell, editors. Arsenic-Exposure and health effects. Chapman & Hall.

McBride, E. F., W. L. Lindemann, and P. S. Freeman. 1968. Lithology and petrology of the Gueydan (Catahoula) Formation in south Texas. University of Texas at Austin, Bureau of Economic Geology Report of Investigations no. 63, 122 p.

McDowell, F. W., and S. E. Clabaugh. 1979. Ignimbrites of the Sierra Madre Occidental and their relation to the tectonic history of western Mexico. Pages 112-124 in C. E. Chapin and W. E. Elston, editors. Ash-flow tuffs: Geological Society of America Special Paper 180: 112-124.

McGowen, J. H., G. E. Granata, and S. J. Seni. 1977. Depositional systems, uranium occurrence and postulated ground-water history of the Triassic Dockum Group, Texas Panhandle-Eastern New Mexico. The University of Texas at Austin, Bureau of Economic Geology, report prepared for the U.S. Geological Survey under grant number 14-08-0001-G410, 104 p.

McGowen, J. H., G. E. Granata, and S. J. Seni. 1979. Depositional framework of the Lower Dockum Group (Triassic), Texas Panhandle. Bureau of Economic Geology Report of Investigations No. 97.

McMahon, P. B. 2001. Vertical gradients in water chemistry in the Central High Plains aquifer, southwestern Kansas and Oklahoma Panhandle, 1999. U.S. Geological Survey Water-Resources Investigations Report 01-4028, 47 p.

McMahon, P. B., J. K. Bohlke, and T. M. Lehman. 2004. Vertical gradients in water chemistry and age in the southern High Plains aquifer, Texas, 2002. U.S. Geological Survey Scientific Investigations Report 2004-5053, 53 p.

Mehta, S., A. E. Fryar, and J. L. Banner. 2000. Controls on the regional-scale of the Ogallala aquifer, Southern High Plains, Texas, USA. Applied Geochemistry 15:849-864.

Meng, X., S. Bang, and G. P. Korfiatis. 2000. Effects of silicate, sulfate, and carbonate on arsenic removal by ferric chloride. Water Research 34:1255-1261.

Miller, C. S., and E. M. Bailey. 1979. Arsenic acid use and hazard assessment in the dessication of cotton. The Texas Agricultural Experiment Station Report MP-1434, The Texas A&M University System, College Station, TX, October 1979, 5 p.

Molenat, N., A. Astruc, M. Holeman, G. Maury, and R. Pinel. 1999. Arsenic speciation by hydride generation-Quartz furnace atomic absorption spectrometry. Optimization of analytical parameters and application to environmental samples. Analusis 27:75-83.

Mosier, E. L. 1998. Geochemical characterization of solid-phase materials in the Central Oklahoma Aquifer. in S. Christenson and J. S. Havens, editors. Ground-water quality assessment of the Central Oklahoma aquifer, Oklahoma: Results of investigations. U.S. Geological Survey Water Supply Paper 2357-A,. 71-105.

Mullican, W. F. I., N. D. Johns, and A. E. Fryar. 1997. Playas and recharge of the Ogallala aquifer on the Southern High Plains of Texas–An examination using numerical techniques. The University of Texas at Austin, Bureau of Economic Geology Report of Investigations No. 242, 72 p.

Nativ, R. 1988. Hydrogeology and hydrochemistry of the Ogallala Aquifer, Southern High Plains, Texas Panhandle and Eastern New Mexico. The University of Texas, Bureau of Economic Geology Report of Investigations No. 177, 64 p.

Nativ, R., and G. N. Guttierez. 1988. Hydrogeology and hydrochemistry of Cretaceous aquifers, Texas Panhandle and Eastern New Mexico. The University of Texas at Austin, Bureau of Economic Geology Geological Circular 88-3, 32 p.

Neeley, R. A. 1994. Facies analysis of the lower Cretaceous (Albian) Goodland and lower Kiamichi Formations of southeast Oklahoma. Oklahoma City Geological Society, The Shale Shaker Digest XIII, Volumes XXXX-XXXXIV (1989-1994):163-192.

Nordstrom, P. L., and R. Quincy. 1999. Ground-water data system dictionary. Texas Water Development Board Report UM-50, 104 p.

Nordstrom, D. K., and D. G. Archer. 2002. Arsenic thermodynamic data and environmental chemistry. Pages 1-26 in A. H. Welch and K. G. Stollenwerk, editors. Arsenic in Ground Water. Kluwer Publishers.

NRC (National Research Council). 1999. Arsenic in drinking water. Subcommittee on arsenic in drinking water. National Academy Press, Washington, D. C.

Nugent, J. E., M. S. Nabers, and B. Williamson. 1994. South Texas uranium district abandoned mine land inventory. Railroad Commission of Texas, Surface Mining and Reclamation Division, variably paginated.

Osterkamp, W. R., and W. W. Wood. 1987. Playa-lake basins on the Southern High Plains of Texas and New Mexico: Part II. A hydrologic model and mass-balance arguments for their development. Geological Society of America Bulletin 99:215-223.

Parker, D. F., J. G. Krystinik, and B. J. Mckee. 1988. Provenance of the Gueydan Formation, south Texas: implications for the late Oligocene-early Miocene tectonic evolution of the Trans-Pecos volcanic field. Geology 16:1085-1088.

Parkhurst, D. L., S. Christenson, and G. N. Breit. 1995. Ground-water quality assessment of the Central Oklahoma aquifer, Oklahoma-Geochemical and geohydrologic investigations. U.S. Geological Survey Water Supply Paper 2357-C, 101 p.

Parkhurst, D. L., and C. A. J. Appelo. 1999. User's guide to PHREEQC (version 2)-a computer program for speciation, batch-reaction, one-dimensional transport, and inverse geochemical calculations. U.S. Geological Survey Water-Resources Investigations Report 99-4259, 312 p.

Parry, W. T., and C. C. J. Reeves. 1968. Clay mineralogy of pluvial lakes sediments, southern High Plains, Texas. Journal of Sedimentary Petrology 38:516-529.

Peacock, C. L., and D. M. Sherman. 2004. Vanadiun(V) adsorption onto goethite (alpha-FeOOH) at pH 1.5 to 12: a surface complexation model based on ab initio molecular geometries and EXAFS spectroscopy. Geochimica et Cosmochimica Acta 68:1723-1733.

Peryea, F. J., and T. L. Creger. 1994. Vertical distribution of lead and arsenic in soils contaminated with lead arsenate pesticide residues. Water, Air and Soil Pollution 78:297-306.

Peryea, F. J., and R. Kammereck. 1997. Phosphate-enhanced movement of arsenic out of lead arsenate-contaminated topsoil and through uncontaminated subsoil. Water, Air and Soil Pollution 93:243-254.

Pierce, M. L., and C. B. Moore. 1980. Adsorption of arsenite on amorphous iron hydroxide from dilute aqueous solutions. Environmental Science and Technology 14:214-216.

Presser, T. S. 1994. Geologic origin and pathways of selenium from the California Coast Range to the west-central San Joaquin Valley. Pages 139-155 in W. T. Frankenberger Jr. and S. Benson, editors. Selenium in the environment. Marcel Dekker, Inc., New York.

Proctor, C. V. J., T. E. Brown, N. B. Waechter, S. Aronow, and V. E. Barmes. 1974. Sequin Sheet. in Geologic Atlas of Texas, scale 1:250,000, The University of Texas at Austin, Bureau of Economic Geology.

Qi, S. L., A. Konduris, D. W. Litke, and J. Dupree. 2002. Classification of irrigated land using satellite imagery, the High Plains aquifer, nominal data 1992. U.S. Geological Survey Water Resources Investigations Report 02-4236, 31 p.

Rahman, M., M. Tondel, S. A. Ahmad, and O. Axelson. 1998. Diabetes mellitus associated with arsenic exposure in Bangladesh. American Journal of Epidemiology 148:198-203.

Rahman, M., M. Tondel, S. A. Ahmad, I. A. Chowdhury, M. H. Faruquee, and O. Axelson. 1999. Hypertension and arsenic exposure in Bangladesh. Hypertension 33:74-78.

Rahman, M., M. Tondel, I. A. Chowdhury, and O. Axelson. 1999. Relations between exposure to arsenic, skin lesion, and glucosuria. Journal of Occupational and Environmental Medicine 56:277-281.

Raven, K. P., A. Jain, and R. H. Loeppert. 1998. Arsenite and arsenate adsorption on ferrihydrite: kinetics, equilibrium, and adsorption envelopes. Environmental Science & Technology 32:344-349.

Redman, A. D., D. L. Macalady, and D. Ahmann. 2002. Natural organic matter affects arsenic speciation and sorption on hematite. Environmental Science & Technology 36:2889-2896.

Reynolds, R. L., and M. B. Goldhaber. 1983. Iron disulfide minerals and the genesis of roll-type uranium deposits. Economic Geology and the Bulletin of the Society of Economic Geologists 78:105-120.

Roddick-Lanzilotta, A. J. 2002. Infrared spectroscopic characterisation of arsenate (V) ion adsorption from mine waters, Macraes Mine, New Zealand. Applied Geochemistry 17:445-454.

Rose, W. I., C. M. Riley, and Dartevelle. 2003. Sizes and shapes of 10-Ma distal fall pyroclastics in the Ogallala Group, Nebraska. Journal of Geology 111:115-124.

Ryder, P. D., and A. F. Ardis. 1991. Hydrology of the Texas Gulf Coast aquifer systems. U.S. Geological Survey Open-File Report 91-64, 147 p.

Ryker, S. J. 2001. Mapping arsenic in ground water - A real need, but a hard problem. Geotimes 46:34 - 36.

Ryker, S. J. 2003. Arsenic in ground water used for drinking water in the United States. Pages 165-178 in A. H. Welch and K. G. Stollenwerk, editors. Arsenic in Ground Water. Kluwer Acad. Publ.

Scanlon, B. R., R. S. Goldsmith, and W. F. I. Mullican. 1994. Methodology and preliminary results of unsaturated flow studies for a proposed Texas low-level radioactive waste repository. Pages 497-506 in A. R. Dutton, editor. Toxic substances and the hydrologic sciences. American Institute Hydrology.

Scanlon, B. R., and R. S. Goldsmith. 1997. Field study of spatial variability in unsaturated flow beneath and adjacent to playas. Water Resources Research 33:2239-2252.

Schlottmann, J. L., E. L. Mosier, and G. N. Breit. 1998. Arsenic, chromium, selenium, and uranium in the central Oklahoma aquifer. in S. Christenson and J. S. Havens, editors. Ground-water quality assessment of the Central Oklahoma aquifer, Oklahoma: Results of investigations. U.S.Geological Survey Water Supply Paper 2357-A,. 119-179.

Seni, S. J. 1980. Sand-body geometry and depositional systems, Ogallala Formation, Texas. The University of Texas at Austin, Bureau of Economic Geology Report of Investigations No 105, 36 p.

Shacklette, H. T., and J. G. Borerngen. 1984. Element concentrations in soils and other surficial materials of the conterminous United States. U.S. Geological Survey Professional Paper 1270, 104 p.

Shelby, C. A., S. Pieper, S. Aronow, and V. E. Barnes. 1992. Beaumont Sheet. in Geologic Atlas of Texas, scale 1:250,000. The University of Texas at Austin, Bureau of Economic Geology.

Sidwell, R. G. 1936. Mineral study of Kiamichi Formation of west Texas. Journal of Sedimentary Petrology 6:31-34.

Smedley, P. L., and D. G. Kinniburgh. 2002. A review of the source, behaviour and distribution of arsenic in natural waters. Applied Geochemistry 17:517-568.

Smedley, P. L., H. B. Nicolli, D. M. J. Macdonald, A. J. Barros, and J. O. Tullio. 2002. Hydrogeochemistry of arsenic and other inorganic constituents in groundwaters from La Pampa, Argentina. Applied Geochemistry 17:259-284.

Smith, G. E., W. E. Galloway, and C. D. Henry. 1982. Regional hydrodynamics and hydrogeochemistry of the uranium bearing Oakville aquifer (Miocene) of south Texas. The University of Texas at Austin, Bureau of Economic Geology Report of Investigations No. 124, 31 p.

Smith, E., R. Naidu, and A. M. Alston. 1998. Arsenic in the soil environment - A review. Adv. Agron. 64:149-195.

Smith, S. M. 2001. National Geochemical Database: Reformatted data from the National Uranium Resource Evaluation (NURE) Hydrogeochemical and Stream Sediment Reconnaissance (HSSR) Program, Version 1.30. U.S. Geological Survey Open-File Report 97-492, WWW release only, URL: http://greenwood.cr.usgs.gov/pub/open-file-reports/ofr-97-0492/index.html , last accessed August, 2005.

Sposito, G. 1984. The surface chemistry of soils. Oxford Univ. Press, Oxford.

Sracek, O., P. Bhattacharya, G. Jacks, J. P. Gustafsson, and M. von Bromssen. 2004. Behavior of arsenic and geochemical modeling of arsenic enrichment in aqueous environments. Applied Geochemistry 192:169-180.

Stanton, M. R., R. F. Sanzolone, S. S. Sutley, D. J. Grimes, and A. M. Meier. 2001. Mineralogical and geochemical Constraints on Fe and As residence and mobility in the Albuquerque Basin: Examples from basin sediments and volcanics. Pages 45-46 in J. C. Cole, editor. U.S. Geological Survey Middle Rio Grande Basin Study: Albuquerque, New Mexico, U.S. Geological Survey Open File Report 00-488.

Stollenwerk, K. G. 1995. Modeling the effects of variable groundwater chemistry on adsorption of molybdate. Water Resources Research 31:347-358.

Stollenwerk, K. G. 2003. Geochemical processes controlling transport of arsenic in groundwater: a review of absorption. Pages 1-26 in A. H. Welch and K. G. Stollenwerk, editors. Arsenic in ground water. Kluwer Publishers.

Swedlund, P., and J. G. Webster. 1999. Adsorption and polymerization of silicic acid on ferrihydrite, and its effect on arsenic adsorption. Water Research 33:3413-3422.

Thelin, G. P., and L. P. Gianessi. 2000. Method for estimating pesticide use for county areas of the conterminous United States. U.S. Geological Survey, Open-File Report 00-250, 62 p.

Tondel, M., M. Rahman, A. Magnuson, I. A. Chowdhury, M. H. Faruquee, and S. A. Ahmad. 1999. The relationship of arsenic levels in drinking water and the prevalence rate of skin lesions in Bangladesh. Environmental Health Perspectives 107:727-729.

Tournassat, C., L. Charlet, D. Bosbach, and A. Manceau. 2002. Arsenic(III) oxidation by birnessite and precipitation of manganese(II) arsenate. Environmental Science & Technology 36:493-500.

Tseng, W. P., H. M. Chu, S. W. How, J. M. Fong, C. S. Lin, and S. Yeh. 1968. Prevalance of skin cancer in an endemic area of chronic arsenicism in Taiwan. Journal of the National Cancer Institute 40:453-463.

Tsuda, T., A. Babazono, E. Yamamoto, N. Kurumatani, Y. Mino, T. Ogawa, Y. Kishi, and H. Aoyama. 1995. Ingested arsenic and internal cancer: a historical cohort followed for 33 years. American Journal of Epidemiology 141:198-209.

U.S. Geolgical Survey. 2004. National Uranium Resource Evaluation (NURE) Hydrogeochemical and Stream Sediment Reconnaissance data, Denver, CO.

Valentine, J. L., S. Y. He, L. S. Reisboro, and P. A. Lachenbruch. 1992. Health response by questionnaire in arsenic-exposed populations. Journal of Clinical Epidemiology 45:487-494.

Vogelmann, J. E., S. M. Howard, L. Yang, C. R. Larson, B. K. Wylie, and N. van Driel. 2001. Completion of the 1990s National Land Cover Data set for the conterminous United States from Landsat Thematic Mapper data and ancillary data sources. Photogrammetric Engin. and Remote Sensing 67:650-662.

Wanty, R. B., and M. B. Goldhaber. 1992. Thermodynamics and kinetics of reactions involving vanadium in natural systems: accumulation of vanadium in sedimentary rocks. Geochimica et Cosmochimica Acta 56:1471-1483.

Warrick, B. E., J. R. Supak, R. B. Metzer, C. R. Stichler, and J. Bremer. 1992. Effects of desiccant rates, defoliation, method of application, and weather on arsenic residues in lint, seed, and burs. Beltwide Cotton Production Research Conference, 570-577.

Welch, A. H., and M. S. Lico. 1998. Factors controlling As and U in shallow ground water, southern Carson Desert, Nevada. Appl. Geochem. 13:521-539.

Welch, A. H., D. B. Westjohn, D. R. Helsel, and R. B. Wanty. 2000. Arsenic in ground water of the United States: occurrence and geochemistry. Ground Water 38:589-604.

Wenzel, W. W., N. Kirchbaumer, T. Prohaska, G. Stingeder, E. Lombi, and D. C. Adriano. 2001. Arsenic fractionation in soils using an improved sequential extraction method. Analytica Chimica Acta 436:309-323.

White, A. F., and N. M. Dubrovsky. 1994. Chemical oxidation-reduction controls on selenium mobility in groundwater systems. Pages 185-221 in W. T. Frankenberger Jr. and S. Bensen, editors. Selenium in the environment. Marcel Dekker, Inc., New York.

Wilkie, J. A., and J. G. Hering. 1996. Adsorption of arsenic onto hydrous ferric oxide: effects of adsorbate/adsorbent ratios and co-occurring solutes. Colloids and Surfaces A- Physicochemical and Engineering Aspects 107:97-110.

Wolery, T. J. 1995. EQ3/6, a software package for geochemical modeling of aqueous systems: package overview and installation guide (version 7.2b). Lawrence Livermore National Laboratory, Livermore, California.

Wood, W. W., and B. F. Jones. 1990. Origin of solutes in saline lakes and springs on the southern High Plains of Texas and New Mexico. Pages 193-208 in T. C. Gustavson, editor. Geologic framework and regional hydrology: Upper Cenozoic Blackwater Draw and Ogallala Formations, Great Plains. Bureau of Economic Geology, The University of Texas at Austin.

Wood, W. W., and W. E. Sanford. 1995. Chemical and isotopic methods for quantifying ground-water recharge in a regional, semiarid environment. Ground Water 33:458-468.

Wood, W. W., and W. E. Sanford. 1995. Eolian transport, saline lake basins, and groundwater solutes. Water Resources Research 31:3121-3129.

Wood, W. W. 2002. Role of ground water in geomorphology, geology, and paleoclimate of the southern High Plains, USA. Ground Water 40:438-447.

Wu, M. M., T. L. Kuo, Y. H. Hwang, and C. J. Chen. 1989. Dose response relation between arsenic concentration in well water and mortality from cancers and vascular diseases. American Journal of Epidemiology 130:1123-1132.

Yan-Chu, H. 1994. Arsenic distribution in soils. Pages 17-49 in J. O. Nriagu, editor. Arsenic in the environment, Part I: cycling and characterization. John Wiley & Sons, Inc., New York.

Yoshida, T., H. Yamauchi, and G. Fan Sunm. 2004. Chronic health effects in people exposed to arsenic via the drinking water: dose-response relationships in review. Toxicology and Applied Pharmacology 198:243-252.

APPENDIX I: Arsenic Geochemistry

I-1 Introduction

Behavior of all chemical elements is dependent upon environmental conditions, mainly represented by pH and redox (Eh) conditions. By definition, a low pH represents an abundance of H^+, whereas a high pH is characterized by scarce H^+. Natural water pH values range from 5 to 9. Oxidizing conditions are characterized by a high Eh (>400 mV). They can be associated with acidic, neutral, or alkaline pH values. On the other hand, reducing conditions, characterized by a low (<100 mV) or negative Eh, tend to be associated with neutral to alkaline conditions (this is because reduction reactions often tend to consume H^+). By definition, trace chemical elements, such as arsenic, do not control pH and Eh. They will be under the chemical form/species directed by thermodynamics to be the most stable under those conditions. As will be seen later, thermodynamics equilibrium is not always reached for kinetics reasons (slow reaction rate).

The geochemistry of arsenic is complex because of the possible coexistence of two or even three redox states (-III, III, V), because of the rich chemistry of organo-arsenicals, and because of the strong interaction of most arsenic compounds with soil particles, particularly iron oxides (and to a lesser degree, aluminum and manganese oxides). The fully deprotonated arsenate AsO_4^{-3} is the expected form of arsenic in most soils under aerobic conditions only at high pH (**Figure 1**). At more neutral and acid pH levels, the $HAsO_4^{-2}$ and $H_2AsO_4^{-1}$ forms, respectively, are dominant. The general understanding of arsenic mobility in soil and aquifers is that it will increase with increasing pH and phosphate concentration and with decreasing clay and iron oxide content. A more thorough discussion of arsenic sorption is presented in Appendix I. As pH increases, the negative charge of the arsenate ion increases, making it less likely to sorb on negatively charged soil particles. Phosphates have a chemical structure very similar to that of arsenates and sorb to soils preferentially under some conditions. Nitrogen also belongs to the same periodic table group (Va) but does not show the same competing behavior as phosphate. Other structurally similar oxyanions, such as sulfate and selenate, are also weak sorbers. Under less oxidizing conditions, the arsenite ion H_3AsO_3 is most stable. The lack of charge renders the ion more mobile and less likely to sorb to soil particles. Its pH stability spread ranges from very acidic to alkaline. The first deprotonated form $H_2AsO_3^{-1}$ exists at significant concentrations only above a pH of approximately 9 (Table 10). The redox processes seem to be mediated by microorganisms (Welch et al., 2000) and to occur next to mineral surfaces.

Under even more reducing conditions, arsenide is the stable ionic form of arsenic. Arsenic has a complex geochemistry with sulfur, both in solution where several thioarsenic ions can form and in the associated minerals. Arsenic metal –As(0)- rarely occurs. Methylated arsenic compounds are generally present at low aqueous concentrations (<1 ug/L), if at all, except maybe when there is an abundance of organic matter (Welch et al., 2000). If not of anthropogenic origin, their formation from inorganic substrates, however, is not thermodynamically favored (Pierce and Moore, 1980) and requires the intervention of organisms (arsenic is often metabolized to render it less toxic). Methylated arsenic compounds are stable in both oxic and reducing environments (Stollenwerk, 2003). The standard Eh of the couple As(V)/As(III) is close to 0 at pH=7, that is, between the Fe^{2+}/Fe^{3+} and SO_4^{-2}/H_2S couples (**Figure 77**).

As(V) and As(III) minerals are fairly soluble and do not control arsenic solubility in oxidizing and mildly reducing conditions, except maybe if barium is present (Henry et al., 1982a, p. 21). This is in contrast to other companion oxyanions not as mobile under reducing conditions, except vanadium. In reducing conditions, As precipitates as arsenopyrite (FeAsS) but more commonly in solid solution with pyrite. Realgar (AsS) and orpiment (As_2S_3) require a high sulfur

activity and are unlikely in the southwestern Gulf Coast and High Plains. There are more than 500 As-containing minerals, but because of their relatively high solubility, arsenate minerals are typically confined to mining districts, particularly those containing copper, lead, and zinc. The most common arsenate mineral is probably scorodite ($FeAsO_4.2H_2O$). However, scorodite is stable only under a small range of acidic pH values. More generally, during the mineral-forming process, arsenate ion associates itself most frequently with trace metals. Notable minerals include $Zn_2(AsO_4)(OH)$ (adamite) and $Co_3(AsO_4)_2.8H_2O$ (erythrite), Arsenate can also substitute for phosphate in apatite and other phosphate minerals (e.g., $Ca_5(AsO_4)_3Cl$ or $Ca_5(AsO_4)_3OH$) A thermodynamic database distributed with the geochemical modeling code PHREEQC gives a reaction constant of logK = -17.81 for $Ca_3(AsO4)_2$, used as an insecticide in the early 1900's. Assuming a reasonable molar concentration in calcium of 2 mmol/L, the lowest arsenic concentration at which precipitation might occur is 2 mg/L.

Distribution coefficient K_d (L/kg), $K_d = C_s/C_w$, where C_s (mg/kg) and C_w (mg/L) are concentrations in solid and water, respectively, is a common way to quantify how much arsenic is sorbed to a soil. As discussed later, it is not the best way to model arsenic distribution between solid particles and aqueous phase. Total concentration C_T and water concentration are then related by

$$C_T = C_w\left(K_d + \frac{\theta_w}{\rho_b}\right)$$

where θ_w and ρ_b are water content and bulk dry density, respectively. Distribution coefficient data for arsenic were computed and gathered by EPA (EPA, 1996, Part 2, p. 40). The coefficient, in the average conditions assumed by EPA, varies linearly from 25 to 31 L/kg for pH values from 4.9 to 8, respectively. For an average porosity of 25 percent and a water saturation of 50 percent, this translates into an additional 9 L/kg to the K_d for the concentration ratio. Distribution coefficients for specific minerals are listed in Smedley and Kinniburgh (2002, Table 6).

Phosphorus commonly exists under only one valence state, P(V), in natural conditions. Orthophosphate (PO_4^{-3}) is the final dissociation product of phosphoric acid (H_3PO_4). The most common ionic form of phosphate in natural conditions is $H_2PO_4^{-1}$. Condensed forms of phosphates, including polyphosphates, are not stable in water and degrade to phosphate. Phosphate sorbs strongly to oxides, as well as to organic and clay phases. Polyphosphates are strong metal ligands. Phosphate concentration is controlled by apatite (complex calcium phosphate). Fertilizers can increase phosphate concentration in water by several orders of magnitude.

I-2 Oxyanions and Other Related Ions

In many geochemical environments, arsenic is regionally associated with selenium, molybdenum, vanadium, and uranium (Smedley and Kinninburgh, 2002 and, e.g., for Texas, Lee, 2005). There is a well-dcumented association of uranium deposits with those trace elements (e.g., Guilbert and Park, 1986, p.912). It can be seen in the roll-front uranium deposits of the western United States (Wyoming, Colorado, Texas). Volcanic ash is the accepted mineralization source. Uranium and other trace elements are leached by oxidizing and ~neutral pH water and transported downgradient and/or downdip by migrating groundwater until reducing environments are encountered. All those elements share the property of being soluble in oxidizing conditions and insoluble in reducing conditions. Other trace elements, such as iron and manganese, have the opposite characteristics. Reduced Fe(II) is soluble, whereas Fe(III) precipitates as iron oxide in oxidizing conditions (~neutral and alkaline pH levels). Similarly, manganese Mn^{+2} is soluble for a larger pH range at reduced Eh. Other light volatile elements, such as fluoride, boron, and beryllium, are also typically found with acidic (rhyolitic) volcanism

and are frequently associated with those oxyanions. They accumulate in the acidic volcanic melt because they do not enter the structure of feldspars and other higher temperature minerals. They typically end up as accessory minerals in intrusive rocks unless they are released during volcanic events. The next few paragraphs give a short review of the behavior of these elements (Se, Mo, V, U, F, B, Be) as well as that of phosphate. Table 10 displays the pH range of stability for the different oxyanions. The pKa is the pH at which the concentrations of the protonated and deprotonated forms are equal.

Selenium has a chemistry similar to that of sulfur, existing naturally in four redox states VI, IV, 0, and –II, with selenate, selenite, and selenide ions occurring in Eh-pH conditions largely parallel to those of arsenic. In oxic conditions, the selenate ion, SeO_4^{-2}, is the dominant species across all natural pH levels. In slightly reducing conditions, the selenite ion exists from the fully deprotonated form, SeO_3^{-2}, at alkaline pH levels to the neutral H_2SeO_3 at acid pH values and the $HSeO_3^{-1}$ form at neutral pH. However, there are several differences with arsenic. The selenate ion is a weak sorber, and its behavior more closely resembles that of sulfate than that of arsenate ion (White and Dubrovsky, 1994). Organo-selenium compounds and possibly native selenium are also more widespread. The standard Eh values for redox couples Se(VI)/Se(IV) and Se(VI)/Se(-II) are ~450 and ~-100 mV, respectively (Figure 77). All selenate and selenite minerals are highly soluble. Native selenium or more likely ferroselite (pyrite with some Se substituted for S) can precipitate at high Eh (~100 mV) at neutral pH. However, kinetics issues may keep selenium in solution even at reducing Eh levels (Henry et al., 1982a, p. 21). No controlling minerals for selenium solubility have been observed in the Gulf Coast.

Molybdenum exists naturally in two redox states: Mo(VI) and Mo(IV). The molybdate ion Mo (VI) (MoO_4^{-2}) is stable across all natural pH levels but the most acidic. Mo(IV) is present mainly in molybdenite MoS_2. Molybdate ion sorbed onto iron oxides and is displaced by arsenate and phosphate. The only common molybdenum mineral is molybdenite (MoS_2). Ilsemannite (Mo_3O_8) has also been described in the southwestern Gulf Coast. It typically forms a low pH for the Mo concentrations considered in this study. Molybdenite typically forms at Eh lower than -200 mV (Henry et al., 1982a, p. 18). Both minerals are insoluble but do not control the Mo chemistry in the southwestern Gulf Coast because pH is generally neutral to alkaline and reducing conditions so low are rare.

The geochemistry of uranium is complicated in the details but can be summarized by the following. Uranium(VI) in oxidizing conditions exists as the soluble positively charged uranyl UO_2^{++}. Solubility is higher at acid pH levels, decreases at neutral pH, and increases slightly at alkaline pH. However, the uranyl ion, to the contrary of oxyanions, can easily form aqueous complexes, including with hydroxyl, fluoride, carbonate, and phosphate ligands. Hence, in the presence of carbonates, uranium solubility is considerably enhanced in the form of uranyl-carbonate (UO_2CO_3) and other higher order carbonate complexes: uranyl-di- and uranyl-tri-carbonates ($UO_2(CO_3)_2^{-2}$ and $UO_2(CO_3)_3^{-4}$). Adsorption of uranium is in inverse proportion to its solubility and is highest at neutral pH (De Soto, 1978, p. 11). Uranium(IV) is the other commonly found redox state. In that state, however, uranium has low solubility and precipitates as uraninite, UO_2, coffinite, $USiO_4.nH_2O$ (if SiO_2>60 mg/L, Henry et al., 1982a, p.18), or related minerals. In the southwestern Gulf Coast, there is no mineral controlling uranium solubility in oxidizing conditions. However, uranite and coffinite are the controlling minerals if the Eh drops below 0-100 mV.

Vanadium naturally exists in three different redox states: V(III), V(IV), and V(V). V(III) is present only in extremely reducing environments and most likely precipitates as $V(OH)_3$ or VO(OH) (Wanty and Goldhaber, 1992). V(IV) generally forms vanadyl cations VO^{+2} (low pH) and $VO(OH)^{+1}$ (higher pH). V(V), in the form of vanadate -$H_2VO_4^{-1}$ and HVO_4^{-2}, sometimes written as $VO_2(OH)_2^{-1}$ and $VO_3(OH)^{-2}$-, is expected to be prevalent in well-oxygenated systems, but both V(IV) and V(V) are often present together. Vanadyl ions are strongly sorbed by organic

and oxide phases. Vanadate ions form strong inner-sphere complexes with iron oxides (Peacock and Sherman, 2004). Although vanadate minerals have been described in the south Texas uranium province, no reduced vanadium minerals have been found. Vanadium sulfides are rare, and reduced vanadium generally integrates crystal structure of other minerals such as titaniferous magnetite. Both minerals are unlikely in the southwestern Gulf Coast, and no mineral is controlling vanadium concentration.

Phosphorus commonly exists under only one valence state, P(V), in natural conditions. Orthophosphate (PO_4^{-3}) is the final dissociation product of phosphoric acid (H_3PO_4). The most common ionic form of phosphate in natural conditions is $H_2PO_4^{-1}$. Condensed forms of phosphates, including polyphosphates, are not stable in water and degrade to phosphate. Phosphate sorbs strongly to oxides, as well as to organic and clay phases. Polyphosphates are strong metal ligands. Phosphate concentration is controlled by apatite (complex calcium phosphate). Fertilizers can increase phosphate concentration in water by several orders of magnitude.

Fluorine exists naturally in solution under one valence, F^-, the fluoride ion. Fluoride tends to make complexes and ion pairs with trace elements. It can also sorb significantly to oxides, especially aluminum oxides, and clays (Hem, 1985, p. 121). Its concentration is controlled by calcium, as fluorite (CaF_2) is the most common fluorine mineral. Apatite can also contain a significant amount of fluorine. Fluorine accumulates in felsic rocks, as well as in sedimentary rocks with the order shale>carbonate>sandstone (Hitchon et al., 1999).

Borate is the only natural form of boron in solution. Orthoboric acid, H_3BO_3, has a pKa of ~9.2 and occupies most of the Eh-pH diagram (Hitchon et al., 1999). Boron is an essential constituent of tourmaline, an accessory mineral highly resistant to weathering. Boron is a frequent component of volcanic gases. Borate can sorb to clays and metal oxides, but minerals controlling its solubility precipitate only in a saline lake type of environment. Beryllium is a rather rare element occurring typically at concentrations <1 ug/L and is found naturally as Be(II) and related aqueous complexes.

Figure 77 presents the redox ladder or the order in which the trace elements would precipitate in given conditions, assuming instantaneous reactions. At ~neutral pH, the precipitation order is selenium (0,-II) $\approx$ uranium (IV)> molybdenum (IV) > arsenic (-II) > vanadium (III). Molybdenum and arsenic solubility at low pH are a strong function of sulfur activity. More genrally the order can be altered depending on other ions present in the solution.

I-2 Surface Complexation

The geochemistry of arsenic is largely impacted by sorption on particles also called surface complexation. Chemists usually make a distinction between weak sorption (or physisorption or outer complex sorption) and strong sorption (or chemisorption or inner complex sorption). The latter involves true chemical bonds between the sorbate and the sorbent, whereas the former entails electrostatic interactions. Surface complexation can be modeled with empirically derived isotherms for a given set of experimental conditions. Arsenic sorption on goethite has been fitted to experimental data with a Langmuir isotherm (Pierce and Moore, 1980) and with a Freundlich isotherm. However, experimental isotherms are not as general as theoretically derived surface complexation models and are not as suitable to predict adsorption behavior outside of the range of experimental data. The double-layer model presented in Dzombak and Morel (1980) and implemented in several geochemical codes, including the U.S. Geological Survey PHREEQC numerical code, is widely used. An understanding of transport of arsenic in porous media necessitates a thorough knowledge of the sorbing materials exposed to fluid flow.

I-2.1 Release Mechanisms

It has been known for a long time that aqueous ions interact with soil or aquifer particles, particularly organic matter, clays, and metal oxides. Soil particles and, in particular, metal oxides have pH-dependent surface charges. A surface includes broken bonds that readily interact with water molecules generating strongly binding OH-type groups. These groups are amphoteric. At lower pH levels, the OH_2^+ group is dominant, whereas at relatively higher pH, the group O^- is the dominant form. In between, there is a pH where both groups are numerically balanced, leading to a globally neutral surface at the ZPC (Zero-Point of Charge; also called isoelectric point; terminology depends on the method used to measure it). Anion sorption decreases past the ZPC of the surface. ZPCs are generally in the 2-5 pH range for silicates, including most clays, leading to mostly negatively charged surfaces in the subsurface. In contrast, iron oxides have a ZPC in the 7-9 range, positioning them as strong anions sorbents except for the highest natural pH. An example describing surface hydrolysis reactions that was extracted from the PHREEQC database follows:

$Hfo\text{-}OH + H^+ = Hfo\text{-}OH_2^+ \qquad \log(K_1) = pK_{a1} = 7.29$

$Hfo\text{-}OH = Hfo\text{-}O^- + H^+ \qquad \log(K_2) = -pK_{a2} = -8.93$

$pH_{ZPC}=0.5(pK_{a1}+ pK_{a2})=8.11$

These pKas are intrinsic values that do not account for electrostatic interactions (this is automatically done in the code). Note that ZPCs can be complexly affected by other ions present in the solutions and that ZPC values usually given strictly apply for minerals in pristine conditions with no sorbing ions besides H^+. ZPCs can be shifted by background ions. For example, Appelo et al. (2002) suggested that carbonate sorption on ferrihydrite moves the ZPC of oxides to lower values. The same observation was made experimentally by Lumsdom and Evans (1994) on pristine goethite in a pure N_2 environment where the theoretical ZPC of ~9.5 can be shifted to values <8 in simpler operational conditions.

Carbonates also have a ZPC in the high pH range. They, however, lack significant specific surface area. Iron oxides, on the other hand, are characterized by high specific surface areas, as high as that of clays, especially if they are amorphous or small grained. Hydrated ferric oxides “Hfo” are very high specific area iron oxides and are particularly active just after genesis and precipitation. The same group includes amorphous iron oxides and other ill-defined species such as ferrihydrite ($\sim Fe_5HO_8.4H_2O$). They age to goethite and other FeOOH oxides with a lower specific surface. Hematite (Fe_2O_3) is typically more crystalline and has a specific surface lower by a factor of ~10. Experiments tend to prove that the “fresher” and the more hydrated the oxide, the higher the As sorption (Smedley and Kinniburgh, 2002). This aspect of arsenic chemistry is well exploited in some water treatment plants where arsenic removal is handled by first oxidizing any As(III) to As(V), more likely to sorb, and by the introduction of ferric salts that evolves into fresh high specific surface area ferric hydroxides scavenging arsenate ions during the coagulation/flocculation/filtration treatment. An alternative is activated alumina. Direct adsorption on oxides or activated carbon is also used.

Several theories tackle the surface-ion interactions, including some developed by Dzombak and Morel (1990) (diffuse double-layer surface complexation model). They suggested that the chemistry of adsorption on iron oxide surfaces is ultimately adequately modeled by an acid-base model whose reaction constant is corrected by local electrostatic factors. The model input, as implemented in PHREEQC, requires the mass of oxide per unit mass of water, the specific surface area of the oxide, and the density of active sites. Dzombak and Morel (1990) estimated adsorption site density at 0.2 mole/mole of iron (the so-called weak sites Hfo_w). An additional less numerous set of sites was deemed necessary to fit their experimental data for cations (the so-called strong sites Hfo_s). Their density was estimated at 0.005 mole/mole of iron. They also suggested a typical specific surface area of 600 m^2/g of Hfo, defined as FeOOH; this translates

into ~53x10^3 m^2/mole of Fe. Dixit and Hering (2003) suggested a similar site density for all iron oxides; they would differ only by their specific surface area and by their intrinsic reaction constant. For a stoichiometric formula of FeOOH and a specific surface area of 600 m^2/g, a site density of 0.2 and 0.005 mol/mol Fe for weak and strong sites, respectively, translates into a site density of 3.84 umol/m^2. Stollenwerk (1995) found that the average site density of ~50 aquifer cores was 3.33 umol/m^2, in agreement with recommendation by Dzombak and Morel (1990). The sorption sites were attached to coatings of Fe and Al oxides on quartz and feldspar grains.

In aqueous systems where arsenic anions are the main sorbates, arsenite sorption does not display large variations in the normal pH range and is slightly higher for neutral pH and maybe alkaline pH. Sorption drops beyond the first pKa of H_3AsO_3 at ~9.2. Arsenate anions sorb most effectively at pH below 7, and then the fraction sorbed decreases to small values (Manning and Goldberg, 1996; Figure 1 of Wilkie and Hering, 1996, who experimented with [As]~100 mg/L). At higher As concentrations (1000's of ppm), work by Raven et al. (1998) suggest that this general model still holds, although arsenite is now more sorbed than arsenate.

Aluminum oxides follow the same general model of high arsenate sorption at pH<7, progressively decreasing as the pH becomes more alkaline (experiments by Halter and Pfeifer, 2001, with [As]~ppm's). However, at equivalent surface area, they sorb more arsenate than iron oxides, particularly at higher pH because of their higher ZPC (~9.5 for amorphous aluminum hydroxides; Manning and Golberg, 1996). In a modeling exercise with their own Al data and Fe data from Dzombak and Morel (1990), Halter and Pfeifer (2001) found that iron oxides sorbed more than Al oxides only at pH<4. They also suggested that α-Al_20_3 (corundum) is a good proxy for arsenic sorption on clays because of the similarity of their mineralogical structure. Lin and Wu (2001) looked at sorption of both arsenite and arsenate on activated alumina across the pH range and also found that the general model is similar to that of sorption on iron oxides.

Manganese oxides have a low ZPC (around 2-3) and are negatively charged in most natural conditions. They sorb little arsenate but some arsenite (because the molecule is not charged). More complex mechanisms are involved, in particular arsenite oxidation and manganese reduction. Silica (SiO_2) ZPC is around 2. Silica has been described as barely sorbing arsenic (Stollenwerk, 2003). Carbonates have also been observed sorbing arsenic (Stollenwerk, 2003). Calcite has a ZPC of approximately 9, suggesting positive charges on the surface. On the other hand, their specific surface area is low.

Clay charges are thought to be due to substitution of Al^{+3} for tetrahedral Si^{+4} or Mg^{+2} for octahedral Al^{+3}, creating a pH-independent deficit of negative charges, typically covered by metal cations. Clays can also sorb anions, especially at the edges of their planar structure where hydroxyl groups can be found (Sposito, 1984). However, because clay ZPCs are typically less than 5, substantial sorption on clays is expected only in acidic conditions. In any case, studies by Roddick-Lanzilotta (2002) suggested that kaolinite does not sorb much As, and when it does, the latter is easily washed off. Wenzel et al (2001) suggested that arsenic sorption on clay follows the following model: As[mg/kg]=12.2exp(0.0057xCEC[mmol$_c$/kg]) [mmol$_c$ = mmol of charge = milliequivalent].

Although organic matter binds metals strongly, it does not seem to play a large role in arsenic inorganic processes. Organic matter is often negatively charged and does not interact readily with anions. Soluble organic molecules may enhance or interfere with As sorption. Bowell (1994) found that fulvic acids compete with arsenates for sorption sites on iron oxides.

The amounts sorbed to different media can be reconstructed by doing a sequential extraction of arsenic on the samples. Within the limits of the extraction techniques, Wenzel et al. (2001) determined that the median fractions of arsenic for 20 Austrian As-contaminated soils in the following states—within the solid phase, sorbed onto well-crystallized hydrous Fe and Al

oxides, sorbed onto amorphous and poorly crystallized hydrous Fe and Al oxides, and more lightly sorbed and readily labile (likely weak physisorption on oxides and clays)—were 17.5%, ~29%, ~42%, and ~10%, respectively. The arsenic concentration ranged from 96 to 2,183 mg/kg with a median of 259 mg/kg. The mean soil composition was ~18% clay and 0.053% carbon on a mass basis. The mean Cation Exchange Capacity (CEC) is 184 $mmol_c/kg$. The average iron and aluminum oxide fraction is 0.5% Fe and 0.2% Mn on a mass basis. Despite abundant clay, most of the arsenic is sorbed on the metal oxides.

I-2.2 Competition in Surface Complexation

In natural waters, many types of ions coexist, several possibly competing for the same absorption sites. The final coverage of the surface depends essentially on two parameters: the relative abundance of each ion and their relative attraction to the surface. More generally, sorption phenomena follow the general chemistry principle of mass action. Equilibrium results of competing sorbates is function of the sorption strength of the individual sorbates but also of the sorbate ratio. For example, at some pH levels, arsenates sorb more strongly than phosphates on iron oxides but phosphate concentration is much higher, resulting in most sites being occupied by phosphate anions. Those competing aspects are captured by the modeling software.

Common anions in the subsurface are sulfates and (bi)carbonates, to which can be added nitrates and phosphates in agricultural areas. Other common aqueous species, such as silica, can also impact arsenic absorption. Trace elements, in particular those forming oxyanions (Mo, Se, V), can also compete for the same sites and may locally affect the As-soluble fraction. Many other aqueous components present in groundwater have been suggested to have some effect on arsenic sorption on soil particles; dissolved organic matter has been described as having some negative impact on As sorption on hematite (Redman et al., 2002), especially for As(III). Some chemical elements, such as calcium, may increase the sorbing capacity of soil particles because they create additional positive charges (cationic bridges) favorable to As sorption. In most studies, nitrates and sulfates had no impact on arsenic sorption. Nitrate (Meng et al., 2000, table 1) and sulfates form weak outer sphere complexes.

Manning and Goldberg (1996) and Hiemstra and Van Riemsdijk (1999) looked at the complexity of oxyanion interactions in surface complexation. Both arsenate and phosphate ions behave very similarly relative to sorption on iron oxides. In an agricultural context, phosphates are applied in the form of polyphosphates and progressively degrade to orthophosphates. They can then be adsorbed by plants and also be sorbed by oxides. Introduced in a clean medium in the same molar concentration, it appears that Al-based groups (gibbsite, kaolinite) preferentially sorb phosphates, whereas iron and manganese oxides preferentially sorb arsenates (Violenta et al., 2002; Manning and Goldberg, 1996). Welch et al. (2000) mentioned several instances where phosphate fertilizers displaced sorbed arsenic from soils. Peryea and Davenport (1991) and Peryea and Kammereck (1997) did columns studies on impact of phosphates on arsenic-contaminated soils. They found that arsenic desorbed by phosphate would move downward but sorb again on deeper subsoil.

Carbonate ions have also been suspected of displacing arsenate but at a much smaller scale (Goh and Lin, 2005), although Meng et al. (2000) found that carbonate has no effect on arsenic sorption. Carbonate sorption on HFO was investigated by Appelo et al. (2002). They suggested that sorption of carbonate ions by iron oxides is more widespread than commonly recognized. Swedlund and Webster (1999) found that silica adsorption on ferrihydrite does compete for adsorption sites with arsenate, and not so much for arsenite, especially at high alkaline pH (>9), where arsenate adsorption is at the lowest and silica adsorption at its highest. Meng et al. (2000) also found silica to negatively impact arsenic adsorption.

I-3 Kinetics

Thermodynamics can only suggest what spontaneous reactions are permissible. It does not provide information on how fast a reaction will proceed. This is the realm of mainly experiment-based kinetics. According to Raven et al. (1998), who experimented with arsenic aqueous concentrations on the order of 50 to a few hundred ppm, adsorption on fresh ferrihydrite is completed within a few hours. They found that arsenite sorption is faster at higher arsenic concentrations, but arsenate is faster at low concentrations and low pH. Lombi et al. (1999), experimenting with natural soils and [As]~100 mg/L, suggested that the equilibrium was reached in 5 days and also that arsenite sorbs faster.

Sorption kinetics are important in the presence of competing sorbates because one can sorb faster and occupy more sites than it should relative to equilibrium. It will then take time for it to desorb and reach true equilibrium. Desorption kinetics is generally slower than adsorption ("aging"), that is, sorption is not fully reversible or slower than adsorption, as observed in many contaminated sites. Lomdi et al. (1999) noted that in an extraction sequence after 1, 10, and 30 days, less and less As was released by the weak extractants, suggesting that the bonds were getting stronger.

Redox reactions are generally microbially mediated. Redox kinetics for As(III) to As(V) can take a few days, whereas As(V) to As(III) can take a few weeks/months. Stollenwerk noted that As(III) tends to be metastable in an oxic environment and that oxidation to As(V) could take years in the presence of only atmospheric oxygen. Other inorganic oxidants (Fe^{3+}, Mn), however, increase the rate of oxidation. In reducing environments, reduction of As(V) to As(III) is faster. Manganese oxide can mediate oxidation of As(III) to As(V) (Tournassat et al., 2002; Manning et al, 2002). This transformation has not been observed for goethite (Wilkie and Hering, 1996, p. 104). Manning and Goldberg (1996) suggested that kaolinite and illite have catalytic abilities in redox reactions of As(III) to As(V).

I-4 Geochemical Data

All geochemical numerical modeling is strongly dependent on the conceptual model, but also, in a less obvious fashion, on the thermodynamic database used for the simulations. The PHREEQC modeling software (Parkhurst and Appelo, 1999) is included with three thermodynamic databases: wateq4f, minteq, and EQ3/6. Arsenic inorganic aqueous species are few. Unlike most metals, oxyanions do not form complexes in solution with ions such as Cl^-, SO_4^{-2}, OH^-, CO_3^- or HCO_3^- common in typical natural water conditions (F^- may be an exception). In strongly reducing environments, combinations with sulfur at different redox states add complexity to the arsenic aqueous chemistry. Homogeneous aqueous reaction constants are reasonably well known and consistent in the different databases, as well as with the published literature. In contrast, if, overall, adsorption studies are in general qualitative agreement (but not always), they are somewhat conflicting in their result on the pH having the highest adsorption and on the value of the intrinsic reaction constant. The generalized double-layer model used to fit experimental data simplifies very complex processes and does not capture all aspects, even if experimentally understood. Experiments are done at different temperatures, at different ionic strengths, at different arsenic and other sorbate concentrations, and using diversely prepared sorbents.

The wate4f database has been recently updated (Nordstrom and Archer, 2002) and contains thermodynamic data for H_3AsO_4, H_3AsO_3 and derived anions, as well as ions $H_4AsO_3^+$ ($H_nAsO_4^{n-3}$, n=0 to 4; $H_nAsO_3^{n-3}$, n=0 to 4). Data for required solid phases, such as hydrated calcium arsenate, are also given, as well as sorption data on iron oxides for arsenate, arsenite, and phosphates. The EQ3/6 and Minteq databases show similar but slightly different information (Table 19). None of the databases provides information on organo-arsenicals.

APPENDIX II: The Uranium Province of South Texas and Other Uranium Showings

Uranium Province of South Texas

The Gulf Coast hosts numerous uranium deposits, particularly in Live Oak, Karnes, and Duval counties. Their grade ranges from 0.04 to 0.30 percent U_2O_3 with individual deposits containing 500-10,000 tons U_2O_3 (Reynolds and Goldhaber, 1983; Finch, 1996) for a cumulative resource of ~100,000 tons U_2O_3 (Finch, 1996), of which one third has been produced (Finch, 1997). They are found in the Whitsett Fm. of the Jackson Group of late Eocene age, in the Oligocene Catahoula tuffs, and in the Miocene Oakville sandstone, as well as in the Pliocene Goliad sands (Henry et al., 1982b, p. 6 and Figure 78)

Mineralization consists of iron sulfides (pyrite and marcasite in variable proportions) at 1-2% weight (Fishman et al., 1982; Goldhaber and Reynolds, 1977). Uranium is found in the form of oxide (uraninite, UO_2) or silicate (coffinite, $USiO_4.nH_2O$). In association with the mineralization, selenium, molybdenum, and arsenic are also found. The Lamprecht deposit (Live Oak County) yields hundreds to thousands of ppm of uranium and a few hundreds of ppm of selenium in the mineralized section. Native selenium has been observed in the nearby Felder mine (Eargle et al., 1975). No arsenic or vanadium is associated with this deposit. When deposits are brought to the surface by erosion, as in the Karnes County area, oxidized ore comprises iron oxides, uranyl calcium phosphate and vanadate (Eargle et al., 1975), uranium silicates (boltwoodite, weeksite, uranophane), and some uranium oxides (schoepite).

The origin of the deposits has been described in many publications, including Hobday and Galloway (1999), Guilbert and Park (1986), Galloway (1982), Galloway et al. (1982), and Galloway and Kaiser (1980). The deposits result from the movement of oxidizing waters carrying uranium and other oxyanions into a reducing environment. The reducing conditions were created by carbonaceous material (Fisher et al., 1970, p.257), authigenic sulfide, dissolved H_2S and/or CH_4 leakage along contemporaneous growth faults from underlying hydrocarbon accumulations, and/or previous pyrite mineralization, also thought to have been created by earlier H_2S leakage, as demonstrated by sulfur isotope studies (Goldhaber et al., 1978) or Mesozoic sulfidic water leakage (Galloway, 1982). Leakage of H_2S is still active, as shown by the odor in some mines (Eargle et al., 1975). Hydrogen sulfide leakage seems to be the trap for most deposits in the Oakville sandstone, whereas organic matter in lignite seems to have played a larger role in the late Eocene deposits (Ilger et al., 1987) and Catahoula deposits (Galloway, 1977, p. 45). Reductants intrinsic to the depositional system, e.g., organic matter or primary pyrite, are more likely present in finer grained facies. In that case, mineralization will occur near permeability contrasts. Conversely, an exogen reductant will be transported through the most permeable zones where the mineralization will also be found (Hobday and Galloway, 1999).

Oxidizing waters flowing downdip along permeable sandstone layers create the well-known roll-front morphology where a tongue of oxidized water progressively invades the reduced section of the aquifer. The mineralization occurs at the generally sharp interface. However, the detailed depositional history can be more complex. In some Gulf Coast deposits, a later phase of resulfidization, probably corresponding to another discharge from a fault, can alter the previously oxidized zone and mask the previous morphology. The mineralization can also be exposed to surficial conditions. The sulfides are then oxidized and trace elements remobilized.

Some deposits show a chromatographic separation of trace metals relative to their position on the redox ladder. Selenium typically precipitates first at higher Eh than uranium; thus, higher selenium concentrations occur behind the front, whereas molybdenum precipitates ahead of the uranium mineralization because molybdenite (MoS_2) requires a lower Eh to form (Galloway,

1982, his Figure 12; see core analyses in Fishman et al., 1982). At the Lamprecht deposit (Live Oak County), the gradation occurs in 100-200 m.

The host formations include the basal sands of the Miocene Oakville Fm. and the Catahoula tuffs (=Gueydan) and the upper section of the underlying Jackson Group of Eocene age (e.g., Whitsett Fm.). Some deposits are also found in the Pliocene Goliad Fm. (Finch, 1996). One controlling factor for mineralization in the Eocene Whitsett Fm. of the Jackson Group is whether the Frio Clay, a downdip marine clay facies, is present to separate the Catahoula and Whitsett units. The fact that, where present, the Jackson is typically not mineralized suggests that the mineralization is at least Oligocene and that the Whitsett was merely used as a high-transmissivity conduit (Figure 21 of Galloway et al., 1979).

The source of uranium and other trace elements is volcanic ash (Galloway and Kaiser, 1980). Ash layers are thought to have contained 10-15 ppm of uranium, about half of which was leached during pedogenesis or later (Ledger et al., 1984). The volcanic rocks at the emission centers in west Texas also contained uranium concentration at 5-6 ppm (Ledger et al., 1984), about twice the average concentration for igneous rocks. Uranium could be sorbed onto glass shards and crystals. It is then readily leached. This process is thought to be minor. Uranium may also be disseminated in the groundmass and is then released at a later time during devitrification and recrystalization (De Soto, 1978, p.66). Volcanic ash has a high specific surface area favorable for leaching. Leaching releases trace elements under oxidizing mildly alkaline conditions in a dry climate. Uranium solubilization is most effective in the thick, aerated unsaturated zone (Hobday and Galloway, 1999). The evidence of this statement lies in the reduced uranium content of most acidic ash layers in the Gulf area relative to their counterparts elsewhere. It is also supported by an increase in the thorium/uranium ratio because thorium does not leach as easily (Dickinson, 1976). Some ash layers preserved in reducing lacustrine environments also show higher uranium content. Ash can be directly deposited aerially. It can also be reworked and deposited as tuffaceous material in an aqueous environment shortly after aerial emplacement. Most layers are currently degraded to clays and zeolites. Ledger et al. (1984) also suggested that uranium leaching continues far later than pedogenesis. In particular, leaching of uranium from volcaniclastics in the southwestern Gulf Coast is still occurring, especially during calichification and its typical higher pH and carbonate concentration.

Mineralization of layers older than the Catahoula Fm. could be explained by local ash beds of the same age or by leaching of uranium from the Catahoula Fm. during pedogenesis by recharging waters. Uranium in younger formations could result from general cross-formational flow or reworking of older accumulations. Galloway et al. (1982) contrasted the Oakville sands in this region and concluded that the generally higher TDS and uranium mineralization of South Texas is due to the higher fault density in the south, allowing more reducing material, as well as deep brines, to invade the aquifer. Galloway and Kaiser (1980, p. 18-19) also suggested that in the Catahoula Fm. of East Texas, more abundant recharge may dilute uranium concentration in groundwater, limiting downdip accumulations. The higher precipitation regime can also increase rejected recharge, in effect, shunting the accumulation engine (Galloway, 1977, p. 48). The uranium-rich solution would then be discharged to the ocean through stream base flow. Had the precipitation been lower in Gueydan times, deep recharge would have been too small to generate economic accumulations.

In addition, despite important lignite deposits earlier in the stratigraphic section, no economical uranium accumulation is associated with them. Large low-grade uranium deposits are associated with lignite in the western United States. The source for these deposits seems to be interbedded volcanic tuffs.

Uranium Showings in the Texas Panhandle:

Minor production (~1 ton U_2O_3) is recorded from Triassic sandstones of the Texas Panhandle and Tertiary rocks of the Hagan Basin in New Mexico (Finch, 1997). Finch (1975) stated that uranium anomalies have been found across the stratigraphic section from the Dockum to the Pleistocene. The Trujillo sandstone in the Dockum Group has yielded 800 tons of ore near the town of Post in Garza County, southeast of Lubbock on the Llano Estacado. McGowen et al. (1979) displayed a map of grab samples from a campaign in the Dockum. Most samples having concentrations >10 ppm are in Garza County, and some are in the Palo Duro Canyon area. A single occurrence of uranium-vanadates minerals in the Edwards limestone of Upton County has also been reported (Eargle, 1956).

McGowen at al. (1977) compiled gamma-ray information from Dockum cores outside of the outcrop areas. They noticed numerous anomalies (their Figures 43 to 47) but mainly in the Midland basin, not on the Central platform. They postulated (p. 69) that a positive structural feature was oxidizing and maybe periodically recharging basinward sandstone aquifers during the Triassic Period. The anomalies are diffuse over large areas and were attributed to the presence of uranium. Contemporary sources for Triassic volcanites have been described east, south, and west of the current outline of the formation (McGowen at al., 1977, p. 77). In addition, the age of the mineralization has not been well constrained. Another hypothesis is leaching of Cretaceous volcanites or shales before deposition of the Ogallala Fm. Ash layers of Ogalalla age are also a possible source, according to McGowen at al. (1977). The Dockum section of the Delaware Basin on the western side of the Central Platform does not exhibit any anomaly (McGowen at al., 1977, p. 69). McGowen et al. (1977, p. 78) concluded their study by stating that the uranium concentration in the Dockum is most likely derived from leaching of Ogallala ash layers and downward flow, especially in the valley fills where the Ogallala is the thickest.

Uranium Showings in Central and East Texas

There are some uranium mineralization or radioactivity anomalies in the Catahoula Fm. of Central and East Texas (Galloway, 1977, Plate III; Ledger, 1981).

APPENDIX III: Evaluation of Geophysical Logs to Determine Potential Sources of Contaminants in the High Plains

Introduction

A preliminary survey of geophysical well logs recorded in the Ogallala Formation in the Southern High Plains indicated potential occurrences of locally extensive, anomalously radioactive shale beds. These beds were interpreted to record local accumulations of volcanic-ash-rich shales, probably in lacustrine (lake) environments. Volcanic ash contains potassium-40 (a radioactive isotope that decays to argon), as well as uranium. Radioactive decay of these and associated isotopes allows volcanic ash to be used for geologic-age-dating. Volcanic ash has been observed in the Ogallala section in Potter County, Texas (Capeda, 2001) and Nebraska (Rose and others, 2003). Younger volcanic ashes also occur. There is a 10-my record of volcanic ash in the High Plains, the source of which has been suggested to be in the Yellowstone area of northern Wyoming (Izett, 1977). It was observed during this investigation that greater numbers of these beds occurred in the southern parts of the study area than in the north and that, coincidentally, greater relative numbers of water wells with elevated arsenic levels also occurred in the south. Volcanic materials have been shown to be a natural source for arsenic. Therefore, it was decided to further investigate the apparent correspondences between groundwater arsenic concentrations and presumed volcanic ash distribution in the Ogallala of the Southern High Plains.

Data and Methods

Over 700 geophysical well logs procured from the well log library of the Bureau of Economic Geology and the Surface Casing Unit of the Texas Commission on Environmental Quality were reviewed. These logs represented geologic sections from 21 counties (**Figure 58**). Approximately 250 of these logs had gamma ray responses recorded for sufficiently thick portions of the Ogallala for the purposes of evaluating presence or absence of elevated gamma ray values. The criteria for usefulness of a given well log were 1) an anomalously elevated gamma ray value was generally defined as one that exceeded 100 API units; 2) that logging began within 8 m (25 ft) of the ground surface for logs that showed no anomalously elevated gamma ray values; and 3) that logging began within 30 m (100 ft) of the surface for logs that did show anomalously elevated values.

The gamma-ray value criterion was applied somewhat subjectively because it was obvious that not all of the well logs had been calibrated to the same standards. All logs were not of the same vintage. In the end a gamma ray value was deemed to be anomalous if it exceeded values for other shale beds in the upper 300 m (1000 ft) of geologic section, which also included Cretaceous and Triassic strata. Also, ash-rich beds less than 2 ft thick may not have produced gamma-ray-log responses that achieved full expression of their actual radioactivity. The second criterion assured that most of the Ogallala was measured prior to judging it free of volcanic beds. Most of the Ogallala is overlain by varying thicknesses of overburden, including the Blackwater Draw Formation and other alluvial material. The third criterion recognized that it was important only that a volcanic bed was observed in the Ogallala, not that it occurred in any pre-defined part of the section.

An attempt was made to provide as spatially consistent data coverage as was possible. Some counties have hundreds of hydrocarbon-prospective boreholes while others have few. The distribution of well data that was collected should be adequate to detect local concentrations of volcanic ash of such extent as to justify further investigation to determine the boundaries of the deposits.

Results

The presence of anomalously elevated gamma ray values for strata within the Ogallala Formation was observed in logs from approximately 110 of the 250 locations for which data were gathered (Figure 58). The most areally extensive occurrences are in Andrews, Gaines, and Yoakum Counties, based on contour mapping of data that was classified according to bed thickness. Three bed-thickness classes were defined: greater than 5 ft thick, 1-5 ft thick, and 0 ft thick (no ash bed present). Contour mapping, in this instance, suggests lateral continuity of the geologic setting between data points. For example, if two data points show indications of the presence of an ash bed then any point between them (if data were available for the point) would also show presence of an ash bed. There is no implication that individual ash beds are laterally continuous between locations, although this is more likely between closer-spaced data locations. In other words: contours envelop areas within which ash beds are expected to have been deposited, but not necessarily at the same time in all places within the contour envelope. If ash beds are a source of arsenic, then the areas within contour envelopes are suggested to mark areas within which potential arsenic sources occur.

Groundwater arsenic generally is more concentrated in the southern than in the northern parts of the Southern High Plains (Figure 44). There appears to be some association between estimated accumulations of interpreted volcanic ash and occurrences of elevated arsenic beneath them and down hydraulic gradient toward the southeast. These associations may indicate that arsenic-bearing constituents may have been extracted from ash deposits and are being transported by groundwater advection. Sparcity of volcanic-ash indicators (elevated gamma-ray responses) in more northern areas and coincident overall with lower levels of arsenic is strongly suggestive that the volcanic deposits and elevated groundwater-arsenic in the south are interrelated. The following section will test this hypothesis.

Mass Balance Computation

In order to assess the possibility of arsenic leaching from Ogallala-age ash beds, a crude mass balance was performed. The total mass of arsenic currently contained in the southern region of the southern High Plains is 1.2×10^{6} kg. This calculation assumes an average saturated thickness of 15 m with a porosity of 0.15 and an average arsenic concentration of 20 ug/L over an approximate area of 25,000 km^2. If the reasonable value of 500 for the number of pore volumes that went through the aquifer in the past 5 millions years, and the assumption that the average arsenic concentration has stayed constant since sediment deposition are used, approximately 0.57×10^{9} kg of arsenic have exited the aquifer through seeps and springs on the escarpment. The footprint of the operationally-defined ash beds (mainly in Gaines and Yoakum counties) is approximately 4,900 km^2. The beds are assumed continuous with an average thickness of 1 m. A total volume for the ash beds of 4.9×10^{9} m^3 follows. Assuming a arsenic content of 6 mg/kg and that half of it is leached, the total mass released is 0.033×10^{9} kg. This mass falls short by one order of magnitude of the amount required. It can however be almost matched if one assumes that the arsenic was leached when the ash covered the whole area (most of it would have washed away to the Gulf of Mexico and only relicts remained within the Ogallala Fm.) and that upgradient areas in New Mexico also provided arsenic.

Conclusions

The apparent association between distribution of groundwater arsenic and anomalously elevated radioactivity in Ogallala Fm. is intriguing and merits additional investigation. More stratigraphic and hydrochemical data should be analyzed than was allowed within the scope of this work. Hundreds of additional well-logs are available that may allow more detailed stratigraphic and geographic mapping of interpreted volcanic ash deposits. A lower cutoff of gamma ray values for inclusion in the thickness map would more completely capture the geographical extent of lake deposits that contain ash material at presumably lower

concentrations than were mapped for this survey. Stratigraphically controlled hydrochemical surveys may allow precise identification of Ogallala strata that convey arsenic-bearing groundwater. Use of stable isotopes may clarify the actual geologic source of arsenic, which conceivably could be Cretaceous (Edwards-Trinity aquifer) or Triassic (Dockum aquifer) strata.

APPENDIX IV: Soil Sampling Results

The following tables display results from the soil sampling campaign. In Table IV.1, chemical analyses are posted with 2 significant digits. Units are kg/kg for water content and mg/kg for other columns. Analyses from nitrite, nitrate, sulfate, and phosphate represent the ion, not the chemical element. Table IV.2 includes texture analyses for sampled boreholes. In Table IV.3, method 1 indicates a matric potential measurement made with a UMS model T5 Tensiometer; method 2 indicates a water potential measurement made with a Decagon model WP4 psychrometer.

Table IV.1 Chemical analyses of soil core samples

Sample ID	Bore hole	Depth (m)	Water Content	As	Cl	Br	NO_2	NO_3	SO_4	PO_4
05-001	A1	0.08	0.020	4.1	1.7	0.0	0.1	0.4	1.7	0.2
05-002	A1	0.38	0.031	4.3	0.8	0.1	0.1	0.5	1.3	3.1
05-003	A1	0.69	0.061	1.8	0.8	0.0	0.2	0.3	0.9	0.2
05-004	A1	0.99	0.076	1.3	1.2	0.0	0.1	0.5	15.9	0.1
05-005	A1	1.30	0.092	2.1	1.3	0.2	0.4	0.5	94.4	1.1
05-006	A1	1.60	0.073	1.5	14.4	0.2	0.3	6.7	104.1	0.2
05-007	A1	2.21	0.032	4.2	19.4	0.1	0.3	0.4	43.6	0.4
05-008	A1	2.97	0.039	3.1	26.6	0.2	0.4	0.7	113.7	0.1
05-009	A2	0.08	0.021	9.7	2.0	8.0	1.1	1.6	6.2	0.5
05-010	A2	0.38	0.046	15.5	0.5	7.1	0.8	0.7	1.8	0.0
05-011	A2	0.69	0.069	19.2	0.4	8.5	0.8	0.9	9.9	0.0
05-012	A2	0.99	0.058	24.5	0.9	8.4	0.8	0.6	27.7	0.0
05-013	A2	1.30	0.039	19.1	0.7	12.4	0.5	0.1	65.0	0.0
05-014	A2	1.60	0.044	19.1	2.8	9.7	0.5	0.0	107.3	0.0
05-015	A2	2.21	0.065	26.0	34.1	7.4	0.4	1.6	205.3	0.1
05-016	A2	2.82	0.061	24.1	30.6	9.1	0.3	1.2	37.3	0.0
05-017	A2	3.43	0.070	33.9	24.2	9.2	0.3	1.2	38.1	0.0
05-018	A2	4.04	0.100	28.6	21.4	10.7	0.5	1.5	37.2	0.0
05-019	A2	4.65	0.066	14.5	13.5	10.1	0.2	1.4	33.9	0.0
05-020	A2	5.26	0.038	16.4	12.0	5.6	0.2	0.0	26.2	0.0
05-021	A2	5.87	0.099	71.9	36.0	6.5	0.1	0.0	91.5	0.0
05-022	A2	6.48	0.066	77.0	31.4	0.2	0.0	0.2	112.1	0.6
05-023	A2	7.09	0.071	36.6	53.0	0.4	0.1	0.1	203.0	0.5
05-024	A2	7.70	0.155	23.0	202.7	1.5	0.3	0.2	523.8	0.3
05-025	A2	8.31	0.136	13.1	180.6	1.6	0.2	0.3	496.7	0.2
05-026	T1	0.08	0.073	3.6	1.0	0.1	0.0	12.7	8.2	0.7
05-027	T1	0.38	0.093	5.8	0.3	0.0	0.2	5.1	10.9	0.5
05-028	T1	0.69	0.109	4.5	0.4	0.1	0.8	1.3	21.0	0.3
05-029	T1	0.99	0.108	3.3	0.7	0.2	0.6	1.4	31.7	0.1
05-030	T1	1.30	0.140	2.1	1.2	0.4	0.4	1.9	86.3	0.0
05-031	T1	1.60	0.140	3.8	1.0	0.3	0.5	4.6	98.4	0.0
05-032	T1	2.21	0.109	4.2	1.4	0.3	0.3	31.2	30.3	0.1
05-033	T1	2.82	0.136	14.0	0.9	0.2	0.4	11.0	42.9	0.1
05-034	T1	3.43	0.130	15.2	0.4	0.3	0.3	3.6	69.6	0.1
05-035	T1	4.04	0.120	14.7	0.5	0.1	0.1	7.4	119.8	0.4

Sample ID	Bore hole	Depth (m)	Water Content	As	Cl	Br	NO_2	NO_3	SO_4	PO_4
05-036	T1	4.65	0.172	29.0	1.0	0.2	0.3	12.0	236.1	0.1
05-037	T1	5.26	0.131	16.9	1.4	0.0	0.2	8.8	335.3	0.5
05-038	T1	5.87	0.141	17.2	4.6	0.0	0.3	10.8	485.9	0.0
05-039	T1	6.48	0.126	14.4	14.3	0.2	0.1	13.6	401.9	0.1
05-040	T1	7.09	0.083	16.8	19.7	0.2	0.1	12.0	248.8	0.1
05-041	T2	0.08	0.197	3.1	0.9	0.1	0.6	12.8	15.0	0.6
05-042	T2	0.38	0.183	8.1	0.5	0.1	0.2	3.8	5.4	1.2
05-043	T2	0.69	0.211	3.0	0.7	0.1	0.6	12.6	14.6	0.6
05-044	T2	0.99	0.127	20.2	0.5	0.2	0.4	0.9	2.2	7.2
05-045	T2	1.30	0.163	32.6	0.6	0.0	0.1	0.1	1.5	6.6
05-046	T2	1.60	0.184	30.9	0.5	0.2	0.3	0.1	1.9	4.3
05-047	T2	2.21	0.183	64.3	1.1	0.1	0.5	0.1	4.8	2.8
05-048	T2	2.82	0.199	203.5	0.4	0.6	0.5	0.1	7.4	1.0
05-049	T2	3.43	0.226	99.2	0.7	0.1	0.7	0.6	20.5	0.6
05-050	T2	4.04	0.160	78.6	0.4	0.0	0.3	0.3	8.3	1.7
05-051	T2	4.65	0.126	59.3	0.4	0.2	0.2	0.3	6.4	1.8
05-052	T2	5.26	0.117	59.6	0.5	0.1	0.2	0.3	6.6	0.6
05-053	T2	5.87	0.213	0.6	1.0	0.0	0.1	1.0	43.3	0.1
05-054	T2	6.48	0.228	0.7	1.5	0.2	0.2	1.7	12.8	0.1
05-055	T2	7.09	0.204	4.6	1.0	0.2	0.2	1.0	24.6	0.1
05-056	T2	7.70	0.127	4.8	0.6	0.0	0.1	0.4	15.4	0.1
05-057	T2	8.31	0.114	5.7	0.4	0.1	0.1	0.5	18.2	0.1
05-058	T2	8.92	0.099	7.1	0.6	0.1	0.1	0.4	14.8	0.1
05-059	T3	0.08	0.070	45.0	4.0	0.2	1.9	6.7	6.9	10.5
05-060	T3	0.38	0.063	18.3	1.9	0.1	0.9	5.2	9.1	1.7
05-061	T3	0.69	0.104	4.2	2.6	0.3	1.2	1.5	35.7	0.2
05-062	T3	0.99	0.107	2.8	3.3	0.3	1.1	1.6	235.3	0.1
05-063	T3	1.30	0.197	4.3	62.3	0.9	1.3	42.7	1127.7	0.0
05-064	T3	1.60	0.157	2.3	243.7	0.1	0.7	31.8	504.7	0.0
05-065	T3	2.21	0.147	4.5	116.8	1.1	0.8	21.7	198.7	0.1
05-066	T3	2.82	0.124	8.0	37.8	0.5	0.5	13.2	78.5	0.0
05-067	T3	3.43	0.114	24.8	25.0	0.2	0.6	12.3	31.1	0.1
05-068	T3	4.04	0.103	34.4	21.3	0.2	0.4	11.8	22.6	0.2
05-069	T3	4.65	0.121	29.4	26.4	0.3	0.5	13.4	11.6	0.1
05-070	T3	5.26	0.109	35.7	24.7	0.3	0.2	11.5	28.7	0.3
05-071	T3	5.87	0.128	41.1	20.0	0.2	0.2	8.5	23.1	0.1
05-072	T3	6.48	0.116	54.4	13.0	0.5	0.2	4.8	20.5	1.3
05-073	T3	7.09	0.090	62.1	6.1	0.1	0.1	2.1	11.1	0.6
05-074	T3	7.70	0.136	43.6	7.5	0.4	0.1	2.0	13.8	0.1
05-075	T3	8.31	0.110	30.0	4.4	0.1	0.0	1.1	13.7	0.1
05-076	T3	8.92	0.109	16.5	3.4	0.4	0.1	0.8	22.8	0.1
05-077	T3	9.53	0.092	11.4	2.4	0.3	0.1	0.5	15.5	0.1
05-078	T3	10.13	0.080	20.1	1.2	0.1	0.1	0.4	30.1	0.1
05-079	T3	10.74	0.072	8.2	0.8	0.1	0.0	0.3	28.1	
05-080	T3	11.35	0.088	17.0	1.1	0.3	0.1	0.4	21.0	0.1
05-081	T3	11.96	0.087	24.0	1.1	0.2	0.1	0.3	11.6	0.1
05-082	T3	12.57	0.064	10.4	1.3	0.2	0.1	0.4	13.5	0.1
05-083	T4	0.08	0.054	33.2	46.4	0.1	1.5	8.9	64.1	7.4

Sample ID	Bore hole	Depth (m)	Water Content	As	Cl	Br	NO_2	NO_3	SO_4	PO_4
05-084	T4	0.38	0.042	62.2	2.7	0.0	0.2	1.4	10.0	54.8
05-085	T4	0.69	0.052	2.1	2.2	0.2	0.5	0.8	21.4	0.1
05-086	T4	0.99	0.043	2.1	4.5	0.0	0.4	0.5	23.5	0.2
05-087	T4	1.30	0.101	1.4	4.2	0.0	0.8	0.7	107.2	0.0
05-088	T4	1.60	0.162	0.4	19.1	0.1	0.5	1.1	663.0	0.0
05-089	T4	2.21	0.127	0.5	115.7	0.4	0.3	8.7	368.7	0.0
05-090	T4	2.82	0.158	3.1	375.6	6.8	1.1	19.6	212.7	
05-091	T4	3.43	0.153	2.5	288.3	7.7	0.7	11.4	73.2	0.0
05-092	T4	4.04	0.123	1.7	176.6	4.0	0.5	7.2	86.0	0.0
05-093	T4	4.65	0.147	2.2	97.0	4.2	0.3	5.3	126.3	0.0
05-094	T4	5.26	0.156	3.8	55.7	4.1	0.2	4.5	122.3	0.0
05-095	T4	5.87	0.083	1.7	21.0	3.4	0.1	2.7	63.9	0.0
05-096	T4	6.48	0.107	4.3	23.0	3.7	0.0	3.7	53.5	0.0
05-097	T4	7.09	0.110	2.0	28.2	3.4	0.2	4.6	64.1	0.1
05-098	T4	7.70	0.135	2.3	42.4	5.6	0.2	7.0	73.2	0.0
05-099	T4	8.31	0.147	6.1	60.3	6.2	0.5	8.8	116.2	0.0
05-100	T4	8.92	0.123	3.7	58.4	5.8	0.2	7.1	106.3	0.4
05-101	T4	9.53	0.170	5.5	71.2	6.2	0.1	7.6	156.0	0.3
05-102	T4	10.13	0.115	3.5	36.4	3.7	0.2	4.6	122.9	0.0
05-103	L1	0.08	0.099	6.5	1.7	0.5	0.8	5.1	5.5	0.2
05-104	L1	0.38	0.130	1.3	0.9	0.4	0.7	1.9	21.5	0.0
05-105	L1	0.69	0.124	0.6	0.8	0.3	0.5	0.9	16.7	0.0
05-106	L1	0.99	0.098	1.2	1.1	0.6	0.6	0.6	8.4	0.0
05-107	L1	1.30	0.124	1.3	0.6	0.3	0.5	0.9	24.7	0.1
05-108	L1	1.60	0.118	2.1	0.4	0.4	0.6	0.9	58.6	0.1
05-109	L1	2.21	0.136	9.9	1.6	0.6	0.3	3.4	69.2	0.1
05-110	L1	2.82	0.115	15.9	2.7	0.8	0.3	10.2	56.2	0.1
05-111	L1	3.43	0.201	37.1	7.6	0.9	0.4	5.4	141.4	0.1
05-113	L1	4.65	0.156	28.8	55.8	0.7	0.3	22.5	390.5	0.1
05-114	L1	5.26	0.119	12.6	75.3	0.4	0.2	20.1	409.4	0.1
05-115	L1	5.87	0.128	9.9	114.5	0.5	0.3	18.0	738.4	0.1
05-116	L1	6.48	0.089	7.3	127.3	0.7	0.1	7.3	319.1	0.1
05-117	L1	7.09	0.084	5.6	154.4	0.6	0.1	3.2	321.1	0.1
05-118	L1	7.70	0.099	18.9	181.2	0.8	0.2	1.5	270.3	0.1
05-119	L1	8.31	0.101	17.7	212.2	0.8	0.2	0.8	279.7	0.1
05-120	L1	8.53	0.078	5.5	163.3	0.5	0.2	0.4	220.4	0.0
05-121	B1	0.08	0.119	4.2	0.6	0.4	0.9	8.7	3.4	0.2
05-122	B1	0.38	0.119	0.7	0.4	0.1	0.5	2.2	1.4	0.6
05-123	B1	0.69	0.121	1.0	0.3	0.8	1.0	1.1	4.2	0.0
05-124	B1	0.99	0.112	1.6	0.4	0.3	1.3	1.0	7.6	0.1
05-125	B1	1.30	0.112	2.3	0.2	0.1	0.8	1.0	18.3	0.1
05-126	B1	1.60	0.122	3.5	0.3	0.2	0.8	0.8	25.3	0.0
05-127	B1	2.21	0.109	3.8	0.4	0.2	0.4	0.5	33.5	0.6
05-128	B1	2.82	0.093	7.6	0.5	0.1	0.3	0.8	26.1	0.1
05-129	B1	3.43	0.106	4.1	1.7	0.3	0.6	5.3	40.2	0.1
05-130	B1	4.04	0.141	11.0	0.7	0.1	0.3	4.6	79.7	0.1
05-131	B1	4.65	0.126	12.1	0.4	0.0	0.2	0.7	138.0	0.1
05-132	B1	5.26	0.136	7.2	0.4	0.1	0.3	0.7	438.2	0.1

Sample ID	Bore hole	Depth (m)	Water Content	As	Cl	Br	NO_2	NO_3	SO_4	PO_4
05-133	B1	5.87	0.127	5.9	0.5	0.1	0.2	0.6	460.8	0.1
05-134	B1	6.48	0.107	19.4	0.6	0.0	0.1	0.5	384.6	0.3
05-135	B1	7.09	0.128	16.1	1.5	0.0	0.1	0.8	502.4	0.2
05-136	B1	7.70	0.120	17.4	4.0	0.1	0.2	1.2	529.9	0.4
05-137	B1	8.31	0.105	10.6	11.8	0.1	0.2	2.5	507.8	0.2
05-138	B1	8.92	0.096	15.5	32.6	0.2	0.2	4.4	447.2	0.2
05-139	B1	9.53	0.084	7.2	51.2	0.2	0.1	4.7	376.2	0.2
05-140	B1	10.13	0.088	4.5	96.2	0.5	0.1	5.4	407.0	0.2
05-141	B1	10.74	0.083	4.8	110.9	0.5	0.2	4.0	333.6	0.2
05-142	B1	11.35	0.100	3.9	164.0	0.7	0.1	2.9	331.1	0.0
05-143	B2	0.08	0.097	4.5	2.4	4.5	1.1	15.4	6.3	0.3
05-144	B2	0.38	0.155	1.6	0.9	4.0	0.1	1.5	6.0	0.1
05-145	B2	0.69	0.121	0.8	1.0	10.2	0.4	1.7	27.2	0.0
05-146	B2	0.99	0.127	0.8	0.8	7.6	0.6	1.3	47.3	0.0
05-147	B2	1.30	0.129	3.6	0.7	8.0	0.4	0.8	25.8	0.0
05-148	B2	1.60	0.127	6.9	0.6	8.8	0.5	0.7	25.0	0.0
05-149	B2	2.21	0.123	17.4	0.3	13.5	0.4	0.1	45.8	0.0
05-150	B2	2.82	0.131	13.5	7.2	8.8	0.4	0.6	224.6	0.1
05-151	B2	3.43	0.145	14.4	19.0	7.6	0.2	0.7	418.5	0.0
05-152	B2	4.04	0.166	18.2	86.2	4.1	0.4	4.4	346.9	0.0
05-153	B2	4.80	0.136	10.8	42.3	7.9	0.3	0.9	521.2	0.6
05-154	B2	5.26	0.109	10.0	45.9	6.7	0.3	0.9	365.6	0.0
05-155	B2	5.87	0.087	8.1	120.6	2.7	0.5	3.4	235.1	0.0
05-156	B2	6.17	0.068	3.4	93.6	2.3	0.3	3.0	167.4	0.0
05-157	G1	0.08	0.064	6.2	6.5	0.2	1.5	18.4	28.4	0.7
05-158	G1	0.38	0.085	4.6	0.9	0.1	1.0	6.4	3.7	0.4
05-159	G1	0.69	0.101	2.4	1.0	0.3	0.6	0.9	5.8	1.2
05-160	G1	0.99	0.102	2.7	1.9	0.2	0.4	0.9	9.4	0.0
05-161	G1	1.30	0.492	14.2	9.2	0.6	1.5	2.6	71.7	0.3
05-162	G1	1.60	0.155	9.9	3.9	0.3	0.4	2.7	57.2	1.0
05-163	G1	2.21	0.180	10.4	51.4	1.2	0.5		130.5	0.2
05-164	G1	2.82	0.123	6.9	84.1	0.5	0.0	3.0	332.9	0.2
05-165	G1	3.43	0.168	8.9	149.9	0.9	0.2	6.2	602.8	0.2
05-166	G1	4.04	0.201	17.7	191.1	1.3	0.3	10.4	712.9	0.0
05-167	G1	4.65	0.153	17.2	88.2	0.7	0.5	4.8	381.5	0.3
05-168	G1	4.95	0.162	15.9	88.2	0.6	0.4	4.5	364.0	0.0
05-169	G2	0.08	0.101	5.6	0.7	0.3	0.1	1.7	3.5	2.3
05-170	G2	0.38	0.052	5.9	0.5	0.4	0.0	1.0	1.5	1.0
05-171	G2	0.69	0.084	2.2	0.3	0.5	0.1	0.8	3.4	0.3
05-172	G2	0.99	0.102	2.2	0.4	3.0	0.4	0.5	15.1	0.1
05-173	G2	1.30	0.072	1.1	0.3	3.7	0.4	0.4	17.8	0.1
05-174	G2	1.60	0.084	1.6	0.3	2.6	0.4	0.6	31.4	0.1
05-175	G2	2.21	0.111	3.7	1.4	0.9	0.7	25.6	12.5	0.1
05-176	G2	2.82	0.126	7.9	1.1	4.2	0.3	12.5	15.8	0.1
05-177	G2	3.43	0.060	6.8	0.4	5.9	0.2	3.7	22.2	0.0
05-178	G2	4.04	0.079	9.9	0.4	5.4	0.2	2.6	26.2	0.0
05-179	G2	4.65	0.084	13.7	0.4	7.4	0.2	2.0	13.1	0.1
05-180	G2	5.26	0.156	23.3	0.5	10.3	0.2	2.1	20.2	0.1

Sample ID	Bore hole	Depth (m)	Water Content	As	Cl	Br	NO_2	NO_3	SO_4	PO_4
05-181	G2	5.87	0.103	23.0	0.5	8.5	0.2	1.5	19.6	0.1
05-182	G2	6.48	0.090	37.2	0.5	8.2	0.2	1.4	27.1	0.2
05-183	G2	7.09	0.079	14.3	0.5	6.4	0.0	1.3	162.2	0.1
05-184	G2	7.70	0.066	9.6	0.6	4.2	0.0	2.0	3035.2	0.0
05-185	G2	8.31	0.102	8.0	1.6	3.1	0.1	4.7	2530.1	0.1
05-186	G2	8.92	0.125	9.3	2.7	0.6	0.2	5.3	485.8	0.0
05-187	G2	9.53	0.135	3.3	35.5	0.1	0.1	15.0	514.9	0.0
05-188	G2	10.13	0.200	8.8	145.1	0.4	0.3	12.3	664.5	0.0
05-189	G2	10.74	0.178	5.8	137.0	0.3	0.2	8.6	471.4	0.0
05-190	H1	0.08	0.071	39.2	1.2	1.6	0.6	4.6	4.6	1.2
05-191	H1	0.38	0.114	11.3	0.1	6.3	0.6	1.8	2.3	0.1
05-192	H1	0.69	0.132	5.5	0.2	6.9	0.5	1.4	8.3	0.0
05-193	H1	0.99	0.129	4.5	0.4	6.2	0.4	1.6	25.2	0.0
05-194	H1	1.30	0.123	5.1	0.2	6.5	0.5	1.5	39.4	0.0
05-195	H1	1.60	0.122	4.9	0.2	0.1	0.4	3.0	25.3	0.1
05-196	H1	2.21	0.119	6.1	1.3	0.3	0.2	30.2	17.2	0.1
05-197	H1	2.97	0.124	18.9	1.1	0.2	0.3	18.6	28.1	0.1
05-198	H1	3.43	0.171	49.9	0.6	0.2	0.2	5.4	36.7	0.3
05-199	H1	4.04	0.127	74.5	0.8	0.1	0.2	1.6	28.6	0.2
05-200	H1	4.65	0.116	76.8	0.4		0.1	1.0	58.8	0.2
05-201	H1	5.26	0.149	34.4	0.5	0.2	0.2	1.5	83.1	0.2
05-202	H1	5.87	0.160	22.3	0.7	0.3	0.4	1.7	112.8	0.2
05-203	H1	6.17	0.130	52.7	0.8	0.1	0.6	1.0	78.0	0.2
05-204	H2	0.08	0.107	34.8	0.4	0.3	1.3	3.2	11.7	0.3
05-205	H2	0.38	0.156	3.2	1.1	0.1	1.0	5.2	60.0	0.1
05-206	H2	0.69	0.115	3.8	6.0	0.6	0.5	43.9	76.8	0.1
05-207	H2	0.99	0.153	4.1	51.3	0.6	0.5	92.5	158.3	0.1
05-208	H2	1.30	0.152	6.3	185.3	0.8	0.2	96.7	313.2	0.1
05-209	H2	1.60	0.146	10.9	288.0	1.7	0.5	64.6	402.2	0.1
05-210	H2	2.21	0.089	10.5	258.8	1.0	0.3	25.6	280.2	0.1
05-211	H2	2.82	0.069	0.0	203.6	0.8	0.1	8.1	206.6	0.0
05-212	H2	3.43	0.072	0.8	185.7	0.7	0.2	3.5	203.0	0.1
05-213	H2	4.04	0.069	0.8	184.7	0.6	0.3	2.2	154.6	0.1
05-214	H2	4.65	0.071	0.9	196.9	0.8	0.1	1.9	115.2	0.1
05-215	H2	5.26	0.071	0.6	213.7	0.8	0.1	1.8	96.2	0.1
05-216	H2	5.87	0.078	1.9	265.8	0.9	0.1	1.9	109.9	0.1
05-217	H2	6.48	0.076	2.4	274.5	0.9	0.1	1.9	116.1	0.0
05-218	H2	7.09	0.068	3.9	224.3	0.8	0.1	1.7	117.5	0.0
05-219	H2	7.70	0.071	3.9	263.0	1.1	0.1	2.0	122.5	0.1
05-220	H2	8.31	0.031	2.2	121.6	0.4	0.0	1.0	63.0	0.0
05-221	D1	0.08	0.060	35.9	1.0		1.5	6.7	7.2	1.6
05-222	D1	0.38	0.083	34.8	0.2		0.2	4.0	2.6	1.1
05-223	D1	0.69	0.134	7.4	0.4		0.7	2.3	3.5	0.1
05-224	D1	0.99	0.118	8.3	0.2		0.6	3.1	5.2	0.8
05-225	D1	1.30	0.132	5.0	0.1		0.5	1.5	5.3	0.0
05-226	D1	1.60	0.134	4.2	0.1		0.5	0.9	4.2	0.0
05-227	D1	2.21	0.144	2.8	0.5		0.3	0.9	20.5	0.0
05-228	D1	2.82	0.106	23.0	1.2		0.3	2.4	42.5	0.0

Sample ID	Bore hole	Depth (m)	Water Content	As	Cl	Br	NO_2	NO_3	SO_4	PO_4
05-229	D1	3.43	0.170	7.7	0.5		0.1	2.3	24.1	0.0
05-230	D1	4.04	0.065	9.3	0.4		0.2	1.0	25.5	0.0
05-231	M1	0.08	0.055	32.8	0.2		0.5	3.4	1.9	1.1
05-232	M1	0.38	0.086	2.4	0.2	8.0	0.4	1.4	1.5	0.1
05-233	M1	0.69	0.081	2.4	0.1	5.2	0.1	0.8	0.7	0.1
05-234	M1	0.99	0.154	0.1	0.2	6.3	0.2	0.7	1.0	0.0
05-235	M1	1.30	0.205	3.2	0.2	9.4	0.7	1.4	12.0	0.0
05-236	M1	1.60	0.168	4.4	0.2	8.7	0.7	3.0	20.6	0.0
05-237	M1	2.21	0.133	8.4	0.3	8.5	0.2	2.3	6.7	0.0
05-238	M1	2.82	0.125	17.8	0.3	8.4	0.2	2.1	4.4	0.0
05-239	M1	3.43	0.134	13.4	0.8		0.5	3.5	7.1	0.0
05-240	M1	4.04	0.128	13.9	1.2	7.7	0.2	2.7	7.1	0.0
05-241	M1	4.65	0.123	27.4	0.7	8.4	0.2	2.4	7.0	0.1
05-242	M1	5.26	0.119	16.8	0.5	8.0	0.2	1.4	6.9	0.0
05-243	M1	5.87	0.114	15.6	0.4	8.0	0.1	1.5	18.4	0.0
05-244	M1	6.48	0.147	29.6	0.5	8.3	0.3	1.1	11.6	0.0
05-245	M1	7.09	0.131	22.8	0.5	8.3	0.3	1.4	30.5	0.0
05-246	M1	7.54	0.090	22.5	0.4	8.9	0.2	1.1	17.1	0.0
05-247	M2	0.08	0.125	29.6	2.0	0.2	4.4	13.1	10.1	2.3
05-248	M2	0.38	0.081	10.1	0.3	0.2	1.6	1.4	3.4	0.2
05-249	M2	0.69	0.087	9.8	0.3	0.3	1.6	1.1	13.7	0.2
05-250	M2	0.99	0.067	7.8	0.6	0.4	1.2	1.3	20.6	0.1
05-251	M2	1.30	0.079	4.2	0.2	0.2	0.9	0.5	41.6	
05-252	M2	1.60	0.077	6.8	0.7	0.2	0.9	1.0	36.1	0.1
05-253	M2	2.21	0.117	17.0	8.8	0.6	0.7	20.4	48.6	0.1
05-254	M2	2.82	0.102	3.4	5.6	0.4	0.3	16.0	84.4	0.1
05-255	M2	3.43	0.102	5.2	1.0	0.2	0.6	2.4	200.2	0.7
05-256	M2	4.04	0.088	11.7	6.3	0.1	0.3	1.3	212.3	1.1
05-257	M2	4.65	0.100	9.9	34.3	0.3	0.1	4.0	305.5	0.2
05-258	M2	5.26	0.074	6.6	36.9	0.2	0.1	3.7	186.5	0.2
05-259	M2	5.87	0.091	6.5	50.1	0.3	0.2	4.8	234.0	0.2
05-260	M2	6.48	0.079	8.0	75.1	0.5	0.2	6.7	162.8	0.2
05-261	M2	7.09	0.097	12.1	124.3	0.9	0.2	9.2	136.9	1.2
05-262	M2	7.70	0.077	13.6	111.8	0.7	0.1	6.4	65.9	0.2
05-263	M2	8.31	0.083	18.4	148.3	0.8	0.2	6.0	45.7	1.3
05-264	M2	8.92	0.105	22.6	192.5	1.1	0.3	5.8	64.6	0.2
05-265	M3	0.08	0.170	35.4	0.8		2.2	18.5	8.6	1.4
05-266	M3	0.38	0.101	34.0	0.2		0.8	2.0	2.0	0.1
05-267	M3	0.69	0.112	13.7	0.1		0.9	1.4	2.1	0.0
05-268	M3	0.99	0.148	6.0	0.3		0.6	1.2	4.7	5.7
05-269	M3	1.30	0.137	6.6	0.2	8.2	0.5	0.8	8.0	0.1
05-270	M3	1.60	0.117	7.2	3.7	8.7	0.4	0.7	2.8	0.1
05-271	M3	2.21	0.188	8.2	0.2	11.0	0.4	0.9	20.9	0.1
05-272	M3	2.82	0.172	11.0	0.2	10.9	0.2	0.9	3.2	0.1
05-273	M3	3.43	0.138	9.2	0.7	10.2	0.2	0.8	6.6	0.0
05-274	M3	4.04	0.155	9.7	0.5	9.0	0.3	0.8	22.4	0.0
05-275	M3	4.65	0.173	8.0	0.7	8.6	0.3	0.7	10.0	0.0
05-276	M3	5.26	0.153	8.7	0.2	8.0	0.2	0.6	8.9	0.0

Sample ID	Bore hole	Depth (m)	Water Content	As	Cl	Br	NO_2	NO_3	SO_4	PO_4
05-277	M3	5.87	0.112	5.7	0.1	7.5	0.2	0.5	17.6	0.0
05-278	M3	6.48	0.116	6.1	0.2	10.4	0.3	0.1	14.0	0.0
05-279	M4	0.08	0.092	20.1	1.0	0.1	1.2	11.8	5.5	0.8
05-280	M4	0.38	0.081	14.1	1.2	0.2	1.0	3.4	1.8	0.0
05-281	M4	0.69	0.136	3.7	0.3	0.2	1.2	1.4	6.1	0.1
05-282	M4	0.99	0.065	4.3	0.5	0.4	1.2	1.6	22.0	0.1
05-283	M4	1.30	0.084	3.4	1.3	0.1	0.9	1.9	25.6	0.1
05-284	M4	1.60	0.088	4.9	0.7	0.1	0.9	0.9	34.2	0.1
05-285	M4	2.21	0.110	2.8	1.0	0.1	0.2	1.0	43.0	0.8
05-286	M4	2.82	0.072	5.6	0.9	0.1	0.3	1.5	51.0	0.1
05-287	M4	3.43	0.137	6.7	8.0	0.3	0.3	11.9	70.2	0.2
05-288	M4	4.04	0.113	10.1	31.2	0.5	0.3	9.9	48.8	0.3
05-289	M4	4.50	0.080	10.2	51.6	0.5	0.3	4.9	48.2	0.5
05-290	DU1	0.08	0.093	0.7	43.7	2.1	0.0	0.2	43.4	0.0
05-291	DU1	0.38	0.086	72.3	38.5	2.8	0.0	0.3	27.7	0.1
05-292	DU1	0.69	0.074	63.3	32.8	2.3	0.1	0.2	18.0	0.1
05-293	DU1	0.99	0.013	81.6	2.7	2.6	0.1	0.7	1.7	3.4
05-294	DU1	1.30	0.128	99.9	146.8	12.6	0.3	0.4	28.9	0.3
05-295	DU1	1.60	0.132	123.7	106.5	12.9	0.2	0.3	35.3	0.2
05-296	DU1	2.21	0.116	49.9	164.5	11.9	0.3	0.3	29.8	0.2
05-297	DU1	2.82	0.125	122.7	86.9	13.7	0.3	0.5	102.2	0.1
05-298	DU1	3.43	0.127	96.4	88.3		0.3		159.1	0.2
05-299	DU2	0.08	0.052	4.6	16.6	10.7	2.3	2.9	9.3	0.3
05-300	DU2	0.38	0.062	5.4	7.5	9.3	0.5	1.6	7.8	0.1
05-301	DU2	0.69	0.071	5.0	7.7	8.5	0.4	1.0	3.7	0.0
05-302	DU2	0.99	0.079	4.5	7.1	7.5	0.2	0.9	9.3	0.1
05-303	DU2	1.30	0.077	2.9	11.9		0.4		31.5	0.1
05-304	DU2	1.60	0.061	4.4	8.7	7.5	0.1		56.3	0.0
05-305	DU2	2.21	0.133	17.9	398.5	8.5	0.8	0.3	159.7	0.0
05-306	DU2	2.82	0.142	68.8	360.3		1.6		347.1	0.0
05-307	DU3	0.08	0.039	5.9	7.2		2.3	10.2	12.5	0.2
05-308	DU3	0.38	0.072	3.6	7.0	8.4	1.5	2.8	15.1	0.1
05-309	DU3	0.69	0.073	3.7	8.0		1.3	6.8	28.4	0.0
05-310	DU3	0.99	0.067	4.4	12.5	7.2	1.3	2.1	43.2	0.0
05-311	DU3	1.30	0.061	3.4	44.1		0.9	4.6	65.1	0.0
05-312	DU3	1.60	0.052	2.8	24.0	6.2	0.7	11.9	17.3	0.0
05-313	DU3	2.21	0.058	3.0	31.2		0.3	31.3	14.4	0.0
05-314	HI1	0.08	0.024	138.1	14.1		2.1	5.8	8.3	18.4
05-315	HI1	0.38	0.039	301.2	6.1	7.5	0.1	1.4	2.8	23.4
05-316	HI1	0.69	0.054	719.2	9.7	11.1	0.2	1.4	8.4	14.9
05-317	HI1	0.99	0.058	613.0	5.6	13.4	0.2	1.7	9.0	46.6
05-318	HI1	1.30	0.071	1854.1	5.4	14.6	1.0	1.9	24.5	47.4
05-319	HI1	1.60	0.067	748.2	6.5	15.3	0.9	2.0	20.6	17.7
05-320	HI1	2.21	0.071	8.1	32.8		0.5	0.5	789.2	0.2
05-321	HI1	2.82	0.075	10.7	99.0		0.3	3.3	3103.3	0.1
05-322	HI1	3.43	0.089	11.9	281.1		0.3	21.1	2764.4	0.0
05-323	HI1	4.04	0.095	13.3	442.6		0.2	34.9	1699.1	0.1
05-324	HI1	4.65	0.104	27.2	540.4		0.1	36.4	504.3	0.7

Sample ID	Bore hole	Depth (m)	Water Content	As	Cl	Br	NO_2	NO_3	SO_4	PO_4
05-325	HI1	5.11	0.105	65.3	533.5		0.3	23.1	350.0	2.1
05-326	HI2	0.08	0.017	5.6	3.9	9.0	0.3	1.6	4.4	3.7
05-327	HI2	0.38	0.045	3.5	4.1	9.1	0.1	0.9	3.1	1.4
05-328	HI2	0.69	0.087	2.0	1.4	5.8	0.1	0.5	1.4	0.3
05-343	KE1	0.08	0.021	3.9	9.5	0.0	0.7	12.1	9.2	1.4
05-344	KE1	0.38	0.007	4.0	0.7	0.0	0.1	0.7	1.5	0.4
05-345	KE1	0.69	0.016	8.2	1.1	0.1	0.2	0.9	2.4	0.6
05-346	KE1	0.99	0.017	12.6	1.7	0.1	0.2	0.3	5.4	0.1
05-347	KE1	1.30	0.023	11.3	4.9	0.0	0.2	0.2	5.0	0.1
05-348	KE1	1.60	0.095	7.9	1.5	0.0	0.2	0.2	3.3	0.0
05-349	KE1	2.21	0.064	29.8	0.4	0.0	0.2	0.1	2.0	0.1
05-350	KE1	2.82	0.062	7.3	2.2	0.1	0.2	0.1	5.2	0.1
05-351	KE1	3.43	0.017	12.3	1.2	0.0	0.2	0.1	1.9	0.4
05-352	KE1	4.04	0.013	1.2	0.8	0.0	0.1	0.1	2.2	0.2
05-353	KE1	4.65	0.030	5.3	3.6	0.1	0.2	0.1	6.0	0.7
05-354	KE1	5.26	0.023	12.7	0.8	0.0	0.1	0.2	2.7	0.7
05-355	ST1	0.08	0.018	8.3	5.7		0.4		6.6	14.7
05-356	ST1	0.38	0.034	2.0	3.2	0.0	0.2	2.0	6.2	1.0
05-357	ST1	0.69	0.033	1.9	2.2	0.0	0.2	0.5	1.6	0.5
05-358	ST1	0.99	0.034	12.4	0.7		0.0		2.6	1.1
05-359	ST1	1.30	0.036	7.3	0.8	0.1	0.3	0.8	5.5	0.5
05-360	ST1	1.60	0.035	7.9	2.1	0.0	0.3	0.2	2.4	0.4
05-361	ST1	2.21	0.043	11.6	0.6	0.0	0.4	0.2	2.9	0.3
05-362	ST1	2.82	0.072	13.1	9.6	0.8	0.3	0.2	30.4	0.4
05-363	ST1	3.43	0.091	16.6	27.7	0.1	0.1	0.4	19.6	0.4
05-364	ST2	0.08	0.052	13.7	5.8	7.0	1.2	13.1	8.7	0.4
05-365	ST2	0.38	0.084	10.4	2.0		0.3	2.8	10.1	0.1
05-366	ST2	0.69	0.096	8.8	0.5		0.3	3.0	26.2	0.1
05-367	ST2	0.99	0.094	7.9	0.5		0.3	2.6	55.4	0.1
05-368	ST2	1.30	0.093	8.3	1.6		0.4	4.3	114.4	0.0
05-369	ST2	1.60	0.099	6.9	36.9	5.7	0.3	33.7	226.5	0.0
05-370	ST2	2.21	0.107	4.9	330.4		0.8	43.7	160.2	0.0
05-371	ST2	2.82	0.124	8.2	633.3		1.3	7.8	177.7	0.5
05-372	ST2	3.43	0.120	14.9	796.8		1.8	5.5	229.9	0.0
05-373	ST2	4.00	0.129	23.9	926.1		0.5	4.1	248.4	0.0
05-374	ST2	4.65	0.137	48.3	1462.5		0.0	6.2	358.2	0.0
05-375	ST2	5.26	0.118	136.6	1093.2		0.1	4.4	4328.6	0.0
05-376	ST3	0.08	0.008	4.9	9.0	3.2	0.4	4.0	8.2	8.4
05-377	ST3	0.38	0.011	3.3	2.4	2.6	0.1	1.2	6.0	0.7
05-378	ST3	0.69	0.011	2.1	1.0	2.2	0.0	0.4	2.6	0.3
05-379	ST3	0.99	0.010	1.9	1.0	2.0	0.0	0.4	2.5	0.3
05-380	ST3	1.30	0.010	2.4	2.3	4.4	0.1		4.0	0.6
05-381	ST3	1.60	0.011	1.4	0.5	2.2	0.0	0.2	3.0	0.3
05-382	ST3	2.21	0.009	1.1	0.1	1.9	0.0	0.2	1.7	0.2
05-383	ST3	2.82	0.060		5.4	1.1	0.0	0.8	23.4	0.1
05-384	ST3	3.43	0.099	8.0	29.9	13.4	0.1	3.3	93.9	0.2
05-385	ST3	4.04	0.086	7.2	25.4	2.9	0.1	3.1	55.5	0.2
05-386	ST3	4.65	0.094	18.5	31.8	3.0	0.1	2.6	59.6	0.3

Sample ID	Bore hole	Depth (m)	Water Content	As	Cl	Br	NO_2	NO_3	SO_4	PO_4
05-387	ST3	5.26	0.102	24.5	39.3	5.6	0.1	5.9	67.5	0.1
05-400	NU1	0.08	0.157	75.7	34.3	2.8	0.0	53.0	18.8	2.1
05-401	NU1	0.38	0.196	30.4	181.2	0.8	0.9	18.4	36.2	0.2
05-402	NU1	0.69	0.222	8.6	1029.1	0.3	3.9	43.0	236.3	0.2
05-403	NU1	0.99	0.234	11.0	1580.7	0.2	5.3	45.2	4424.6	0.1
05-404	NU1	1.30	0.229	12.0	1931.2	0.1	6.0	25.7	4537.1	0.0
05-405	NU1	1.60	0.227	14.3	1852.9	0.1	5.7	16.2	4367.9	0.1
05-406	NU1	1.91	0.214	14.2	1898.4	0.1	5.5	9.9	4374.1	0.1
05-407	NU1	2.21	0.220	14.3	2181.6	0.0	6.1	7.6	1651.9	0.3
05-408	NU1	2.51	0.254	12.6	2958.2	0.0	8.1	4.2	723.0	0.3
05-409	NU1	2.82	0.291	11.9	3512.6	0.0	9.6	4.2	770.7	0.1
05-410	NU1	3.12	0.252	9.4	3069.2	0.0	8.3	3.5	634.8	0.0
05-411	NU1	3.73	0.225	8.0	2885.4	0.1	7.7	3.0	563.2	0.0
05-412	NU1	4.04	0.215	5.0	3017.1	0.0	7.9	1.1	460.9	0.1
05-413	NU1	4.34	0.203	4.7	2704.4	0.0	6.8	0.7	423.9	0.1
05-414	NU1	4.65	0.215	6.0	2749.2	0.0	7.7	2.5	480.2	0.1
05-415	NU1	4.95	0.215	3.6	2751.4	0.0	6.9	1.5	430.7	0.0
05-416	NU1	5.26	0.186	2.2	1673.8	0.0	4.5	1.4	316.5	0.0
05-417	NU1	5.56	0.146	3.0	1425.9	0.1	3.6	1.8	359.9	0.0
05-418	NU1	5.87	0.147	3.5	1238.7	0.0	3.0	2.0	421.0	0.0
05-419	NU1	6.17	0.157	1.9	1329.7	0.0	3.2	2.5	417.4	1.3
05-420	NU1	6.48	0.148	1.6	1336.3	0.0	3.2	2.3	388.0	0.1
05-421	NU1	6.78	0.204	1.3	2020.0	0.0	4.8	2.9	573.1	0.2
05-422	NU1	7.09	0.232	0.7	2757.5	0.0	7.2	3.3	566.4	0.0

Table IV.2 Texture analysis for borehole samples

Sample ID	Borehole	Sand (%)	Silt (%)	Clay (%)
05-001	A1	84.5	5.6	9.9
05-003	A1	69.4	7.7	22.9
05-005	A1	52.7	27.5	19.9
05-007	A1	64.4	20.4	15.2
05-008	A1	57.1	24.3	18.6
05-009	A2	80.5	10.4	9.0
05-010	A2	72.7	10.7	16.6
05-011	A2	62.3	12.7	25.0
05-012	A2	66.8	10.4	22.8
05-013	A2	76.8	7.2	16.1
05-014	A2	78.3	6.9	14.8
05-015	A2	76.9	6.2	16.9
05-016	A2	62.5	15.2	22.3
05-017	A2	58.6	15.3	26.1
05-018	A2	71.6	15.3	13.1
05-019	A2	74.3	12.6	13.1
05-020	A2	74.1	13.7	12.2
05-021	A2	82.0	8.9	9.1
05-022	A2	84.4	6.5	9.1
05-023	A2	74.2	13.1	12.7
05-024	A2	69.0	15.9	15.1
05-025	A2	62.1	18.9	19.0
05-026	T1	76.5	5.7	17.8
05-028	T1	65.6	9.8	24.7
05-031	T1	43.7	22.7	33.6
05-032	T1	42.8	27.9	29.3
05-033	T1	52.5	18.3	29.3
05-035	T1	42.4	28.3	29.3
05-036	T1	40.3	22.0	37.8
05-037	T1	41.1	20.3	38.6
05-038	T1	42.0	17.8	40.3
05-040	T1	76.4	5.2	18.4
05-041	T2	16.9	20.7	62.4
05-043	T2	21.5	23.7	54.7
05-044	T2	61.9	9.7	28.4
05-046	T2	42.4	15.7	41.9
05-048	T2	34.8	23.2	42.0
05-049	T2	22.8	24.7	52.5
05-050	T2	57.7	8.0	34.3
05-052	T2	77.4	5.0	17.6
05-053	T2	37.5	11.0	51.5
05-055	T2	23.5	51.1	25.5
05-056	T2	44.5	34.4	21.1
05-058	T2	55.4	24.8	19.8
05-059	T3	80.8	4.2	15.0
05-061	T3	66.2	10.9	22.9

Sample ID	Borehole	Sand (%)	Silt (%)	Clay (%)
05-063	T3	43.7	26.6	29.6
05-065	T3	51.1	16.7	32.2
05-067	T3	63.0	9.1	27.9
05-069	T3	70.9	2.8	26.3
05-071	T3	70.6	1.9	27.5
05-073	T3	76.9	1.8	21.3
05-075	T3	69.8	11.5	18.7
05-077	T3	53.4	26.0	20.7
05-079	T3	56.3	25.9	17.8
05-081	T3	71.7	13.9	14.4
05-082	T3	70.6	18.4	11.0
05-083	T4	83.5	2.8	13.8
05-086	T4	78.1	5.3	16.6
05-088	T4	54.9	10.9	34.2
05-090	T4	53.6	24.1	22.3
05-092	T4	64.4	14.9	20.6
05-094	T4	65.5	6.1	28.3
05-096	T4	61.7	22.3	16.0
05-097	T4	43.5	34.8	21.7
05-099	T4	55.2	27.2	17.6
05-101	T4	58.8	25.3	15.9
05-102	T4	55.4	29.5	15.0
05-103	L1	68.0	13.0	19.0
05-106	L1	70.3	8.4	21.3
05-107	L1	52.3	20.4	27.4
05-109	L1	46.1	24.0	29.9
05-111	L1	30.9	31.8	37.4
05-113	L1	48.0	18.1	33.9
05-115	L1	39.3	25.8	34.8
05-117	L1	59.3	16.6	24.1
05-118	L1	74.9	6.3	18.8
05-120	L1	72.4	12.6	15.0
05-123	B1	62.7	9.3	28.0
05-125	B1	59.0	14.2	26.7
05-126	B1	59.0	13.8	27.1
05-128	B1	65.4	13.4	21.2
05-131	B1	42.0	24.9	33.1
05-132	B1	45.9	21.9	32.2
05-134	B1	69.8	8.9	21.3
05-135	B1	66.7	11.6	21.7
05-137	B1	50.1	27.5	22.4
05-139	B1	70.9	13.4	15.8
05-141	B1	53.1	25.8	21.1
05-142	B1	52.3	27.8	19.9
05-144	B2	48.0	20.2	31.8
05-145	B2	62.8	15.9	21.3
05-147	B2	52.0	23.4	24.6
05-149	B2	56.9	18.4	24.6

Sample ID	Borehole	Sand (%)	Silt (%)	Clay (%)
05-151	B2	35.2	32.4	32.4
05-152	B2	46.7	27.0	26.3
05-153	B2	49.2	19.8	31.0
05-156	B2	64.6	19.3	16.0
05-157	G1	87.7	2.6	9.7
05-159	G1	76.2	5.4	18.4
05-160	G1	81.3	1.1	17.6
05-162	G1	67.2	2.7	30.1
05-163	G1	40.6	29.0	30.3
05-164	G1	52.1	29.3	18.6
05-166	G1	73.6	15.2	11.2
05-168	G1	69.5	17.2	13.3
05-169	G2	86.3	2.4	11.3
05-171	G2	72.3	6.4	21.3
05-173	G2	82.6	1.1	16.3
05-175	G2	76.0	1.4	22.6
05-176	G2	72.3	3.9	23.8
05-178	G2	85.2	2.2	12.6
05-179	G2	86.5	2.2	11.3
05-180	G2	90.3	1.3	8.4
05-181	G2	72.1	7.0	20.9
05-183	G2	83.8	2.4	13.8
05-184	G2	87.6	2.7	9.7
05-186	G2	77.3	13.1	9.6
05-189	G2	76.0	17.8	6.2
05-191	H1	66.5	13.1	20.5
05-192	H1	55.9	18.6	25.5
05-194	H1	44.4	23.7	31.9
05-196	H1	41.8	24.1	34.1
05-198	H1	39.3	29.9	30.7
05-199	H1	40.5	29.6	29.8
05-200	H1	45.8	29.2	25.0
05-202	H1	59.7	29.7	10.5
05-203	H1	71.9	19.5	8.6
05-204	H2	62.4	18.1	19.5
05-205	H2	33.3	27.2	39.5
05-207	H2	37.9	36.6	25.5
05-208	H2	48.4	34.8	16.9
05-211	H2	56.2	34.1	9.7
05-214	H2	62.9	29.8	7.3
05-218	H2	59.4	28.2	12.4
05-219	H2	68.9	23.3	7.8
05-223	D1	66.3	13.3	20.4
05-224	D1	68.9	13.2	17.9
05-227	D1	48.8	19.7	31.5
05-228	D1	78.2	12.5	9.3
05-229	D1	68.1	21.3	10.6
05-231	M1	92.4	1.3	6.3

Sample ID	Borehole	Sand (%)	Silt (%)	Clay (%)
05-233	M1	86.0	3.6	10.4
05-235	M1	23.7	38.6	37.8
05-237	M1	66.5	10.6	22.9
05-239	M1	36.3	30.6	33.1
05-241	M1	68.7	10.5	20.8
05-243	M1	59.7	16.3	24.0
05-244	M1	62.3	22.1	15.6
05-246	M1	58.7	24.9	16.3
05-247	M2	57.9	20.2	21.9
05-249	M2	50.6	16.9	32.5
05-251	M2	45.4	19.2	35.4
05-253	M2	34.5	27.2	38.3
05-255	M2	64.5	20.6	14.9
05-256	M2	72.6	16.3	11.1
05-258	M2	72.7	15.0	12.4
05-260	M2	73.9	13.6	12.5
05-261	M2	72.6	14.9	12.5
05-262	M2	70.0	16.2	13.8
05-264	M2	67.3	16.9	15.8
05-266	M3	66.0	12.8	21.2
05-268	M3	39.2	28.8	32.0
05-269	M3	51.8	20.3	27.8
05-271	M3	32.3	24.4	43.3
05-273	M3	55.5	14.9	29.6
05-275	M3	63.4	17.1	19.6
05-277	M3	44.4	33.1	22.5
05-278	M3	44.4	34.3	21.4
05-279	M4	73.8	10.4	15.8
05-284	M4	61.6	20.3	18.1
05-285	M4	45.3	38.1	16.6
05-286	M4	59.4	26.6	14.0
05-287	M4	57.0	27.9	15.1
05-288	M4	60.7	24.5	14.7
05-290	DU1	54.9	5.9	39.3
05-292	DU1	76.5	5.6	17.9
05-293	DU1	89.4	1.2	9.4
05-294	DU1	64.9	4.9	30.2
05-296	DU1	67.8	4.6	27.7
05-298	DU1	62.6	14.8	22.6
05-299	DU2	69.0	14.6	16.4
05-301	DU2	61.3	13.5	25.2
05-303	DU2	48.5	20.6	30.9
05-304	DU2	48.2	21.3	30.5
05-305	DU2	20.1	48.2	31.8
05-306	DU2	26.6	40.9	32.6
05-314	HI1	84.4	6.2	9.4
05-316	HI1	70.4	7.7	21.9
05-319	HI1	66.4	8.4	25.1

Sample ID	Borehole	Sand (%)	Silt (%)	Clay (%)
05-321	HI1	58.8	14.4	26.7
05-323	HI1	53.5	20.7	25.8
05-325	HI1	53.7	19.2	27.1
05-326	HI2	82.0	5.8	12.2
05-328	HI2	57.8	6.2	36.0
05-343	KE1	88.2	1.2	10.6
05-345	KE1	90.7	<0.1	9.4
05-347	KE1	85.7	<0.1	14.4
05-348	KE1	80.6	5.5	13.8
05-349	KE1	76.8	4.3	18.9
05-351	KE1	90.7	<0.1	9.4
05-353	KE1	88.2	<0.1	11.9
05-354	KE1	89.5	<0.1	10.6
05-355	ST1	84.5	2.4	13.1
05-357	ST1	81.9	3.7	14.4
05-359	ST1	83.2	4.6	12.2
05-361	ST1	81.9	4.6	13.5
05-363	ST1	78.0	14.4	7.6
05-364	ST2	57.9	25.5	16.6
05-366	ST2	43.9	23.8	32.2
05-368	ST2	35.6	29.2	35.2
05-370	ST2	37.8	27.1	35.2
05-372	ST2	29.4	32.8	37.7
05-375	ST2	66.2	25.8	7.9
05-376	ST3	88.2	2.4	9.4
05-378	ST3	92.6	<0.1	7.5
05-380	ST3	90.1	2.4	7.5
05-382	ST3	95.3	<0.1	5.0
05-384	ST3	77.5	2.5	20.0
05-385	ST3	82.6	2.4	15.0
05-387	ST3	65.8	15.9	18.2
05-400	NU1	19.5	32.0	48.5
05-402	NU1	20.2	22.8	56.9
05-404	NU1	18.2	37.4	44.3
05-406	NU1	26.6	47.3	26.1
05-409	NU1	10.5	22.3	67.2
05-410	NU1	14.4	22.8	62.9
05-412	NU1	20.9	25.7	53.4
05-414	NU1	20.2	25.6	54.2
05-416	NU1	26.9	26.5	46.6
05-418	NU1	42.6	28.1	29.2
05-420	NU1	45.7	26.7	27.6
05-422	NU1	10.5	22.9	66.6

Table IV.3 Matric potential data for borehole samples

Borehole	Depth (m)	Potential (-m)	Method
A05-01	0.15	-394	2
A05-01	0.76	-240	2
A05-01	1.37	-65.0	2
A05-01	2.13	-118	2
A05-01	2.90	-214	2
A05-02	0.15	-726	2
A05-02	0.76	-347	2
A05-02	1.37	-366	2
A05-02	2.29	-93.4	2
A05-02	2.90	-125	2
A05-02	3.51	-103	2
A05-02	4.11	-170	2
A05-02	4.88	-198	2
A05-02	5.79	-266	2
A05-02	6.71	-200	2
A05-02	7.62	-107	2
A05-02	8.53	-142	2
B05-01	0.23	-3.39	1
B05-01	1.14	-6.70	1
B05-01	2.67	-6.98	1
B05-01	4.50	-7.93	1
B05-01	7.24	-7.85	1
B05-01	9.68	-8.52	1
B05-01	11.20	-9.11	1
B05-02	0.23	-5.33	1
B05-02	0.53	-6.85	1
B05-02	1.14	-4.92	1
B05-02	1.60	-7.33	1
B05-02	2.36	-6.58	1
B05-02	2.82	-4.15	1
B05-02	4.04	-3.49	1
B05-02	5.11	-7.69	1
D05-01	0.23	-4.76	1
D05-01	0.53	-3.18	1
D05-01	0.84	-2.47	1
D05-01	1.14	-2.37	1
D05-01	1.45	-1.39	1
D05-01	1.75	-0.70	1
D05-01	2.29	-0.10	1
D05-01	2.90	-0.65	1
D05-01	3.58	-2.58	1
DU05-01	0.15	-166	2
DU05-01	0.76	-128	2
DU05-01	1.37	-121	2
DU05-01	2.29	-115	2
DU05-01	2.90	-67.0	2

Borehole	Depth (m)	Potential (-m)	Method
DU05-01	3.35	-71.1	2
DU05-02	0.15	-335	2
DU05-02	0.76	-209	2
DU05-02	1.37	-200	2
DU05-02	2.29	-128	2
DU05-02	2.74	-228	2
DU05-02	2.90	-301	2
DU05-03	0.15	-876	2
DU05-03	0.76	-429	2
DU05-03	1.37	-241	2
DU05-03	1.83	-276	2
DU05-03	2.44	-274	2
G05-02	0.53	-3.14	1
G05-02	1.14	-4.96	1
G05-02	1.75	-5.04	1
G05-02	2.36	-6.61	1
G05-02	2.97	-4.88	1
G05-02	4.50	-3.72	1
G05-02	5.41	-3.43	1
G05-02	6.63	-4.68	1
G05-02	7.85	-2.67	1
G05-02	9.07	-4.30	1
G05-02	10.29	-0.60	1
H05-01	0.23	-25.4	2
H05-01	0.53	-32.5	2
H05-01	1.14	-4.12	1
H05-01	1.45	-4.50	1
H05-01	2.29	-3.40	1
H05-01	2.97	-62.9	2
H05-01	4.19	-51.8	2
H05-01	6.02	-28.4	2
H05-02	0.23	-55.8	2
H05-02	0.53	-59.9	2
H05-02	1.14	-55.8	2
H05-02	1.75	-65.0	2
H05-02	2.97	-110	2
H05-02	4.19	-157	2
H05-02	5.41	-209	2
H05-02	6.63	-218	2
H05-02	7.85	-238	2
H05-02	8.46	-255	2
HI05-01	0.15	-683	2
HI05-01	0.76	-413	2
HI05-01	1.37	-434	2
HI05-01	2.29	-352	2
HI05-01	2.90	-320	2
HI05-01	3.51	-298	2
HI05-01	4.11	-228	2

Borehole	Depth (m)	Potential (-m)	Method
HI05-01	5.03	-260	2
HI05-02	0.15	-665	2
HI05-02	0.46	-356	2
HI05-02	0.91	-366	2
KE05-01	0.15	-92.4	2
KE05-01	0.76	-224	2
KE05-01	1.37	-131	2
KE05-01	2.29	-131	2
KE05-01	2.90	-159	2
KE05-01	3.51	-239	2
KE05-01	4.11	-138	2
KE05-01	4.72	-168	2
KE05-01	5.33	-93.4	2
L05-01	0.53	-5.97	1
L05-01	1.14	-5.20	1
L05-01	1.75	-5.22	1
L05-01	2.97	-7.30	1
L05-01	4.19	-7.87	1
L05-01	6.63	-7.80	1
L05-01	7.85	-8.03	1
M05-01	0.23	-0.94	1
M05-01	0.53	-1.30	1
M05-01	0.84	-1.43	1
M05-01	1.75	-2.09	1
M05-01	2.36	-6.90	1
M05-01	2.97	-24.4	2
M05-01	4.11	-17.3	2
M05-01	5.33	-11.2	2
M05-01	7.16	-11.2	2
M05-02	0.23	-6.47	1
M05-02	0.53	-130	2
M05-02	1.14	-89.3	2
M05-02	1.68	-58.9	2
M05-02	2.90	-27.4	2
M05-02	3.51	-16.2	2
M05-02	4.11	-35.5	2
M05-02	4.72	-40.6	2
M05-02	5.94	-76.1	2
M05-02	7.16	-85.3	2
M05-02	8.53	-103	2
M05-03	0.23	-7.35	1
M05-03	0.53	-7.49	1
M05-03	0.84	-4.81	1
M05-03	1.14	-4.98	1
M05-03	1.45	-13.7	2
M05-03	1.75	-13.7	2
M05-03	2.29	-18.4	2
M05-03	2.90	-39.4	2

Borehole	Depth (m)	Potential (-m)	Method
M05-03	3.51	-38.3	2
M05-03	4.11	-19.6	2
M05-03	4.72	-19.6	2
M05-03	5.33	-21.9	2
M05-03	6.25	-19.6	2
M05-04	0.23	-1.90	1
M05-04	0.53	-5.14	1
M05-04	0.76	-8.12	2
M05-04	1.07	-15.2	2
M05-04	1.68	-25.4	2
M05-04	2.29	-25.4	2
M05-04	2.90	-26.4	2
M05-04	3.51	-33.5	2
M05-04	4.42	-50.8	2
ST05-01	0.15	-1046	2
ST05-01	0.76	-318	2
ST05-01	1.37	-268	2
ST05-01	2.29	-91.4	2
ST05-01	2.90	-43.6	2
ST05-01	3.66	-54.8	2
ST05-02	0.15	-247	2
ST05-02	0.76	-109	2
ST05-02	1.37	-115	2
ST05-02	2.29	-117	2
ST05-02	2.90	-117	2
ST05-02	3.51	-163	2
ST05-02	4.04	-182	2
ST05-02	4.72	-157	2
ST05-02	5.33	-180	2
ST05-03	0.15	-758	2
ST05-03	0.76	-518	2
ST05-03	1.37	-464	2
ST05-03	2.29	-263	2
ST05-03	2.90	-56.8	2
ST05-03	3.51	-50.8	2
ST05-03	4.11	-39.6	2
ST05-03	4.72	-43.6	2
ST05-03	5.33	-53.8	2
T05-01	0.15	-2.19	1
T05-01	0.76	-5.37	1
T05-01	1.37	-2.09	1
T05-01	2.29	-5.95	1
T05-01	3.51	-9.34	1
T05-01	4.11	-14.6	2
T05-01	4.72	-29.4	2
T05-01	5.33	-80.0	2
T05-01	5.94	-87.3	2
T05-01	7.01	-69.4	2

Borehole	Depth (m)	Potential (-m)	Method
T05-02	0.23	-8.00	1
T05-02	1.14	-1.85	1
T05-02	1.75	-3.54	1
T05-02	2.97	-6.21	1
T05-02	4.19	-2.80	1
T05-02	5.41	-1.03	1
T05-02	6.63	-8.67	1
T05-02	7.85	-7.59	1
T05-03	0.15	-3.38	1
T05-03	1.07	-3.49	1
T05-03	2.29	-3.10	1
T05-03	2.74	-7.34	1
T05-03	5.33	-8.25	1
T05-03	6.55	-24.0	2
T05-03	7.16	-7.72	1
T05-03	7.77	-18.3	2
T05-03	8.99	-33.5	2
T05-03	11.43	-33.5	2
T05-04	0.15	-4.33	1
T05-04	1.07	-6.09	1
T05-04	2.13	-2.49	1
T05-04	3.51	-7.05	1
T05-04	5.18	-7.38	1
T05-04	6.40	-6.94	1
T05-04	7.01	-8.82	1
T05-04	8.08	-25.4	2
T05-04	9.60	-25.2	2
T05-04	10.06	-30.5	2

Table 1. Overview of arsenic behavior in the subsurface

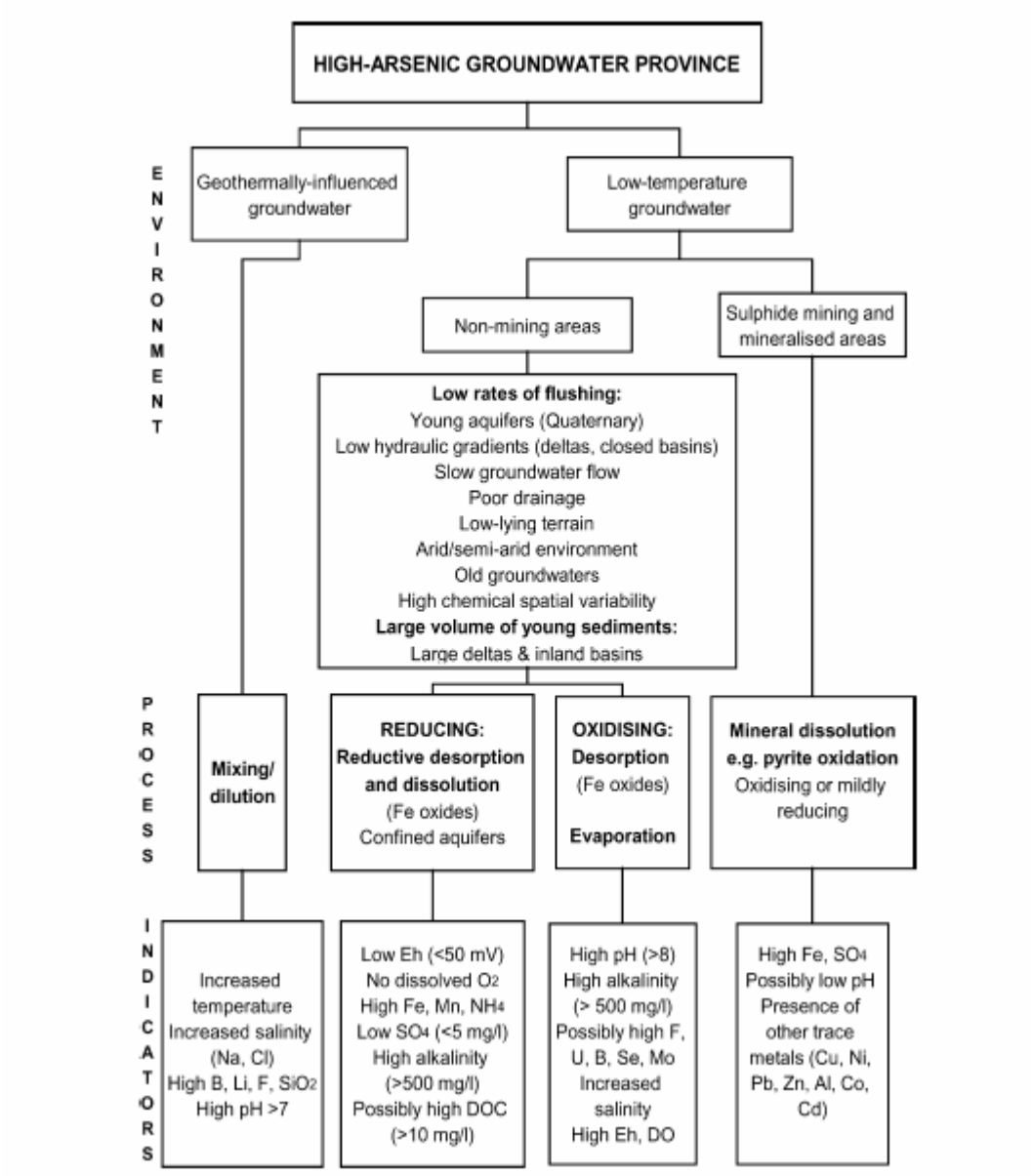

SOURCE: Smedley and Kinninburgh, 2002

Table 2. Arsenic concentration statistics in the High Plains area

	Number of Samples	As<10 ug/L	10<As<50 ug/L	As>50 ug/L
Central High Plains	668	99.7%	0.3%	0.0%
Southern High Plains (Northern)	477	92.7%	7.3%	0.0%
Southern High Plains (Southern)	609	49.3%	48.4%	2.3%
Southern High Plains	1086	68.3%	30.4%	1.3%
Texas High Plains	1754	80.3%	18.9%	0.8%

Table 3. Arsenic concentration statistics in the Gulf Coast area

	Number of Samples	As<10 ug/L	10<As<50 ug/L	As>50 ug/L
Gulf Coast Aquifers				
Chicot A.	386	90.9%	8.5%	0.5%
Evangeline A.	456	90.4%	9.2%	0.4%
Jasper A.	278	77.3%	15.5%	7.2%
Combined	1,120	87.3%	10.5%	2.1%
Southwestern Section of the Gulf Coast Aquifers				
Chicot A.	96	72.9%	25.0%	2.1%
Evangeline A.	209	79.4%	19.6%	1.0%
Jasper A.	101	52.5%	27.7%	19.8%
Combined	406	71.2%	22.9%	5.9%
Northeastern Section of the Gulf Coast Aquifers				
Chicot A.	290	96.9%	3.1%	0.0%
Evangeline A.	247	99.6%	0.4%	0.0%
Jasper A.	177	91.5%	8.5%	0.0%
Combined	714	96.5%	3.5%	0.0%

Table 4. Common arsenical products and their use

Common Name(s)	Formula (CAS#)	As Redox state	Comments (non exhaustive list of trade names)
Arsenic trioxide or white arsenic	As_2O_3 (1327-53-3)	III	Main base product for arsenical compound manufacturing
Arsenic acid or Orthoarsenic acid	H_3AsO_4 (7778-39-4)	V	(also Dessicant L-10; Hi-Yield Dessicant H-10; Zotox; Desiccant L-10; Hy-Yield H-10; Poly Brand Dessicant; CCA Type C; Chemonite Part A; Crab grass killer)
Sodium Arsenite	NaAsO2 (7784-46-5)	III	sodium metaarsenite
Acid lead arsenate	$PbHAsO_4$ (7784-40-9)	V	
Basic lead arsenate	$Pb_4(PbOH)(AsO_4)_3$	V	
Calcium arsenate	$Ca_3(AsO_4)_2$ (7778-44-1)	V	
MSMA	$NaHAsO_3(CH_3)$ (2163-80-6)	V	monosodium methanearsonate, salt of the monomethylarsonic acid (MMA) (also Bueno6, Ansar6-6, Drexel, Zeneca, Helena)
DSMA	$Na_2AsO_3(CH_3)$ (144-21-8)	V	disodium methanearsonate, salt of the monomethylarsonic acid (MMA) (also Ansar8100, Drexel, Zeneca)
Cacodylic acid DMA(A)	$HAsO_2(CH_3)_2$ (75-60-5)	V	dimethylarsinic acid (also Ansar 138, Arsan, Bolls-Eye, Broadside, Check-Mate, Cotton Aide HC, Moncide, Montar, Phytar, Phytar 138, Phytar 600, Rad-E-Cate 25, Dilic, Silvisar 510, Sylvicor)
Chromated Cu Arsenate (CCA)	Complex structure;	Mainly V	comes in 3 types including: $CrO_3.CuO.As_2O_3$

Table 5. Arsenical compound use history

Usage	Start Date	Ban Date	Chemical compound
Animal feed (poultry)	1930's	N/A	Organic form of As
Herbicide - weed killer	1900's	1988	Pb Arsenate, Cu Acetoarsenite ("Paris green")
- ~specific to cotton	1977	N/A	MSMA, DSMA, cacodylic acid
Insecticide: - Sheep and cattle dips - Boll weevil (cotton pest) - Orchard pests	<1900	1988	Na Arsenite Ca Arsenate Pb Arsenate
Defoliant	First marketed in 1956 ~1965	1992	Arsenic acid
Wood preservatives	~1900's ~1975	N/A	Chromated Copper Arsenate

SOURCE: Loebenstein (1994);
NOTE: usages not included are lead batteries, metal alloys, semiconductors, glass manufacturing

Table 6. Timeline for High Plains cotton crop

Season / Month		**Chemical**	**Goal**	**Application Method**
Winter	Field plowed after harvest		Limit pest infestation	N/A
Winter		herbicide	Weed control	Spray
Early Spring / Spring	Pre-plant	P, N fertilizer Herbicide (e.g., MSMA) Insecticide	favor rooting weed control pest control	If dry land, applied into soil If irrigated, applied with water
April/May (last planting date: June 1 in counties north of Lubbock, June 5 in the Lubbock region, and June 10 to the south)	Planting			N/A
June	Emergence, early development stages	Herbicide (e.g., MSMA, DSMA) N, P fertilizer	weed control favor growth	Spray dry land = apply into soil irrigated = with water
May - August	Irrigation if available			
Summer		Insecticide(s)	Pest control	
Fall	Harvest-aid series Sometimes a light freeze plays the role of dessicant.	boll-opener, defoliant, dessicant (previously arsenic acid)	Facilitate harvest	spray
Fall (before first hard freeze)	Harvest			N/A

NOTE: Phases are shifted earlier by a few weeks for the southwestern Gulf Coast region

Table 7. Elemental arsenic and product application rates (loadings)

Substance	Ap. Rate (mg As/m^2)	Cited Ap. Rate	Source and comments
Ca Arsenate	420-630	10-15 lbs/ac	Aurelius (1988)
Arsenic acid	260	3 pts/ac	Miller and Bailey (1979)
ibid	170-260	2.94-4.42 lbs/ac	Aurelius (1988)
ibid	175-260	2-3 pts/ac at 6.22 lbs As/gal	Warrick et al. (1992)
MSMA	78	1.7 kg/ha	Jordan et al. (1997) (in Arkansas)
ibid	100	1.33 qts/ac at 6 lbs product/gal	Baumann (1998) (preplant use)
ibid	100	1.33 qts/ac at 6. lbs product/gal	Baumann (1998) (postemergence use)
ibid	39	0.76 lbs/ac	Gianessi and Marcelli (2000) (state average in 1992)
ibid	59	1.14 lbs/ac	Gianessi and Marcelli (2000) (state average in 1997)
ibid	27-37	0.6 – 0.8 kg/ha	Bridges et al. (2002) (in Florida, Georgia)
ibid	100	2 lbs/ac	LSU (2005) (Louisiana) (preplant)
ibid	50-100	1-2 lbs/ac	LSU (2005) (Louisiana) (postemergence)
DSMA	165	4 qts/ac at 3.6 lbs product/gal	Baumann (1998) (postemergence use)
ibid	91	2 lbs/ac	Gianessi and Marcelli (2000) (state average in 1992)
ibid	70-140	1.5-3 lbs/ac	LSU (2005) (Louisiana) (postemergence)
Pb Arsenate	10,590	490 kg/ha (440 lb./acre)	Welch et al. (2000) – general citation for western US, high bound.
ibid	8,000	80 kg/ha As	Davenport and Peryea (1991) – high bound
ibid	1,660	1.1 mmol/kg	Peryea and Kammereck (1997): experiment mimicking field conditions on a soil with a density of 1.35 g/cm3 and to a depth of 14 cm.

NOTE: Given the diversity of the units used in the references, compiled application rate and dosage values are converted to mg elemental As/m^2 for comparison purposes but also cited as in the original source. Rates are sometimes reported as "active ingredient (a.i)", some other times with no such indication. We assumed all rates are a.i. rates.
Ap. = Application; ac = acre (4046.86 m^2); pts = pints (0.4732×10^{-3} m^3); qts = quarts (0.9464×10^{-3} m^3); lbs = pounds (454,000 mg); ha = hectare (10,000 m^2); As molar weight = 75 g/mole
Unless indicated, rates apply to a Texas location

Table 8. Comparison of arsenic concentrations in wells within and farther than 1000 m from cotton gin locations in the Texas Southern High Plains

Region	Wells	Number	μ_0	ν	P(F<=f)	P(T<=t)
SHP-S	≤ 1000 m	31	1.0775	0.0456	0.002	0.987
	> 1000 m	503	1.0765	0.1069		
SHP-N	≤ 1000 m	11	0.6920	0.0729	0.207	0.808
	> 1000 m	341	0.6746	0.0544		

NOTE: Average (μ_0) and variance (ν) values are for $\log_{10}$ arsenic concentrations. For F-tests, the p-value indicates the probability that the compared sample variances are different. For t-tests, the p-value indicates the probability that the compared sample means are the same.

Table 9. Borehole sampling information

Borehole	Latitude	Longitude	County	Setting	Crop/Vegetation	Depth (ft)	Number of Samples	Arsenic (ug/kg)			Arsenic (ug/L)		
								median	min	max	median	min	max
Southern High Plains													
A1	32.3866	-102.7640	Andrews	Rangeland	Shrubs, grasses	10.0	8	2.6	1.3	4.3	54	17	206
A2	32.3804	-102.7979	Andrews	Rangeland	Shrubs, grasses	28.0	17	23	9.7	77	425	97	1162
T2	33.3560	-102.2329	Terry	Playa	Adjacent irrigated cotton	30.5	18	14	0.55	203	115	2.6	1025
T3	33.2354	-102.2838	Terry	Irrigated	Cotton	41.5	24	19	2.3	62	230	15	687
T4	33.0212	-102.3067	Terry	Irrigated	Cotton	33.5	20	2.4	0.41	62	22	2.6	1490
T1	33.3278	-102.3005	Terry	Dryland	Cotton	23.5	15	14	2.1	29	103	15	203
L1	33.9280	-102.6098	Lamb	Dryland	Cotton	28.3	17	7.3	0.63	37	73	5.0	191
B1	33.9114	-102.6755	Bailey	Dryland	Cotton	36.6	22	5.4	0.68	19	52	5.7	182
B2	34.0051	-102.9440	Bailey	Dryland	Cotton	20.5	14	7.5	0.76	18	67	6.3	142
G1	32.7099	-102.4294	Gaines	Dryland	Cotton	16.5	12	9.4	2.4	18	57	24	113
G2	32.6777	-102.3056	Gaines	Dryland	Cotton	35.5	21	7.9	1.1	37	74	16	415
H1	32.4475	-101.6386	Howard	Dryland	Cotton	20.5	14	21	4.5	77	146	34	662
H2	32.3957	-101.5416	Howard	Dryland	Cotton	28.0	17	3.2	0.05	35	31	0.7	324
D1	32.7072	-102.1747	Dawson	Dryland	Cotton	11.5	10	8.0	2.8	36	63	20	598
M1	32.3844	-102.0458	Martin	Dryland	Cotton	20.5	16	15	0.11	33	123	0.74	598
M2	32.3488	-102.0782	Martin	Dryland	Cotton	27.5	18	9.8	3.4	30	114	34	238
M3	32.1155	-101.7563	Martin	Dryland	Cotton	21.5	14	8.5	5.7	35	59	40	338
M4	32.1305	-101.7563	Martin	Dryland	Cotton	14.5	11	5.6	2.8	20	66	25	218
Southwestern Gulf Coast													
KE1	26.7550	-97.6048	Kenedy	Rangeland	Live Oak, shrubs, grasses	18.0	12	8.0	1.2	30	510	186	753
DU2	27.4581	-98.7189	Duval	Rangeland	Shrubs, grasses	10.0	8	4.8	2.9	69	79	37	486
DU3	27.7999	-98.6301	Duval	Rangeland	Shrubs, grasses	8.0	7	3.6	2.8	5.9	55	50	152
ST1	26.7027	-98.3974	Star	Rangeland	Shrubs, grasses	12.3	9	8.3	1.9	17	206	59	468
HI2	26.5352	-98.1659	Hidalgo	Rangeland	Grasses	3.0	3	3.5	2.0	5.6	79	23	332
HI1	26.5607	-98.1242	Hidalgo	Rangeland	Shrubs, grasses	17.0	12	102	8.1	1854	3168	114	26201
ST3	26.7208	-98.5238	Star	Irrigated	Pasture, grasses	18.0	12	3.3	1.1	24	189	81	586
DU1	27.2934	-98.3157	Duval	Dryland	Peanuts	11.5	9	72	0.69	124	840	7.4	979
ST2	26.4746	-98.7435	Star	Dryland	Corn	17.9	12	9.6	4.9	137	107	46	1156
NU1	27.6726	-97.7076	Nueces	Dryland	Cotton	24.0	23	8.0	0.74	76	36	3.2	483

Table 10. Dominant species and pKa of relevant chemical elements

Oxyanion	**Dominant Species / *pKa***
Arsenate – As(V)	H_3AsO_4 ***2.30*** $H_2AsO_4^-$ ***7.16*** $HAsO_4^{2-}$ ***11.65*** AsO_4^{3-}
Phosphate – P(V)	H_3PO_4 ***2.15*** $H_2PO_4^-$ ***7.20*** HPO_4^{2-} ***12.35*** PO_4^{3-}
Selenate – Se (VI)	$HSeO_4^-$ ***1.8*** SeO_4^{2-}
Molybdate – Mo(VI)	H_2MoO_4 ***~4*** $HMoO_4^-$ ***4.24*** MoO_4^{2-}
Vanadate – V(V)	H_3VO_4 ***4*** $H_2VO_4^-$ ***8.5*** HVO_4^{2-}
Borate – B(III)	H_3BO_3 ***9.24*** $H_2BO_3^-$
Arsenite – As(III)	H_3AsO_3 ***9.15*** $H_2AsO_3^-$
Selenite Se(IV)	H_2SeO_3 ***2.7*** $HSeO_3^-$ ***8.54*** SeO_3^{2-}

NOTE: pKa's are approximately located and thus the table represent the spread of a species under varying pH. Data from Dzombak and Morel (1990, Table 10.9) and other sources

Table 11. Average abundance of arsenic and other elements for different rock types (mg/kg)

Element	**Igneous**	**Sandstone**	**Shale**	**Carbonate**
Arsenic	1.8	1	9	1.8
Boron	7.5	90	194	16
Fluoride	715	220	560	112
Molybdenum	1.2	0.5	4.2	0.75
Antimony	0.5	0.8	0.1	0.2
Selenium	0.05	0.5	0.6	0.3
Uranium	2.8	1.	4.5	2.2
Vanadium	149	20	101	13

SOURCE: Hem (1985, Table 1)

Table 12. Average abundance of arsenic and other elements in soils in the U.S. (mg/kg)

Element	**Geometric Average**	**Range**
Arsenic	7.2	<0.1 - 97
Boron	33	<20 - 300
Fluoride	430	<10 – 3,700
Molybdenum	~1	<3 - 15
Antimony	0.66	<1 – 8.8
Selenium	0.39	<0.1 – 4.3
Uranium	2.7	0.3 - 11
Vanadium	80	<7 - 500

Source: Shacklette and Boerngen (1984, Tables 1 and 2)

Table 13. Current trace element concentration in southwestern Gulf Coast soils. Arithmetic mean (range) in mg/kg

Formation	**Arsenic**	**Molybdenum**	**Selenium**	**Uranium**
Whitsett	5.3 (0.6-17)	2.1 (0.2-4.6)	0.18 (0.01-0.90)	
Catahoula	3.4 (0.2-6.9)	0.9 (0.2-4.0)	0.13 (0.01-0.60)	2-3*
Oakville	No Data	0.9 (0.3-2.0)	0.17 (0.01-0.38)	
U.S. average	~5-6	1-2	0.1-0.5	

NOTE: from a total of ~300 samples

Data from Table 4 of Henry and Kapadia (1980) Arithmetic mean + composite range

* from Galloway (1977, p.39) and Galloway and Kaiser (1980, p.14)

Table 14. Typical dissolved concentration in groundwater

Element	Value or Range (ug/L)	Source
Arsenic	1-50 1-50 <10	Hitchon et al. (1999) Welch et al. (2000, Figure 2) Smedley and Kinninburgh (2002, p.525
Boron	50-1000	Hitchon et al. (1999)
Fluoride	10-1,500 <1,000	Hitchon et al. (1999) Hem (1985, p.120)
Molybdenum	~<10 (?) variable	Hem (1985, p.140)
Antimony	~<5	Hem (1985, p.145)
Selenium	0.1-10 <1	Hitchon et al. (1999) Hem (1985, p.145)
Uranium	0.1-10	Hem (1985, p.148)
Vanadium	<10	Hem (1985, p.138)

Table 15. Typical arsenic concentrations in water

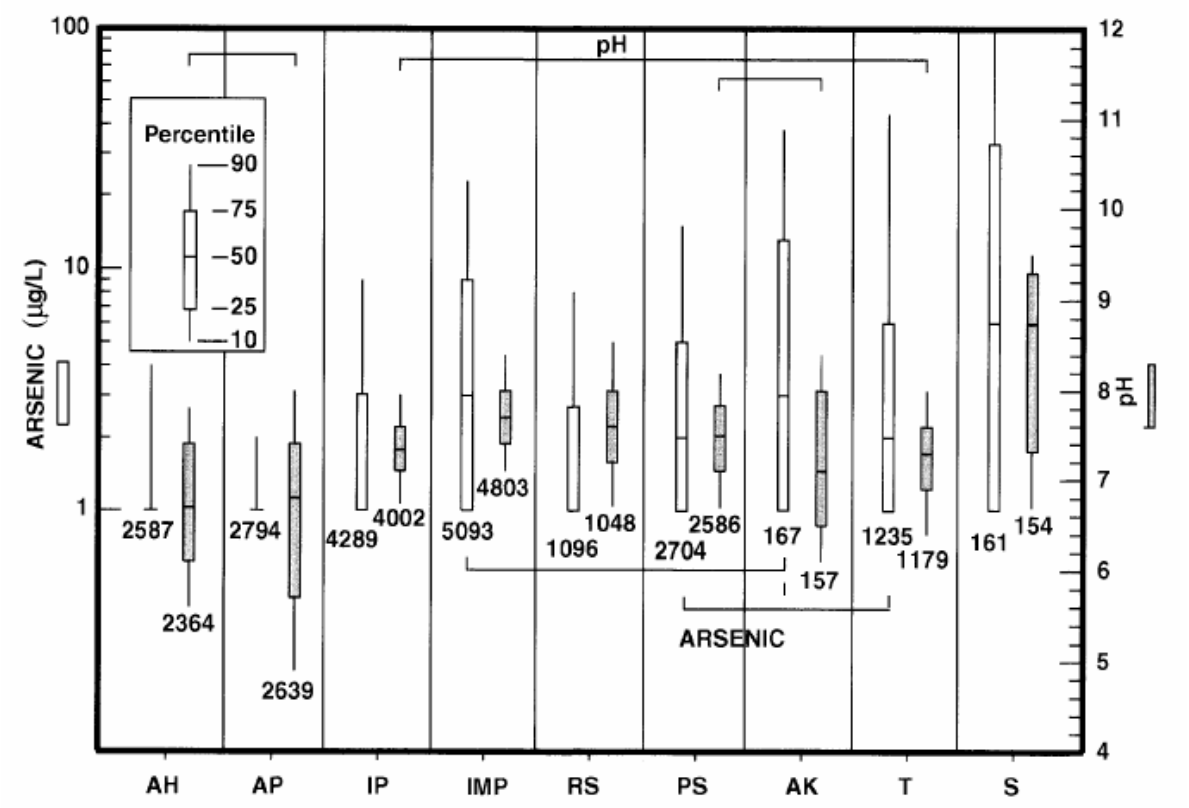

SOURCE: Welch et al., 2000

NOTE: Summary statistics for arsenic and pH in groundwater. “AP” (Atlantic Plains) and “IP” (Interior Plains) apply to the Gulf Coast and High Plains areas, respectively.

Table 16. Summary of regression coefficients between arsenic and other parameters (High Plains)

Covariate	Value	As Source	Parameter Source
Molybdenum	0.180	TWDB	TWDB
Selenium	0.138	TWDB	TWDB
Vanadium	0.653	TWDB	TWDB
Boron	0.170	TWDB	TWDB
Fluoride	0.299	TWDB	TWDB
Silica	0.075	TWDB	TWDB
Iron	0.004	TWDB	TWDB
Bicarbonate	0.056	TWDB	TWDB
Sulfate	0.091	TWDB	TWDB
Chloride	0.058	TWDB	TWDB
Nitrate	0.048	TWDB	TWDB
TDS	0.010	TWDB	TWDB
pH	0.013	TWDB	TWDB
Beryllium	N/A		TWDB – All <DL
Perchlorate	0.100	Jackson et al., 2004	Jackson et al., 2004
Ca/Mg	0.145	NURE	NURE
Ca/Mg	0.101	TWDB	TWDB

Table 17. Summary of regression coefficients between arsenic and other parameters (southwestern Gulf Coast)

Covariate	Value	As Source	Parameter Source
Molybdenum	0.033	NURE	NURE
Molybdenum	0.130	TWDB – All >DL	TWDB – All >DL
Molybdenum	0.358	TWDB	TWDB
Selenium	0.020	NURE	NURE
Selenium	0.014	TWDB – All >DL	TWDB – All >DL
Selenium	0.012	TWDB	TWDB
Vanadium	0.386	NURE	NURE
Vanadium	0.381	TWDB – All >DL	TWDB – All >DL
Vanadium	0.432	TWDB	TWDB
Boron	0.120	NURE	NURE
Boron	0.061	TWDB – All >DL	TWDB – All >DL
Boron	0.004	TWDB	TWDB
Fluoride	0.039	TWDB – All >DL	TWDB – All >DL
Uranium	0.088	NURE	TWDB – All <DL
Silica	0.115	NURE	NURE
Silica	0.089	TWDB – All >DL	TWDB – All >DL
Iron	0.024	NURE	NURE
Alkalinity	0.002	NURE	NURE
Bicarbonate	0.001	TWDB – All >DL	TWDB – All >DL
Sulfate	0.034	NURE	NURE
Sulfate	0.138	TWDB – All >DL	TWDB – All >DL
Chloride	0.040	NURE	NURE
Nitrate	0.000	TWDB – All >DL	TWDB – All >DL
Conductivity	0.052	NURE	NURE
TDS	0.049	TWDB – All >DL	TWDB – All >DL
Disolved Oxygen	0.027	NURE	NURE
Disolved Oxygen	0.002	NURE(if As>10ug/L)	NURE (if As>10ug/L)
Redox – All GC	0.003	TWDB	TWDB
Redox – Sth. GC	0.005	TWDB	TWDB
pH	0.078	NURE	NURE
pH	0.189	TWDB – All >DL	TWDB – All >DL

Table 18. Ashfall events in the Texas Panhandle during Ogallala and Blackwater Draw sediment deposition

Event Name	Age (Ma)	Approximate Source	U (ppm)	Thickness (ft) in Panhandle	Source
Lava Creek B	0.62	Yellowstone area	6.6	1	Izett (1981)
Guaje	1.4	Jemez Mountains	18		Izett (1981) Age in Gustavson et al. (1991)
Huckleberry Ridge	2.2	Yellowstone area	6.2		Izett (1981)
Mount Blanco	2.3	Pacific Northwest	3.3		Izett (1981)
West Amarillo Creek	~10	Yellowstone area		3	Cepeda (2001)

Table 19. pKa for arsenic-based acids at 25°C

Arsenical Compound	pKa	Source
H_3AsO_3	9.17 – (14.1)	Nordstrom and Archer (2003)
	9.15 – (14.7)	Wateq4f
	9.20 – (11.02)	EQ3/6 (Wolery, 1995)
	9.29 – (12.04)	Minteq
Arsenic acid H_3AsO_4	2.30 – 6.99 – 11.80	Nordstrom and Archer (2003)
	2.30 – 7.16 – 11.65	Wateq4f
	2.25 – 6.76 – 11.60	EQ3/6 (Wolery, 1995)
	2.24 –6.96 – 11.50	Minteq
monomethylarsonic acid (MMA) $H_2AsO_3(CH_3)$	4.19 – 8.7	Molenat et al. (1999) and NRC (1999, p.29)
dimethylarsinic acid (DMA) $HAsO_2(CH_3)_2$	1.78? 6.2?	Molenat et al. (1999) NRC (1999, p.29)

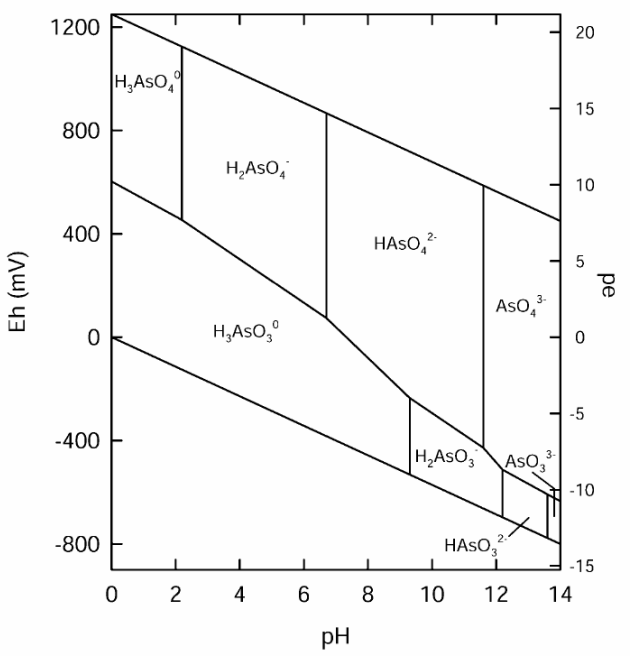

SOURCE: Smedley and Kinniburgh, 2002

Figure 1. Eh-pH diagram for arsenic aqueous species in the As-O_2-H_2O system at 25°C and 1 bar

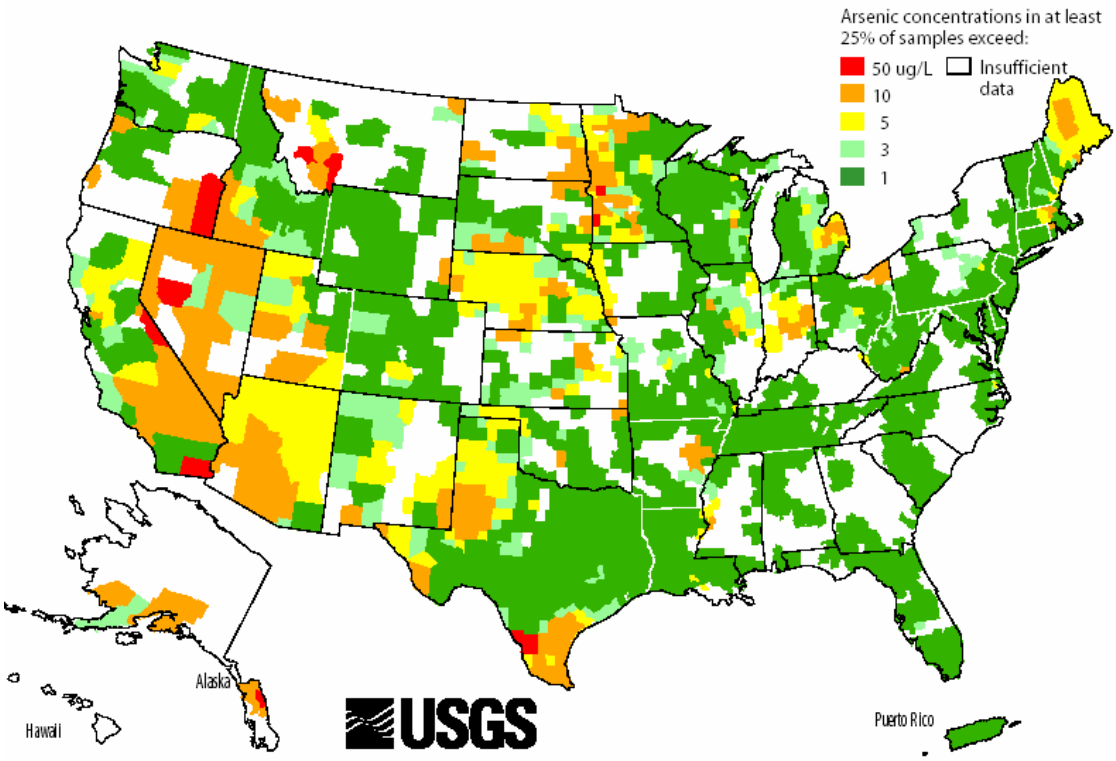

NOTE: Distribution based on 31,350 ground-water samples. The map shows arsenic concentrations found in at least 25% of samples per county

SOURCE: Ryker, 2001

Figure 2. Distribution of arsenic concentration in the U.S.

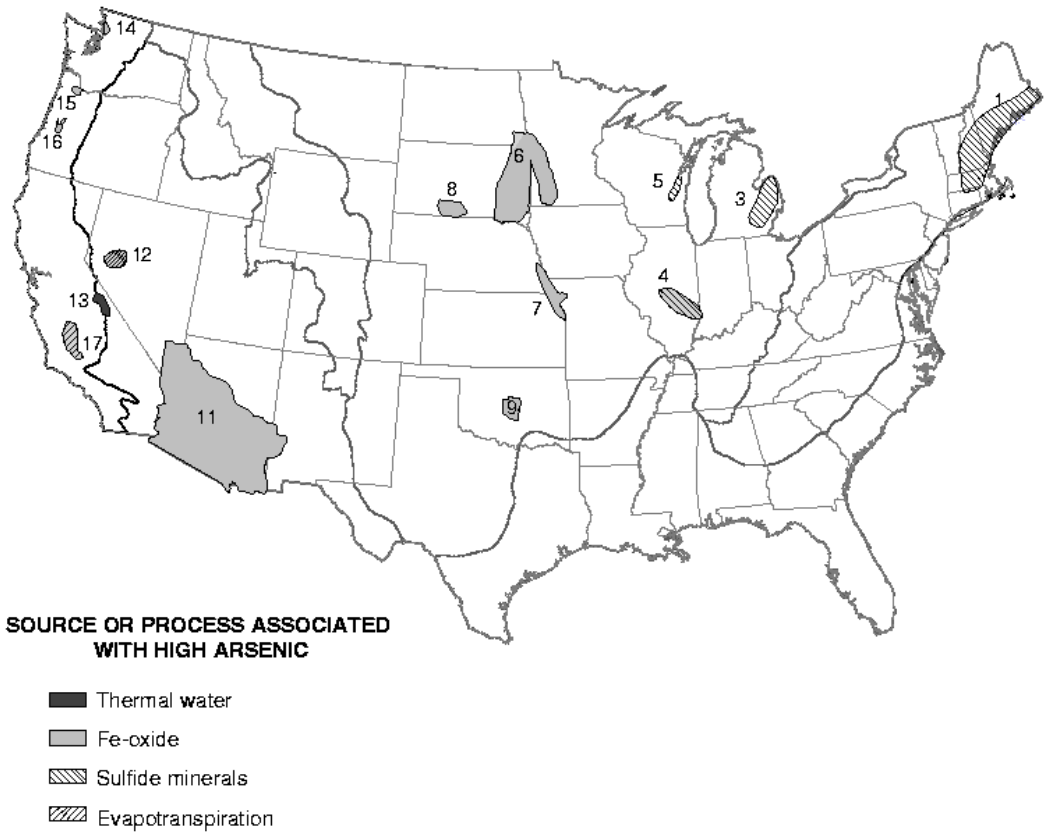

SOURCE: Welch et al, 2000

Figure 3. Distribution of groundwater with elevated arsenic concentrations (> 50 ug/L) and primary source or process resulting in high arsenic concentrations

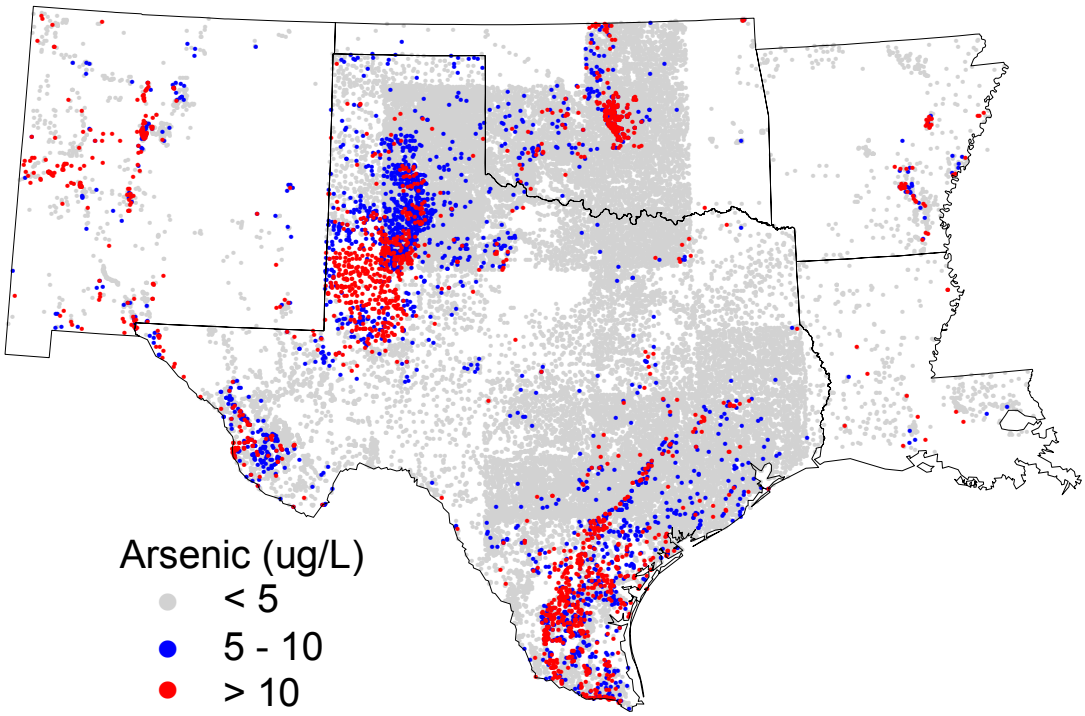

NOTE: Texas Water Development Board, US Geological Survey, National Uranium Resource Evaluation, New Mexico Bureau of Geology and Mineral Resources, Association of Central Oklahoma Governments, and Arkansas Department of Environmental Quality databases

Figure 4. Arsenic concentrations in groundwater in Texas and surrounding states

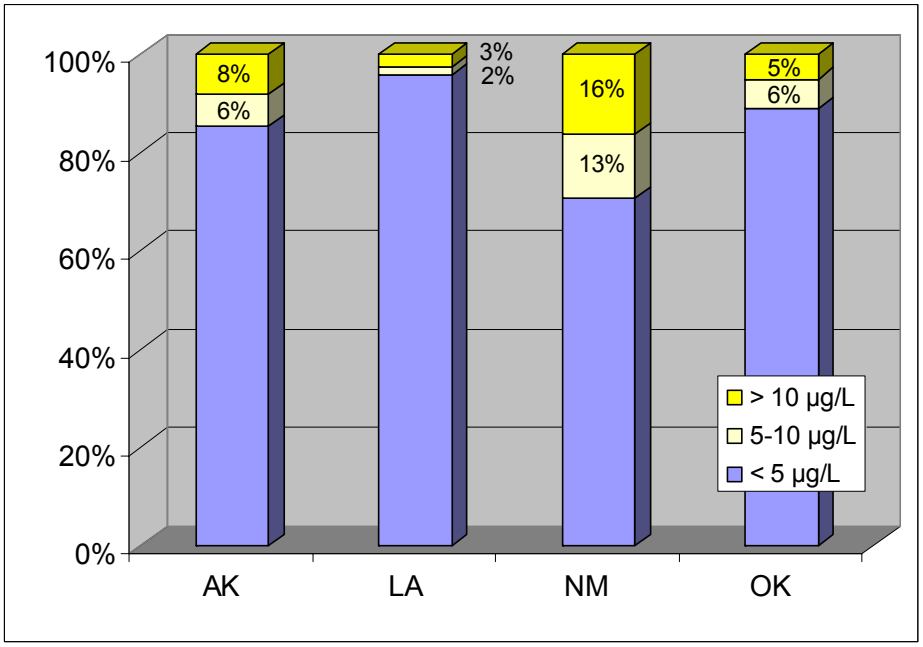

Figure 5. Summary of arsenic concentrations for states surrounding Texas

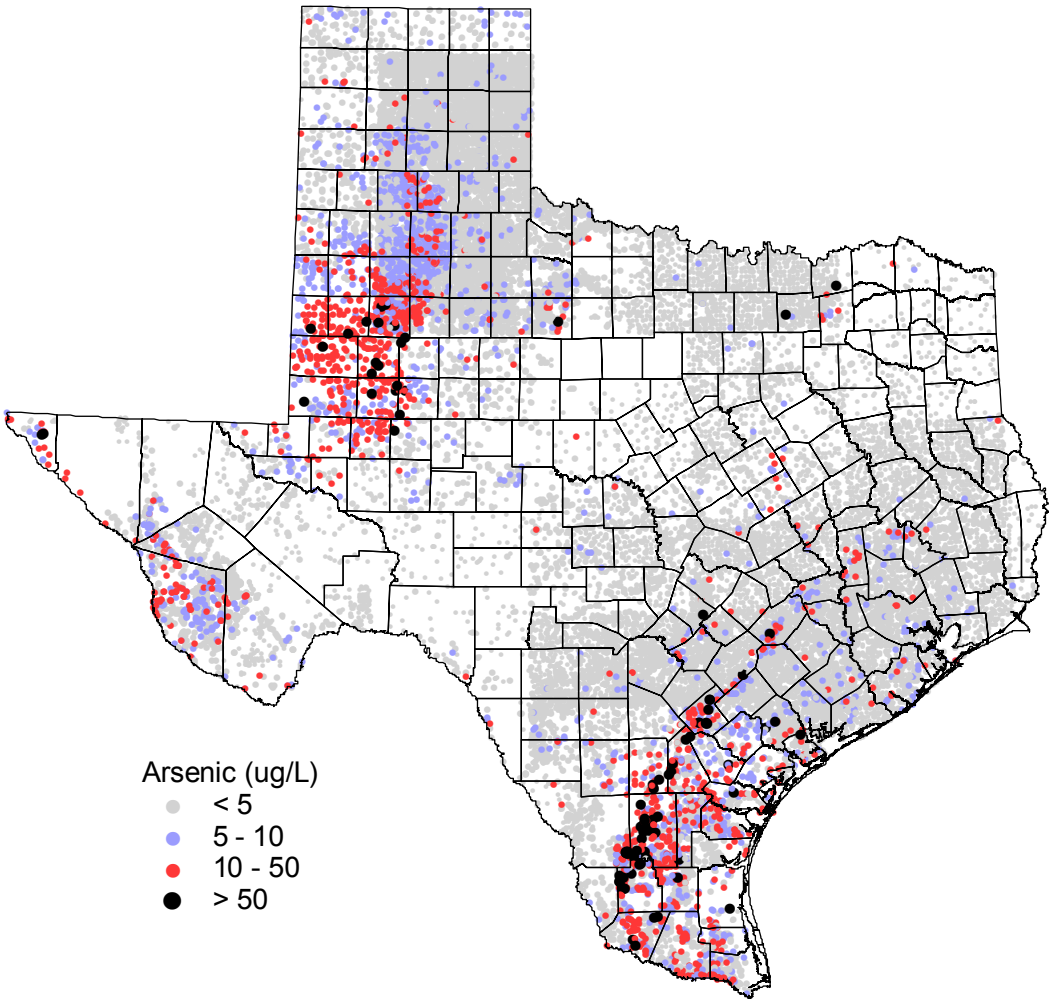

SOURCE : TWDB and NURE databases

Figure 6. Arsenic distribution in groundwater across the state of Texas

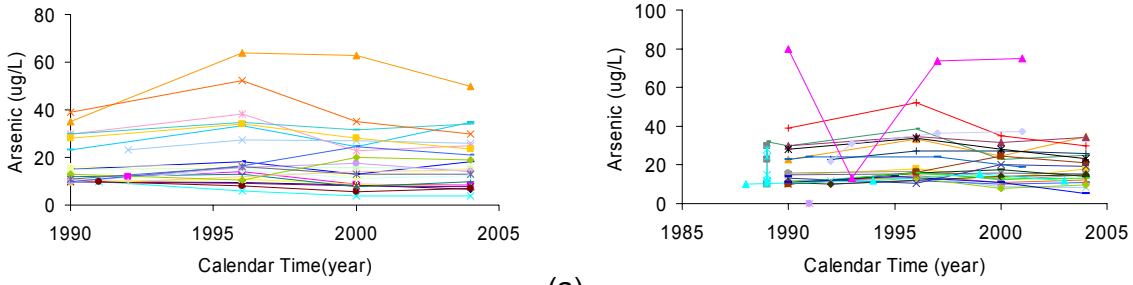

(a) (b)

NOTE: the analysis =13.2 ug/L in plot (b) within the time series with the highest average is likely a typo

Figure 7. Time series for arsenic analyses (a) south of southern High Plains; (b) southwestern Gulf Coast (both from TWDB database)

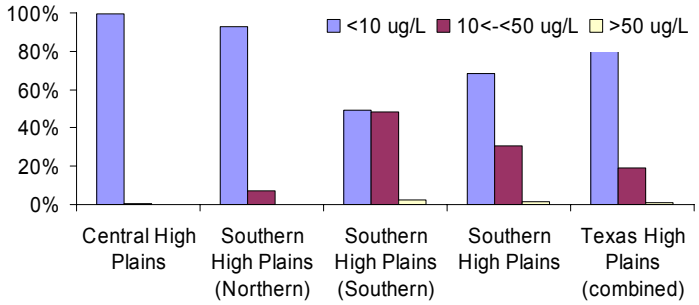

NOTE: Total of 477, 609, and 668 samples in the southern and northern section of the southern High Plains and central High Plains, respectively

Figure 8. Arsenic concentration statistics in the High Plains

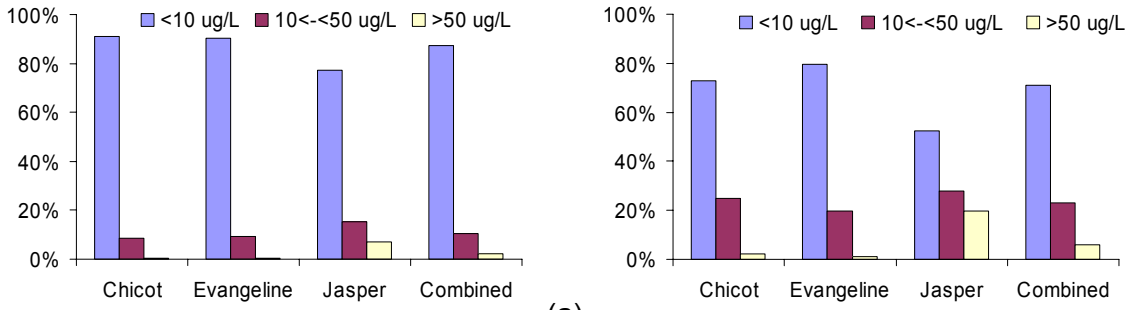

(a) (b)

NOTE: Total of 1,120 and 406 samples for (a) and (b), respectively

Figure 9. Arsenic concentration statistics: (a) whole Gulf Coast aquifer; (b) only southwestern section

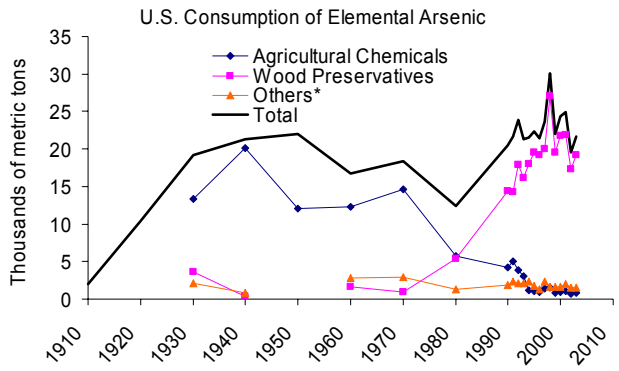

Source: Loebenstein (1994, Table 2)

NOTE: "others" includes glass manufacturing, alloys, electronics; and USGS commodity data (http://minerals.usgs.gov/minerals/pubs/commodity/arsenic)

Figure 10. U.S. consumption of elemental arsenic

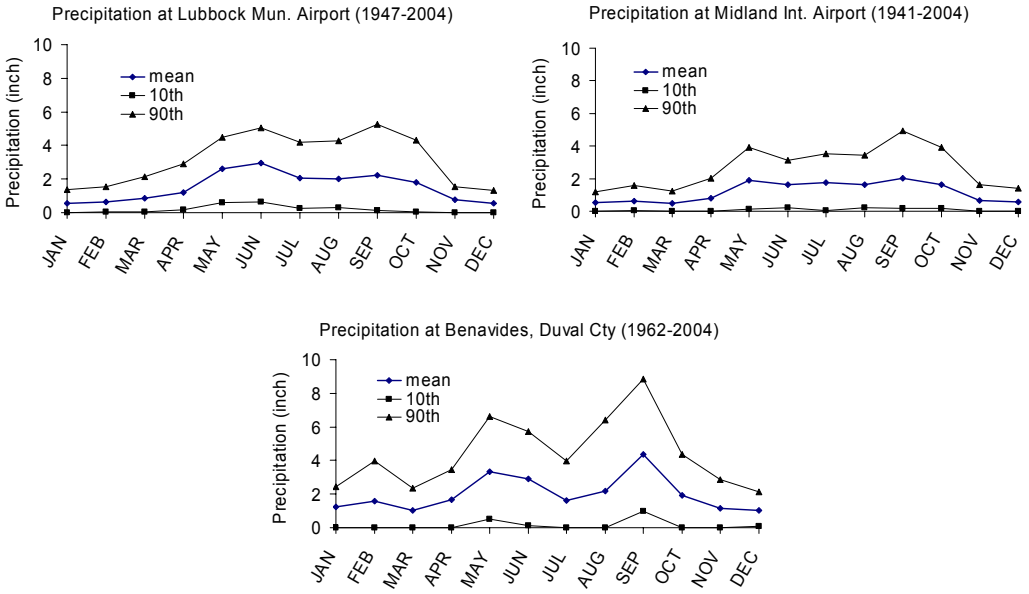

Source: National Weather Service

Figure 11. Precipitation monthly average in Lubbock and Midland in the High Plains and Benavides in the southwestern Gulf Coast

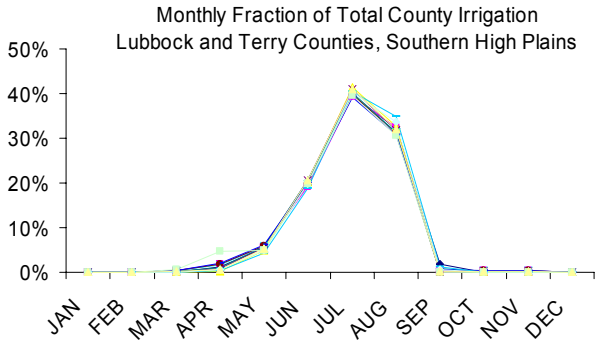

Source: Blandford (2003)

Note: Irrigated cotton crop accounts for 37 and 26% of the total area of Lubbock and Terry counties

Note: data include years 1982, 1983, 1984, 1987, 1992, and 1993

Figure 12. Monthly fraction of total county irrigation in Lubbock and Terry counties

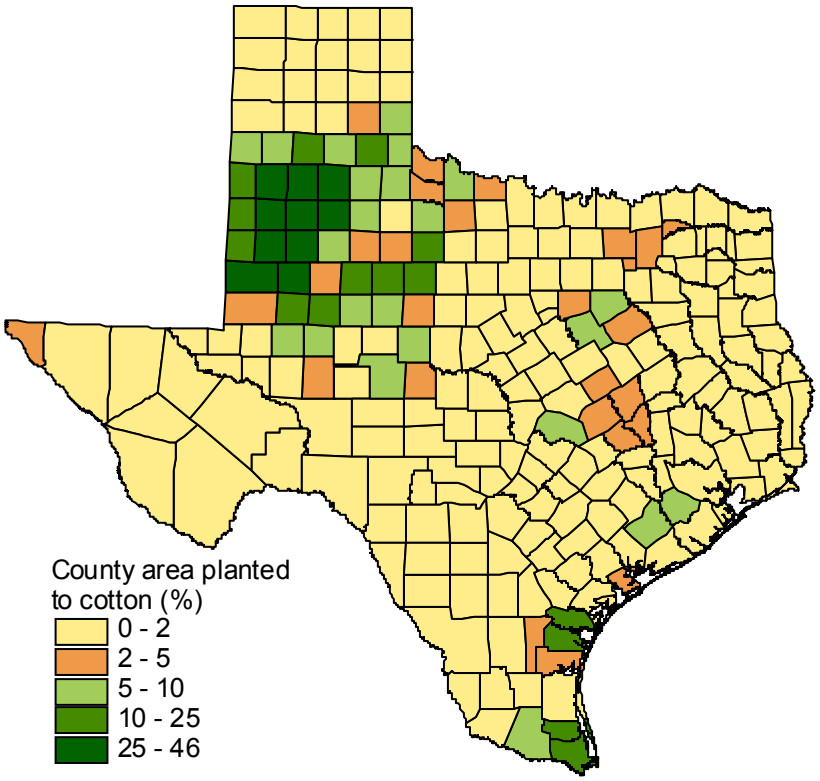

NOTE: Values shown based on median annual planted cotton acreage for the period 1970 to 1995
SOURCE: NASS database
Figure 13. County area planted to cotton

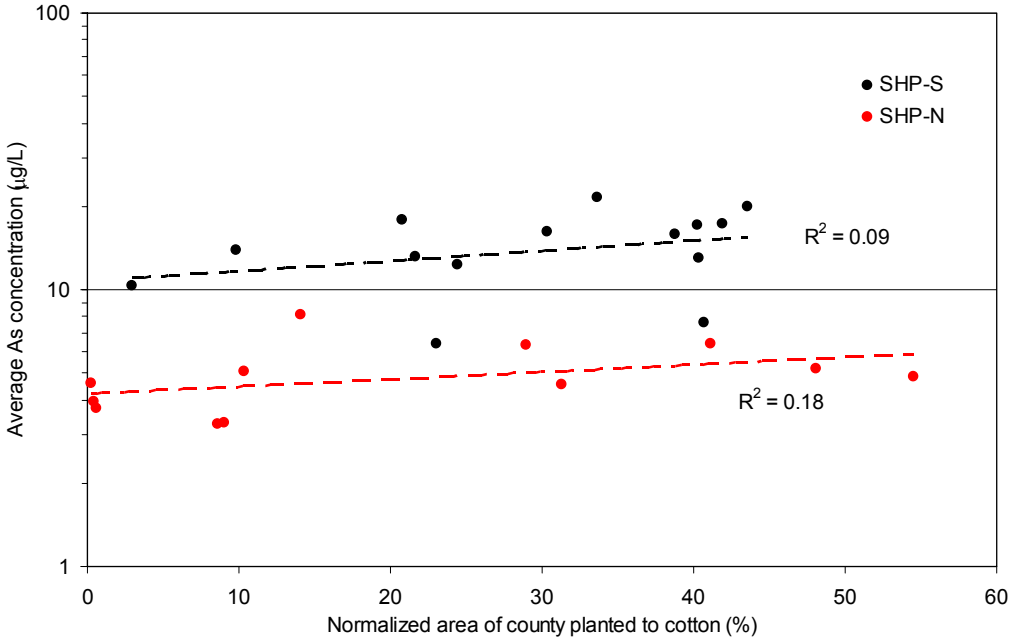

NOTE: SHP-S and SHP-N = Texas southern High Plains southern and northern regions, respectively
Figure 14. Average arsenic concentration in groundwater related to area planted to cotton by county in the southern High Plains

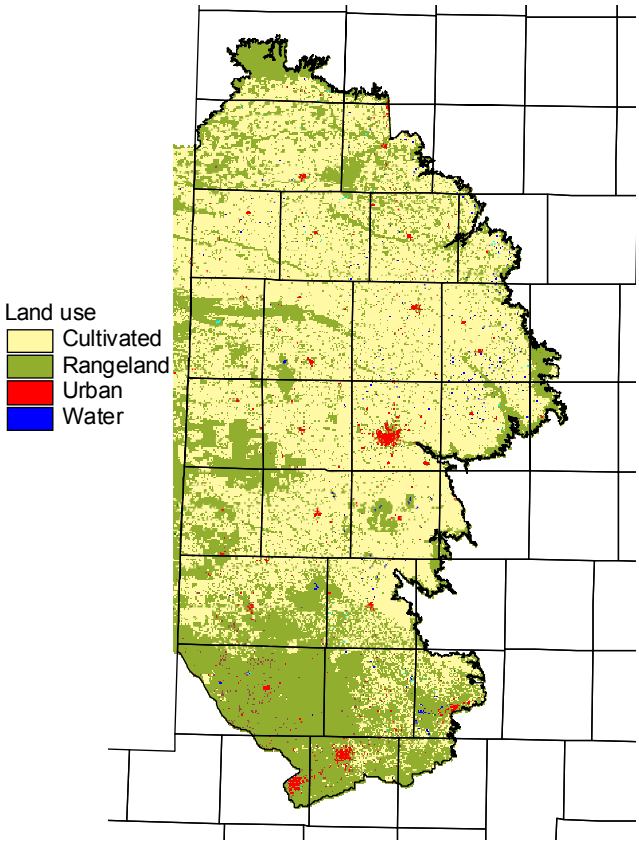

Figure 15. Map of land use in the southern High Plains

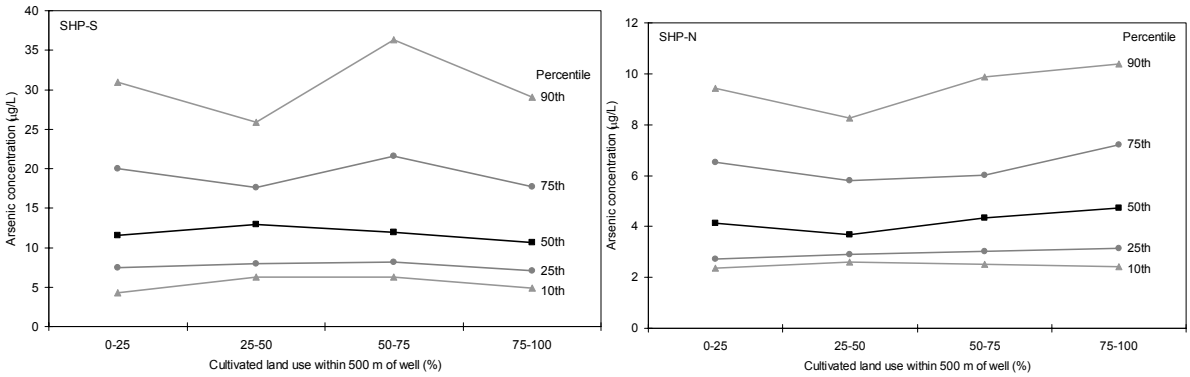

NOTE: Land use derived from NLCD (1992) (Vogelmann *et al*. 2001)
NOTE: SHP-S and SHP-N = Texas southern High Plains southern and northern regions, respectively
Figure 16. Distribution of groundwater arsenic concentrations in the southern High Plains in relation to the percentage of cultivated land use within 500 m of well locations

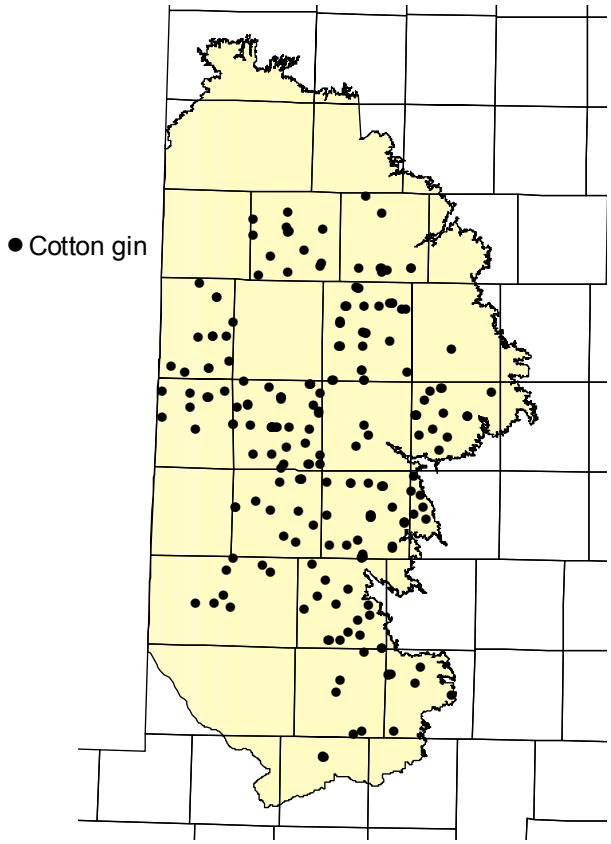

Figure 17. Cotton gin locations in the High Plains

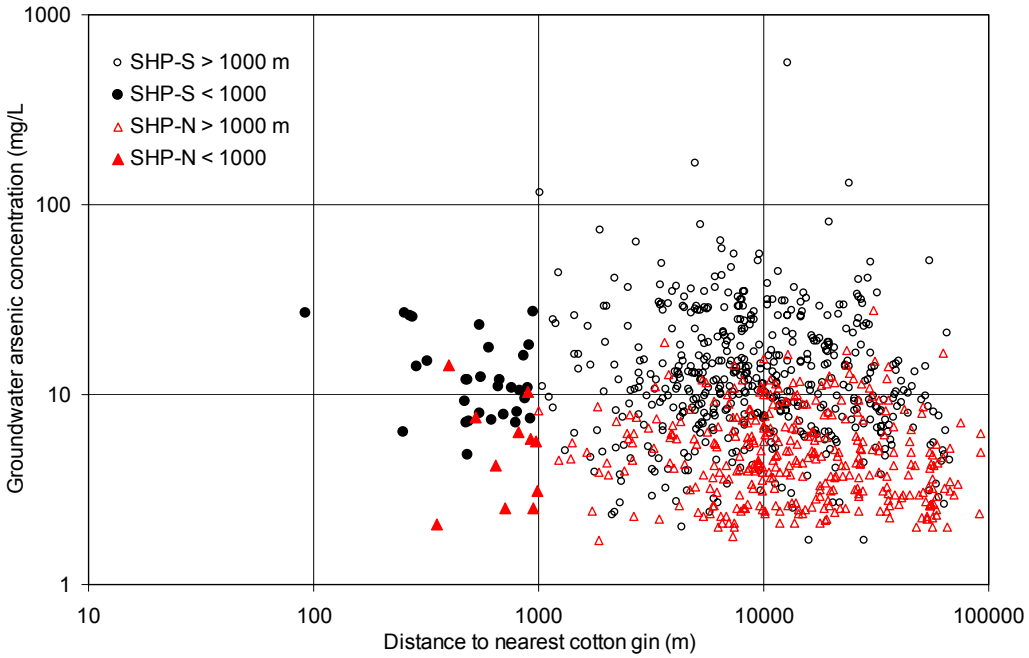

NOTE: SHP-S and SHP-N = Texas southern High Plains southern and northern regions, respectively

Figure 18. Relationship between groundwater arsenic concentrations and distance to cotton gins in the High Plains

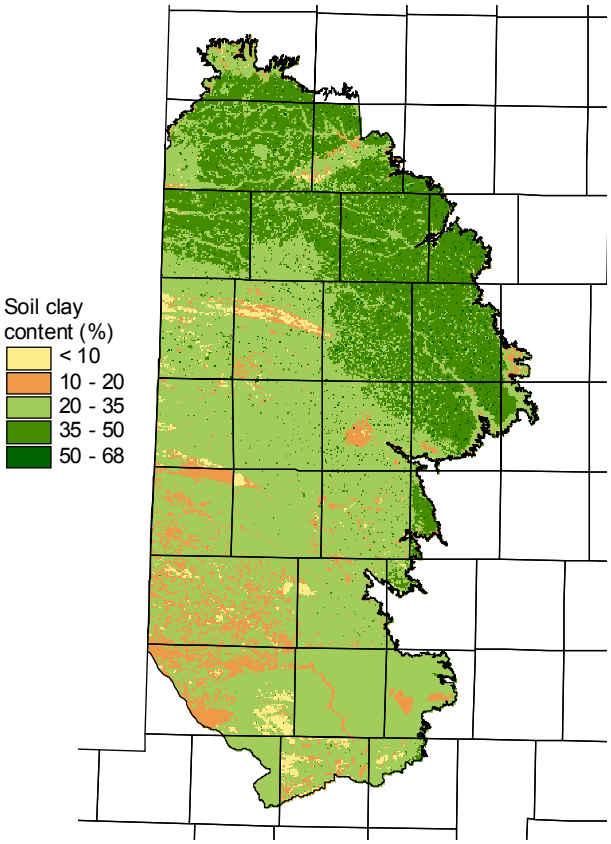

Figure 19. Soil clay content on the footprint of the southern High Plains aquifer

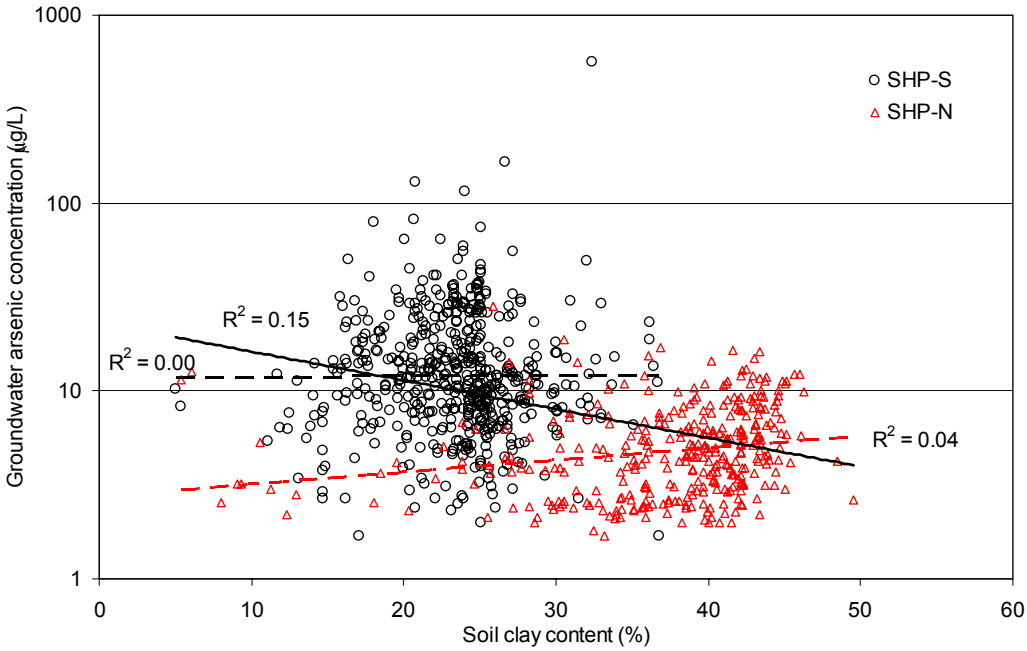

NOTE: Arsenic concentration in groundwater related to average soil clay content within 1000 m of well locations for the southern (SHP-S) and northern (SHP-N) regions. The solid line represents the regression for all points, the dashed lines represent regressions for each region.

Figure 20. Relationship between groundwater arsenic concentrations and soil clay content within 1000 m of well locations for the Texas southern High Plains

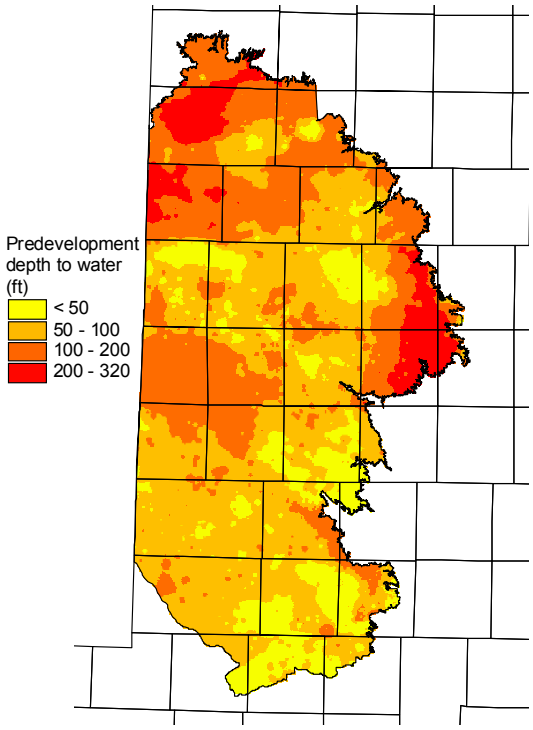

Figure 21. Predevelopment depth to water (southern High Plains aquifer)

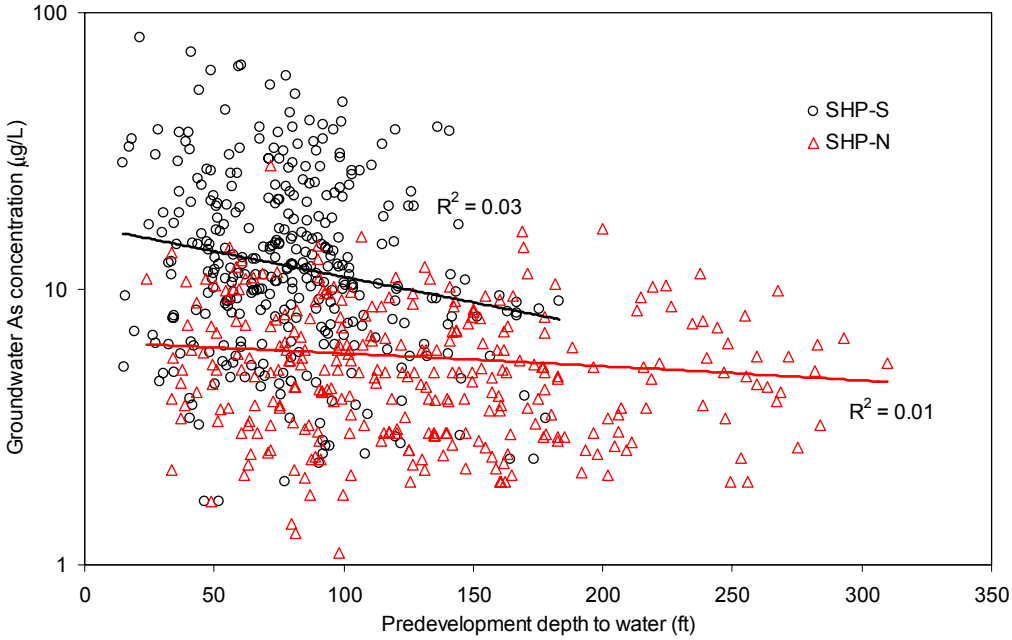

NOTE: Predevelopment depth to water was estimated from the earliest TWDB database information available in a given area

NOTE: SHP-S and SHP-N = Texas southern High Plains southern and northern regions, respectively

Figure 22. Relationship between predevelopment depth to water in the High Plains aquifer and arsenic concentrations in ground water

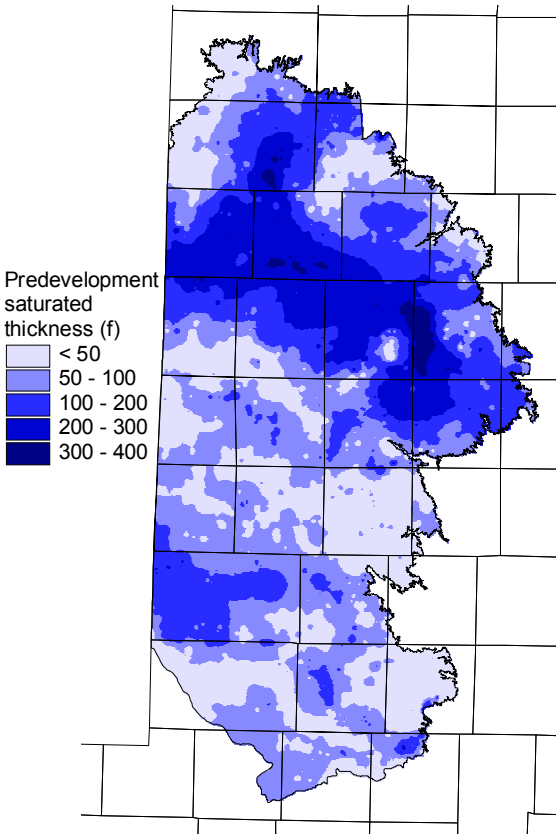

Figure 23. Predevelopment saturated thickness (southern High Plains aquifer)

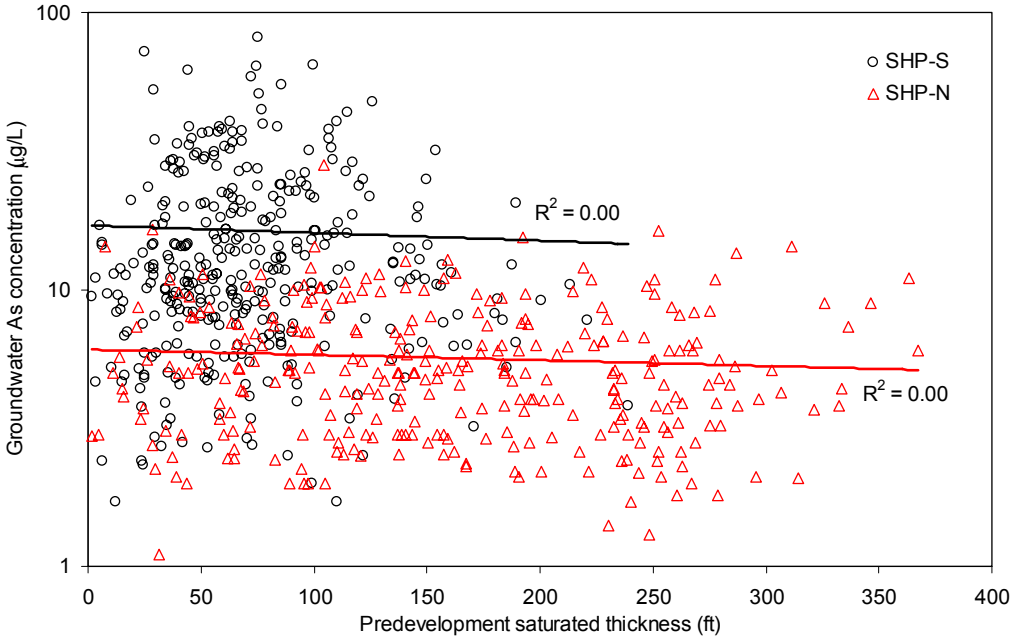

NOTE: Predevelopment saturated thickness was estimated from the earliest TWDB database information available in a given area

NOTE: SHP-S and SHP-N = Texas southern High Plains southern and northern regions, respectively

Figure 24. Relationship between predevelopment saturated thickness of the High Plains aquifer and arsenic concentrations

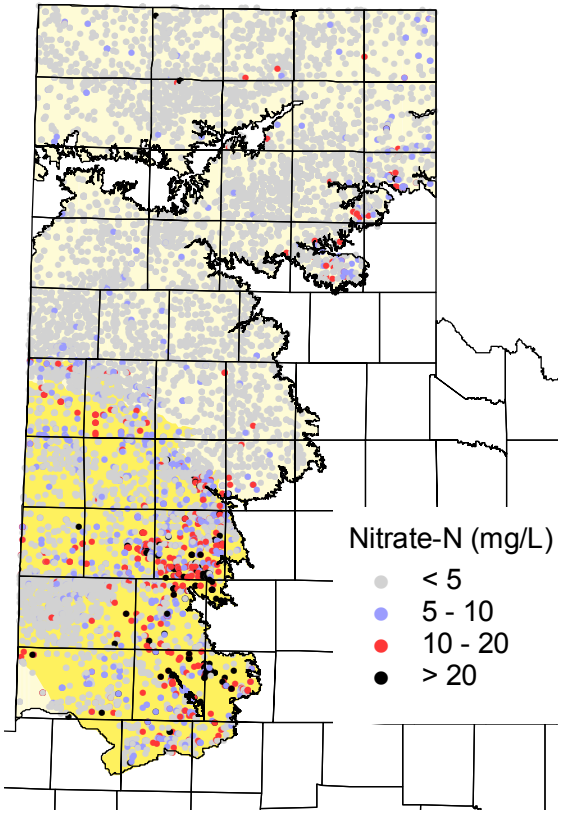

Figure 25. Nitrate distribution in the Texas High Plains

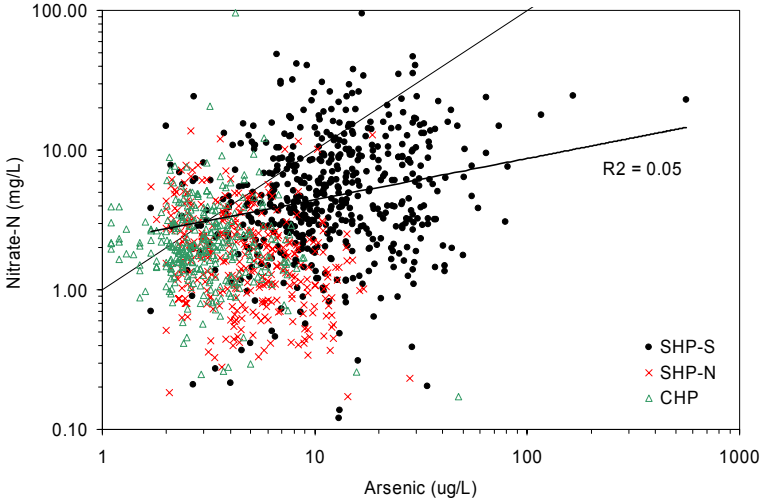

NOTE: trendline uses only SHP-S data points

Figure 26. Crossplot of As vs. Nitrate (High Plains aquifer)

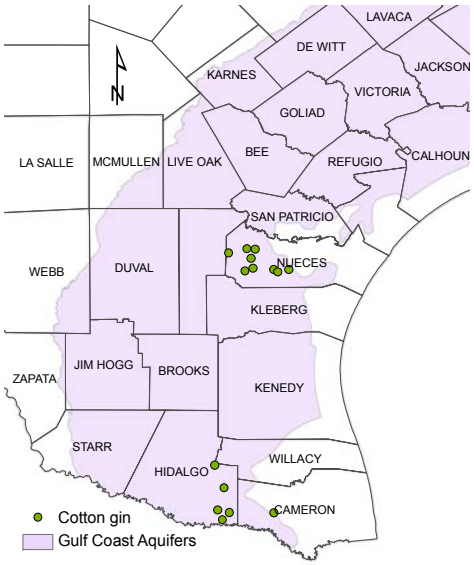

Figure 27. Cotton gin locations in the southwestern Gulf Coast

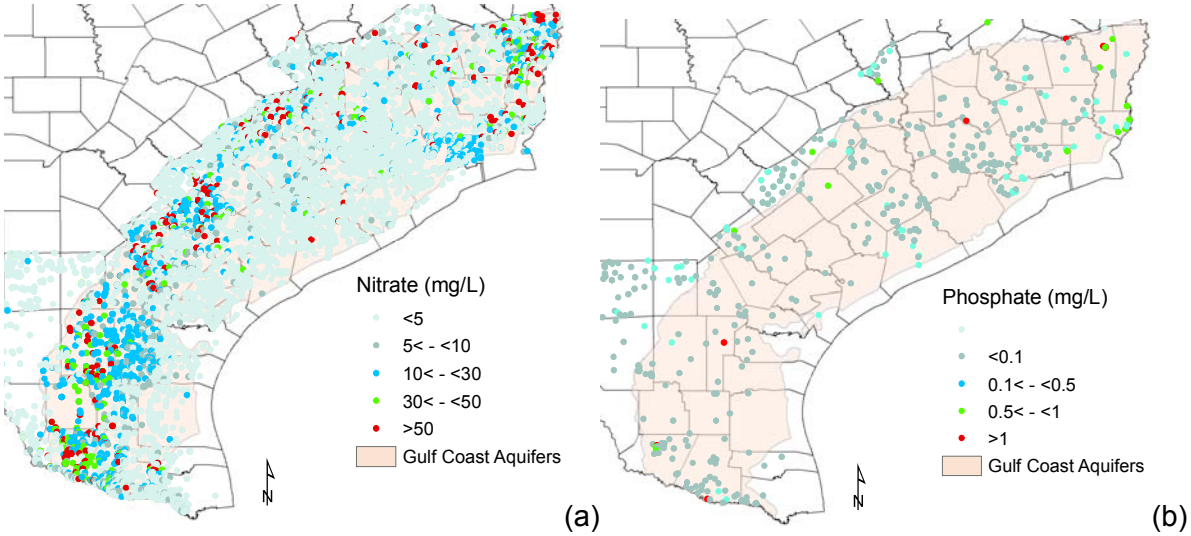

(a) (b)

Figure 28. Nitrate (a) and phosphate (b) distribution in the Gulf Coast

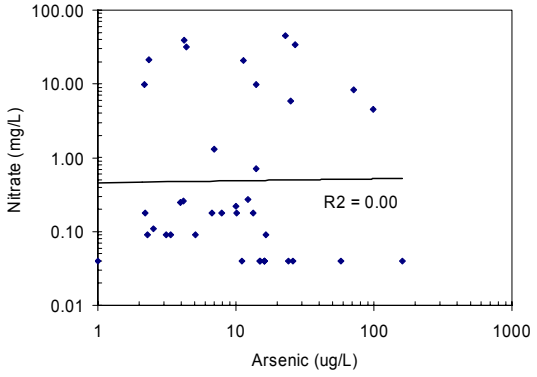

(a)

NOTE: TWDB data (a)

Figure 29. Crossplot of As vs. Nitrate (southwestern Gulf Coast)

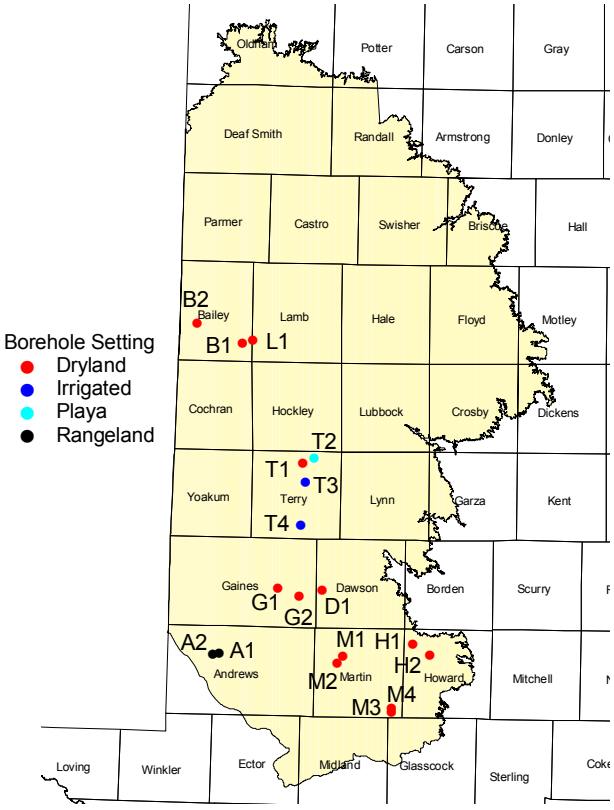

(a)

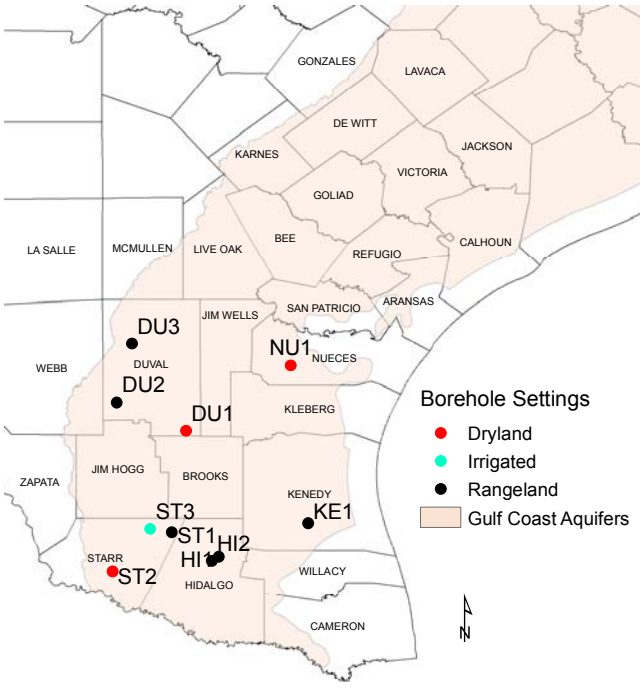

(b)

Figure 30. Drilling sites locations: High Plains (a) and southwestern Gulf Coast (b)

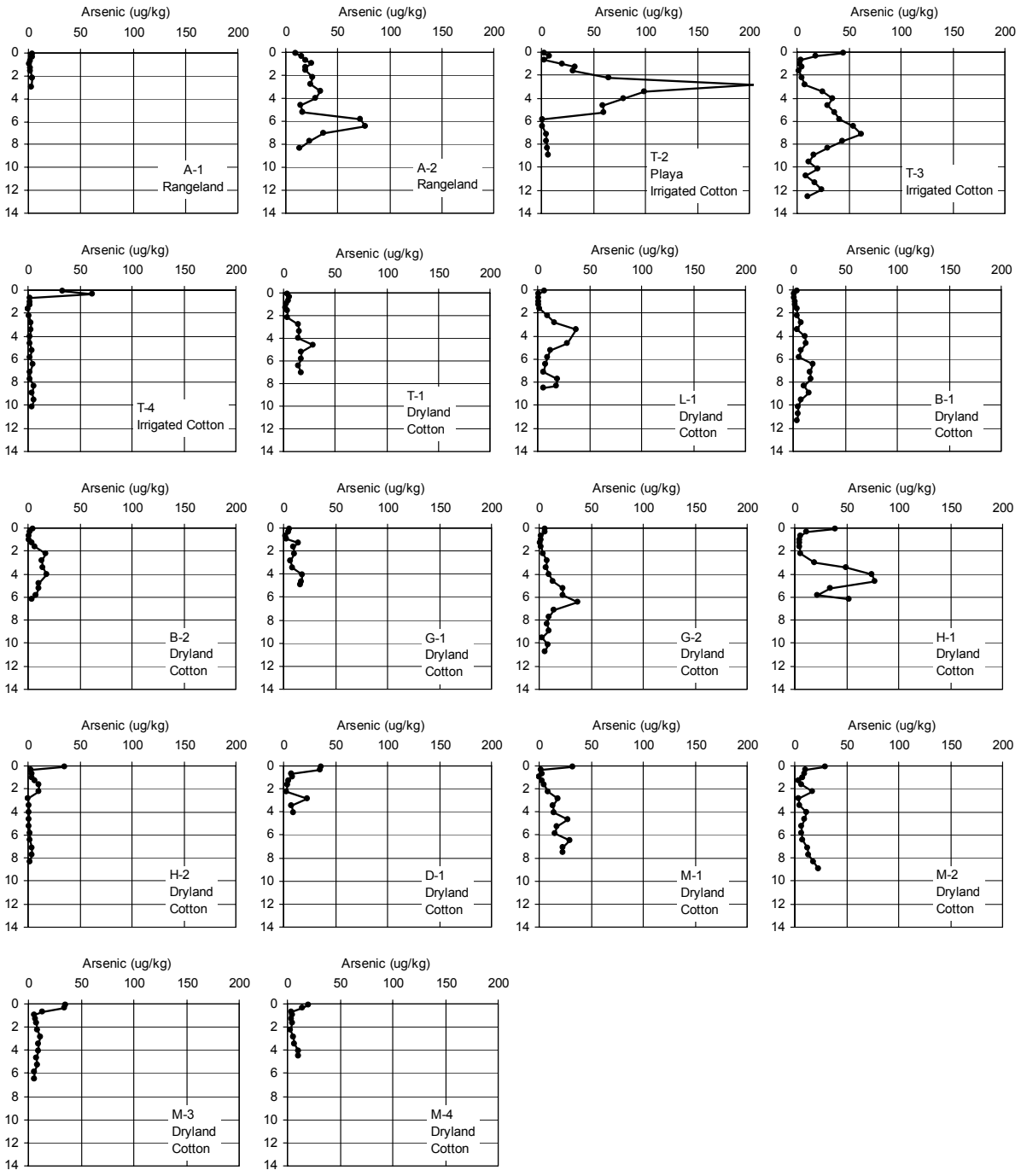

Figure 31. Borehole sample arsenic concentrations in soil in the southern High Plains

.

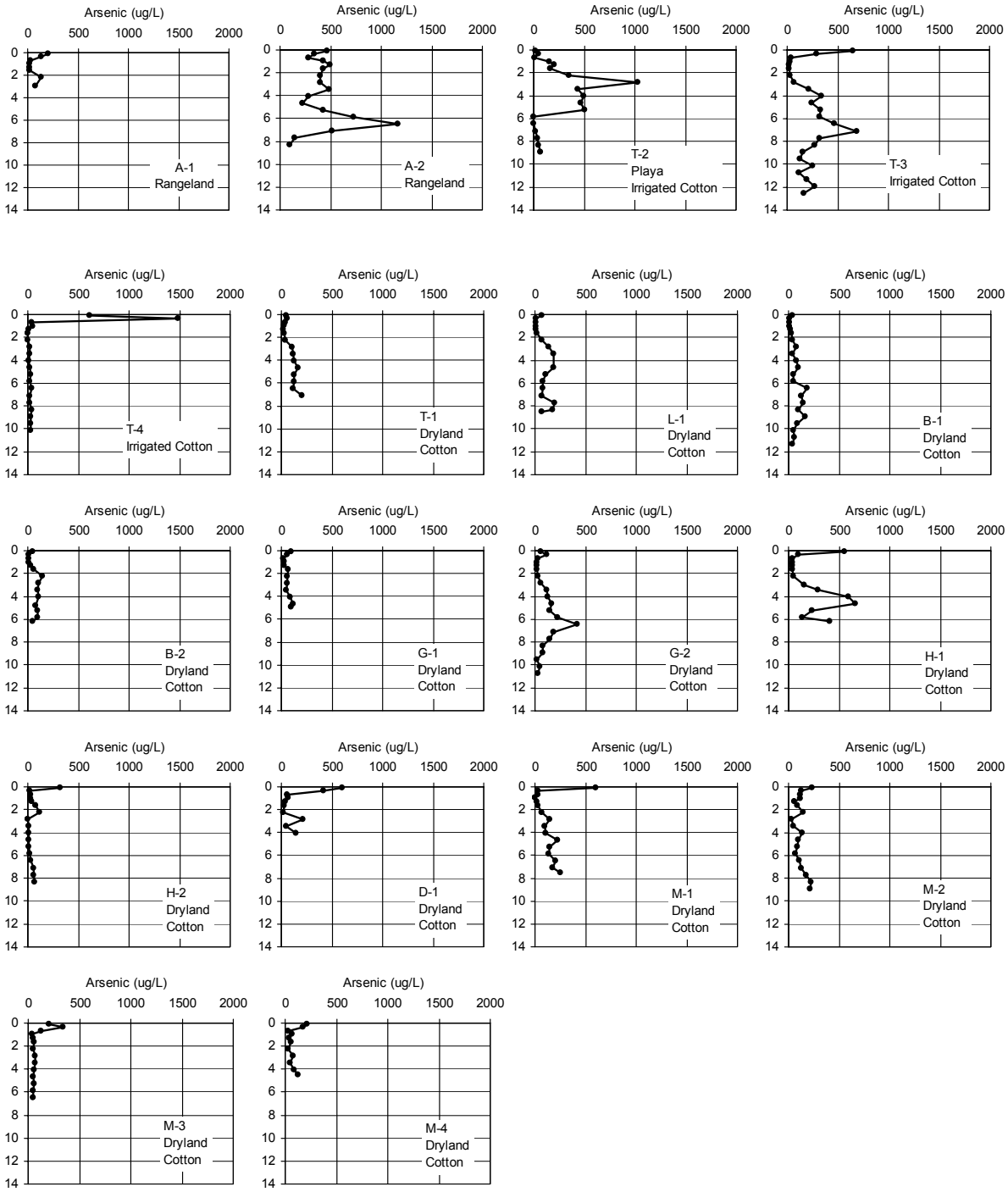

Figure 32. Borehole sample arsenic concentrations in soil water in the southern High Plains

.

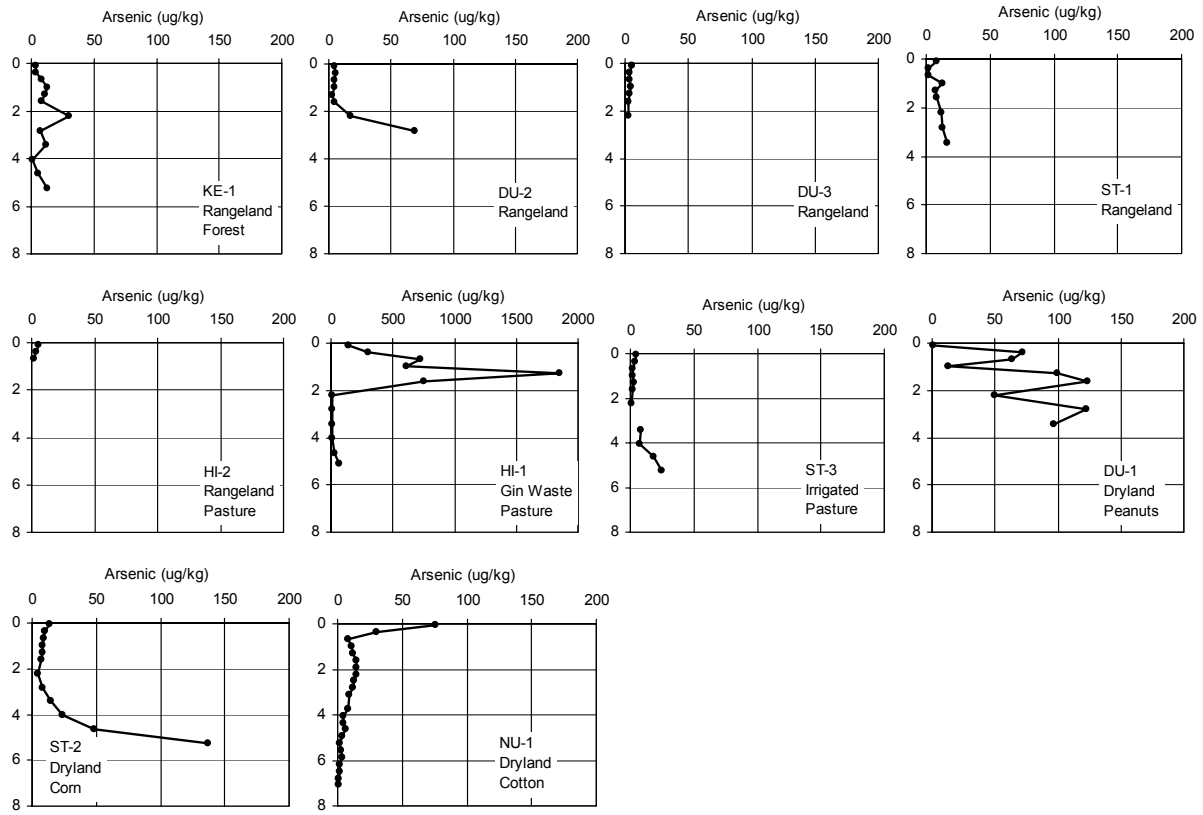

Figure 33. Borehole sample arsenic concentrations in soil in the southwestern Gulf Coast

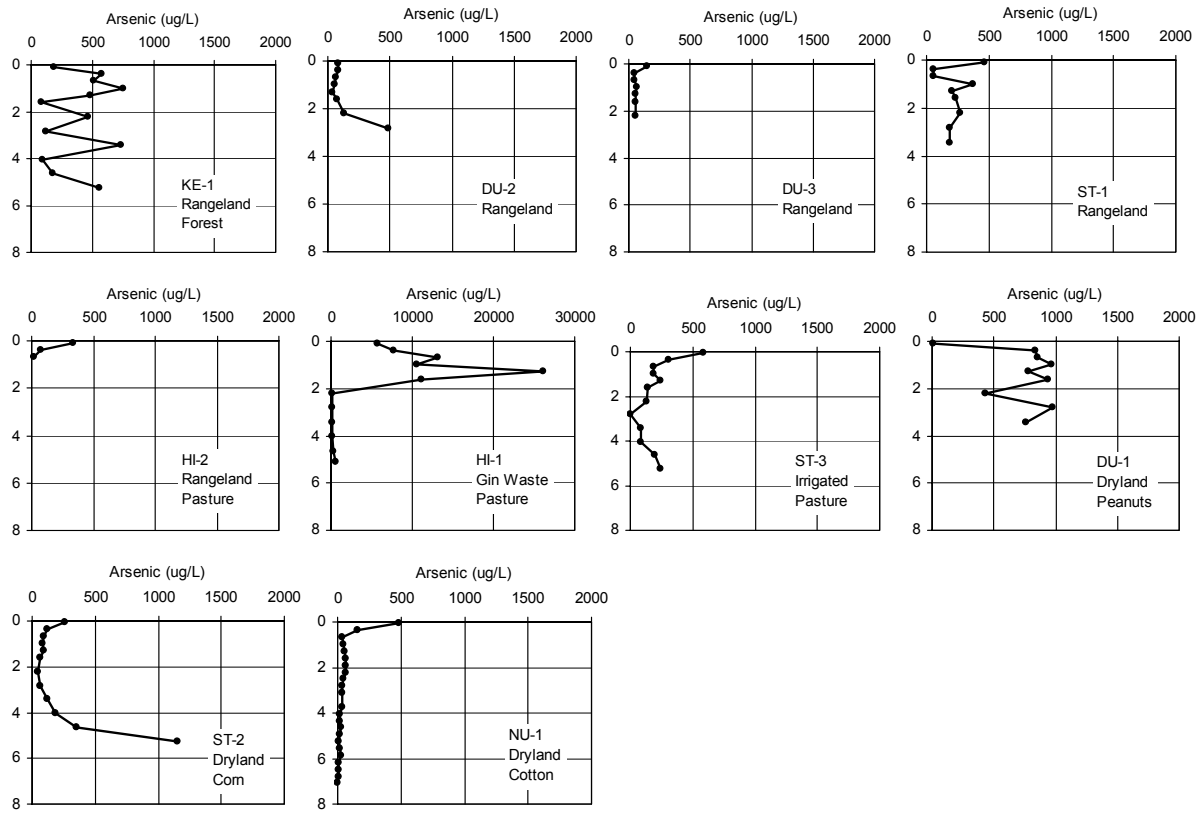

Figure 34. Borehole sample arsenic concentrations in soil water in the southwestern Gulf Coast

Distance = 0.5 m

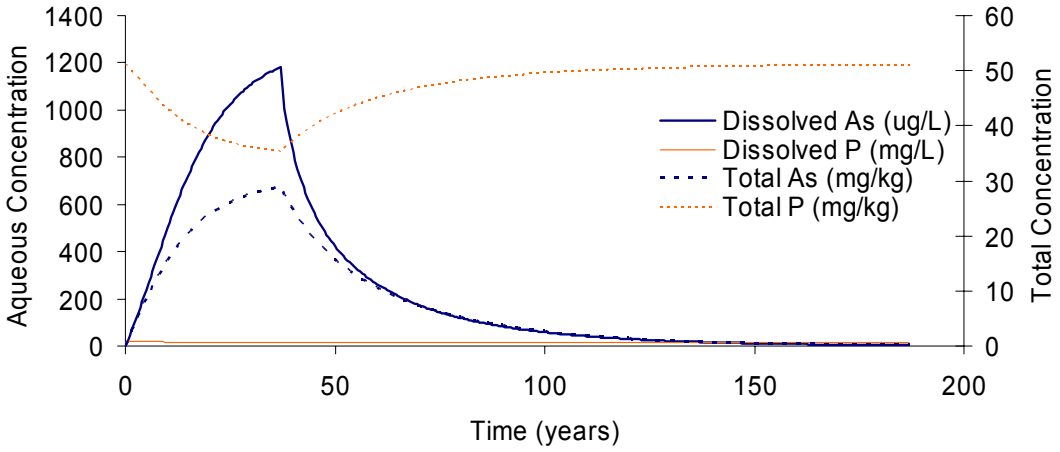

(a)

Distance = 1.5 m

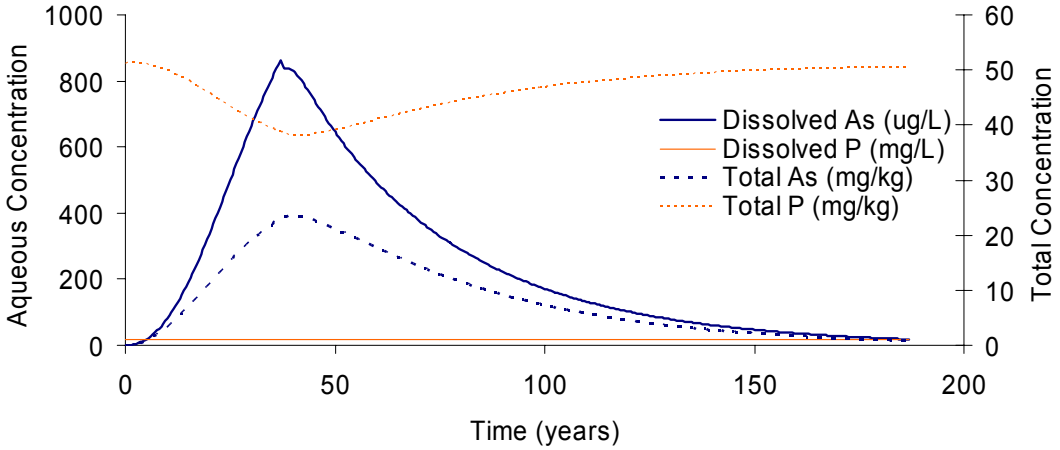

(b)

Distance = 2.5 m

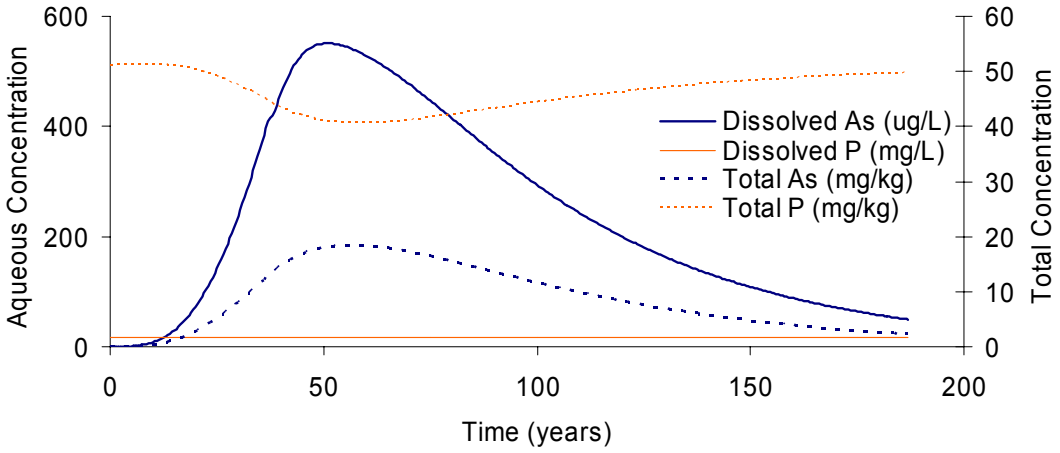

(c)

Figure 35. Soil modeling results with phosphates: As and P breakthrough curves at selected distances

Distance = 0.5 m

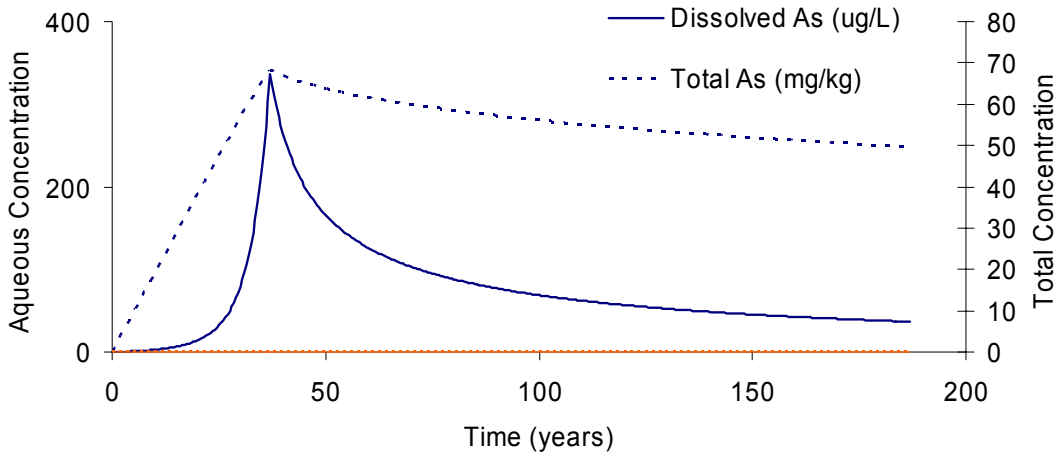

(a)

Distance = 1.5 m

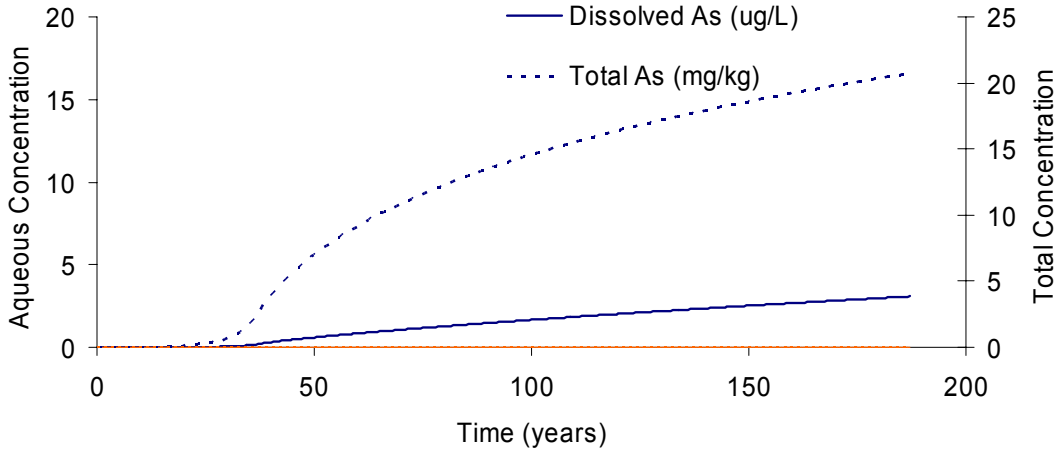

(b)

Distance = 2.5 m

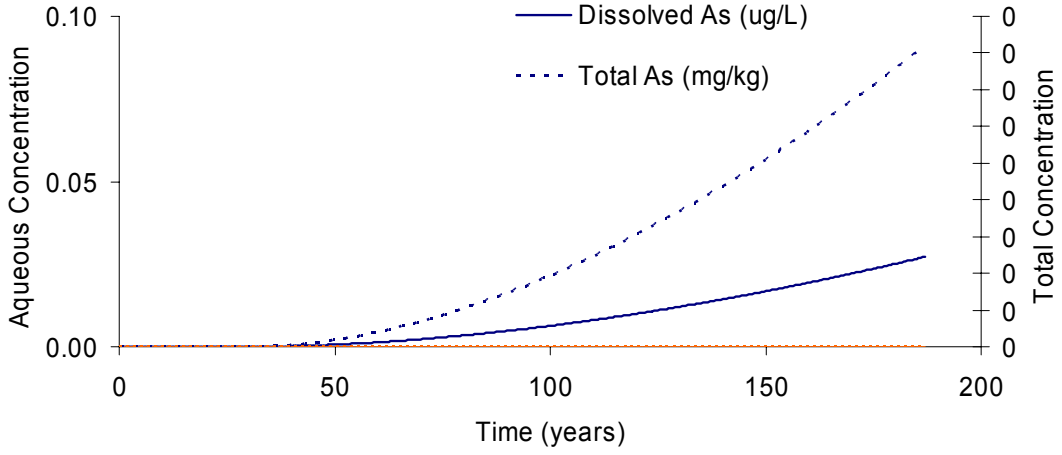

(c)

Figure 36. Soil modeling results without phosphates: As breakthrough curves at selected distances

Time=20 years

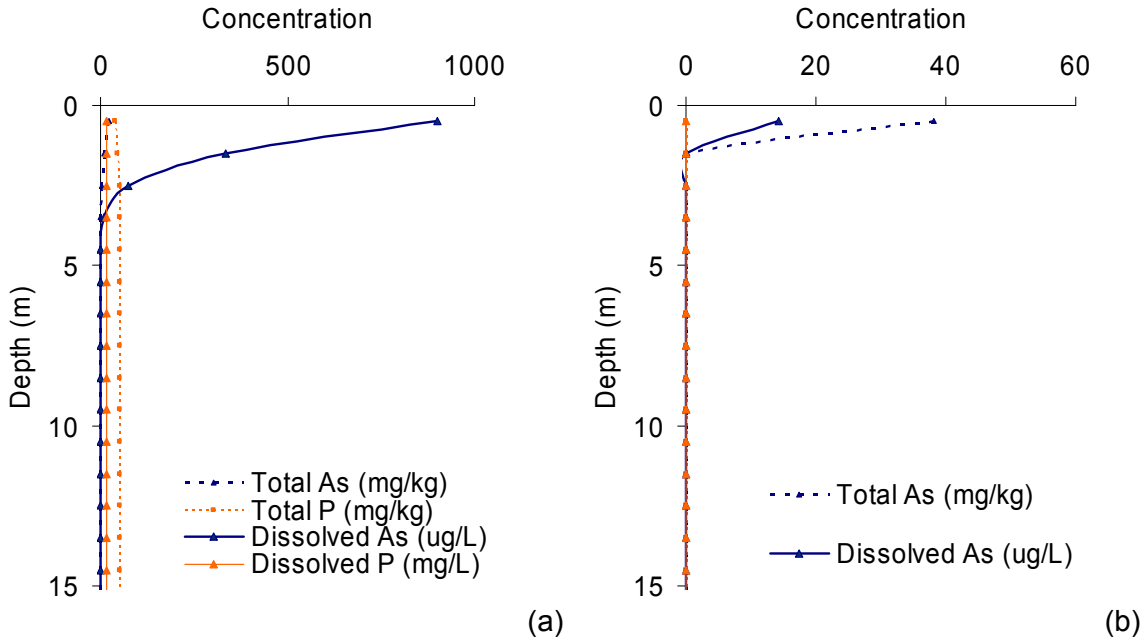

Time = 50 years

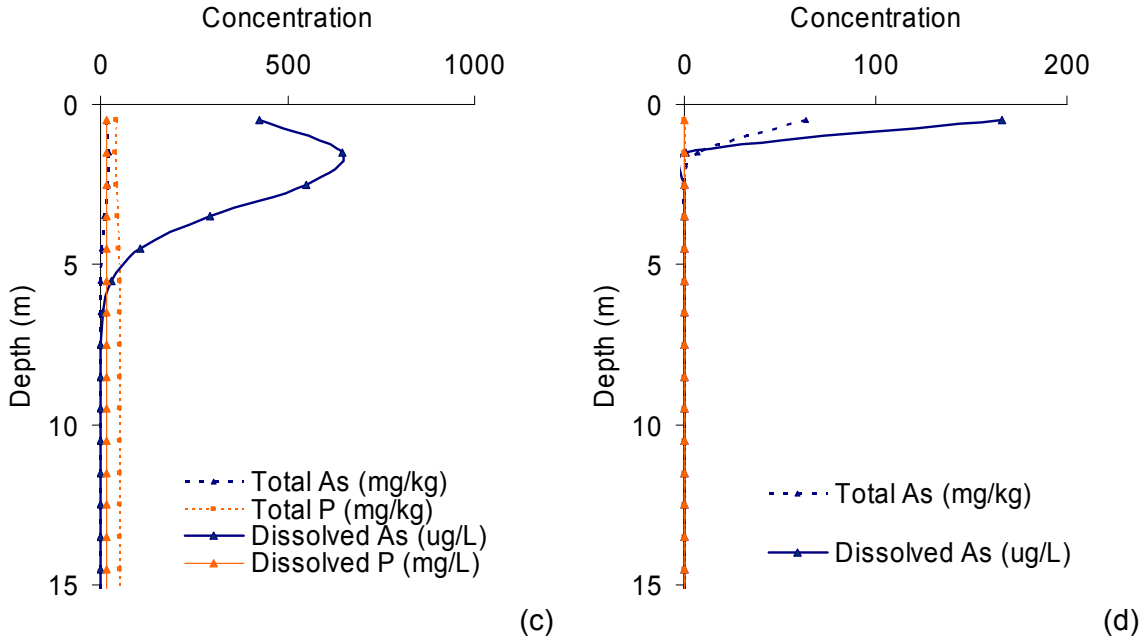

Figure 37. Soil modeling results with and without phosphates: As and P vertical profiles at selected times

Time = 100 years

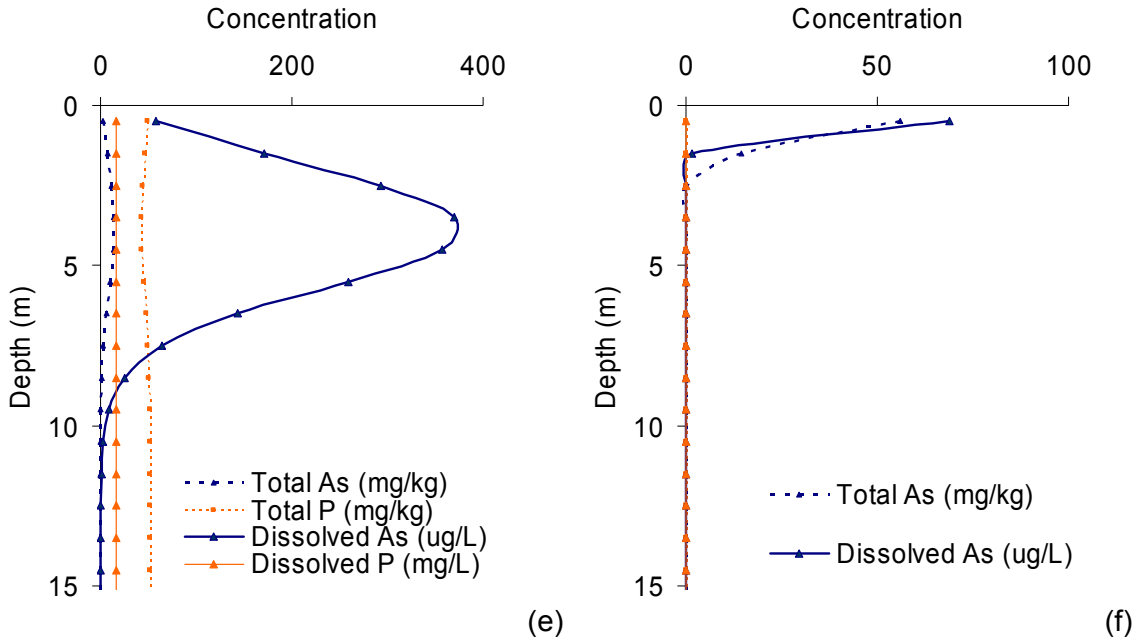

Time = 180 years

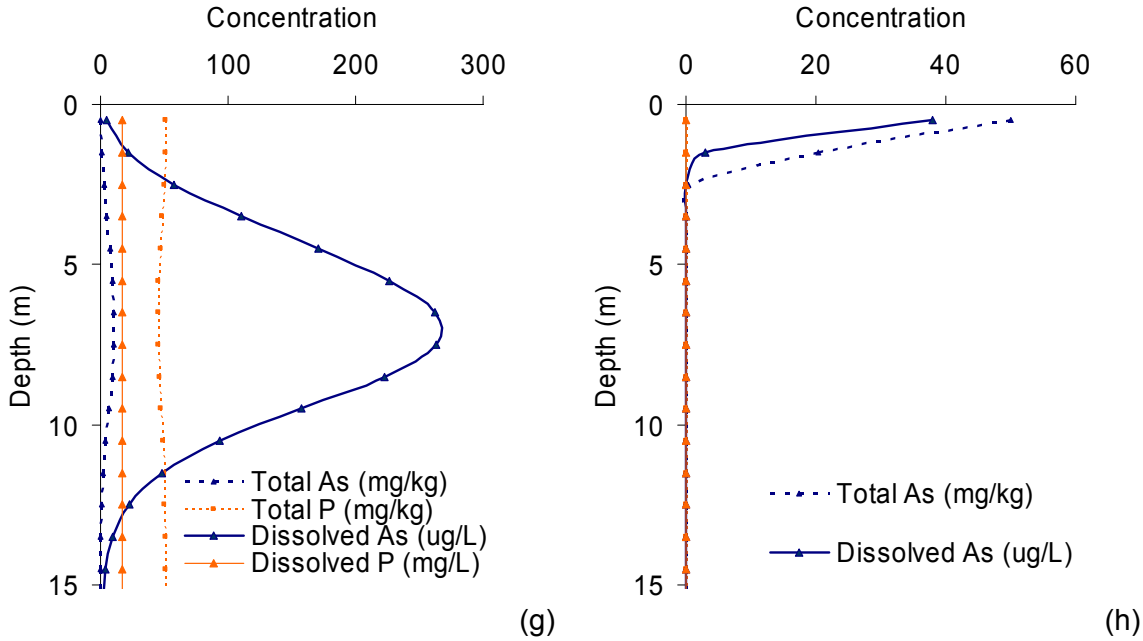

Figure 37. Soil modeling results with and without phosphates: As and P vertical profiles at selected times (continued)

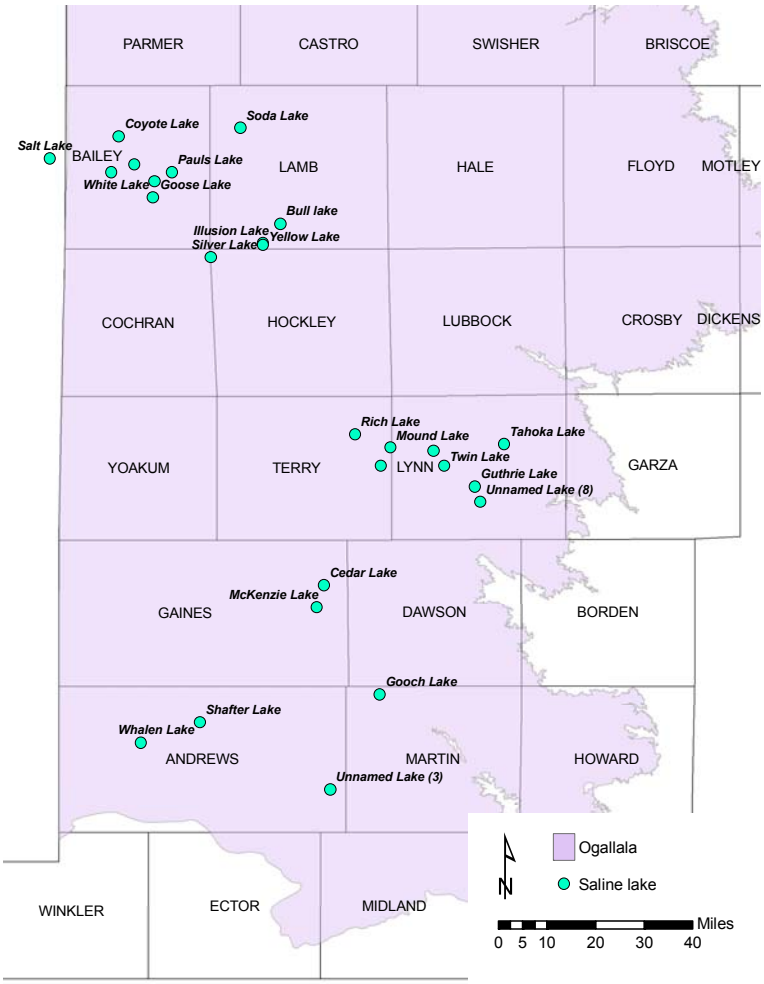

NOTE: Numerals for lakes with unknown lakes are from Wood and Jones (1990)
SOURCE: from Wood and Jones, 1990, and GAT sheets

Figure 38. Location of saline lakes in the Texas High Plains

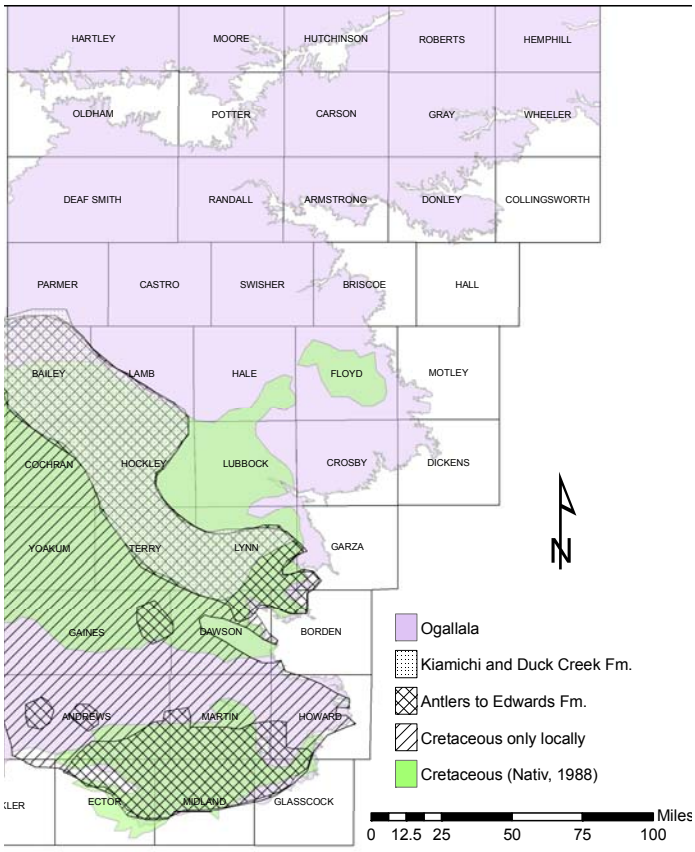

NOTE: Boundaries close to that of Nativ (1988) were adopted by the TWDB as High Plains Edwards-Trinity minor aquifer

SOURCE: (a) Brand et al. (1953) and (b) Nativ (1988)

Figure 39. Location of Cretaceous subcrops in the southern High Plains

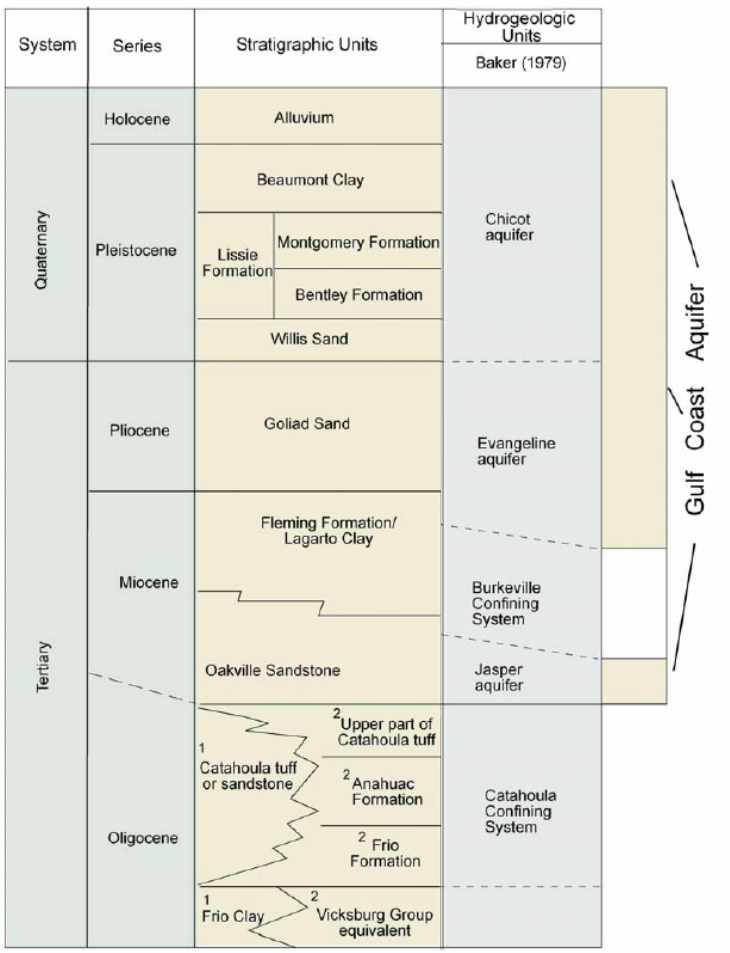

SOURCE: Chowdhury and Mace, 2003

Figure 40. Stratigraphy and hydrostratigrphy of the Gulf Coast aquifers

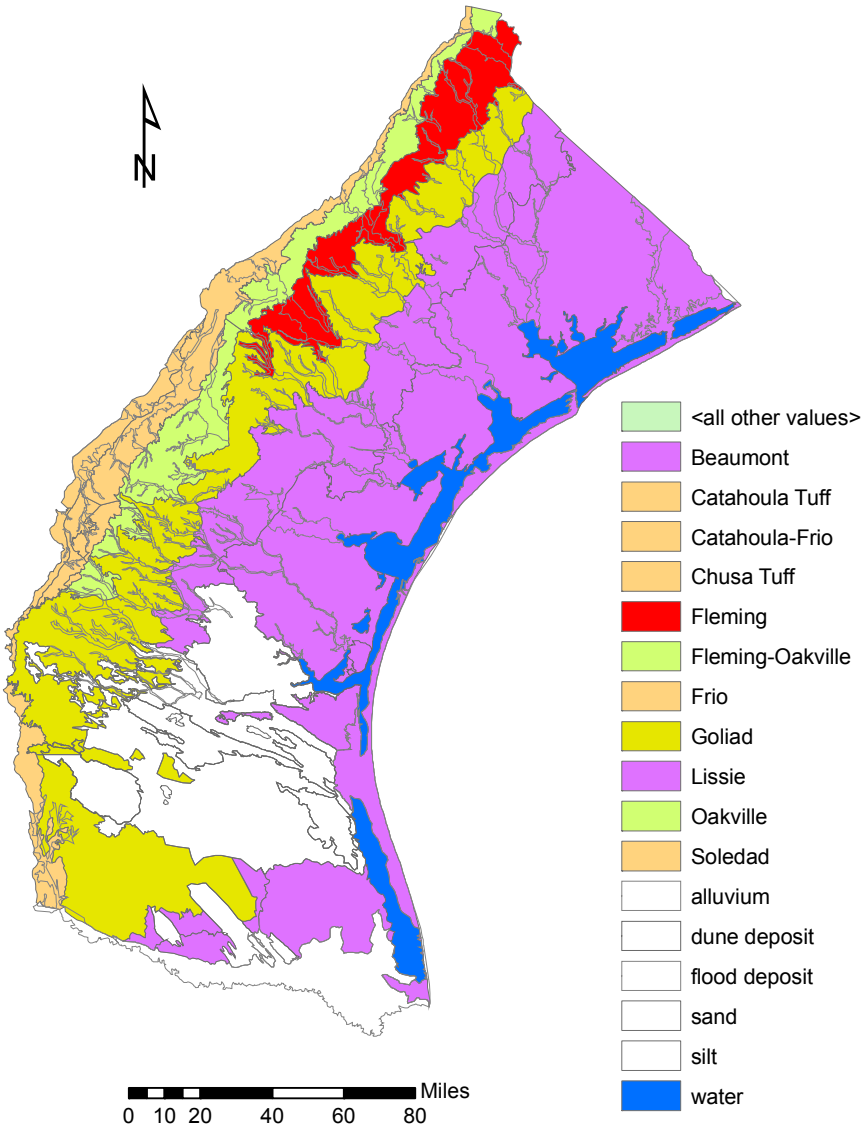

Figure 41. Simplified geologic map of the southwestern Gulf Coast region

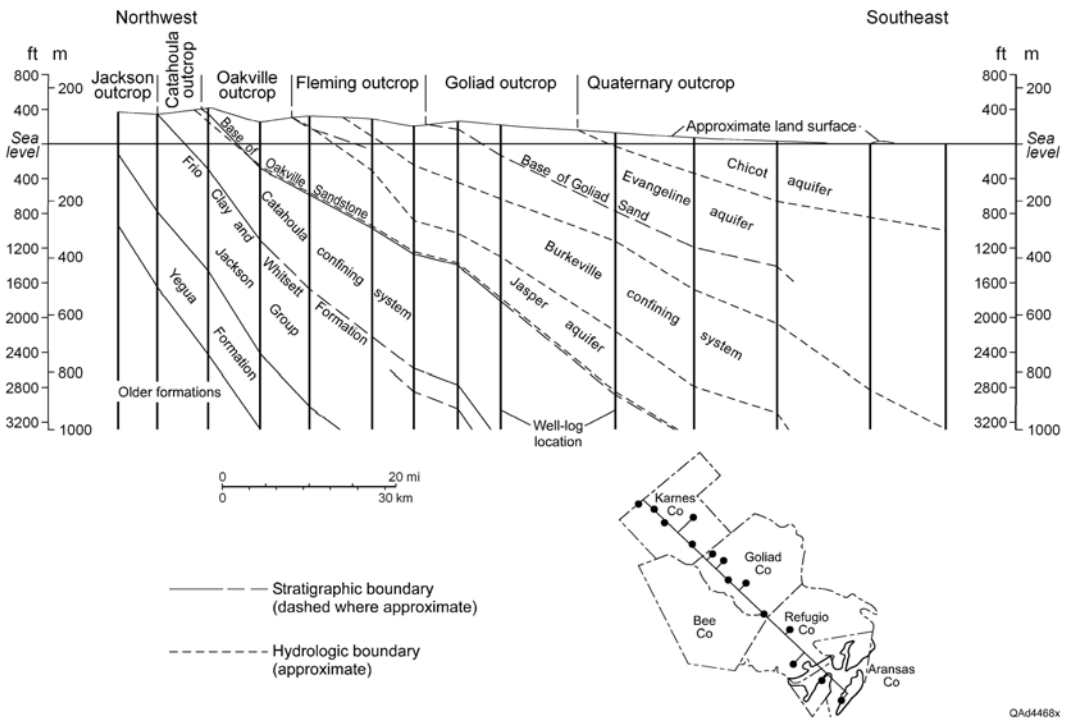

Figure 42. Cross-section along dip in the Gulf Coast aquifer through Karnes, Goliad, and Refugio Counties

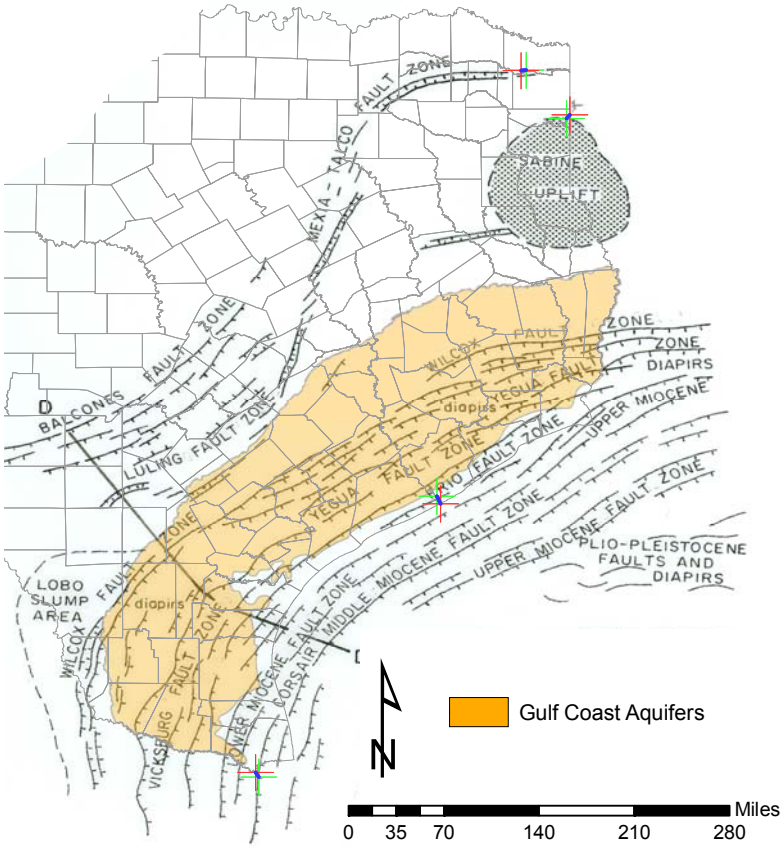

Figure 43. Tectonic map of the Gulf Coast area

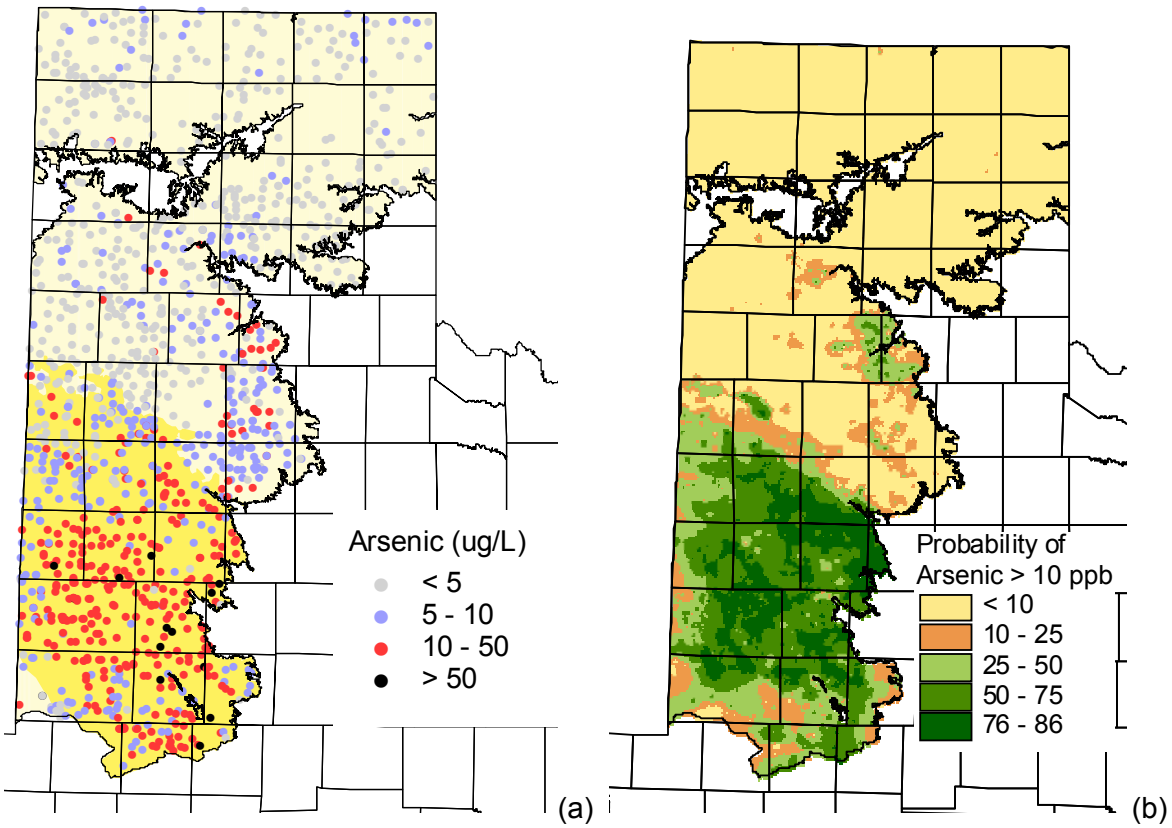

Figure 44. Arsenic distribution in the High Plains aquifer (TWDB database): (a) from arsenic data points; (b) inferred from fluoride data points.

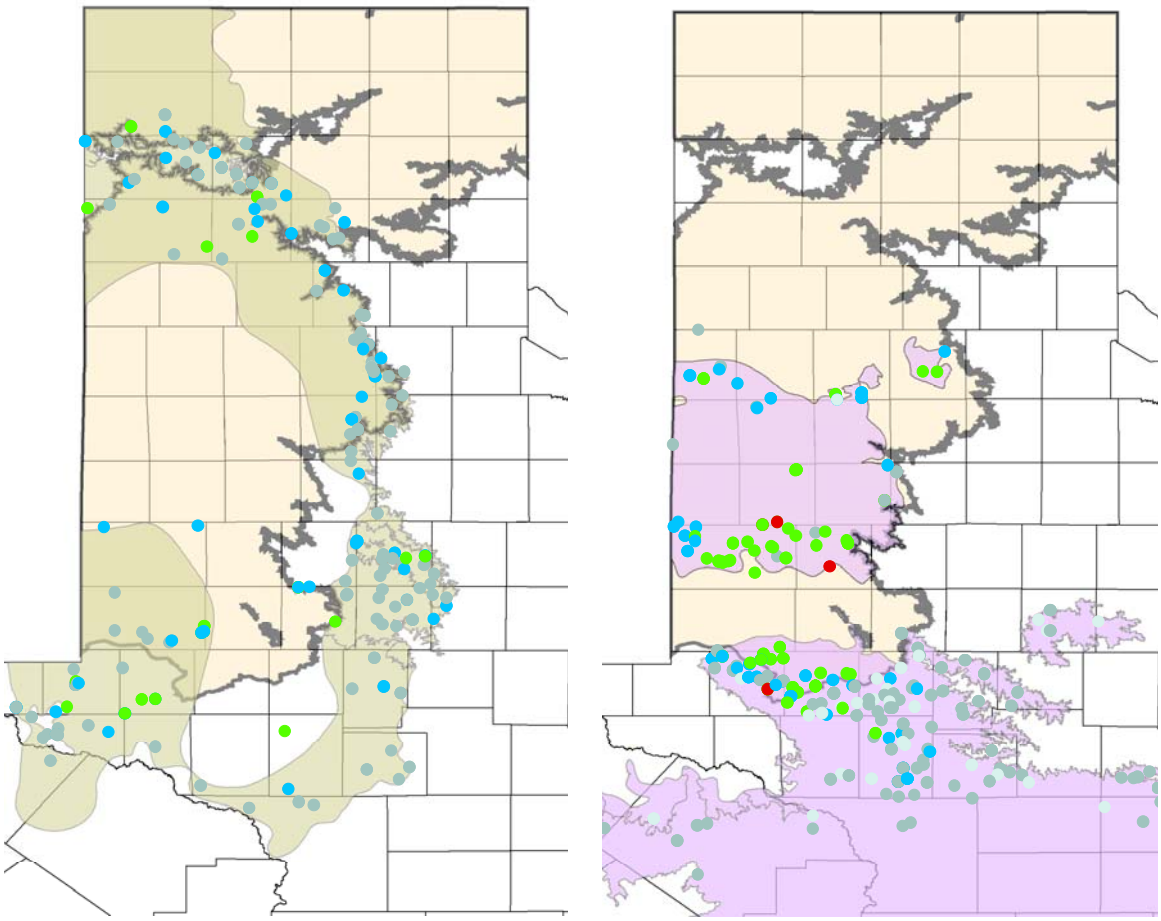

(a) (b)

NOTE: data include those High Plains wells screening in multiple formations
NOTE: only Dockum outcrop and that part of the aquifer with a TDS<5,000 mg/L are shown. Downdip central section is more saline. Dockum Fm. underlies all of the southern High Plains aquifer.
SOURCE: aquifer outlines from TWDB GIS coverage of major and minor aquifers

Figure 45. Arsenic distribution in the Dockum (a), Edwards Trinity (b), and Cenozoic Pecos Alluvium aquifers (c).

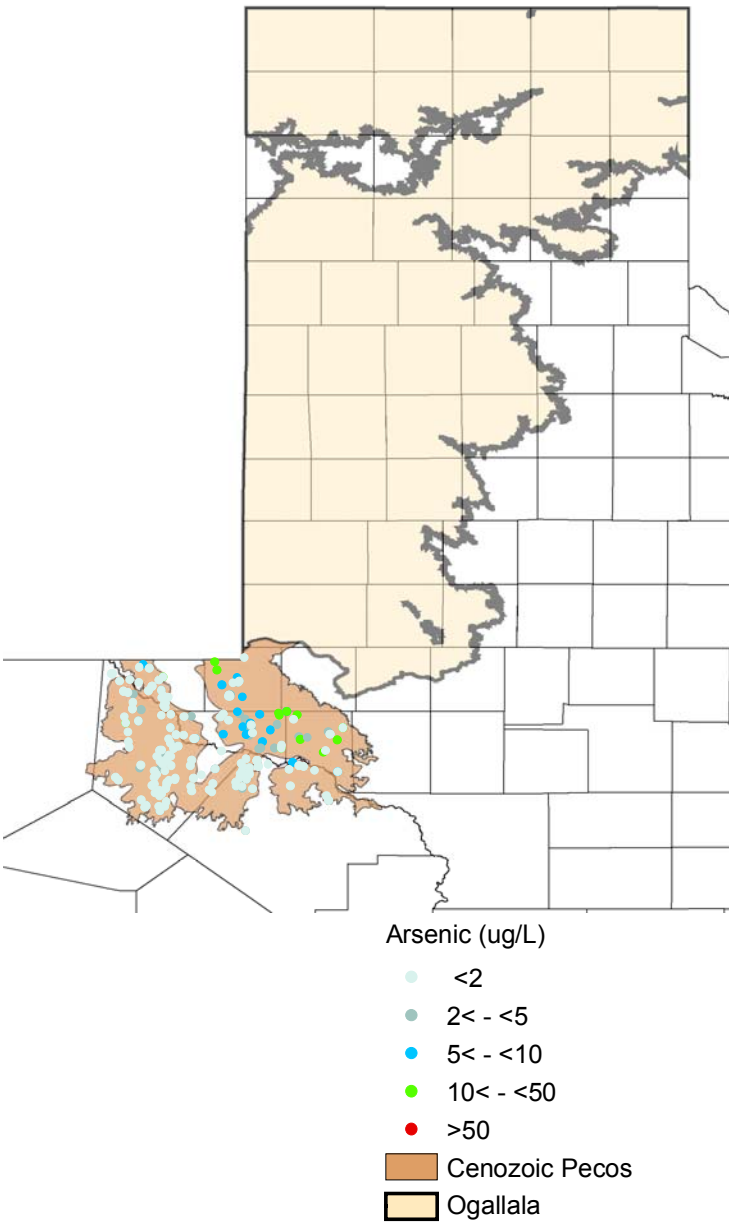

NOTE: data include those High Plains wells screening in multiple formations
SOURCE: aquifer outlines from TWDB GIS coverage of major aquifers

Figure 45. Arsenic distribution in the Dockum (a), Edwards Trinity (b), and Cenozoic Pecos Alluvium aquifers (c). (continued)

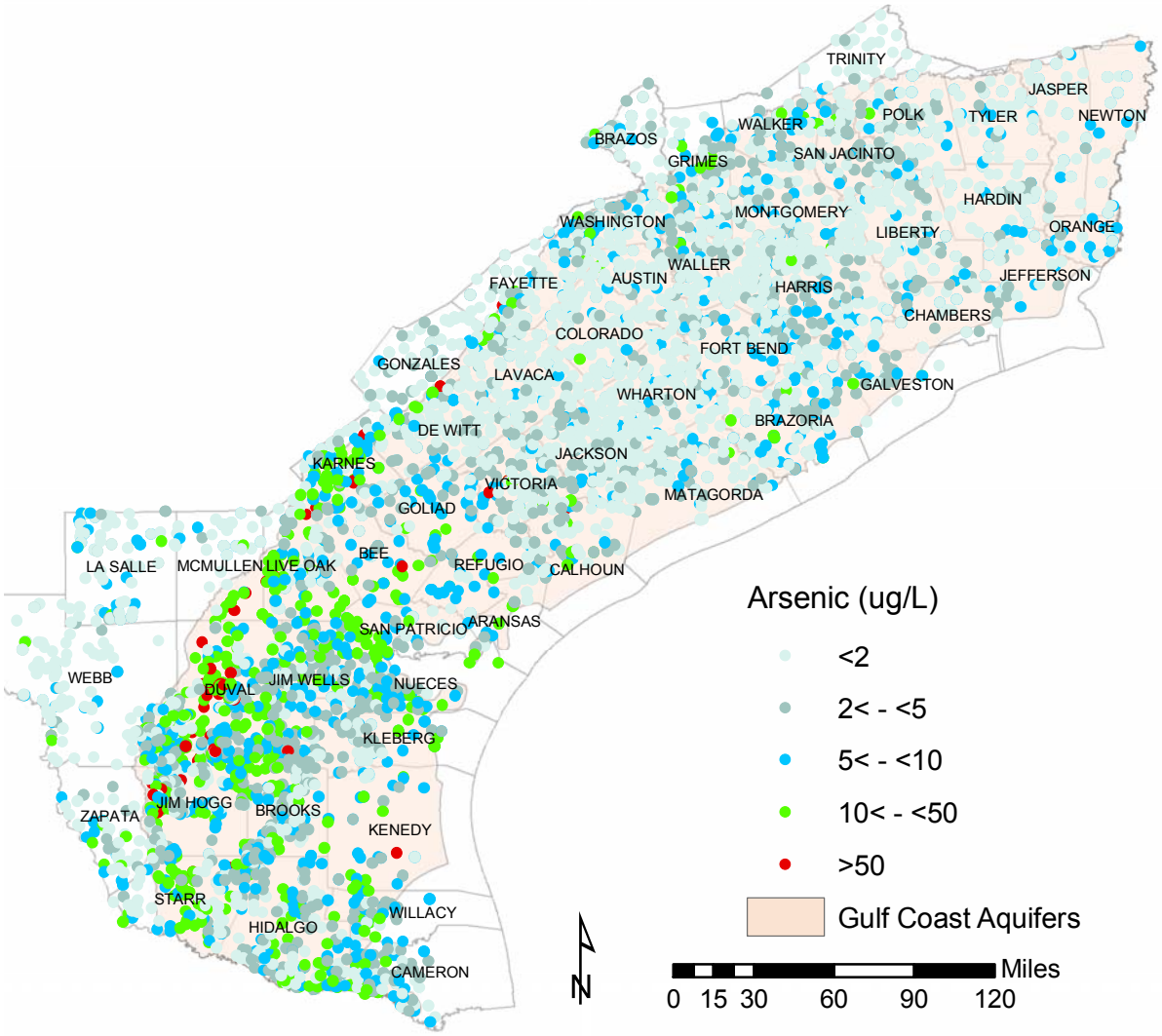

Figure 46. Arsenic distribution in the Gulf Coast aquifers (TWDB and NURE databases)

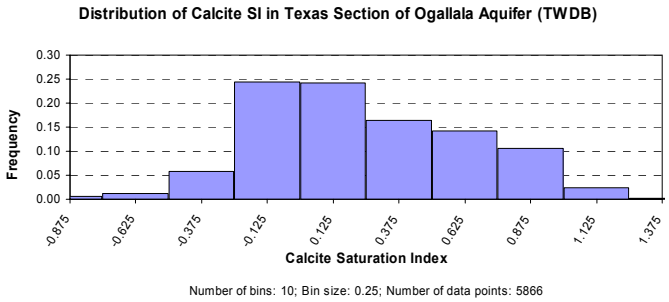

Figure 47. Distribution of calcite saturation index in the southern High Plains aquifer (TWDB data set)

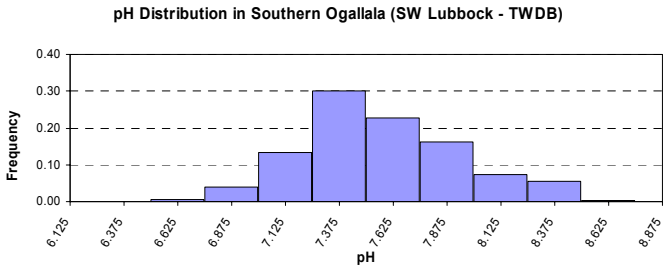

(a)

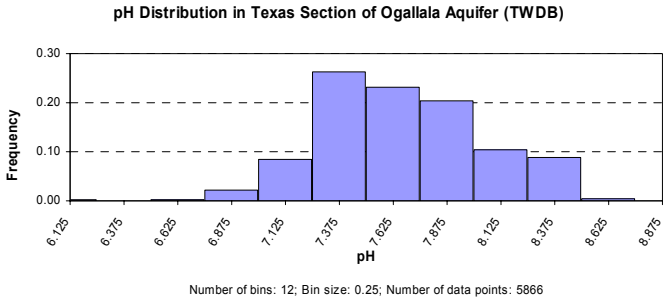

(b)

Figure 48. pH distribution in the High Plains Aquifer: all Texas data points (a); southwestern region of southern High Plains (b). all data points (TWDB database).

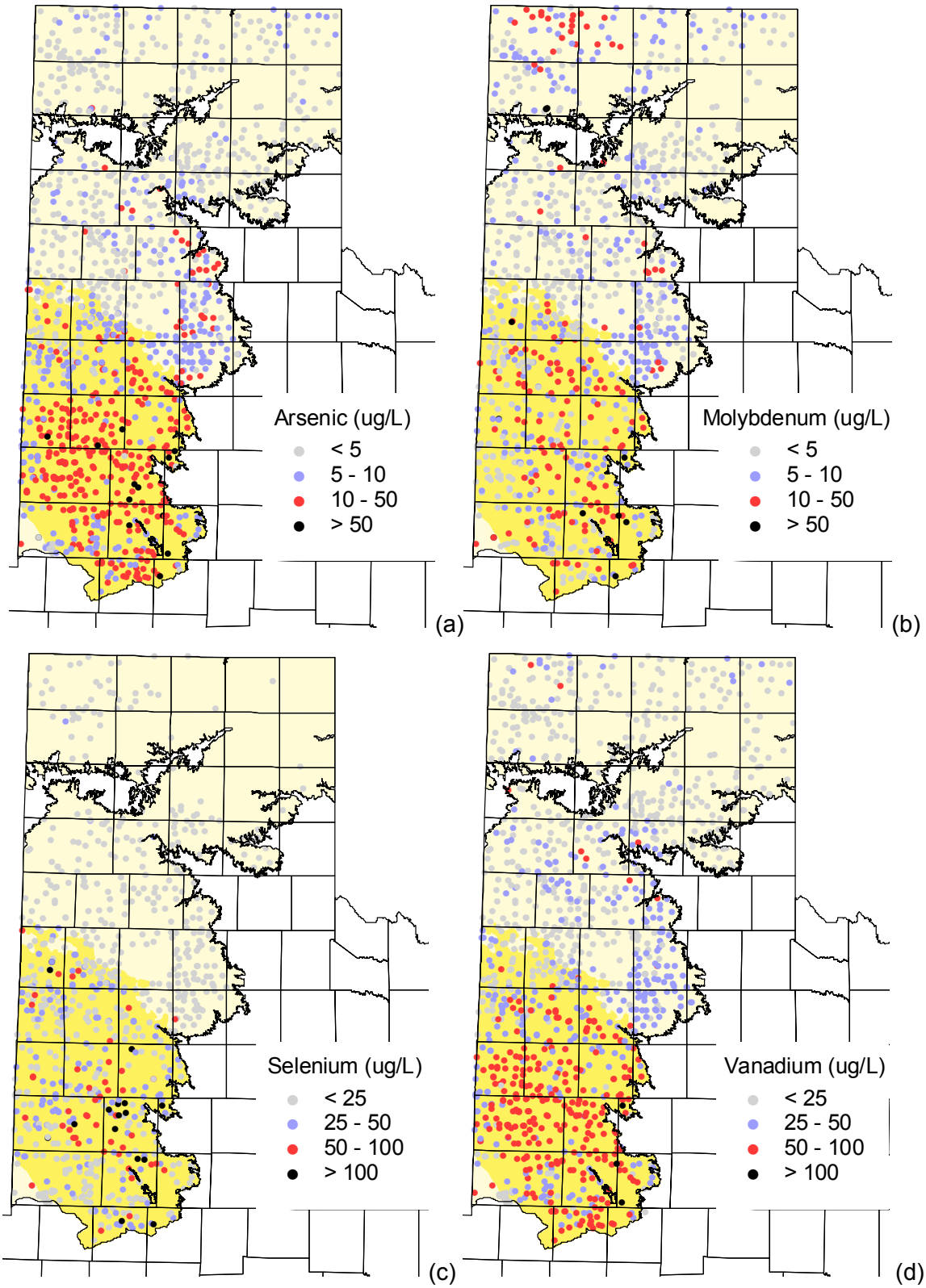

Figure 49. Spatial distribution of As (a), Mo (b), Se (c), V (d), B (e), F (f), U (g), silica (h), Fe (i), chloride (j), sulfate (k), TDS (l), and pH (m) in High Plains aquifers. All plots use only TWDB data except U where NURE data are used.

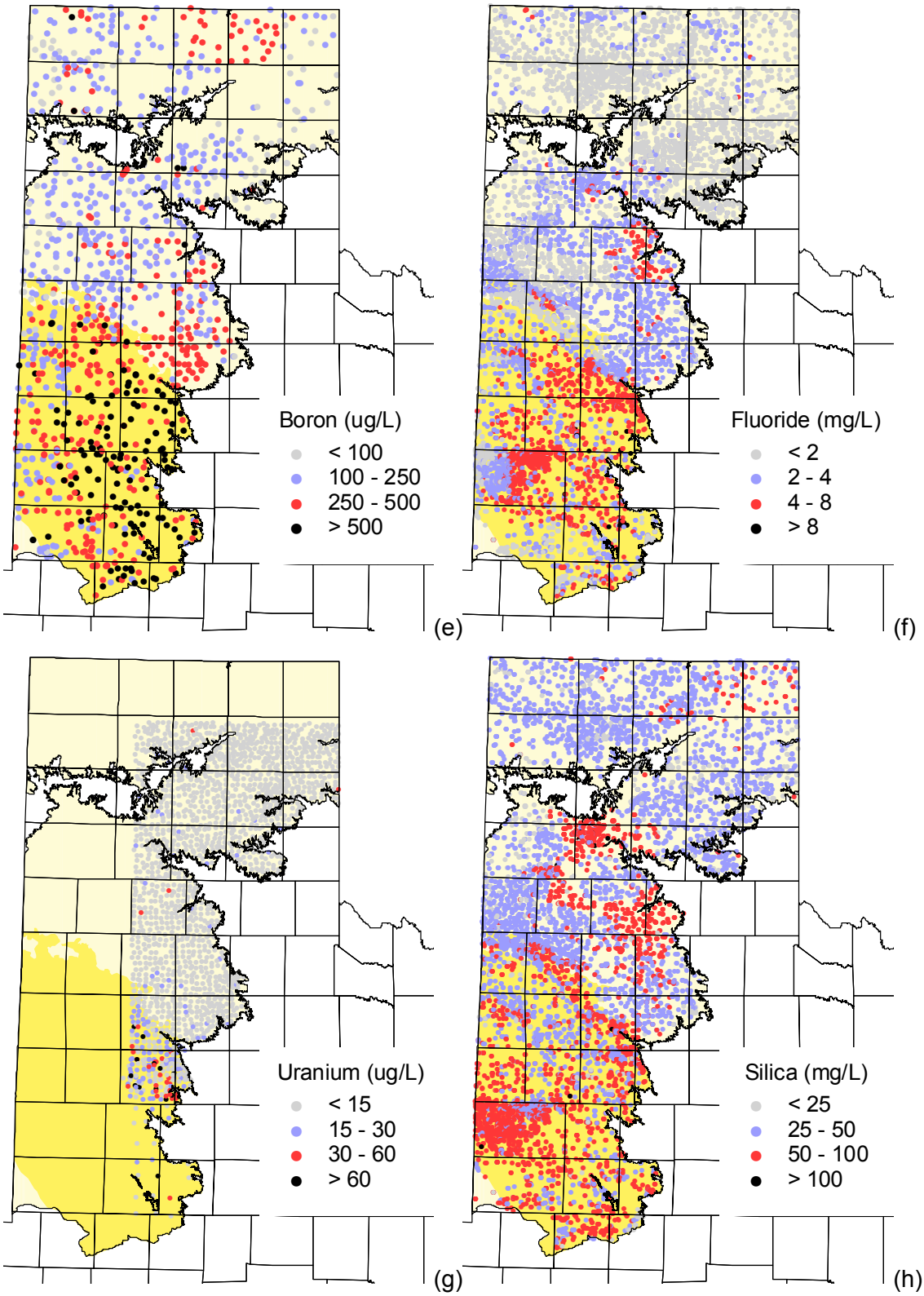

Figure 49. Spatial distribution of As (a), Mo (b), Se (c), V (d), B (e), F (f), U (g), silica (h), Fe (i), chloride (j), sulfate (k), TDS (l), and pH (m) in High Plains aquifers. All plots use only TWDB data except U where NURE data are used. (continued)

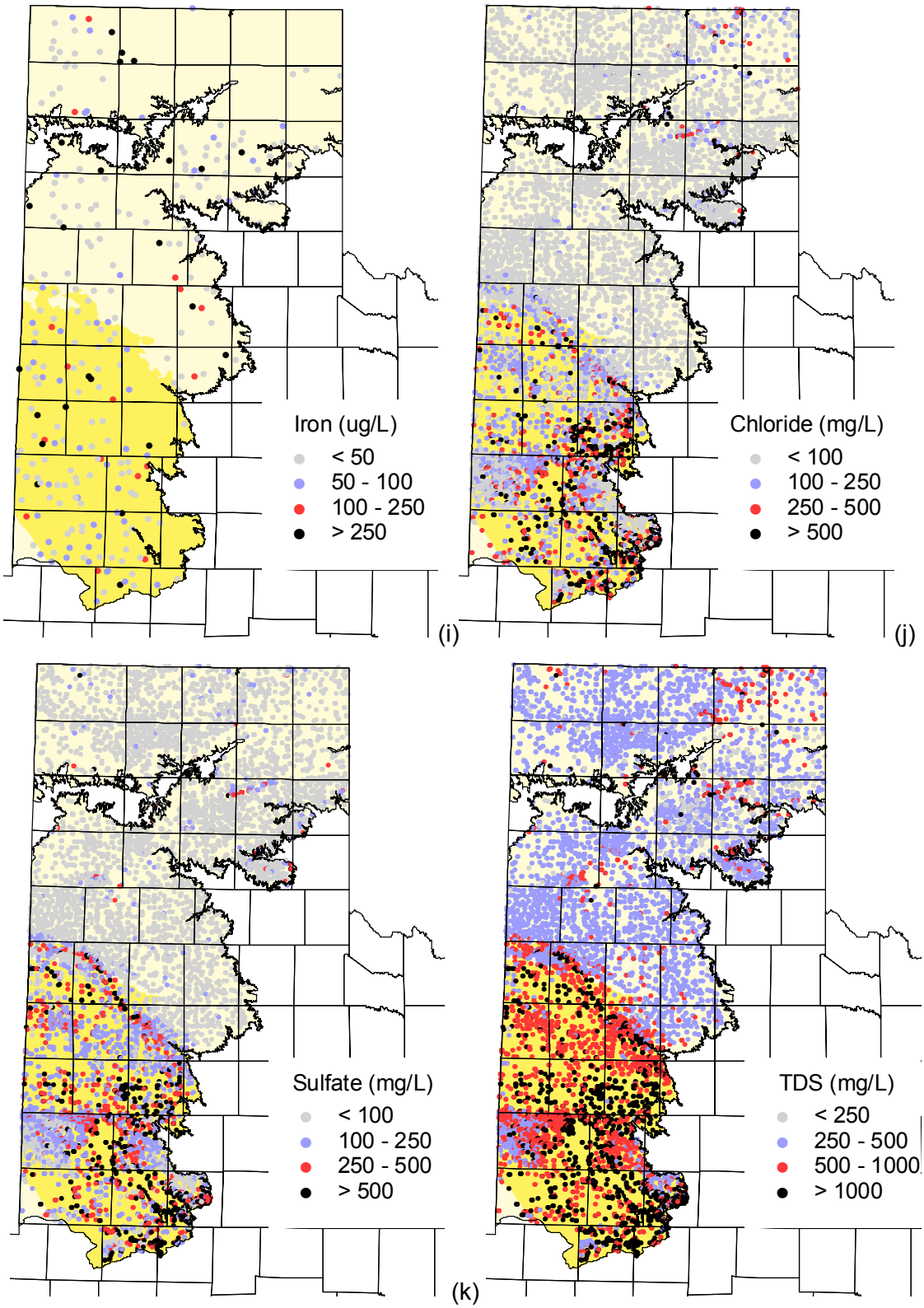

Figure 49. Spatial distribution of As (a), Mo (b), Se (c), V (d), B (e), F (f), U (g), silica (h), Fe (i), chloride (j), sulfate (k), TDS (l), and pH (m) in High Plains aquifers. All plots use only TWDB data except U where NURE data are used. (continued)

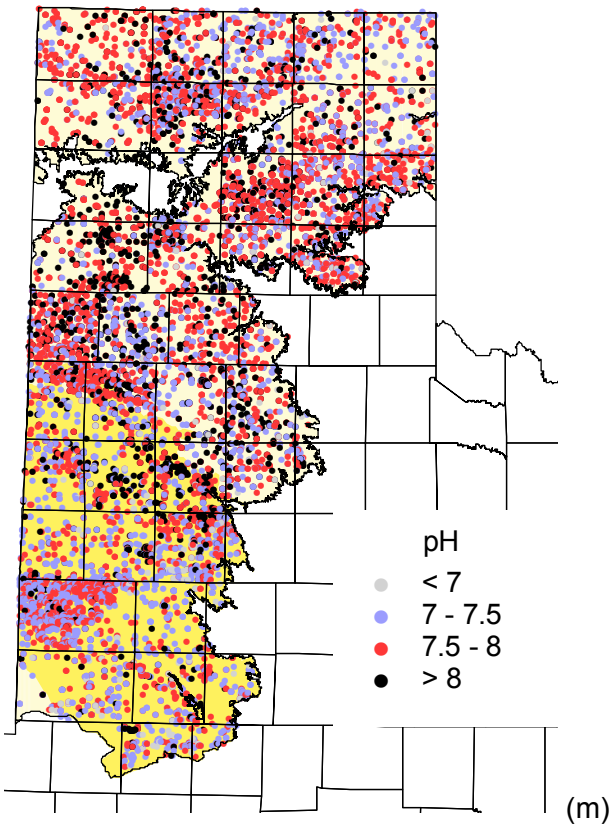

(m)

Figure 49. Spatial distribution of As (a), Mo (b), Se (c), V (d), B (e), F (f), U (g), silica (h), Fe (i), chloride (j), sulfate (k), TDS (l), and pH (m) in High Plains aquifers. All plots use only TWDB data except U where NURE data are used. (continued)

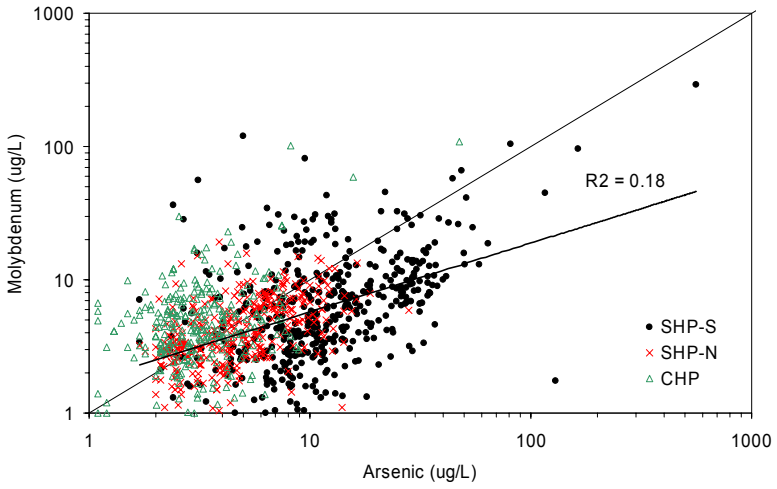

(a)

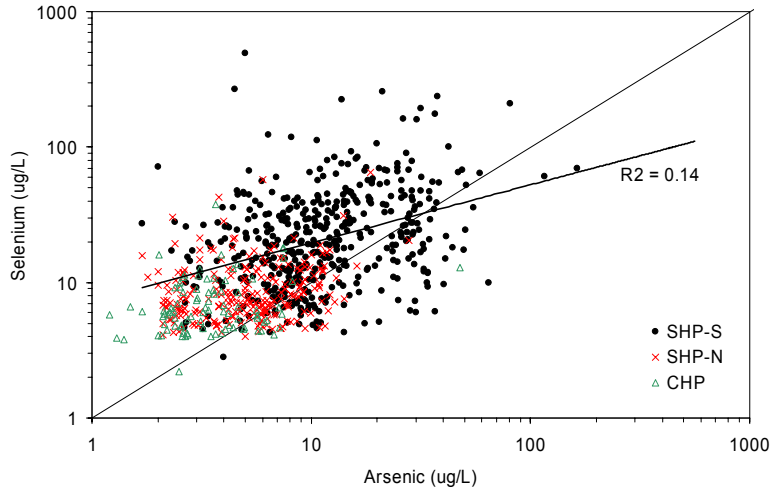

(b)

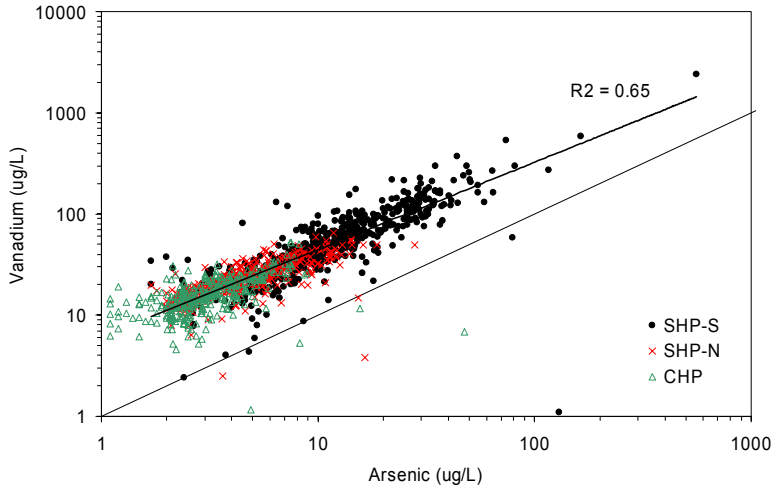

(c)

Figure 50. Cross-plots of (a) As vs. Mo, (b) vs. Se, (c) vs. V, (d) vs. B, (e) vs. F, (f) vs. silica, (g) vs. Fe, (h) vs. bicarbonate, (i) vs. sulfate, (j) vs. chloride, (l) vs. TDS and (m) vs. pH (NURE data set), High Plains aquifers.

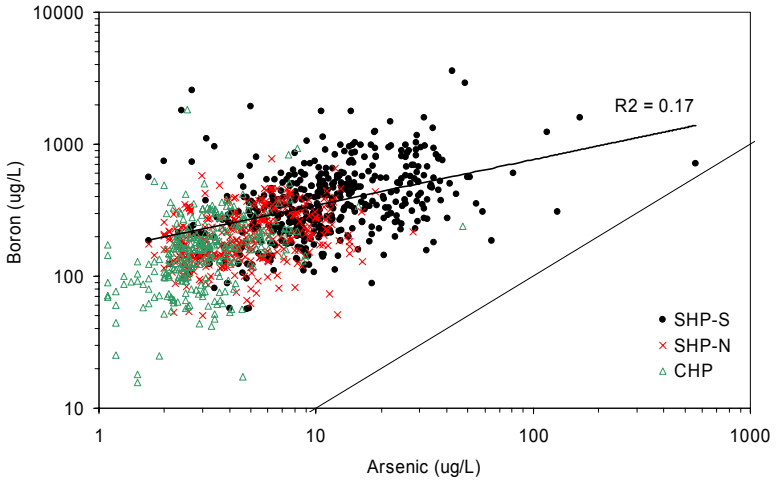

(d)

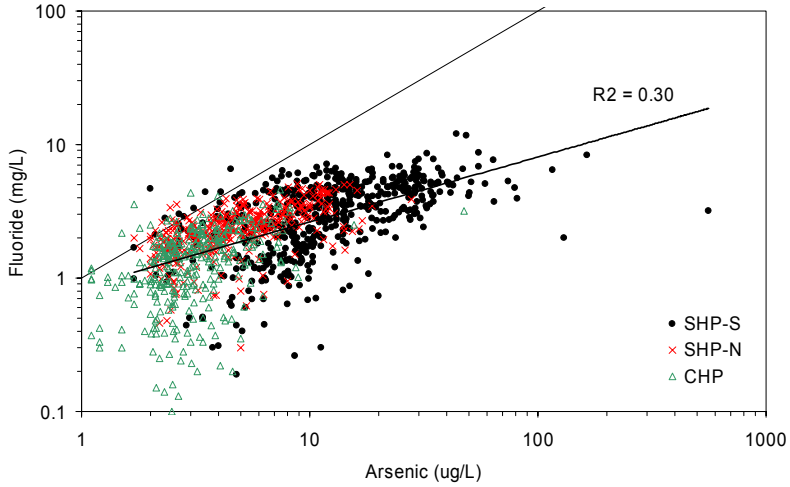

(e)

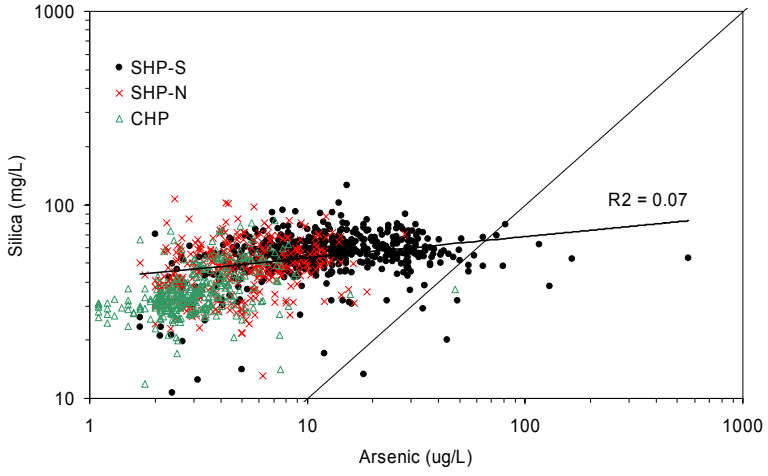

(f)

Figure 50. Cross-plots of (a) As vs. Mo, (b) vs. Se, (c) vs. V, (d) vs. B, (e) vs. F, (f) vs. silica, (g) vs. Fe, (h) vs. bicarbonate, (i) vs. sulfate, (j) vs. chloride, (l) vs. TDS and (m) vs. pH (NURE data set), High Plains aquifers. (continued)

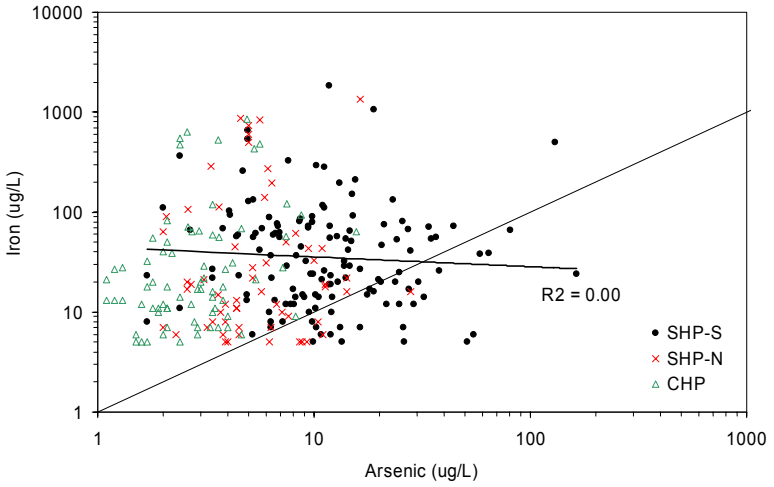

(g)

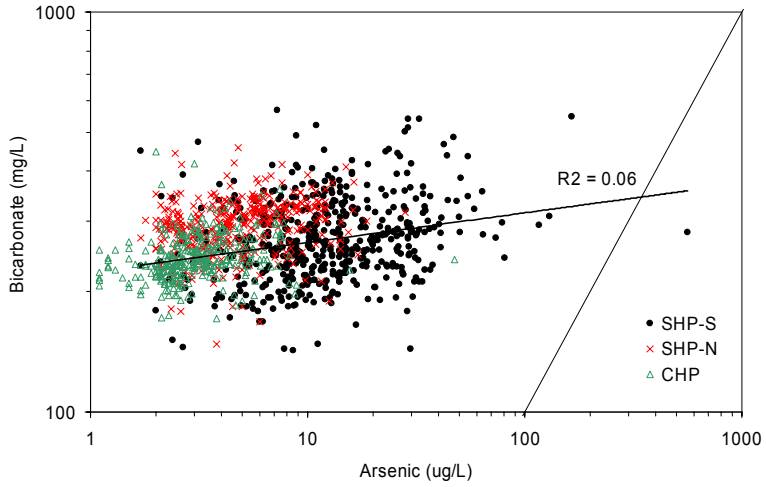

(h)

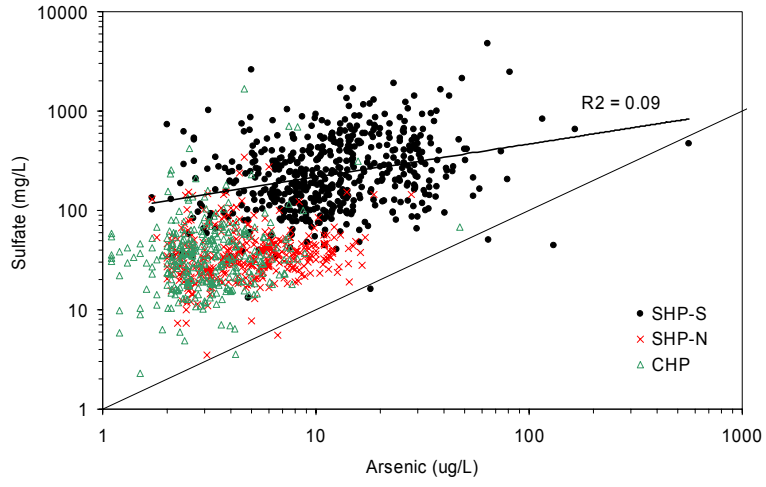

(i)

Figure 50. Cross-plots of (a) As vs. Mo, (b) vs. Se, (c) vs. V, (d) vs. B, (e) vs. F, (f) vs. silica, (g) vs. Fe, (h) vs. bicarbonate, (i) vs. sulfate, (j) vs. chloride, (l) vs. TDS and (m) vs. pH (NURE data set), High Plains aquifers. (continued)

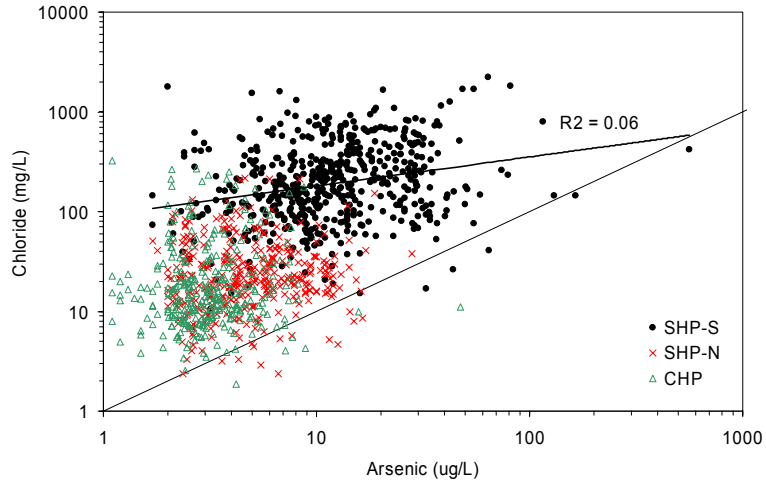

(j)

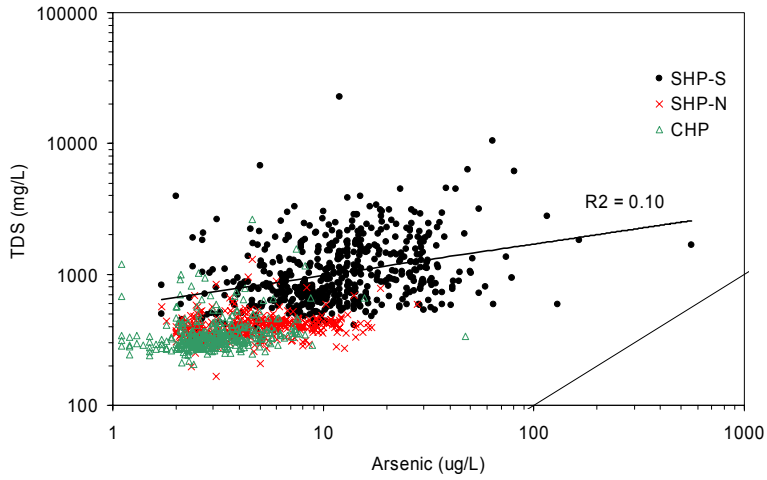

(l)

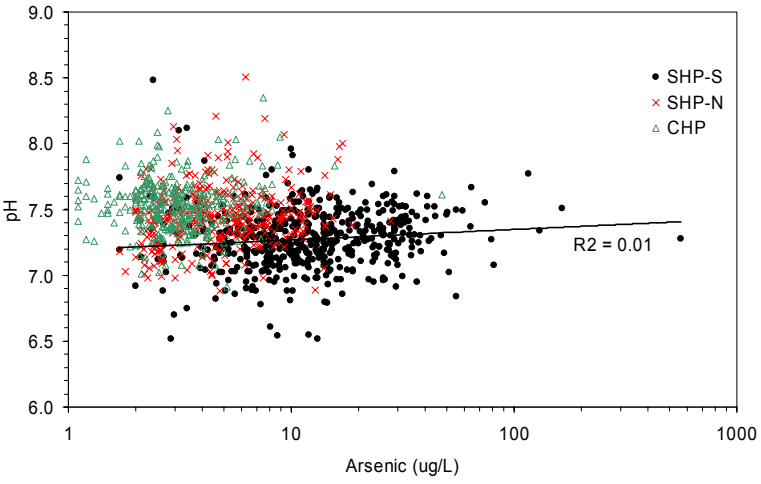

(m)

Figure 50. Cross-plots of (a) As vs. Mo, (b) vs. Se, (c) vs. V, (d) vs. B, (e) vs. F, (f) vs. silica, (g) vs. Fe, (h) vs. bicarbonate, (i) vs. sulfate, (j) vs. chloride, (l) vs. TDS and (m) vs. pH (NURE data set), High Plains aquifers. (continued)

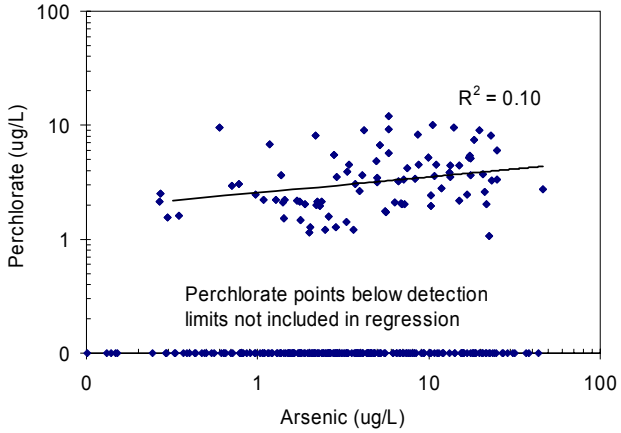

NOTE: Data set from Public Water Supply well sampling (Jackson et al., 2004)
Figure 51. Cross-plot of As vs. perchlorate, southern High Plain aquifers.

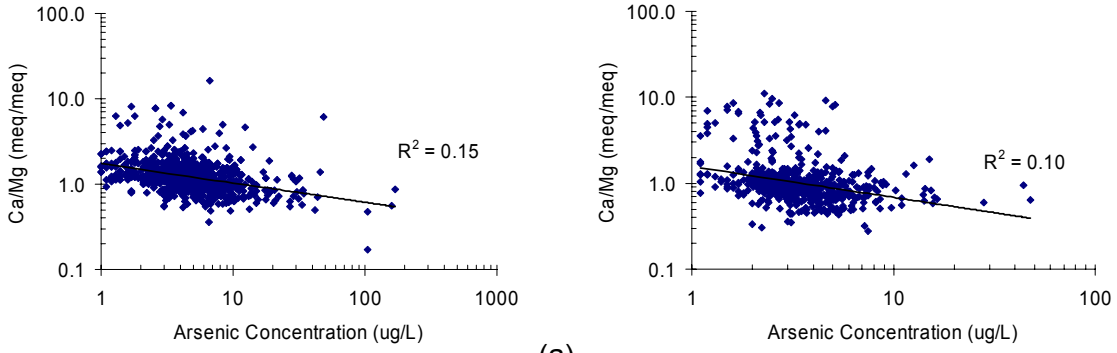

Figure 52. Cross-plot of As vs. Ca/Mg ratio, southern High Plains; NURE (a) and TWDB (b) databases

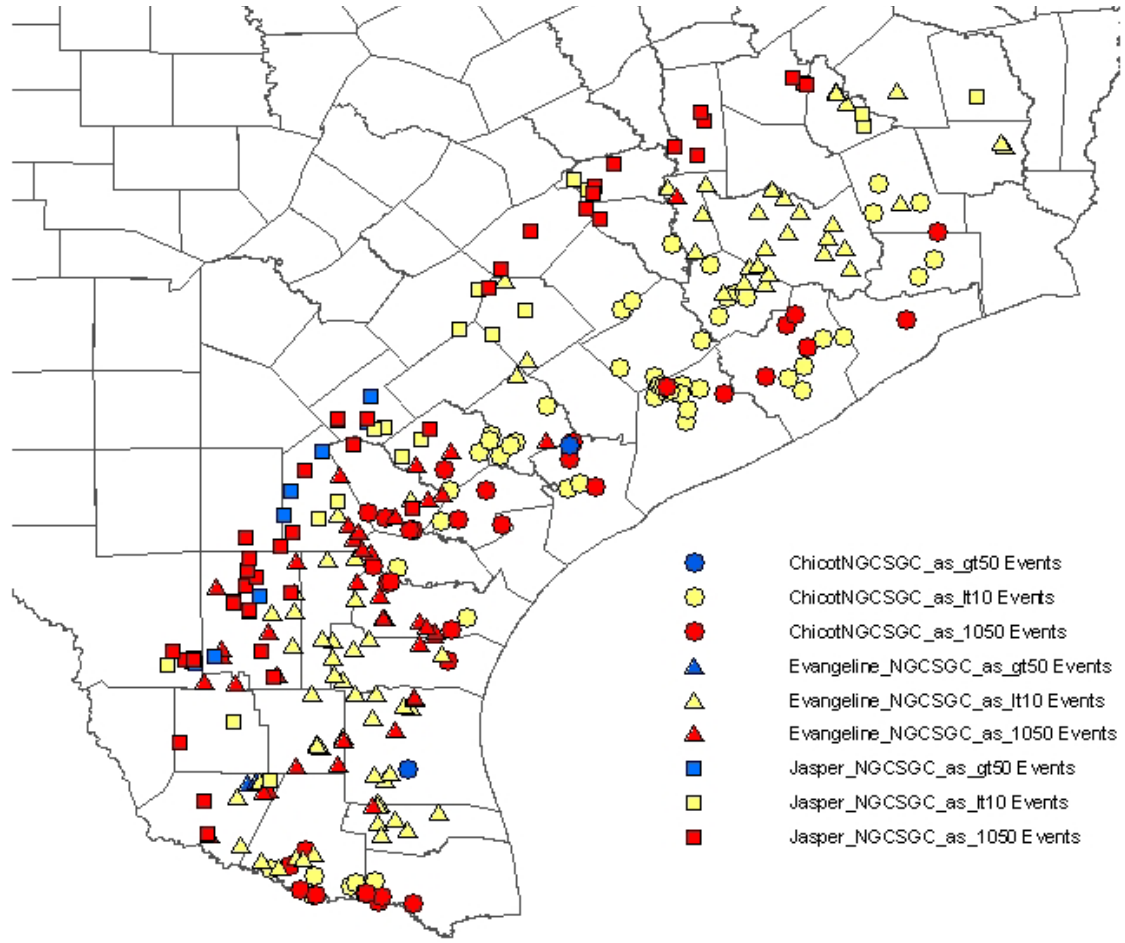

(a)

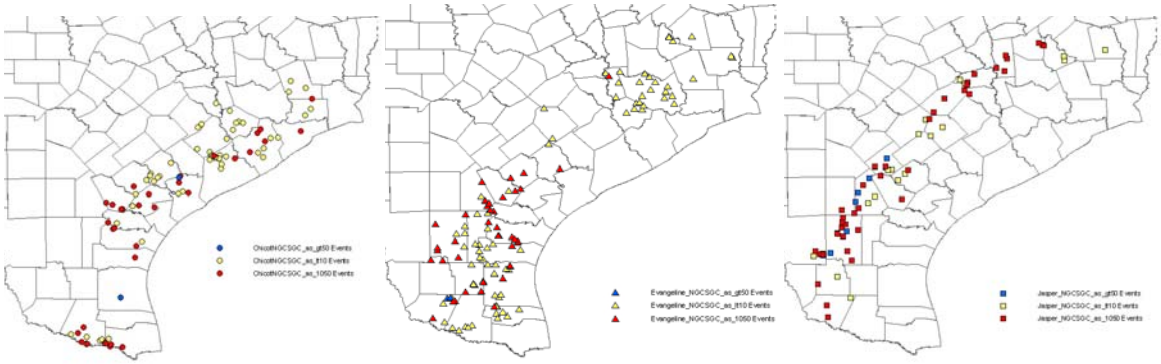

(b)

Figure 53. Arsenic spatial distribution by aquifer: all together (a) and, individually, in Chicot, Evangeline, and Jasper aquifers (b).

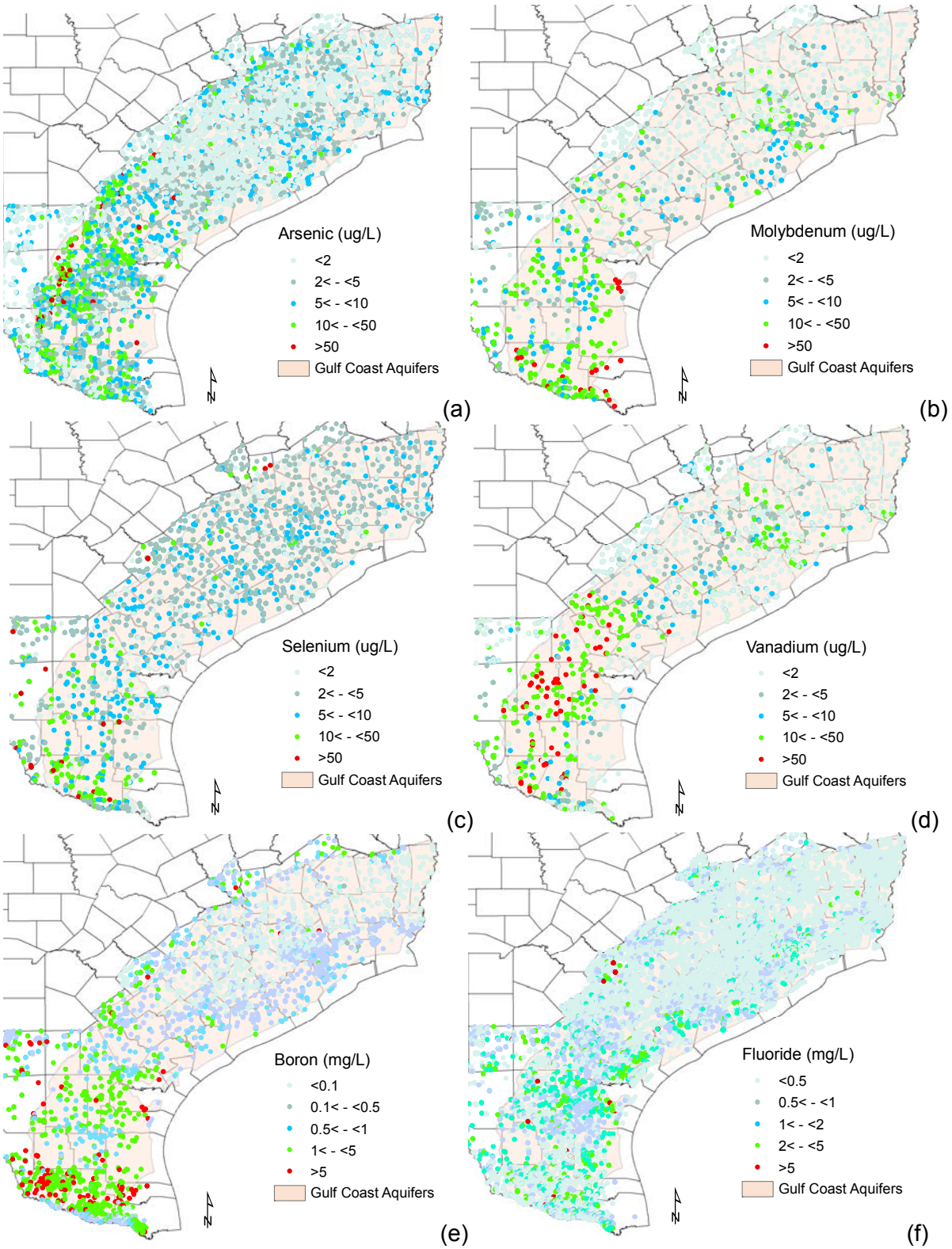

Figure 54. Spatial distribution of As (a), Mo (b), Se (c), V (d), B (e), F (f), U (g), silica (h), Fe (i), chloride (j), sulfate (k), TDS (l), anf pH (m) in Gulf Coast aquifers. All plots use only TWDB data except As and U where NURE data are also included.

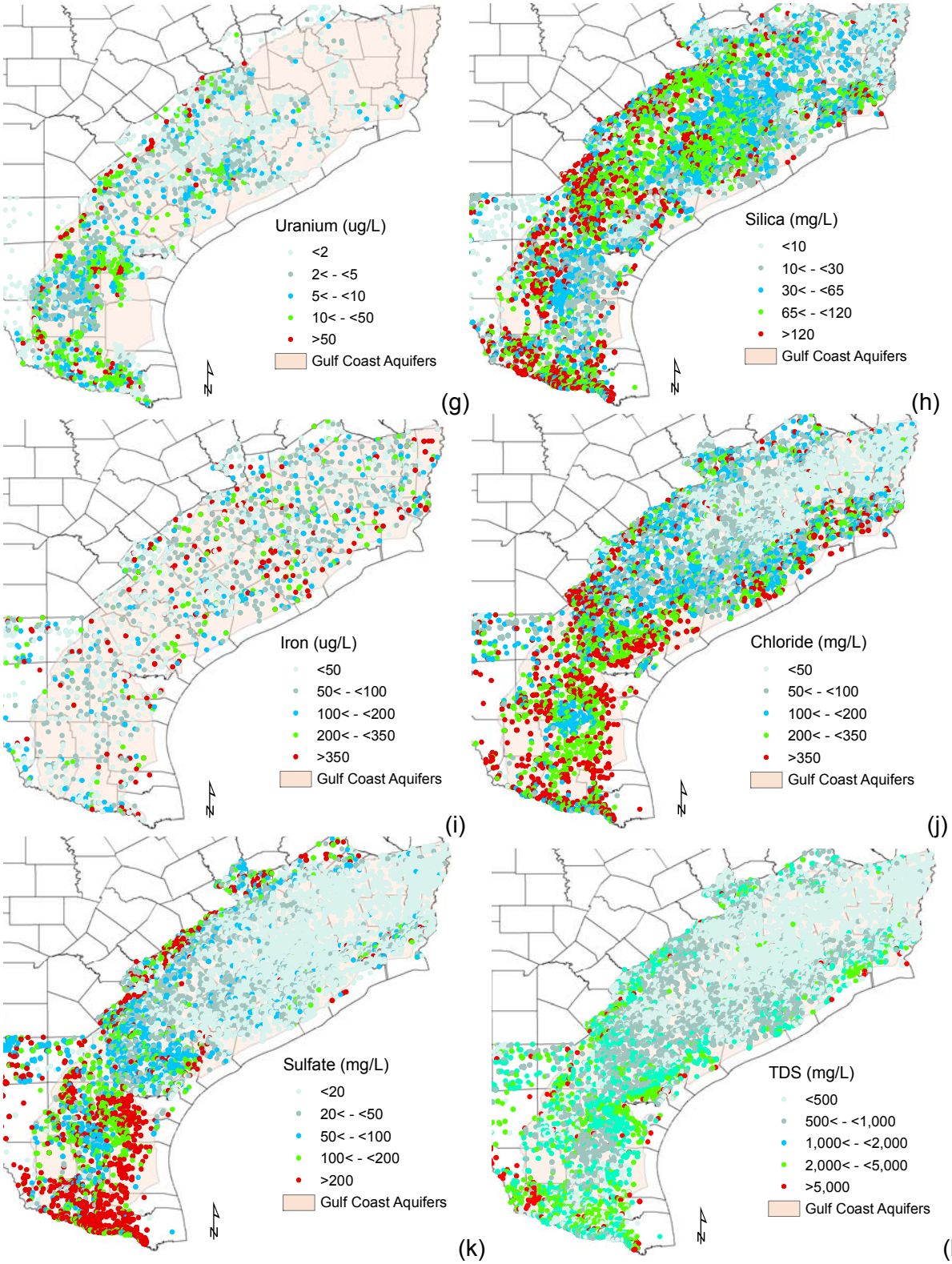

Figure 54. Spatial distribution of As (a), Mo (b), Se (c), V (d), B (e), F (f), U (g), silica (h), Fe (i), chloride (j), sulfate (k), TDS (l), anf pH (m) in Gulf Coast aquifers. All plots use only TWDB data except As and U where NURE data are also included. (continued)

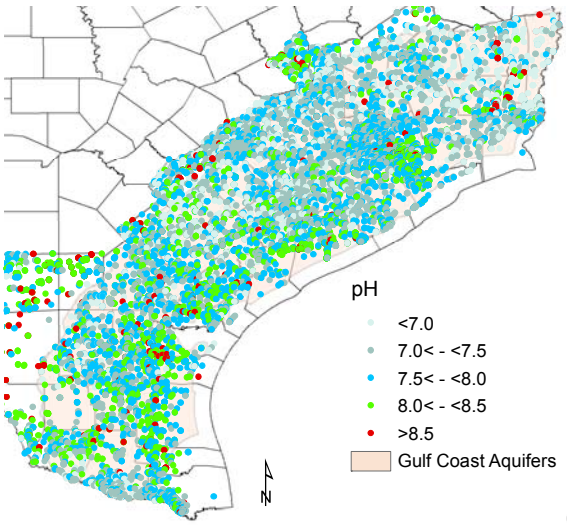

(m)

Figure 54. Spatial distribution of As (a), Mo (b), Se (c), V (d), B (e), F (f), U (g), silica (h), Fe (i), chloride (j), sulfate (k), TDS (l), anf pH (m) in Gulf Coast aquifers. All plots use only TWDB data except As and U where NURE data are also included. (continued)

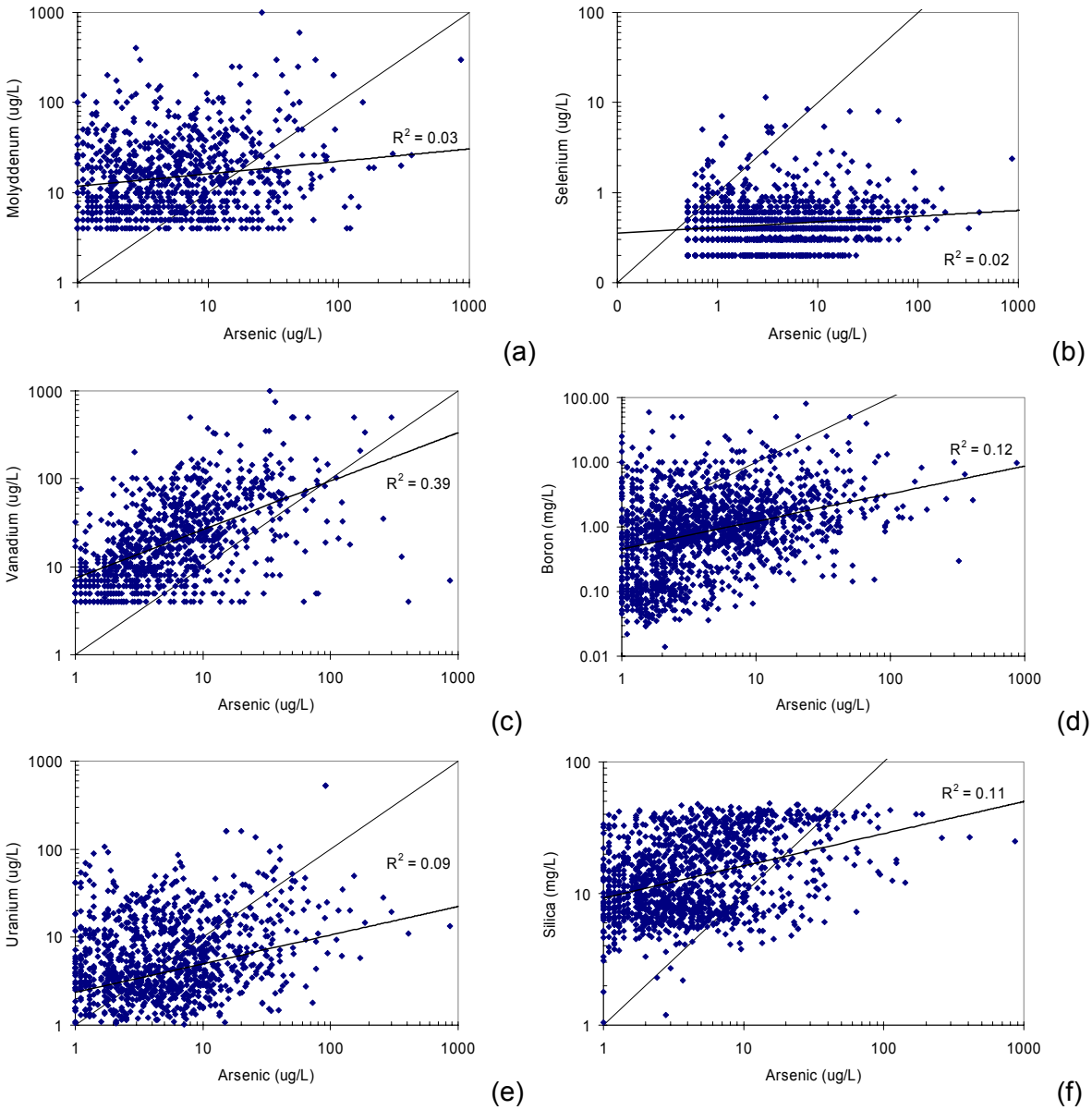

Figure 55. Cross-plots of (a) As vs. Mo, (b) vs. Se, (c) vs. V, (d) vs. B, (e) vs. U, (f) vs. silica, (g) vs. Fe, (h) vs. alkalinity (~bicarbonate), (i) sulfate, (j) vs. chloride, (k) vs. conductivity (~TDS) and (l) vs. pH (NURE data set), southwestern Gulf Coast aquifers.

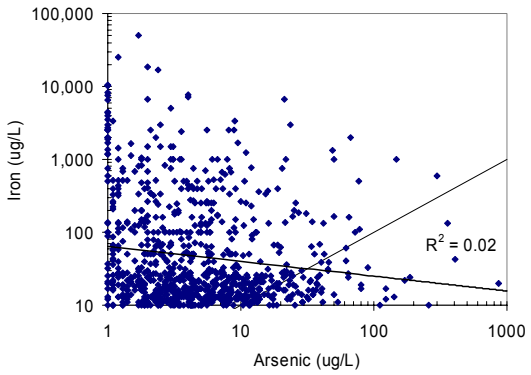

(g)

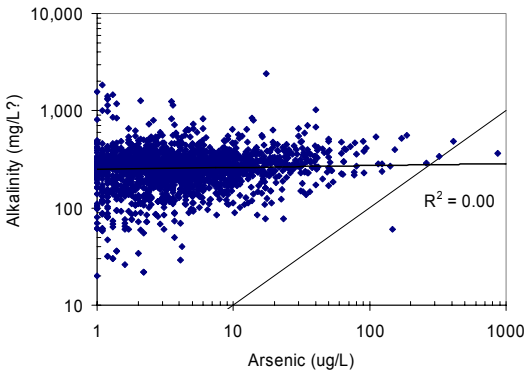

(h)

NOTE: Reporting unit was not given (mg/L?)

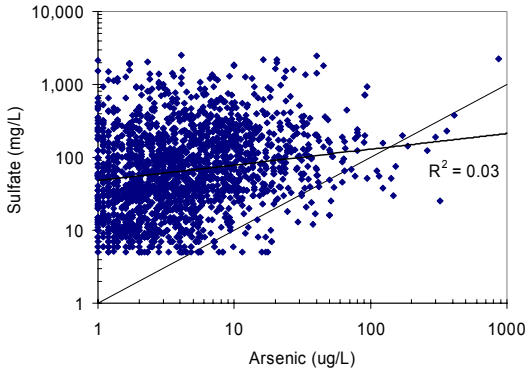

(i)

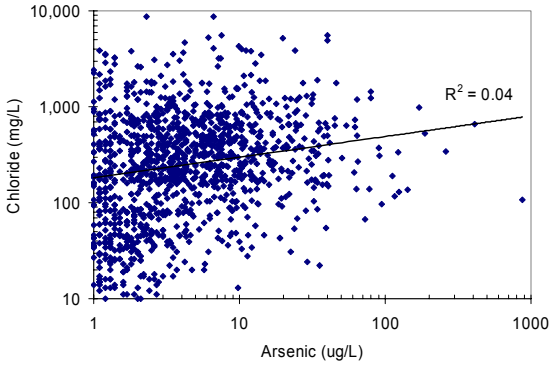

(j)

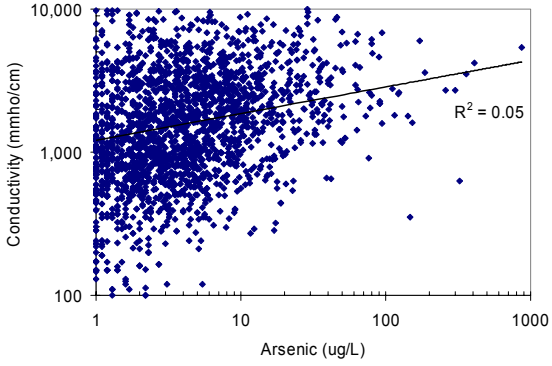

(k)

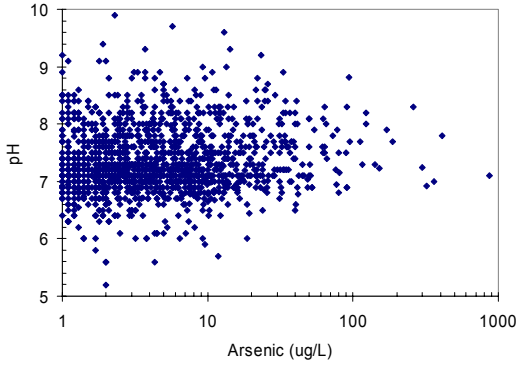

(l)

Figure 55. Cross-plots of (a) As vs. Mo, (b) vs. Se, (c) vs. V, (d) vs. B, (e) vs. U, (f) vs. silica, (g) vs. Fe, (h) vs. alkalinity (~bicarbonate), (i) sulfate, (j) vs. chloride, (k) vs. conductivity (~TDS) and (l) vs. pH (NURE data set), southwestern Gulf Coast aquifers. (continued)

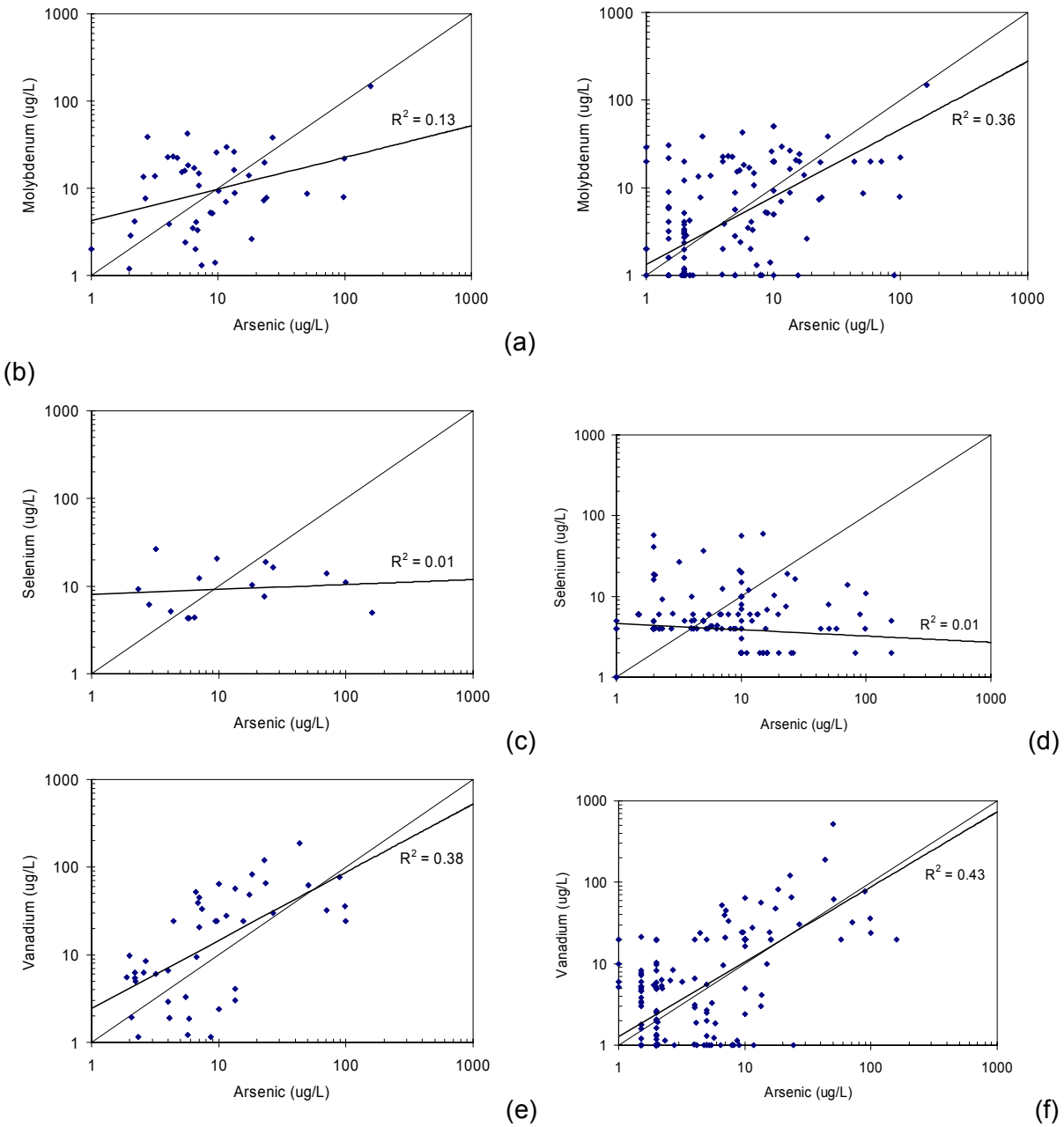

NOTE: Left-hand side plots include only those sample points where both variables are above detection limits; right-hand side plots include all sample points

Figure 56. Cross-plots of (a,b) As vs. Mo, (c,d) vs. Se, (e,f) vs. V, (g,h) vs. B, (i) vs. fluoride and silica, (j) vs. bicarbonate and sulfate, (k) vs. nitrate, and (l) vs. TDS and pH (TWDB database), southwestern Gulf Coast aquifers.

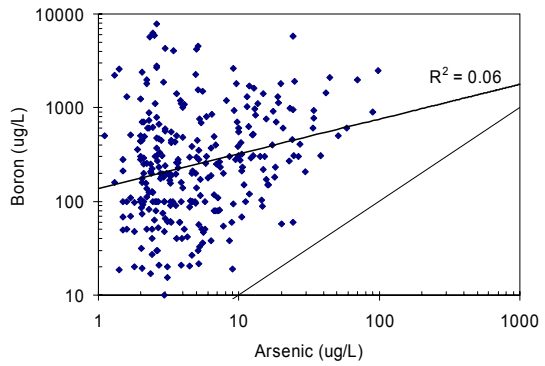

(g)

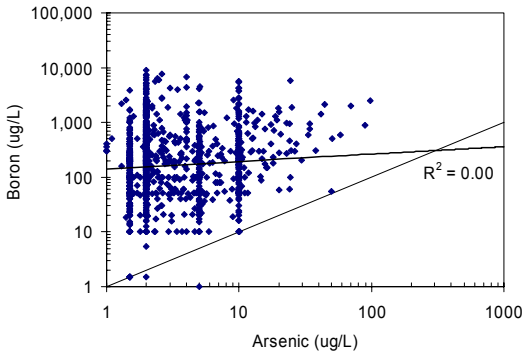

(h)

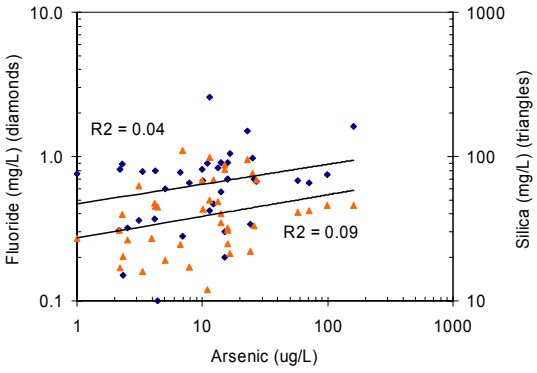

(i)

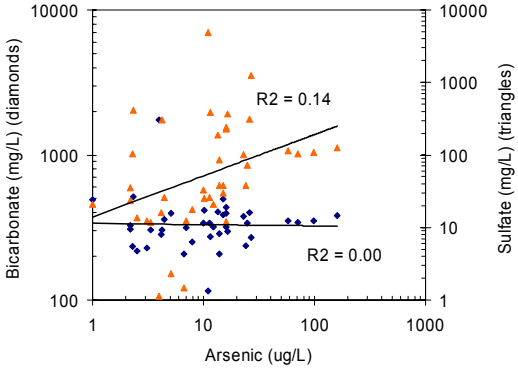

(j)

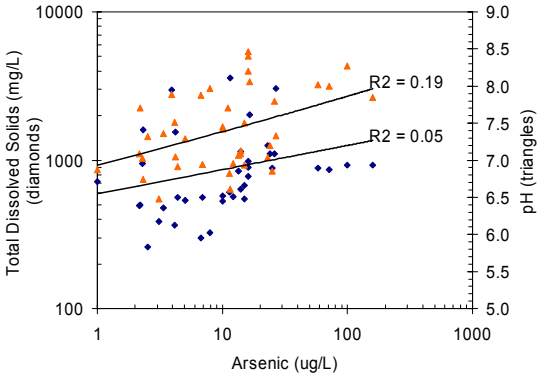

(k)

NOTE: all plots include only those sample points where both variables are above detection limits except (h) that include all sample points.

Figure 56. Cross-plots of (a,b) As vs. Mo, (c,d) vs. Se, (e,f) vs. V, (g,h) vs. B, (i) vs. fluoride and silica, (j) vs. bicarbonate and sulfate, (k) vs. nitrate, and (l) vs. TDS and pH (TWDB database), southwestern Gulf Coast aquifers. (continued)

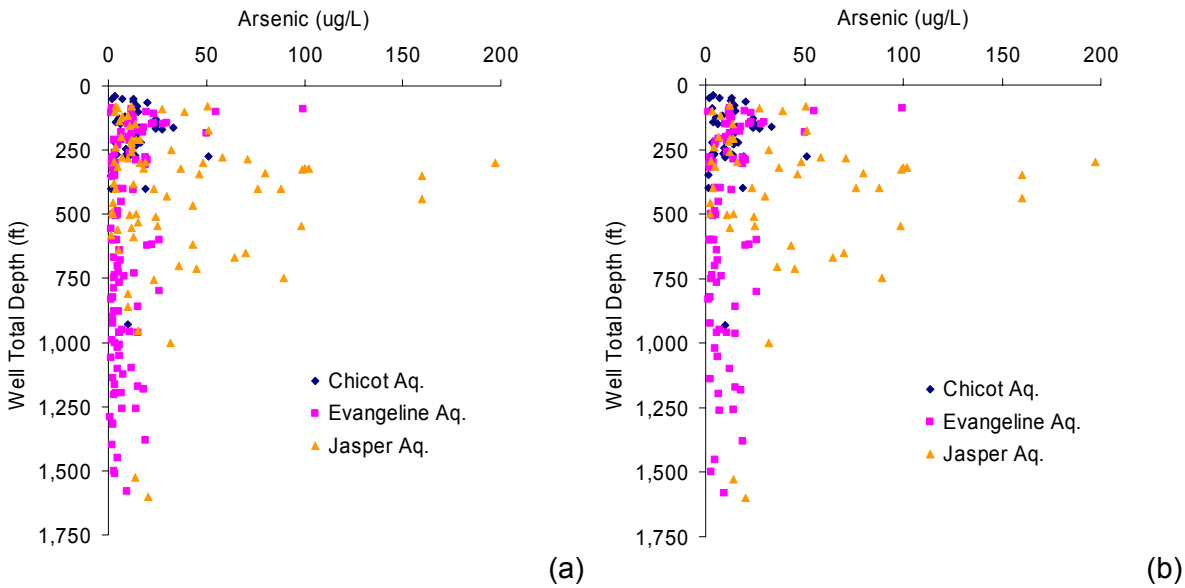

Figure 57. Arsenic concentration vs. total well depth in Gulf Coast Aquifers (a), only southwestern Gulf Coast (b)

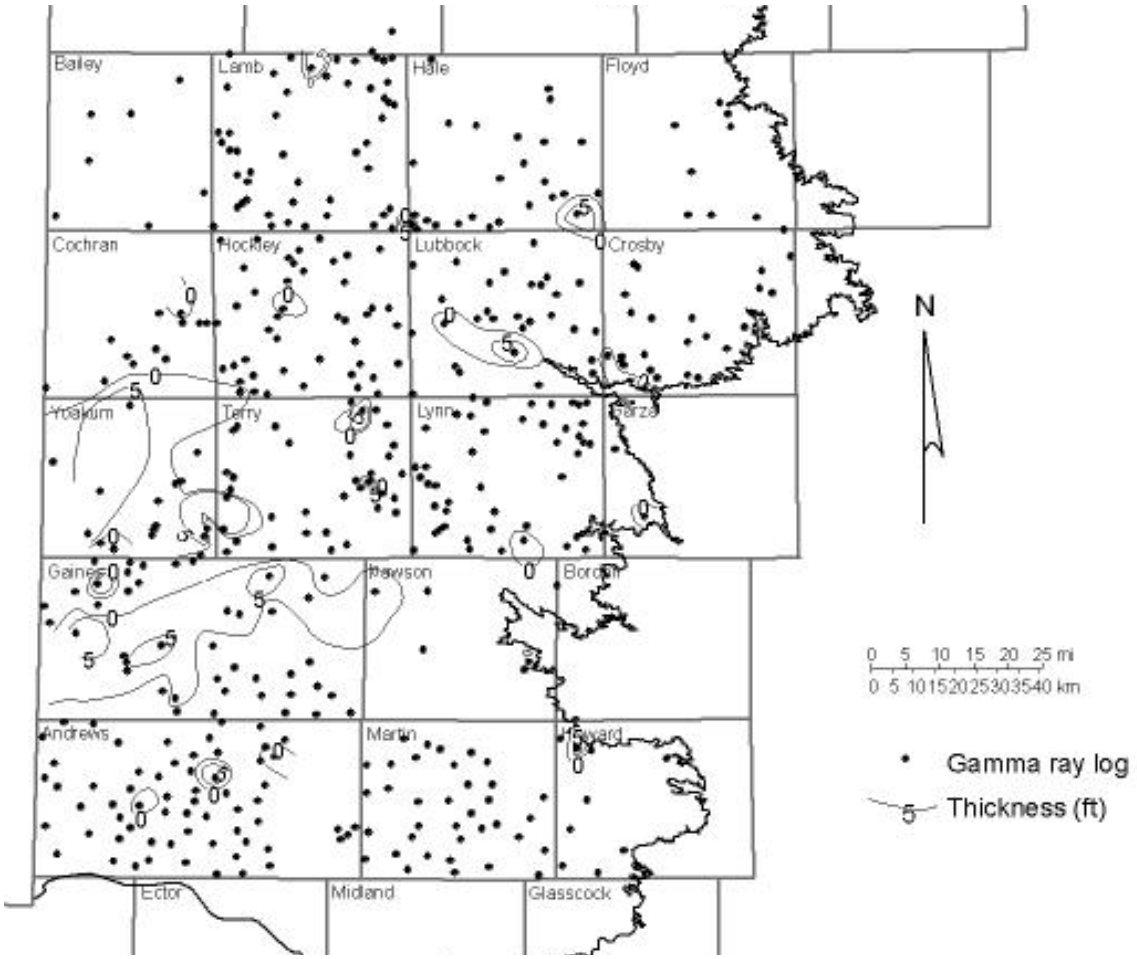

Figure 58. Thickness map of Ogallala-age ash beds based on geophysical logs

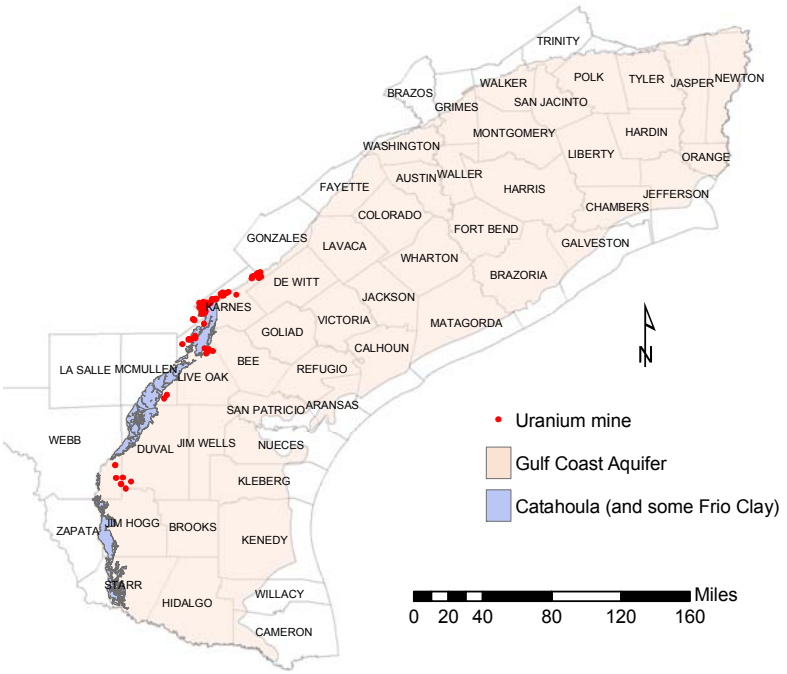

Figure 59. Map of selected uranium mines in the southern Gulf Coast area

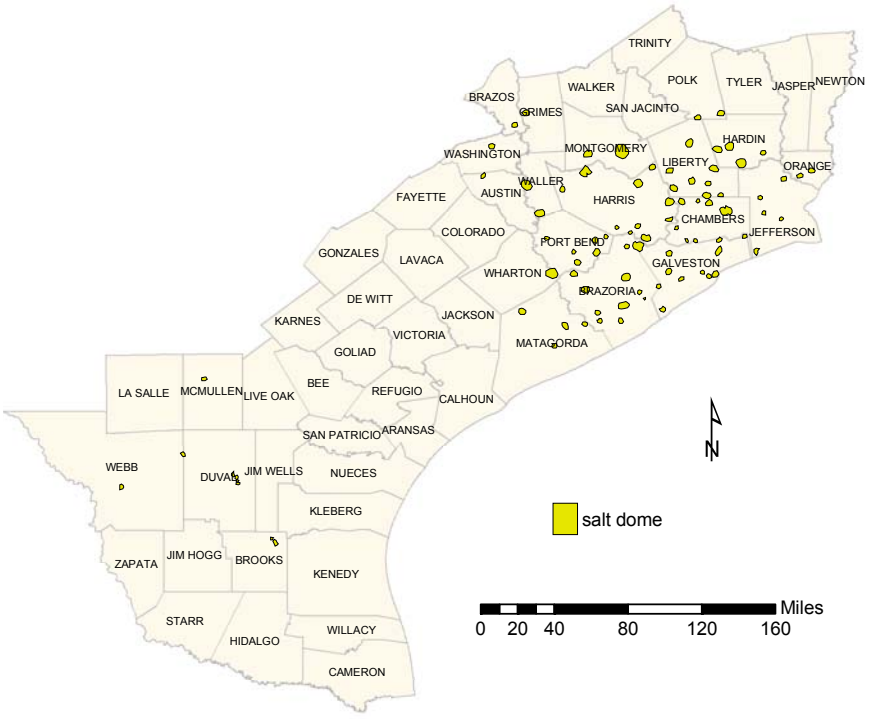

NOTE: locations from Lopez (1995), depth information from Halbouty (1979) and Ewing (1990)
Figure 60. Map of salt domes along the Gulf Coast

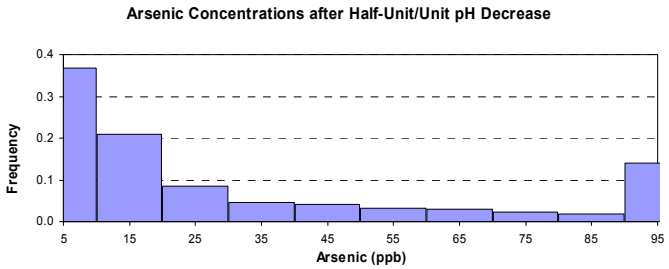

(a)

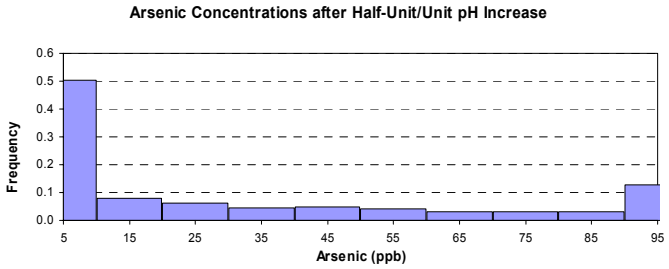

(b)

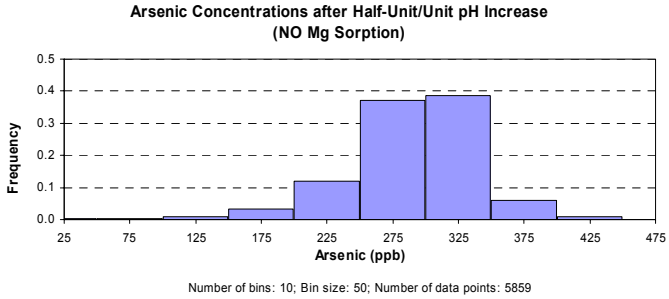

(c)

Figure 61. Histograms of arsenic distribution showing modeling results

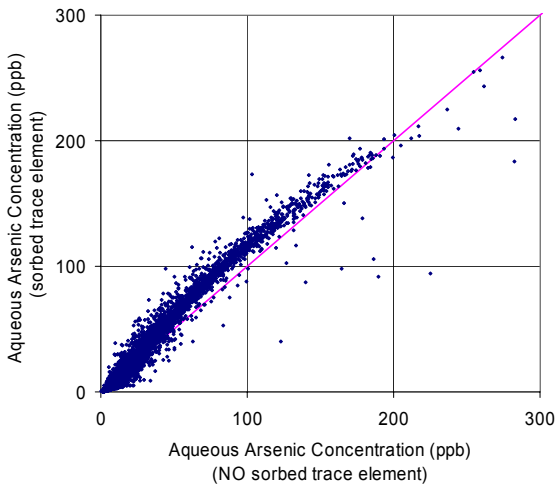

(a)

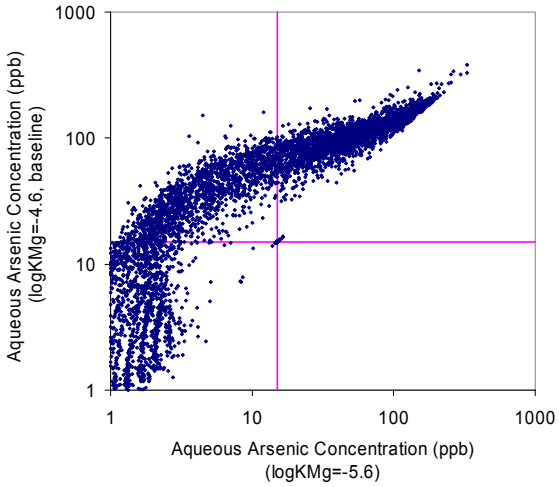

(b)

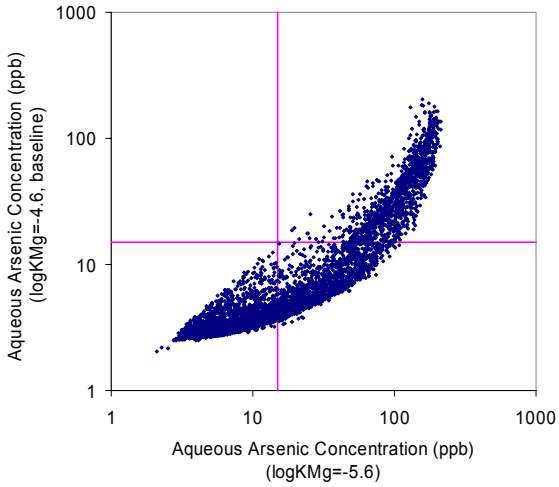

(c)

Figure 62. Crossplot of arsenic concentration with and without including trace elements in the modeling

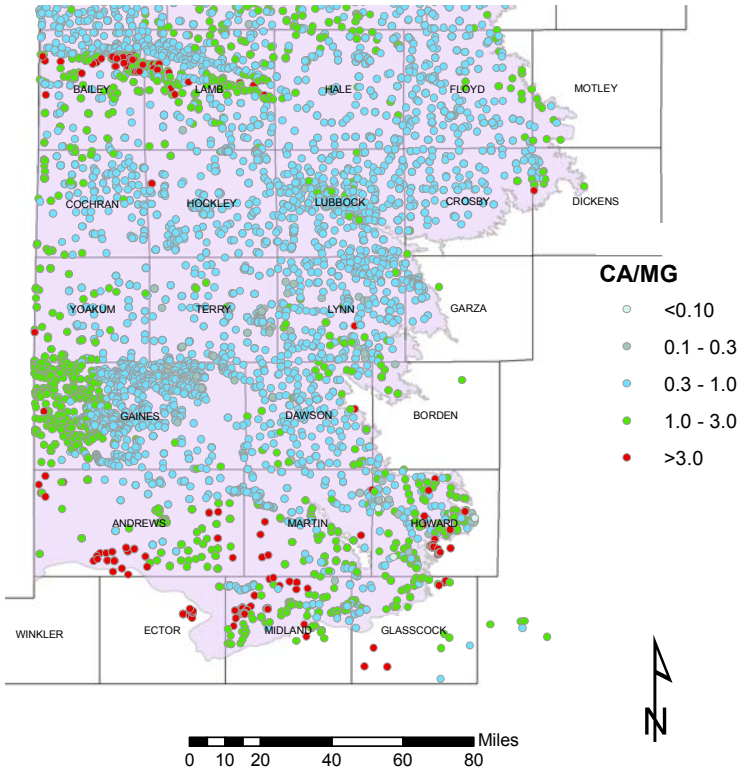

Figure 63. Spatial distribution of the Ca/Mg ratio in the southern High Plains (TWDB database)

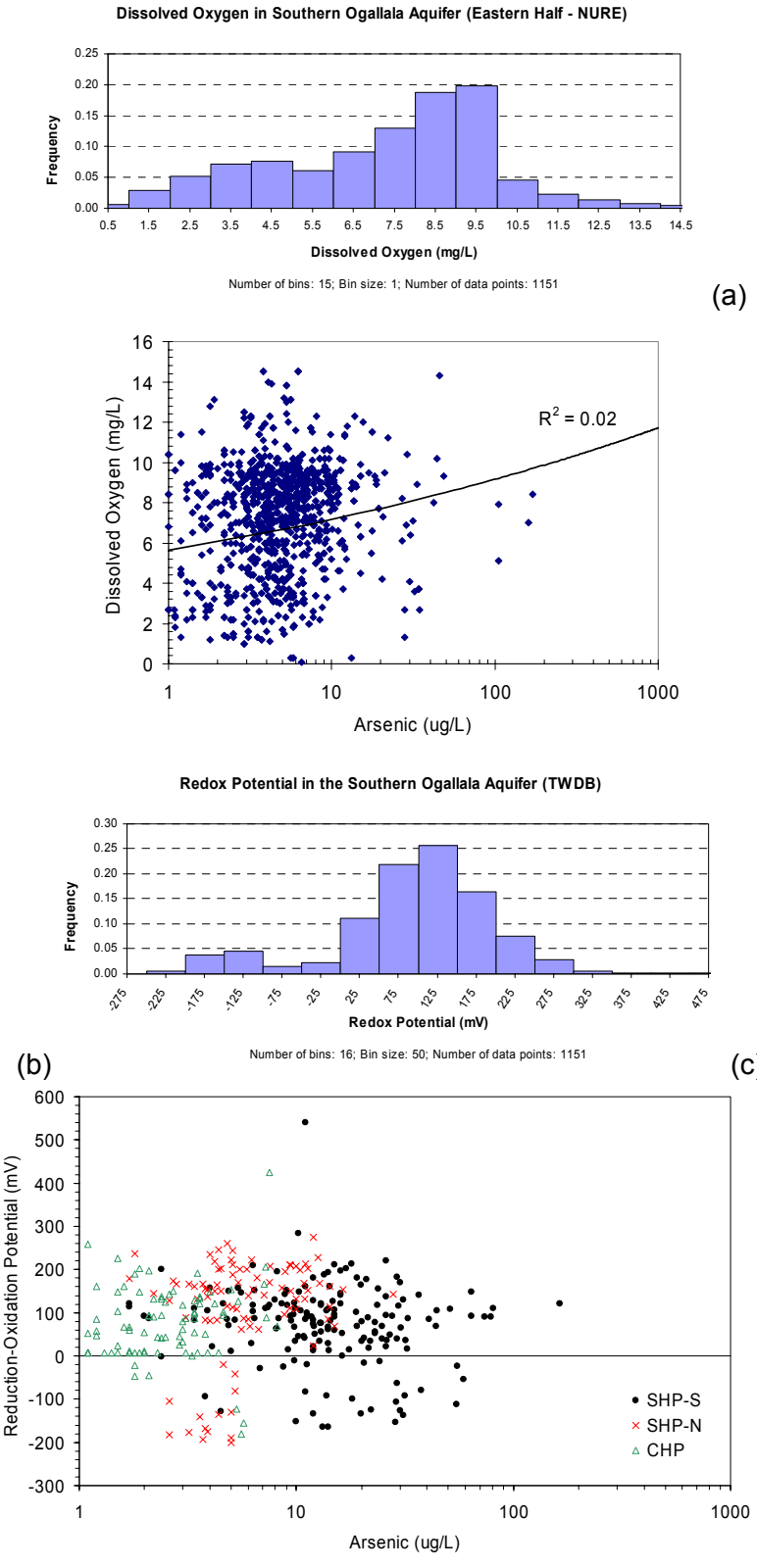

Figure 64. Distribution of dissolved oxygen (NURE) and redox potential (TWDB) in the southern High Plains aquifer

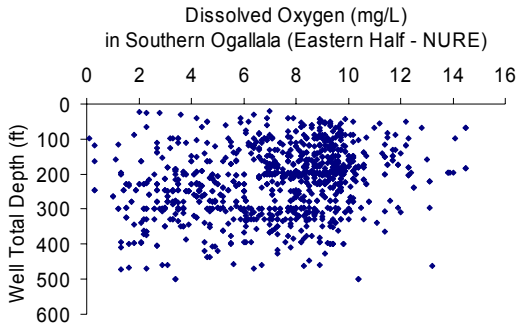

Figure 65. Depth distribution of dissolved oxygen in the eastern half of the southern High Plains aquifer (NURE data)

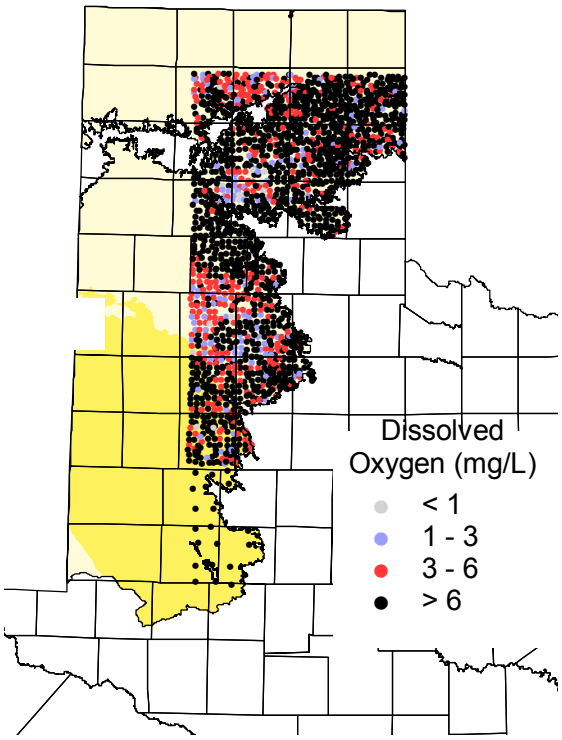

Figure 66. Spatial distribution of dissolved oxygen in the eastern half of the southern High Plains aquifer (NURE data)

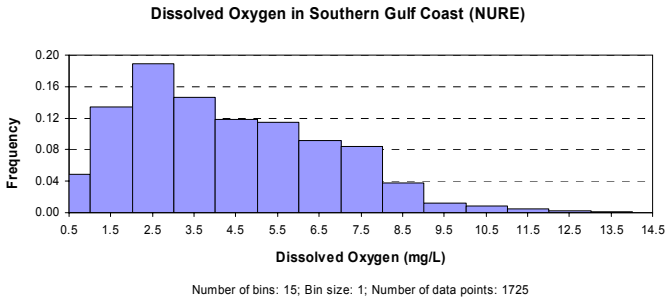

Figure 67. Histogram of dissolved oxygen in the southwestern Gulf Coast aquifers (NURE data)

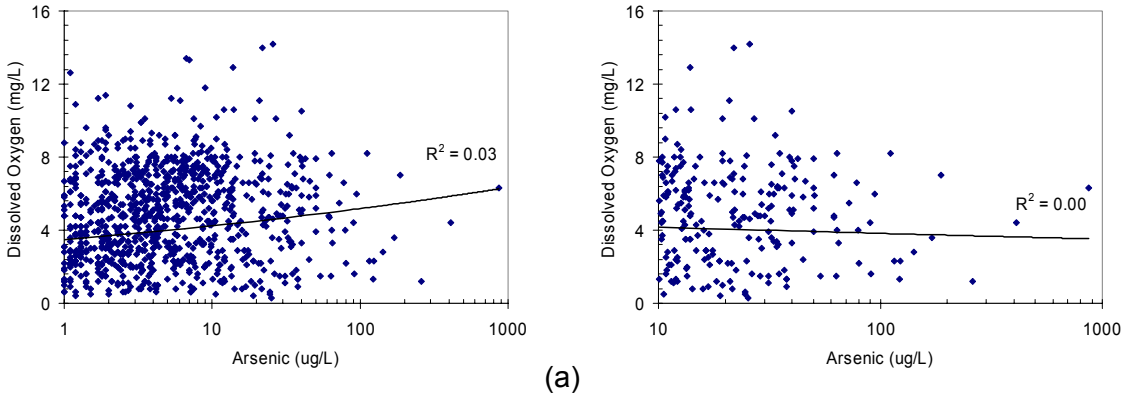

(a) (b)

NOTE: (a) all samples; (b) only samples with As > 10 ug /L are retained

Figure 68. Cross-plots of As vs. dissolved oxygen (NURE data set), southwestern Gulf Coast aquifers:

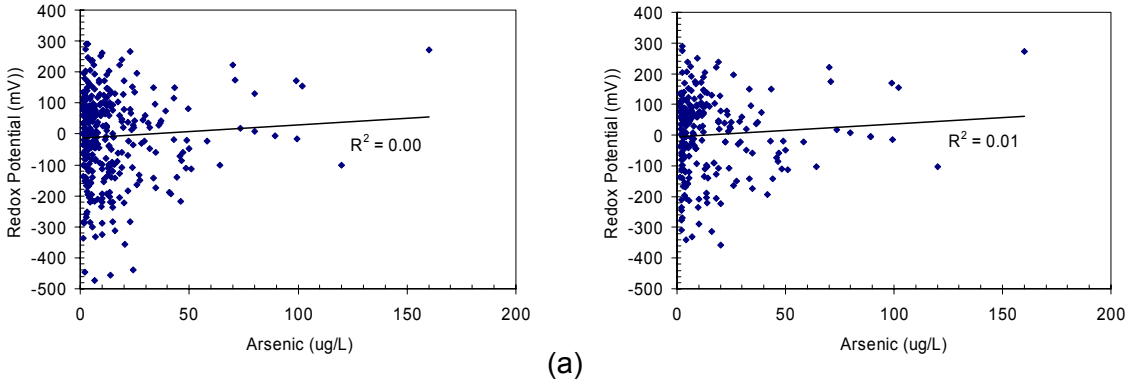

(a) (b)

Figure 69. Redox potential in Gulf Coast aquifers (a) and only southwestern section (b)

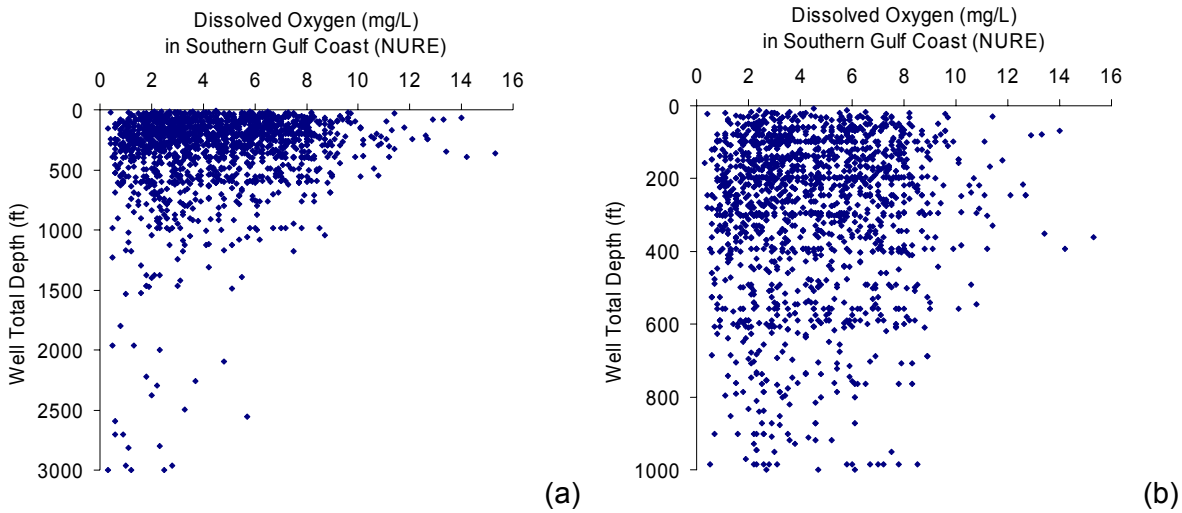

NOTE: (a) to a depth of 3,000 ft; (b) to a depth of 1,000 ft

Figure 70. Depth distribution of dissolved oxygen in the southwestern Gulf Coast aquifers

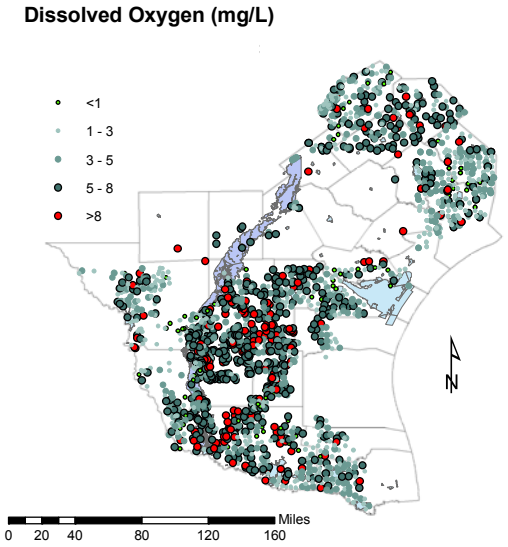

Figure 71. Spatial distribution of dissolved oxygen in the southwestern Gulf Coast aquifers (NURE)

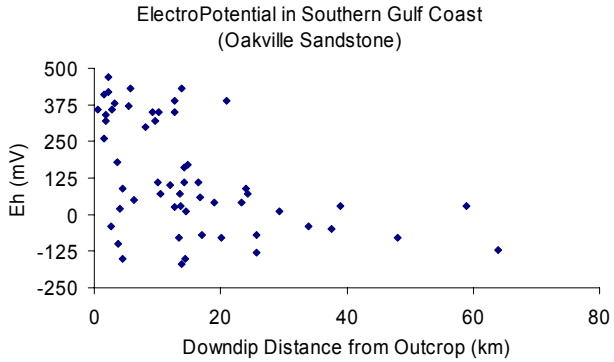

NOTE: data from Henry et al. (1982a, Table A-1)

Figure 72. Eh evolution along groundwater flowlines in Oakville sandstone of the southwestern Gulf Coast

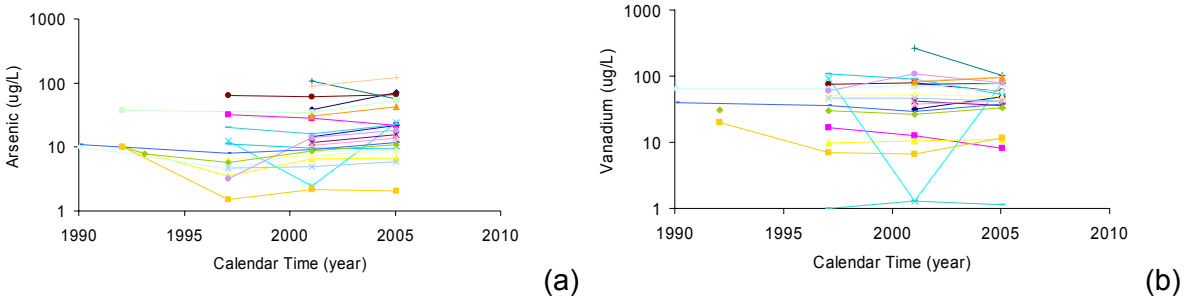

(a) (b)

Figure 73. Time series of arsenic and Vanadium aqueous concentrations in wells recently sampled in Duval County

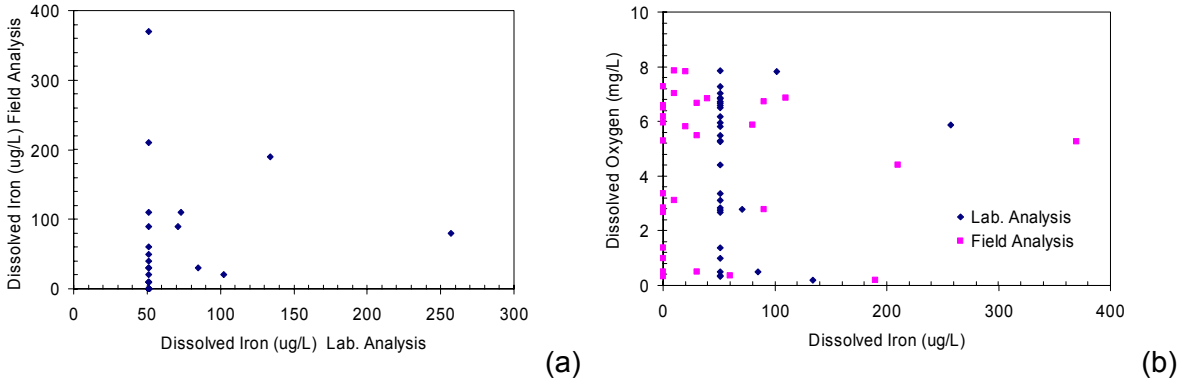

(a) (b)

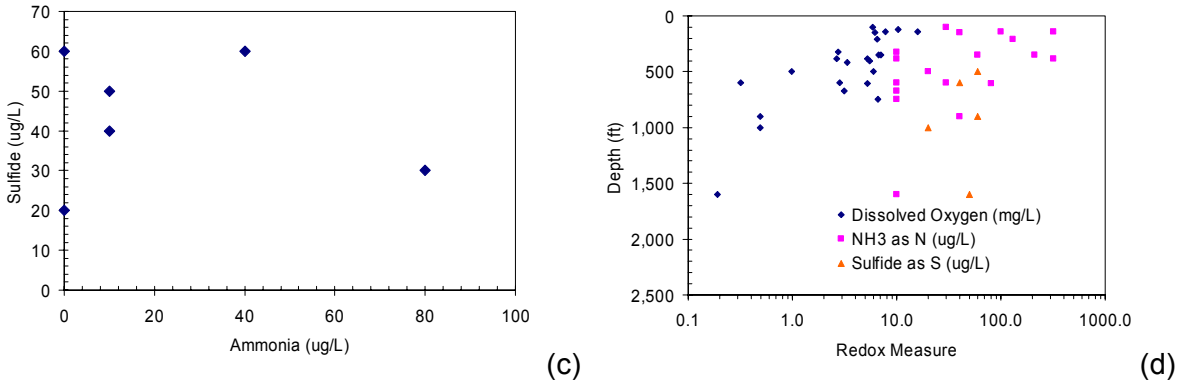

(c) (d)

Figure 74. Analysis of redox pairs (Duval County)

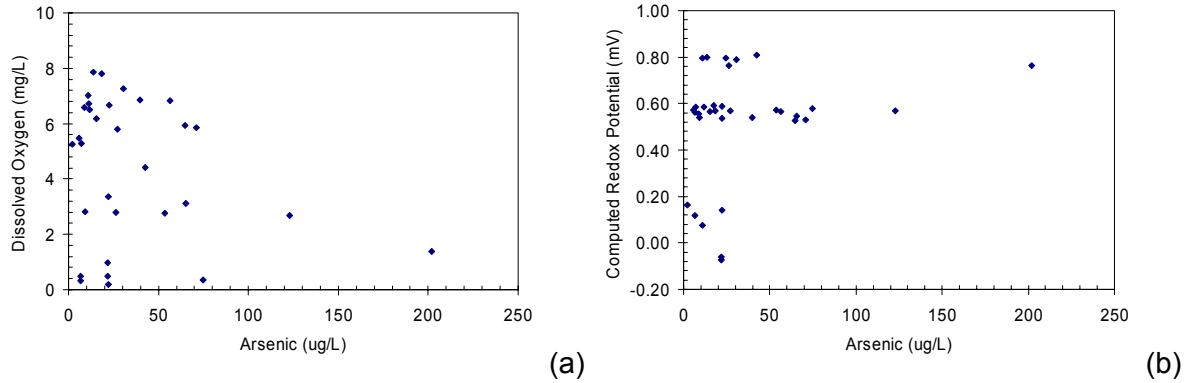

(a) (b)

Figure 75. Cross-plots of As vs. dissolved oxygen (a) and computed redox potential (b) (Duval County)

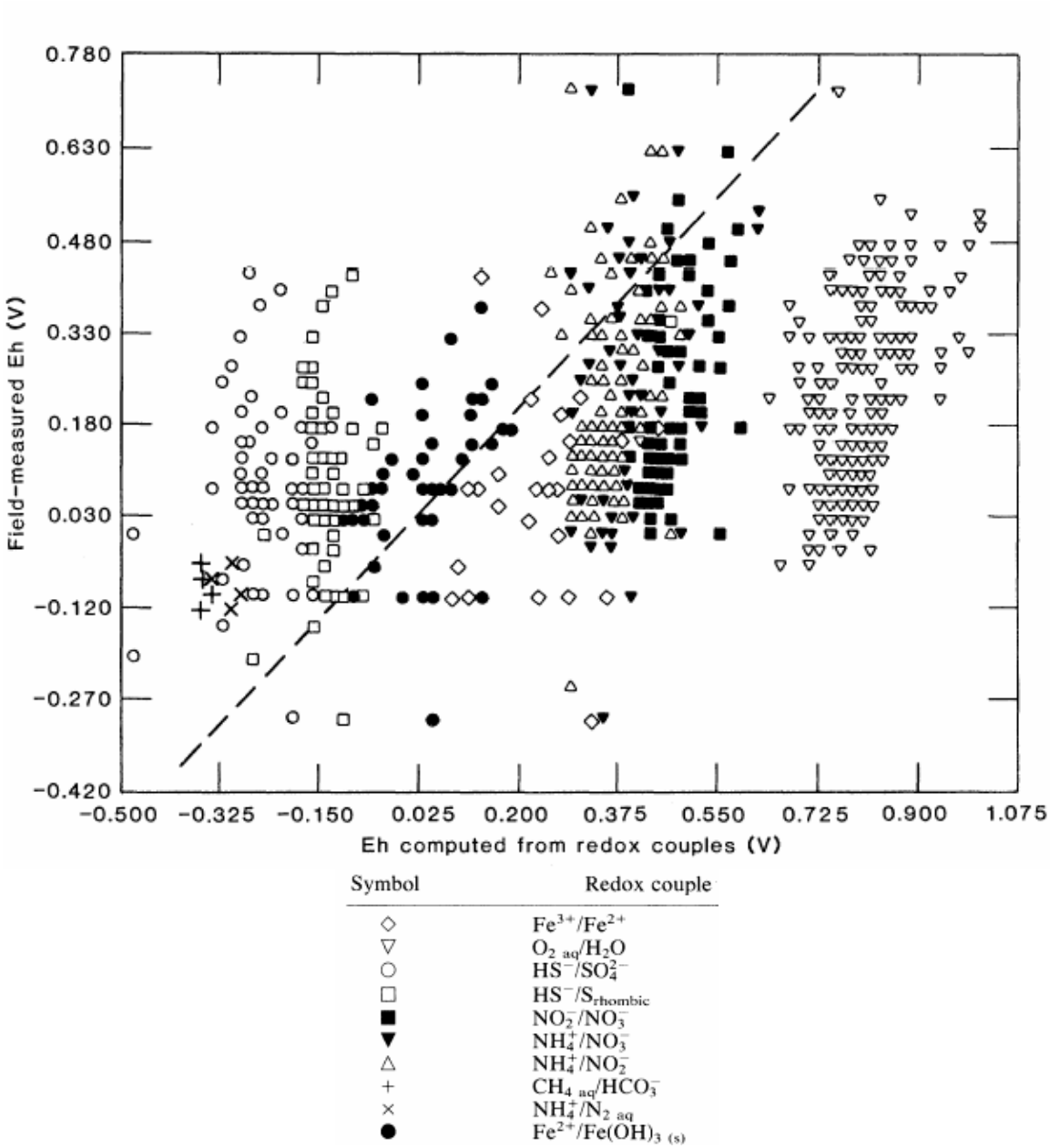

SOURCE: Lindberg and Runnels, 1994

Figure 76. Literature comparison of measured and computed Eh

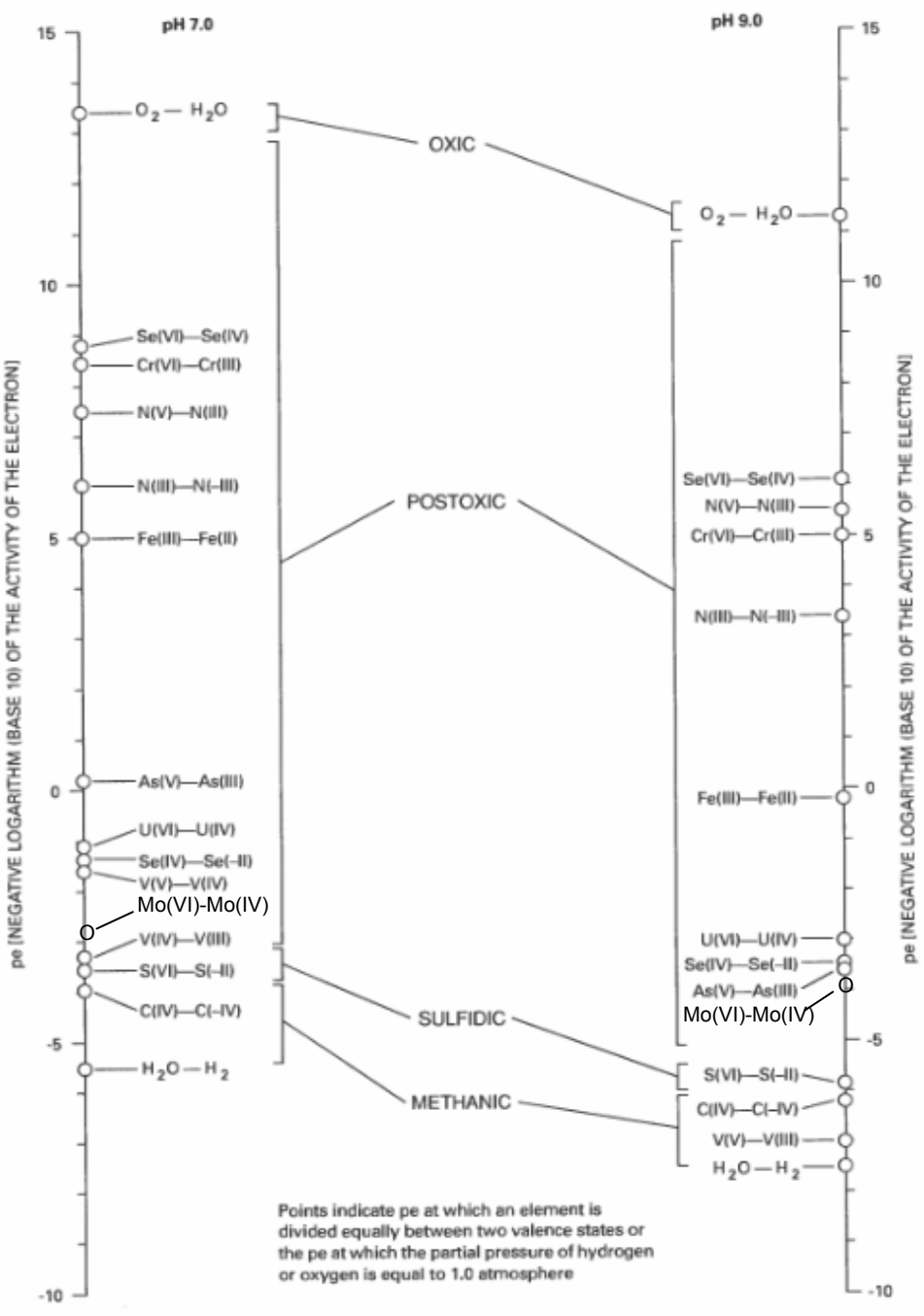

NOTE: at 25°C, pe = 16.9 Eh (V) or Eh (mV) = 59 pe
SOURCE: Parkhurst et al., 1995
Figure 77. Redox ladder for As, Se, U, and V and major redox couples

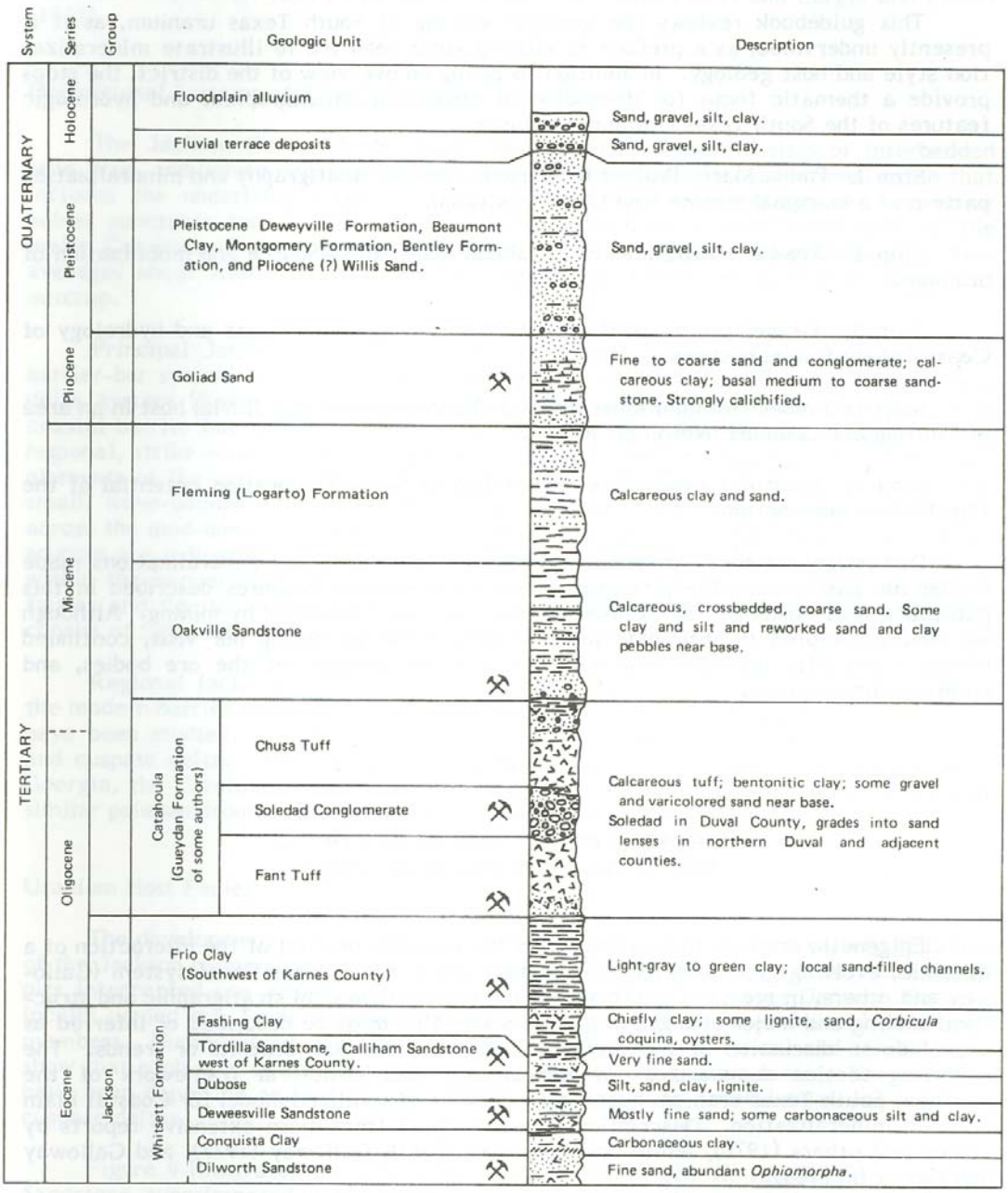

NOTE: Crossed picks indicate units from which uranium has been extracted
SOURCE: Galloway et al., 1979
Figure 78. Stratigraphic section in the South Texas uranium province